

Copyright
by
Dilip Rugnathbhai Maniar
2000

**Preservation Alternatives for Historic Metal Truss Bridges:
Shackelford County Bridge – A Case Study**

by

Dilip Rugnathbhai Maniar, B.S.C.E., L.C.S.E.

Thesis

Presented to the Faculty of the Graduate School of

The University of Texas at Austin

in Partial Fulfillment

of the Requirements

for the Degree of

Master of Science in Engineering

The University of Texas at Austin

August 2000

**Preservation Alternatives for Historic Metal Truss Bridges:
Shackelford County Bridge – A Case Study**

**Approved by
Supervising Committee:**

Michael D. Engelhardt

Joseph A. Yura

Dedication

To my parents, Rugnathbhai and Heeragauri.

Acknowledgements

It's my pleasure to thank each individual who has helped me in the completion of this thesis. Firstly, to Dr. Michael D. Engelhardt, for giving me the opportunity to work on the research project. His way of encouraging and guiding me is highly appreciated. I am very thankful to him for his continuous guidance and support throughout the study. Secondly to, Texas Department of Transportation for funding the research study and giving a unique opportunity to work with them. Thirdly to, the faculty and staff of Ferguson Structural Engineering Laboratory for guiding and helping me by proving me excellent technical knowledge and best working environment.

I would also like to thank Mr. Charles Bowen for his continuous support throughout the study. I am also thankful to Norman Grady, Photis Matsis, and Scott Barney for helping me with load testing. I am very thankful to Mr. Patrick Sparks form Law Engineering, Austin to help me with material evaluation. I would also like to thank all the individuals who helped me directly or indirectly towards completion of my research studies.

From the personal side, I would like to thank my family for supporting me throughout my life. I am exceptionally thankful to my parents who have taken lots of effort to bring me the person I am.

August 2000

Abstract

Preservation Alternatives for Historic Metal Truss Bridges: Shackelford County Bridge – A Case Study

Dilip Rugnathbhai Maniar, M.S.E.

The University of Texas at Austin, 2000

Supervisor: Michael D. Engelhardt

A number of very old metal truss bridges, some dating back more than a century, are still in vehicular service in Texas. Many of these bridges are of historic interest due to their age and other unique features. There is currently a strong interest in saving historic metal truss bridges and keeping them in continued service. However, achieving this goal is frequently problematic due to structural deficiencies found in these old bridges.

A case study was conducted on a historic metal truss bridge constructed in 1885 in Shackelford County Texas. A number of techniques were investigated to address the structural deficiencies of this bridge. This included techniques for data collection, materials evaluation, structural analysis and load rating, field load testing, and finally structural rehabilitation. This case study demonstrated that the structural deficiencies in this bridge could be addressed by simple and inexpensive remedies, thereby permitting continued use of this historic bridge.

Table of Contents

List of Tables	xv
List of Figures.....	xviii
List of Illustrations	xxi
Chapter 1	1
Introduction	1
1.1 Background.....	1
1.2 Project Description and Scope of Report	2
1.2.1 Data Collection and Material Evaluation.....	4
1.2.2 Analysis and Load Rating of the Bridge	4
1.2.3 Rehabilitation Options	5
1.5 Scope of Evaluation.....	6
Chapter 2	7
Data Collection.....	7
2.1 Introduction	7
2.2 Components of Bridge Records.....	8
2.3 Case Study.....	10
2.3.1 Bridge History	10
2.3.2 Bridge Description.....	11
2.3.2.1 Flooring System.....	12
2.3.2.2 Floor Supporting System.....	12
2.3.2.2.1 Main Truss Span.....	12
2.3.2.2.2 South and North Approaches.....	18
2.3.2.3 Substructure	18
2.3.2.4 Railing	20
2.3.3 Field Observations	22

2.3.3.1 Flooring System.....	22
2.3.3.2 Floor Supporting System.....	22
2.3.3.3 Substructure	23
2.3.3.4 Miscellaneous Items	24
Chapter 3	25
Material Evaluation.....	25
3.1 Introduction	25
3.2 Need for Material Evaluation.....	26
3.3 Metals	27
3.3.1 Metal Identification Tests	27
3.3.1.1 Wrought Iron Identification in Field	29
3.3.2 Chemical Composition.....	29
3.3.3 Microstructure	31
3.3.4 Macrostructure.....	31
3.3.5 Hardness Testing	32
3.3.6 Detection of Defects	33
3.4 Structural Timber.....	34
3.5 Masonry.....	35
3.6 Metal Evaluation for Case Study Bridge	38
3.6.1 Laboratory Testing	38
3.6.1.1 Selection of Location for Material Removal.....	38
3.6.1.2 Removal of Material.....	39
3.6.1.3 Test Conducted	40
3.6.2 In-situ Testing.....	40
Chapter 4	42
Analysis and Load Rating	42
4.1 Introduction	42
4.2 Rating Levels	42

4.3 Rating Methods	43
4.4 Rating Equation.....	44
4.5 Loadings	45
4.6 Analysis	46
4.6.1 Truss Analysis	46
4.6.2 Truss Analyses Comparison.....	49
4.6.3 Deck Analysis.....	50
4.6.4 Deck Analyses Comparison	53
4.7 Nominal Capacity Calculations	56
4.7.1 Truss	56
4.7.1.1 Inventory.....	57
4.7.1.2 Operating	57
4.7.2 Timber Deck.....	58
4.7.3 Metal Floor Beams	58
4.8 Load Rating	59
4.8.1 Discussion on Load Rating Results	59
Chapter 5	62
Field Load Testing.....	62
5.1 Introduction	62
5.2 Objective	62
5.3 Overview of Field Load Testing.....	63
5.3.1 Strain Gage Layout	63
5.3.2 Description of Test Equipment.....	64
5.3.3 Loading Vehicle	64
5.3.4 Field Load Testing.....	65
5.4 Analysis of the Field Load Test Data.....	66
5.5 Theoretical Analysis of Load Test Vehicle	67
5.6 Field Load Test Issues.....	67

5.7 Comparison of the Test Data and Theoretical Analysis	68
5.7.1 First Field Load Test	69
5.7.2 Second Field Load Test.....	72
5.8 Conclusions Derived from Field Load Tests	78
Chapter 6	81
Rehabilitation Options	81
6.1 Introduction	81
6.2 Common Deficiencies in Older Metal Truss Bridges	82
6.2.1 Inadequate Load Capacity of Truss	82
6.2.2 Damage and Deterioration to Truss.....	83
6.2.3 Geometrical Deficiencies	86
6.2.4 Deficiencies in Substructure	87
6.3 Rehabilitation Techniques.....	87
6.3.1 Bridge Floor and Deck System.....	87
6.3.2 Damage and Deterioration.....	90
6.3.3 Truss Strengthening.....	90
6.3.4 Truss Strengthening by Post-Tensioning.....	91
6.3.5 Substructures	94
6.4 Case Study Bridge: Rehabilitation Options	95
6.4.1 Timber Deck	95
6.4.2 Metal Floor Beams	100
6.4.3 Truss	101
6.4.4 Substructure and Approach Spans	103
6.5 Case Study Bridge: Rehabilitation Plan.....	103
6.5.1 Plan I: Do Nothing.....	103
6.5.2 Plan II: Rehabilitate the Bridge for H15 Loading	103
6.5.3 Plan III: Rehabilitate the Bridge for HS20 Loading.....	104

Chapter 7	107
Summary and Conclusions	107
7.1 Review of Project Scope and Objectives.....	107
7.2 Summary of Major Project Tasks and Findings	108
7.2.1 Data Collection.....	110
7.2.2 Evaluation of Materials	111
7.2.3 Structural Analysis and Load Rating.....	113
7.2.4 Field Load Testing.....	116
7.2.5 Development of Rehabilitation Options	119
7.3 Conclusions	121
Appendix A.....	123
Photographs of Case Study Bridge	123
Appendix B.....	149
Drawings of Case Study Bridge	149
Appendix C.....	173
Material Testing Results for Metal Samples of Case Study Bridge	173
C.1 Results of Laboratory Testing.....	174
C.2 Field Testing	180
Appendix D.....	182
Wrought Iron.....	182
D.1 Introduction.....	182
D.2 The Manufacturing of Wrought Iron.....	183
D.2.1 The Puddling Process	184
D.2.2 Aston Process or New Byers Process.....	185
D.3 Chemical Composition of Wrought Iron.....	185
D.3.1 Carbon.....	187

D.3.2 Manganese	187
D.3.3 Phosphorous	188
D.3.4 Sulfur	188
D.3.5 Silicon.....	188
D.3.6 Influence of Chemical Composition upon the Welding Properties	188
D.3.7 Influence of Chemical Composition on the Properties of Wrought Iron.....	189
D.4 Structure of Wrought Iron	191
D.4.1 Microscopic Examination.....	191
D.4.2 Macroscopic Examination.....	194
D.5 Mechanical Properties	195
D.5.1 Tensile Strength.....	196
D.5.2 Shear Strength.....	198
D.5.3 Torsion Strength.....	201
D.5.4 Impact Strength.....	201
D.5.5 Compressive Strength of Wrought Iron.....	202
D.5.6 Modulus of Elasticity.....	202
D.5.7 Fatigue Resistance	203
D. 5.8 Hardness	203
D.5.9 Machinability.....	203
D.5.10 Specific Gravity.....	204
D.5.11 Coefficient of Linear Expansion.....	204
D.6 Effect of High and Low Temperatures on the Physical Properties	204
D.7 Effect of Rolling Temperature	204
D.8 Effect of Repeated Heating.....	205
D.9 Effect of Work upon Wrought Iron.....	205
D.10 Influence of Reduction in Rolling from Pile to Bar on the Strength of Wrought Iron.....	206
D.11 Effect of Overstrain and Cold Work.....	207

D.12 Fabrication.....	207
D.12.1 Forming	207
D.12.2 Threading and Machining.....	208
D.12.3 Forging.....	208
D.12.4 Bending.....	208
D.12.5 Welding	209
D.12.6 Protective Coatings	210
D.12.6.1 Adherence and Weight of Protective Coatings	211
D.12.7 Corrosion Resistance	212
D.13 Use of Wrought Iron.....	213
D.13.1 Forms Available	214
D.13.2 Applications	214
D.14 Wrought Iron versus Steel.....	215
D.14.1 Test for Distinguishing Wrought Iron from Steel	215
D.15 The Nick-Bend Test for Wrought Iron.....	216
D.16 Alloyed Wrought Iron.....	219
D.17 Average Properties of Wrought Iron from Various References.....	220
Appendix E.....	222
Analysis and Load Rating of Case Study Bridge	222
E.1 Truss Member Properties.....	222
E.2 Truss Member Axial Forces.....	222
E.3 Truss Member Capacities.....	224
E.4 Load Rating of the Truss.....	224
E.5 Timber Deck Member Properties.....	229
E.6 Forces in the Timber Deck Members.....	229
E.7 Capacity of the Timber Deck Members	230
E.8 Load Rating of the Timber Deck	231
E.9 Metal Floor Beam Properties	231

E.10 Forces on the metal floor beam.....	232
E.11 Capacity of the Metal Floor Beam.....	232
E.12 Load Rating of the Metal Floor Beam	233
E.13 Load Rating of the Bridge	234
Appendix F	235
Field Load Testing of Case Study Bridge	235
F.1 Strain Gage Layout for the First Test.....	235
F.2 Strain Gage Layout for the Second Field Load Test	242
F.3 Comparison of Field Load Test Data and Structural Analysis Results	246
References	296
Vita	305

List of Tables

Table 3.1:	Average test results for metal specimen.....	40
Table 4.1:	Summary of controlling load rating for the truss	60
Table 4.2:	Summary of controlling load rating for the floor beam (beam section under the wheel load)	61
Table 5.1:	Details of first load testing runs	66
Table 5.2:	Details of second load testing runs	66
Table.C.1:	Metal sample identification.....	174
Table.C.2:	Results of tension test	175
Table C.3:	Results of hardness measurements	175
Table C.4:	Chemical analysis	176
Table C.5:	In-situ hardness values measured on members of upstream truss ..	180
Table C.6:	In situ hardness values measured on members of downstream truss.....	181
Table D.1:	Typical chemical composition of wrought iron.....	186
Table D.2:	Distribution of impurities between the base metal and the slag.....	186
Table D.3:	Influence of chemical composition on the properties of wrought iron.....	190
Table D.4:	Order of qualities graded from no. 1 to No. 19	190
Table D.5:	Longitudinal and transverse tensile properties of wrought iron.....	197
Table D.6:	Average tensile properties of plain and alloyed wrought iron	199
Table D.7:	Physical properties of different varieties of wrought iron.....	200

Table D.8: ASTM Specifications for tensile properties of wrought iron.	
Longitudinal properties – minimum requirements.....	200
Table D.9: British standard specification of wrought iron.....	201
Table D.10: Impact strength of wrought iron.....	202
Table D.11: Effect of temperature on the physical properties of wrought iron. .	204
Table D.12: Effect of repeated heating.....	205
Table D.13: Physical properties of wrought iron plates from shear and universal mills	206
Table D.14: Effect of rolling on the tensile strength of wrought iron.....	206
Table D.15: Chemical composition of wrought iron specimen used for test series	217
Table D.16: Physical properties of wrought iron tested	217
Table D.17: Properties of wrought iron tested	218
Table D.18: Properties of Alloyed wrought iron.....	219
Table D.19: Chemical analysis o f wrought iron.....	220
Table D.20: Average properties of wrought iron.....	221
Table E.1: Truss member properties	223
Table E.2: Maximum member forces due to dead and live load	224
Table E.3: Truss member capacities in kips.....	225
Table E.4: Truss member “H” load rating	225
Table E.5: Truss member “HS” load rating	226
Table E.6: Timber stringer properties	229

Table E.7: Forces in the timber stringers due to live load of AASHTO H15 truck	230
Table E.8: Forces in the timber stringers due to dead load	230
Table E.9: The capacity of the timber stringers	231
Table E.10: The timber stringer load rating	231
Table E.11: Sectional properties of the metal floor beam.....	232
Table E.12: Forces in the floor beam.....	232
Table E.13: The bending capacity of the floor beam.....	233
Table E.14: The load rating of the floor beam.....	233

List of Figures

Figure 2.1: Side elevation of the bridge	14
Figure 2.2: Details of the timber bridge deck	15
Figure 2.3: Details of the timber approach deck	16
Figure 2.4: Details of the metal floor beam	17
Figure 2.5: Details of the truss	19
Figure 2.6: Details of the metal bent	20
Figure 2.7: Details of the stone masonry piers	21
Figure 2.8: Details of the metal railing	21
Figure 4.1: The simple 2-D model of the truss	47
Figure 4.2: The 3-D model of both the trusses	48
Figure 4.3: The 2-D model of bridge deck with spring supports	51
Figure 4.4: The 3-D model of the bridge deck	52
Figure 5.1: The details of the loading vehicle used for the first test	65
Figure 5.2: The details of the loading vehicle used for the second test	65
Figure 6.1: New timber deck layout with all timber stringers	98
Figure 6.2: New timber deck layout with the steel-timber composite stringers	98
Figure 6.3: New timber deck layout with W-shape stringers	98
Figure 6.4: Addition of member to tension chord	105
Figure 6.5: Connection details for the added member	105
Figure B.1: Overall view of case study bridge	150
Figure B.2: Details of the metal truss	151
Figure B.3: Cross-sections of the truss members	152

Figure B.4: Details of the top compression chord	153
Figure B.5: Details of the vertical members (L2U2, L3U3 and L4U4)	154
Figure B.6: Details of the hangers (L1U1 and L5U5).....	155
Figure B.7: Details of the bottom chord members (L0L1, L1L2, L2L3, L3L4, L4L5 and L5L6).....	156
Figure B.8: Details of the diagonal members (L2U1 & L4U5).....	157
Figure B.9: Details of the diagonal members (L3U2 & L3U4).....	158
Figure B.10: Details of the tension rods (L2U3 & L4U3).....	159
Figure B.11: Details of the timber bridge deck – Plan view	160
Figure B.12: Details of the cross-section of timber bridge deck	161
Figure B.13: Details of the metal floor beam	162
Figure B.14: Details of top lateral bracing	163
Figure B.15: Details of bottom lateral bracing	164
Figure B.16: Details of portal bracing and intermediate bracing	165
Figure B.17: Details of the south approach spans	166
Figure B.18: Details of the north approach spans	167
Figure B.19: Details of the timber deck of the approach spans	168
Figure B.20: Details of metal bent for approach spans	169
Figure B.21: Details of metal bent for approach spans	170
Figure B.22: Details of metal railing	171
Figure B.23: Details of the stone masonry piers.....	172
Figure C.1: Locations of photomicrographs	177
Figure D.1: Longitudinal section of wrought iron.....	192

Figure D.2: Transverse section of wrought iron.....	193
Figure F.1: Field load test No.1 – Locations of instrumented members	237
Figure F.2: Field load test No.1 – Gage identification for upstream truss	238
Figure F.3: Field load test No.1 – Gage identification for downstream truss...	239
Figure F.4: Field load test No.1 – Location of strain gage on member cross- sections	242
Figure F.5: Field load test No.2 – Location of strain gages.....	245

List of Illustrations

Graph 5.1:	Average stress: Bottom chord (L2L3)	73
Graph 5.2:	Stress variation: Top Chord (L0U1)	75
Graph 5.3:	Average stress: Top Chord (U2U3)	76
Graph 5.4:	Stress variation: Vertical Hanger (L1U1)	77
Graph 5.5:	Average stress: Diagonal member (L2U1)	78
Photograph A.1:	Case study bridge – looking towards south	123
Photograph A.2:	Side view of the south approach span	124
Photograph A.3:	Side view of the main truss span of the bridge	124
Photograph A.4:	Side view of the north approach span	125
Photograph A.5:	Details of the upstream truss	125
Photograph A.6:	Details of the downstream truss	126
Photograph A.7:	Details of the southwest roller support	127
Photograph A.8:	Details of the northwest hinge support	128
Photograph A.9:	Details at bottom chord joints L1 and L5	129
Photograph A.10:	Details at bottom chord joints L2, L3, and L4	130
Photograph A.11:	Connection details at bottom chord joint L1	131
Photograph A.12:	Connection details at bottom chord joint L1	131
Photograph A.13:	Details of tension rod L2U3 and L4U3, turnbuckle connection	132
Photograph A.14:	Details at upper chord joints U1 and U5	133
Photograph A.15:	Details at upper chord joints U2, U3, and U4	133
Photograph A.16:	Details of top bracing connection	134

Photograph A.17:	Details of bridge deck.....	134
Photograph A.18:	Details of bridge deck.....	135
Photograph A.19:	Details of the north stone masonry pier and the main span deck	136
Photograph A.20:	Details of the south stone masonry pier and the main span deck	137
Photograph A.21:	Details of the top lateral bracing system.....	138
Photograph A.22:	Details of the turnbuckle of the top bracing tension rods	138
Photograph A.23:	Details of metal railing	139
Photograph A.24:	Details of metal railing connection to truss member	139
Photograph A.25:	Details of the timber deck of the south approach span....	140
Photograph A.26:	Details of the metal bent of the south approach span.....	141
Photograph A.27:	Details of the timber deck of the north approach span....	142
Photograph A.28:	Details of the connection between timber stringers in the north approach span.....	143
Photograph A.29:	Details of the timber stringers of the main span resting on the south pier	143
Photograph A.30:	Details of the ground slope at the base of the south pier .	144
Photograph A.31:	Details of the metal wing wall at the north abutment.....	144
Photograph A.32:	Details at base of pipe column of metal bent for north approach span.....	145
Photograph A.33:	Details of base of pipe column of metal bent for north approach span.....	145

Photograph A.34:	Deteriorated foundation of metal bents for north approach span.....	146
Photograph A.35:	Deteriorated abutment at south end of south approach span.....	146
Photograph A.36:	Details of metal bent for north approach span.....	147
Photograph A.37:	Details of the metal retaining wall at the north abutment	147
Photograph A.38:	Details of the metal retaining wall at the north abutment	148
Photograph C.1:	Photomicrograph on surface “A”	177
Photograph C.2:	Photomicrograph on surface “B”	178
Photograph C.3:	Photomicrograph on surface “C”	179
Graph E.1:	Inventory “H” load rating of the truss	227
Graph E.2:	Operating “H” load rating of the truss.....	227
Graph E.3:	Inventory “HS” load rating of the truss	228
Graph E.4:	Operating “HS” load rating of the truss	228
Graph F.1:	Member L0L1 (Outside) of the upstream truss	247
Graph F.2:	Member L0L1 (Inside) of the upstream truss	247
Graph F.3:	Member L0L1 (Outside) of the downstream truss	248
Graph F.4:	Member L1L2 (Outside) of the upstream truss	248
Graph F.5:	Member L1L2 (Inside) of the upstream truss	249
Graph F.6:	Member L1L2 (Outside) of the downstream truss	249
Graph F.7:	Member L2L3 (outside) of the upstream truss.....	250
Graph F.8:	Member L2L3 (Inside) of the upstream truss	250
Graph F.9:	Member L2L3 (Outside) of the downstream truss	251

Graph F.10:	Member L3L4 (Outside) of the upstream truss	251
Graph F.11:	Member L3L4 (Inside) of the upstream truss	252
Graph F.12:	Member L4L5 (Outside) of the upstream truss	252
Graph F.13:	Member L5L6 (Outside) of the upstream truss	253
Graph F.14:	Member L5L6 (Inside) of the upstream truss	253
Graph F.15:	Member L0U1 of the upstream truss	254
Graph F.16:	Member L0U1 of the downstream truss	254
Graph F.17:	Member U1U2 of the upstream truss	255
Graph F.18:	Member U1U2 of the downstream truss	255
Graph F.19:	Member U2U3 of the upstream truss	256
Graph F.20:	Member U2U3 of the downstream truss	256
Graph F.21:	Member U2U3 of the upstream truss (Near U3 joint, Top).....	257
Graph F.22:	Member U2U3 of the upstream truss (Near U3 joint, Bottom)	257
Graph F.23:	Member U3U4 of the upstream truss	258
Graph F.24:	Member U4U5 of the upstream truss	258
Graph F.25:	Member L6U5 of the upstream truss	259
Graph F.26:	Member L1U1 of the upstream truss	259
Graph F.27:	Member L1U1 of the downstream truss	260
Graph F.28:	Member L2U2 of the upstream truss	260
Graph F.29:	Member L2U2 of the downstream truss	261
Graph F.30:	Member L3U3 of the upstream truss	261
Graph F.31:	Member L3U3 of the downstream truss	262
Graph F.32:	Member L4U4 of the upstream truss	262

Graph F.33:	Member L5U5 of the upstream truss	263
Graph F.34:	Member L2U1 of the upstream truss	263
Graph F.35:	Member L2U1 of the downstream truss	264
Graph F.36:	Member L2U3 of the upstream truss	264
Graph F.37:	Member L2U3 of the downstream truss	265
Graph F.38:	Member L4U3 of the upstream truss	265
Graph F.39:	Member L4U5 of the upstream truss	266
Graph F.40:	Member L3U2 of the upstream truss	266
Graph F.41:	Member L3U2 of the downstream truss	267
Graph F.42:	Member L3U4 of the upstream truss	267
Graph F.43:	Member mid-span section of the metal floor beam.....	268
Graph F.44:	Section at 23" away from the mid span of the metal floor beam	268
Graph F.45:	Bottom chord L2L3 (Inside).....	269
Graph F.46:	Bottom chord L2L3 (Outside).....	269
Graph F.47:	Bottom chord L2L3 (Outside).....	270
Graph F.48:	Bottom chord L1L2 (Outside).....	270
Graph F.49:	Bottom chord L1L2 (Outside).....	271
Graph F.50:	Top chord L0U1	271
Graph F.51:	Top chord L0U1	272
Graph F.52:	Top chord L0U1	272
Graph F.53:	Top chord L0U1	273
Graph F.54:	Top chord L0U1	273

Graph F.55:	Top chord U1U2	274
Graph F.56:	Top chord U1U2	274
Graph F.57:	Top chord U1U2	275
Graph F.58:	Top chord U1U2	275
Graph F.59:	Top chord U2U3	276
Graph F.60:	Top chord U2U3	276
Graph F.61:	Top chord U2U3	277
Graph F.62:	Top chord U2U3	277
Graph F.63:	Top chord U2U3	278
Graph F.64:	Vertical hanger L1U1	278
Graph F.65:	Vertical hanger L1U1	279
Graph F.66:	Vertical hanger L1U1	279
Graph F.67:	Vertical hanger L1U1	280
Graph F.68:	Vertical hanger L1U1	280
Graph F.69:	Vertical hanger L1U1	281
Graph F.70:	Vertical hanger L1U1	281
Graph F.71:	Vertical hanger L1U1	282
Graph F.72:	Vertical hanger L1U1	282
Graph F.73:	Diagonal member L2U1	283
Graph F.74:	Diagonal member L2U1	283
Graph F.75:	Diagonal member L2U1	284
Graph F.76:	Diagonal member L2U1	284
Graph F.77:	Diagonal member L3U2	285

Graph F.78:	Diagonal member L3U2	285
Graph F.79:	Diagonal member L3U2	286
Graph F.80:	Diagonal member L2U3	286
Graph F.81:	Diagonal member L2U3	287
Graph F.82:	Vertical member L2U2	287
Graph F.83:	Vertical member L2U2	288
Graph F.84:	Vertical member L2U2	288
Graph F.85:	Vertical member L2U2	289
Graph F.86:	Vertical member L2U2	289
Graph F.87:	Average stress: Bottom chord (L1L2)	290
Graph F.88:	Average stress: Bottom chord (L2L3)	290
Graph F.89:	Average stress: Top Chord (L0U1)	291
Graph F.90:	Average stress: Top Chord (U1U2).....	291
Graph F.91:	Average stress: Top Chord (U2U3).....	292
Graph F.92:	Average stress: Vertical hanger (L1U1).....	292
Graph F.93:	Average stress: Diagonal member (L2U1).....	293
Graph F.94:	Average stress: Diagonal member (L3U2).....	293
Graph F.95:	Average stress: Diagonal member (L2U3).....	294
Graph F.96:	Average stress: Vertical member (L2U2).....	294
Graph F.97:	Stress variation: Vertical Hanger (L1U1).....	295
Graph F.98:	Stress variation: Top Chord (L0U1).....	295

Chapter 1

Introduction

1.1 BACKGROUND

Nearly 40% of the nations' bridges are structurally and/or geometrically deficient [NCHRP #293, 1987]. Some of the deficient bridges are in service with speed and/or load restrictions and some are out of service. The reasons of closing a particular bridge are numerous including, for example, uncertainty in load carrying capacity, damage to bridge member/s due to accidents, excessive loss of the member cross-sectional area due to corrosion, inadequate geometrical clearances, foundation deficiencies, etc.

Options available for addressing the problems associated with a deficient bridge include both rehabilitation and replacement. Many issues are involved in the decision of whether to rehabilitate or to replace a deficient bridge. The decision becomes even more complex when the bridge in question is of historic interest. Engineering, social and political factors may all play a role when addressing such a bridge. When the decision is made to rehabilitate a bridge, further questions arise as to the most cost effective rehabilitation options that maintain the historical integrity of the bridge and that address the various engineering, social and political constraints.

One class of historic bridge that is frequently found to be either structurally or geometrically deficient is historic metal truss bridges.

Rehabilitation of historic metal truss bridges is the subject of this report. More specifically, this report examines some of the engineering issues involved with the rehabilitation of historic metal truss bridges. The work reported herein is part of a larger project conducted for the Texas Department of Transportation (TxDOT) entitled: “Preservation Alternatives for Historic Metal Truss Bridges.” The overall objective of this larger project was to develop information and tools to aid engineers and decision makers involved with historic metal truss bridges.

Historic metal truss bridges in Texas can be divided into two broad categories: “on-system” bridges and “off-system” bridges. On-system bridges are those on the state highway system, and are found on state highways, US highways, farm-to-market routes, ranch-to-market routes, interstate frontage roads, etc. The surviving on-system historic trusses were typically constructed in the 1920s and 1930s, and were designed by TxDOT, for H10 to H15 loads.

The “off-system” bridges are those not on the state highway system, and are typically found on county roads or city streets. Many of the off-system historic truss bridges in Texas were constructed in the late 1800’s or early 1900’s. These bridges were often designed and erected by private bridge companies. The off-system bridges are typically constructed of light steel, wrought iron or cast iron components and have timber decks. Many of the off-system trusses pre-date the automobile, and originally carried horse traffic and livestock.

1.2 PROJECT DESCRIPTION AND SCOPE OF REPORT

The research reported herein addresses off-system historic truss bridges in Texas. The focus of this research was a case study conducted on a specific off-

system bridge located in Shackelford County, Texas. This case study bridge is located on County Road 188, and crosses the Clear Fork of the Brazos River. The bridge was constructed in 1885 and is currently closed to traffic. Further description of the bridge is provided in Chapter 2.

The purpose of this case was to examine the procedures and diagnostic tools that may prove useful in evaluating an off-system historic truss bridge. The case study is intended to serve as a model for evaluating such a bridge. Work on this case study was divided into three major categories:

- collect data on the bridge and the materials used to construct the bridge;
- conduct a detailed structural evaluation of the bridge, including a structural analysis and field load testing;
- identify rehabilitation options for the bridge.

This report concentrates on the engineering aspects of historic truss evaluation. Preservation issues were addressed in other portions of this TxDOT project, and are not reported herein. The focus of this engineering evaluation was to establish the most realistic and accurate load rating possible for the bridge, identify deficiencies, and identify methods to correct deficiencies and improve the load rating, if needed. The scope of this work primarily covers evaluation of the truss and its supports. Evaluation of approach spans to the truss is not the primary focus of this project.

The following sections provide a brief introduction and overview of the major elements of this case study.

1.2.1 Data Collection and Material Evaluation

This task involved collecting all the relevant data about the bridge and the material used for its construction. Generally, the data required for load rating a bridge is available from construction drawings, specifications, and bridge records. This data may not be available for an old off-system bridge. In this case the required data need to be collected from other sources. This task demonstrates how to collect the required data for an old metal truss bridge. The data required for the load rating are geometry of the bridge, properties of material used for construction of the bridge and the current condition of the bridge. Due to unavailability of the required data for the case study bridge, field observation, field measurements, and material testing were carried out. A description of the data required and data collected is provided in Chapter 2. Methods available for in-situ material evaluation are discussed in Chapter 3. The complete material evaluation report for the case study bridge is included in Appendix C. Additional background information about wrought iron is provided in Appendix D.

1.2.2 Analysis and Load Rating of the Bridge

This task demonstrates the process of analysis and load rating. Different rating levels and load rating methods are described. The rating equation, calculation of nominal capacity and different loadings to be considered are also briefly described in this task. This task involved analysis of the bridge truss and the deck followed by the calculation of nominal capacity and load rating. Both the analyses for the truss and the deck were carried out in two phases: preliminary analysis and detailed analysis. The nominal capacities of the truss and the deck

were calculated based on material testing results and AASHTO manual (1994). The rating of the bridge was based on the analysis results and calculated nominal capacities. The ratings were based on allowable stress design and load factor design methods for both inventory and operating levels. Description of this task can be found in Chapter 4 and all calculations are included in Appendix E. To evaluate the accuracy of the mathematical models used for analyses, a field load test was carried out. The complete details of load testing are provided in Chapter 5 and in Appendix F.

1.2.3 Rehabilitation Options

This task involved looking at different rehabilitation options available for metal truss bridges. From analysis and load rating, the deficiencies in the bridge were identified. For each deficiency, various rehabilitation options were studied. In addition, other rehabilitation methods were also studied to present complete information available on bridge rehabilitation. This will aid TxDOT engineers working on similar bridges with different deficiencies than those encountered in the case study. Common structural deficiencies in off-system truss bridges are inadequate strength of bottom chords of the truss and the deck system. A number of rehabilitation methods are available for these types of deficiencies. Other deficiencies are damaged truss members, excessive corrosion, fatigue damage, welding of nonstructural components to fracture critical members, inadequate railing, and damaged bearings. Common methods of rehabilitation are reducing dead load, adding or modifying to members or supports, adding of external post-tensioning, increasing bridge stiffness, providing continuity, providing composite

action, modifying the load path, and increasing redundancy. Fatigue damaged members and impact damaged members require special techniques for rehabilitation. The rehabilitation options should be economical, easy to construct, durable, maintainable, replaceable and consistent with historic preservation principles. The complete details of this segment of the research work are described in Chapter 6.

1.5 SCOPE OF EVALUATION

The objective of this report is to demonstrate an evaluation of load rating for the main truss span, based on metal truss and deck capacities, of the case study bridge. For rehabilitation of similar bridges, other structural issues related to foundations, approach spans, railing, etc. should also be addressed.

Chapter 2

Data Collection

2.1 INTRODUCTION

This chapter deals with the information that should be available to for bridge condition assessment and load rating. The information should be complete, accurate and up to date. The main objective of collecting the information is to determine the complete history of the bridge including damage to the bridge and all strengthening and repairs made to the bridge. The information collected will aid to better understand the bridge condition and to carry out a realistic analysis and load rating of the bridge based on current condition. All the required information may not be available for a historic truss bridge. In this case, the required data or information has to be collected by carefully inspecting the bridge.

Bridge owners should maintain a complete, accurate and current record of each bridge under their jurisdiction. As per AASHTO manual, [AASHTO, 1994], information about a bridge may be subdivided into three categories: base data which are normally not subject to change, data which are updated by field inspection, and data which are derived from the base and inspection data.

In the case of an off-system historic truss bridge, the owner may be a county or city government, or some other local jurisdiction. Thus, bridge records may be available, for example, in a county courthouse, in city government offices, etc. Local historical societies, museums, community groups, etc. may also be a

source of information. However, finding useful records for very old bridges, particularly pertaining to the original construction, may be difficult or impossible in many cases. In such a case, careful field observation and measurement of the bridge will serve as the primary source of data needed for an engineering assessment of the bridge. Although TxDOT is not the owner of off-system bridges, TxDOT typically inspects these bridges through the BRINSAP program. Consequently, recent inspection records should be available from BRINSAP.

Section 2.2 provides a general discussion of the type of information and data that should be collected for a thorough engineering assessment of an off-system historic truss bridge. Section 2.3 provides a summary of the data collected for the case study bridge in Shackelford County, Texas.

2.2 COMPONENTS OF BRIDGE RECORDS

A detailed discussion of the items that should be included in a complete bridge record is presented in “Manual for Condition Evaluation of Bridges” [AASHTO, 1994]. Following is a summary list of the discussion given in the AASHTO guidelines:

- original construction drawings;
- shop drawings;
- as-built drawings;
- technical specifications used for bridge construction;
- photographs of the overall bridge as well as of key features or details;
- copies of construction logs and other pertinent correspondence related to the design or construction of the bridge;

- material certifications such as: certified mill test reports for steel, concrete delivery slips, manufacturers certifications, etc.
- material test data such as results of concrete compressive strength tests, independent steel tension coupon tests, etc.
- reports from field load tests, if any;
- records of any major maintenance or repairs done on the bridge since original construction;
- records of coatings applied to the bridge;
- records of damage to the bridge due to accidents and any subsequent repairs;
- records of load rating calculations and any resultant load postings on the bridge;
- records of major flood events and scour activity for bridge over waterways;
- traffic data showing the frequency and type of vehicles using the bridge, including ADT (average daily traffic) and ADTT (average daily truck traffic);
- inspection and load rating reports for the bridge;
- bridge inventory data such as geometrical details and general information about the bridge;
- bridge inspection data describing current physical condition of the bridge as well as waterway, if any;

- bridge load rating data evaluated based on inventory and current inspection data.

As noted earlier, it will generally not be possible to collect all of this information for most bridges, particularly in the case of an off-system historic metal truss bridge. Nonetheless, making an effort to collect as much of this data as possible will contribute to the best possible engineering assessment of a bridge.

2.3 CASE STUDY

This section describes the information collected by the author for the Shackelford County case study Bridge. Being an old bridge, only very limited information was available about the bridge. To collect the required data, a thorough field examination of the bridge was conducted. This examination included measuring all the dimensions of the bridge components and member sections and conducting a detailed inspection of the bridge. From the measured dimensions, drawings were prepared. Photographs were taken to document important details and damage. In the following sections, the bridge history, bridge description, and field observations are described.

2.3.1 Bridge History

Historic details of the case study bridge were collected from several references. The main source was a report prepared by the Historic American Engineering Record, [HAER, 1996]. The other source was a file record of the bridge available from the Texas Department of Transportation, [TxDOT]. In addition, an inspection and load rating report prepared by ARS Engineers, Inc. in 1996 was available from TxDOT. A few bridge catalogs of King Iron and Bridge

Manufacturing Company were available from an Austin based structural consulting firm. The details available from these catalogs, however, were different than those found in the case study bridge.

The bridge selected for this case study is located in the Shackelford County, Texas. The bridge is spanning the Clear Fork of the Brazos River on County Road (CR) 188, Shackelford County, Texas. This bridge is referred as the “Fort Griffin Iron Truss Bridge” in the Historic American Engineering Record [HAER, 1996]. The bridge was constructed in 1885 by King Iron and Bridge Manufacturing Company located in Cleveland, Ohio. The company was responsible for design, fabrication and construction of the bridge. The metal for the fabrication of the bridge was supplied by Phoenix Iron Company. The bridge is presently owned by Shackelford County. No vehicular traffic is currently allowed on the bridge. Overall view of the case study bridge is presented in Figure 2.1.

The bridge has historic significance being the oldest surviving bridge in Shackelford County. The bridge was built to accommodate traffic between Albany-Fort Griffin-Throckmorton. Fort Griffin was formerly a military checkpoint and a cattle town. Hence, the bridge was an important crossing at that time. This is the last surviving bridge constructed using pin-connected Pratt through-trusses in Shackelford County.

2.3.2 Bridge Description

The bridge consists of the main truss span, the south approach and the north approach as shown in Figure 2.1. The main components of the bridge are

the floor system, floor-supporting system, substructure and railing. Each of the components is described in the following paragraphs. Photographs and prepared drawings are presented in Appendix A and Appendix B respectively.

2.3.2.1 Flooring System

The flooring system throughout consists of timber planks placed 350mm (14") center-to-center with a gap of 70mm (2¾") between adjacent planks. The planks are 290mm x 90mm thick (11½" x 3½") in cross section and 4.2m (168") long. These timber planks are supported on timber stringers. For the main truss span, there are two 200mm x 400mm deep (8"x16") timber stringers and five 75mm x 300mm deep (3"x12") timber stringers. For both approaches, there are four 200mm x 400mm deep (8"x16") timber interior stringers, and two external metal channel sections. The flooring system of both the main span and approach spans are as shown in Figure 2.2 and Figure 2.3.

2.3.2.2 Floor Supporting System

The floor supporting system for the main truss span consists of metal floor-beams and two trusses. The supporting system for both approaches consist of metal bents with latticed bracing.

2.3.2.2.1 Main Truss Span

The floor-beams are built-up sections from metal plate used for the web and two angles used at top and bottom flanges. The flange angles are connected to the web plate with rivets. These floor-beams are non-prismatic i.e. they are tapered along their span with maximum depth at mid-span and minimum depth at both ends. These floor-beams are connected to the truss lower joints with a U-bar

and a plate or with a plate (at hangers). The details of the metal floor beam is shown in Figure 2.4.

The truss is a pin-connected Pratt through truss. The truss is second-degree indeterminate. It is supported on roller supports at the south end and on hinge supports at the north end. The bottom tension chord is made up of two rectangular eyebars. The top compression chord is continuous and is a built-up section with two channels sections back-to-back connected with a cover plate on the topside and battens at 1050mm (42") center-to-center on the bottom. All remaining tension members are made up of either round eyebars or two rectangular eyebars of smaller cross-section than the bottom tension chord member cross-section. All remaining compression members are built-up sections from two channel sections back-to-back connected with lacing on both sides. There is a bottom horizontal bracing system and a top horizontal bracing system to provide lateral stability to the trusses. The bottom horizontal bracing system consists of crossed round eyebars connected at each end of the floor-beams. The top horizontal bracing system consists of crossed round eyebars connected to each joint of the truss and built-up members connected straight joint to joint. The two end built-up members are rigidly connected to the inclined part of the compression chord. The details of the truss are shown in the Figure 2.5. Other details of truss are documented in the Appendix A and Appendix B.

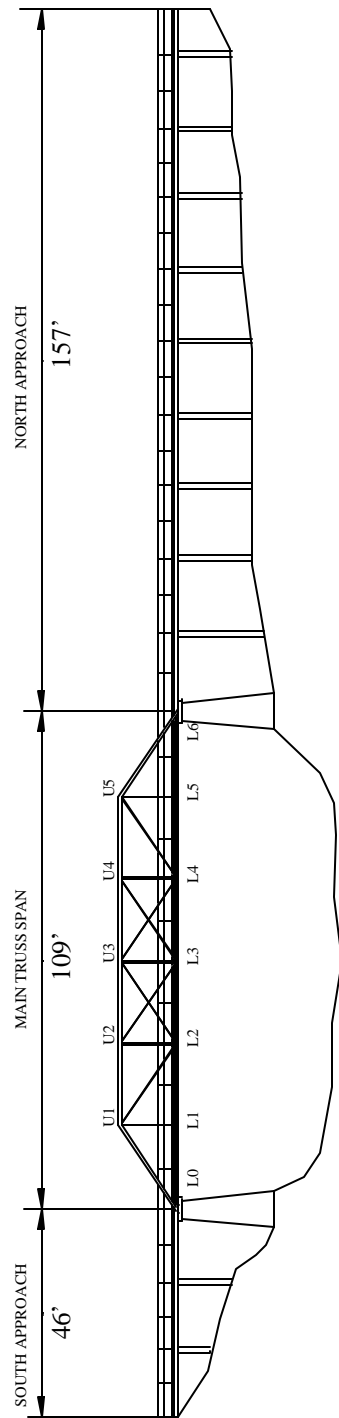


Figure 2.1: Side elevation of the bridge

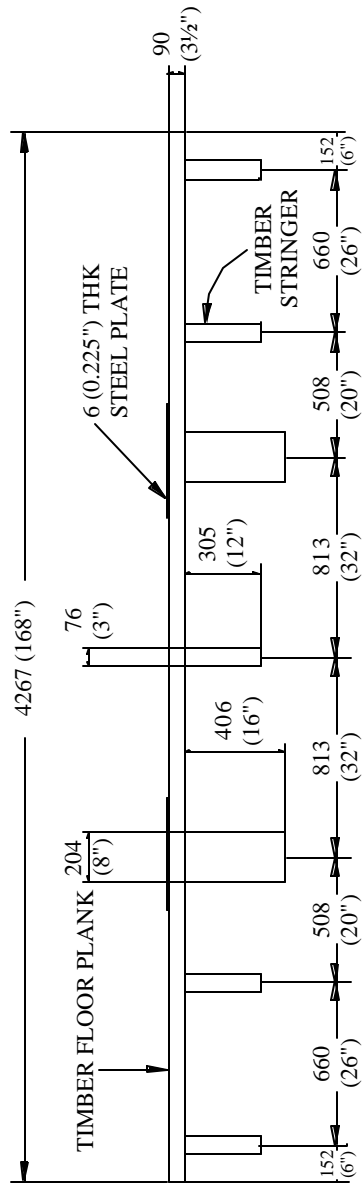


Figure 2.2: Details of the timber bridge deck

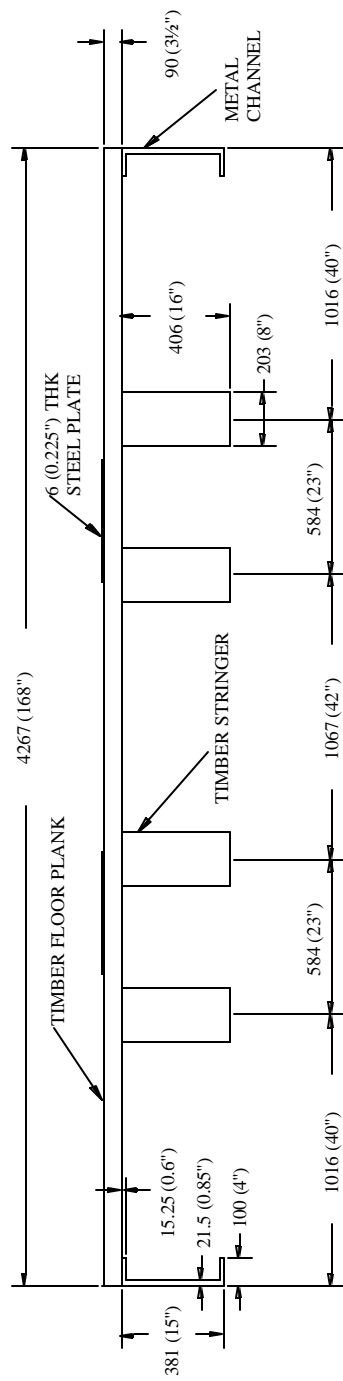


Figure 2.3: Details of the timber approach deck

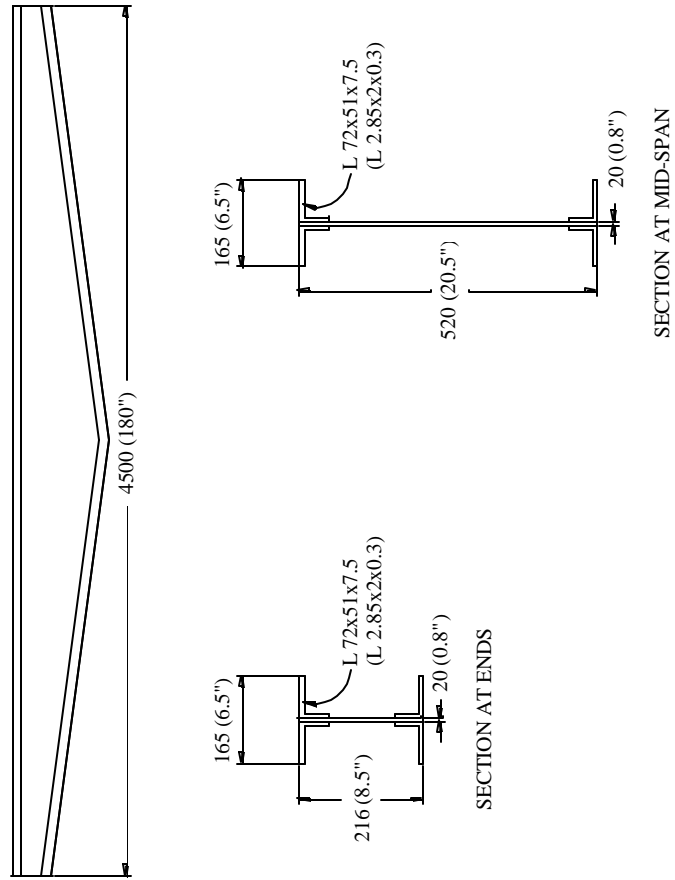


Figure 2.4: Details of the metal floor beam

2.3.2.2.2 South and North Approaches

The floor supporting system for the approach spans consist of built-up metal bents with latticed bracing. The top members of the bents are built-up sections with two angles and two rail sections. The vertical members of the bents are built-up sections with two angles and two pipe sections. The lattice bracing is made from angle sections. The details of metal bent are shown in Figure 2.6.

2.3.2.3 Substructure

The substructure for the main truss span consists of masonry piers at each end. Both roller and hinge supports are directly supported on top of these piers. These piers also support timber stringers of the end truss panels and the approach panels. Foundations for metal bents are shallow masonry type foundations. This was determined based on a few exposed foundations. The abutment of the south approach span is made up of stone masonry without any retaining and wing walls. The abutment of the north approach span is made up of metal plates with retaining wall and wing walls. The details of the masonry piers are shown in the Figure 2.7.

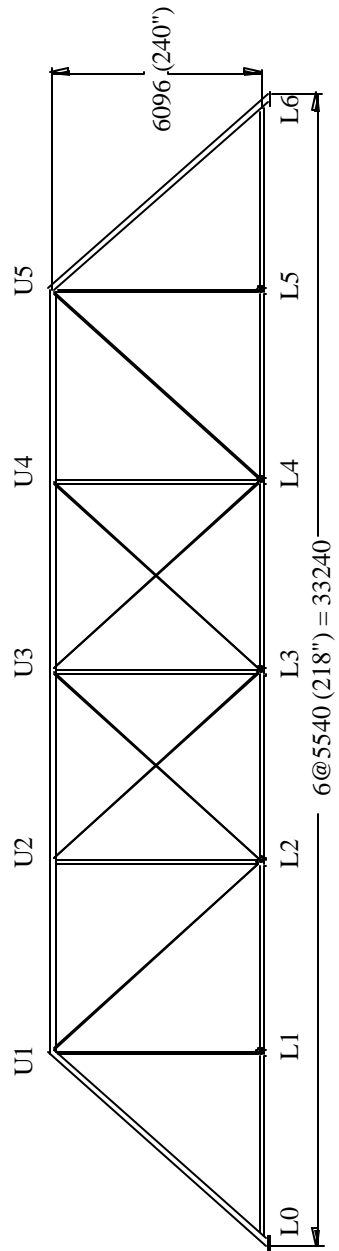


Figure 2.5: Details of the truss

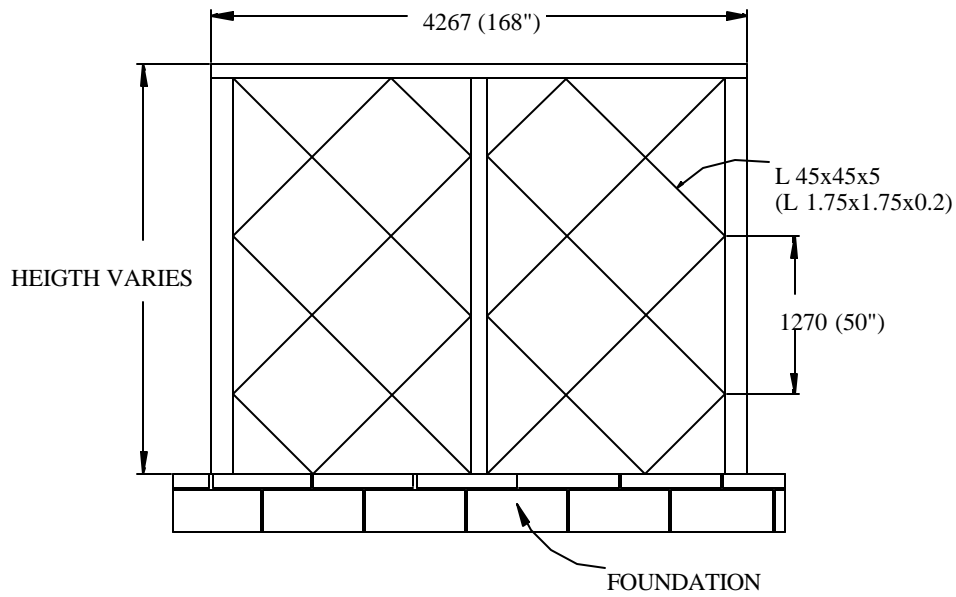


Figure 2.6: Details of the metal bent

2.3.2.4 Railing

The railing runs from the start of the south approach spans to the end of the north approach spans. It is made up of two horizontal metal pipes connected either to vertical truss members or to vertical angle posts. The angle posts are connected to the timber floor planks by horizontal pieces of metal angle. The details of metal railing are as shown in the Figure 2.8.

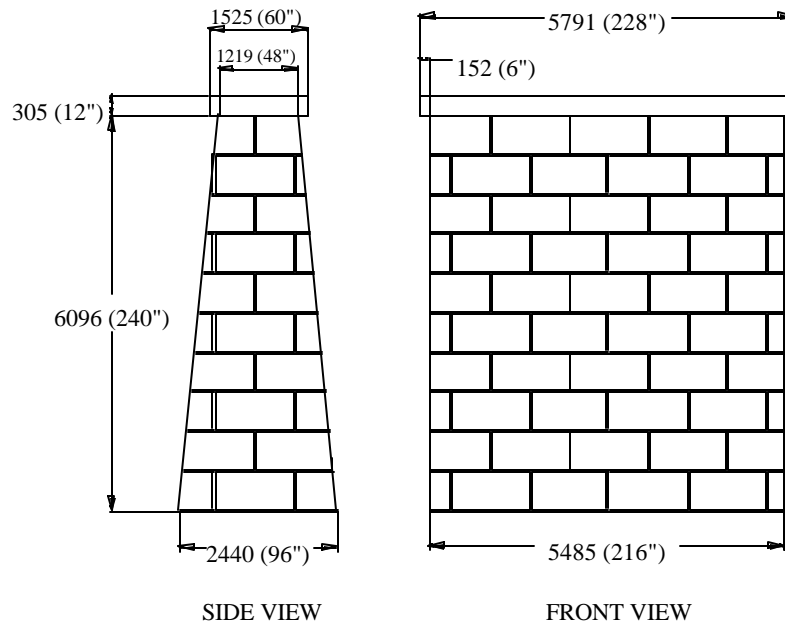


Figure 2.7: Details of the stone masonry piers

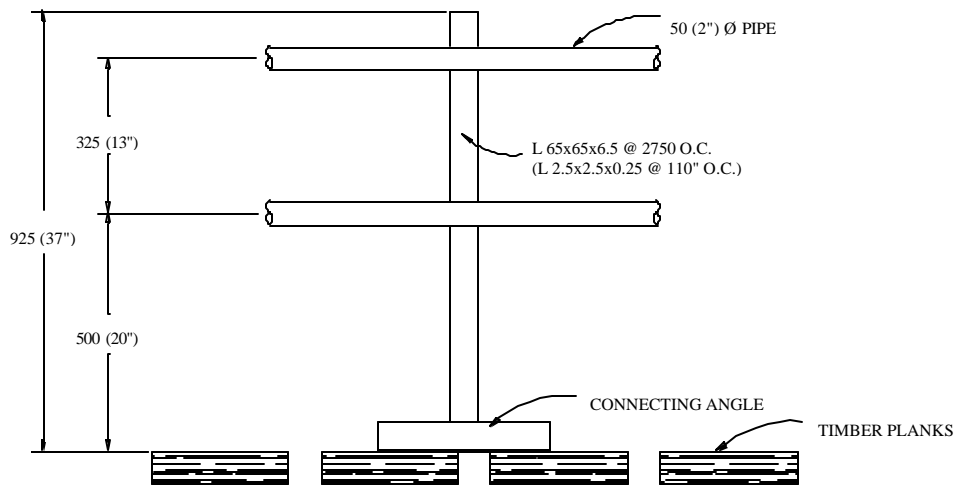


Figure 2.8: Details of the metal railing

2.3.3 Field Observations

This section is based on the observations made by Dilip R. Maniar and Karim Zulfiqar during a site visit to the bridge on August 21 and 22, 1998. Drawings were prepared based on the measured dimensions. Photographs were taken and are documented with notes. The complete sets of photographs and drawings are presented in the Appendix A and Appendix B respectively.

2.3.3.1 Flooring System

Timber planks and timber stringers are deteriorated and are not in good condition. It appears that old timber stringers were replaced with the new ones several years ago. These old timber stringers are still in position but no floor planks are connected to them. The metal channel floor beams located on each side of each approach are made up of several channels that are butt-welded. At the time of construction of this bridge there was no welding available. Therefore, these channels were apparently installed afterwards.

2.3.3.2 Floor Supporting System

Main Truss Span

Metal floor-beams are somewhat corroded, but do not appear to have suffered significant loss of cross section. All truss members are corroded. The section loss is not severe as the amount of corrosion is minor. No large displacements, distress or damage was found on truss members except at one hanger. This tension hanger has a kink at the middle. All joints appear in good condition except the southwest roller support. This roller support is dislocated from its original position.

South and North Approach Spans

All members of the metal bents are corroded. The pipe sections are welded to the angle sections. Therefore, these pipes were apparently added after initial construction of the bridge. These pipes are not connected to the horizontal built-up members of the bents. The pipes are directly supporting the edge channels which are supporting the deck timber planks. The connection of the bents to their foundations is not visible due to soil deposits. There is one horizontal tie rod at the top of the foundation level connecting the bottom of all three legs of the bents. At several places, the pipe sections are not bearing on the foundation.

2.3.3.3 Substructure

Main Truss Span Piers

Masonry joints are deteriorated at many places. Scouring near the foundation has made the slope of the ground very steep. Stones from the pier have come out at several places, especially near top of the north pier.

South and North Approaches

Foundations for metal bents are not visible at many places. At one bent of the north approach, the foundation is visible as it is projecting above the ground. The masonry joints of this foundation are open. This suggests the possibility that the foundations of all bents may have open joints. The south approach span abutment has many stones dislocated from their original position. All the joints of the abutment are filled with soil. The north approach abutment is not visible due to the metal retaining plate.

2.3.3.4 Miscellaneous Items

Railing

All the parts of railing are corroded. The railing-posts are not connected to the bridge deck i.e. to the timber floor planks at many places.

Lateral Bracing

All the members comprising of lateral load resisting system are corroded. No other distress or damage was found to any member of the bracing system.

Metal Retaining wall at the North Approach

This metal retaining wall is heavily corroded. Looking at the plate, it appears that it was not an original part of the bridge but was added afterwards. This plate seems to be taken out from another structure and then added to the bridge.

Chapter 3

Material Evaluation

3.1 INTRODUCTION

Information on the type, grade and properties of material used for relatively new bridges may be obtained from the construction drawings, specifications, and bridge records. This may not be the case with older bridges. In this case, it is necessary to evaluate the material properties before doing analysis and load rating of the bridge. A variety of techniques, tests and methods are available to assess material properties. The final choice of method to be used will depend on the type of material being evaluated, the desired properties, the desired level of reliability in the measured properties, availability of equipment, availability of experienced technicians, and cost.

This chapter describes the need of material evaluation and various methods available for material evaluation both in the laboratory and in the field. At the end of this chapter, material evaluations conducted for the case study bridge are described. Detailed material test results for the case study bridge are provided in Appendix C. Appendix D provides a general discussion on the characteristics of wrought iron, a common material used in off-system historic metal truss bridges, and the material used for the case study bridge.

3.2 NEED FOR MATERIAL EVALUATION

A thorough understanding of the materials used in an older bridge is a key element in developing a realistic load rating for the bridge. Material properties of interest in bridge evaluation include yield strength, ultimate strength, ductility, fracture toughness, modulus of elasticity, weldability and other. In addition to these, identifying the chemical composition and microstructure of the material may be of additional help to better understand the material.

For evaluation of older bridges, AASHTO manual, [AASHTO, 1994], specifies the yield stress of metal to be used for load rating depending on the year of construction of the bridge. These values may be used for preliminary analysis and for load rating. However, these values of yield stress may be quite conservative in some cases. Measuring the actual yield stress of the metals used in the bridge may show a higher value than those specified by AASHTO, and can help increase in load rating of the bridge. Proper material evaluation will also help in identifying any defects or flaws in the material. For older bridges, it is very important to know the presence of cracks or other defects in the members, especially for fracture critical members. Material evaluation will also help identify any changes in the bridge material, such as replacement of some member/s or addition of certain components of the bridge as a part of a prior repair or rehabilitation program.

Various testing methods, both in field and laboratory, are available to assess properties of different materials. In the following sections, several field test methods available for metal, timber and masonry are described. Typical

laboratory methods for metal and wood are well known and hence are not described. However, a brief discussion of laboratory test methods for masonry is included.

3.3 METALS

The evaluation of a metal must identify the type of metal as well as its mechanical properties and condition. For identification of the metal, metal sorting or chemical composition tests can be used to establish if the metal is steel, wrought iron, cast iron, or some other metal. There are various methods available which can give an estimate of mechanical properties of the metal. To evaluate the condition of the metal, visual observation and defect determination tests can be conducted.

3.3.1 Metal Identification Tests

Several methods are available to identify the metal without determining its chemical composition. These methods are fast and simple, and are useful for qualitative judgments.

The following methods can be used for metal identification:

- Ultrasonic;
- Electromagnetic methods;
- Spark testing; and
- Chemical testing.

Ultrasonic testing can be used to identify cast iron by the velocity of longitudinal waves. Ultrasonic testing cannot be used to determine the type of steel because the velocity of sonic waves through different types of steel lies very

near to each other. Metal identification can often be done by using electromagnetic methods, especially using the eddy current method. This is because of the influence of the alloying element on the electrical conductivity and magnetic permeability. Both of these influencing parameters are imaged in the impedance of an eddy current coil. The tests can be carried out using different frequencies. The choice of frequency is based on trials to separate the different classes of metal as far as possible from each other.

Spark testing depends on the oxidation of the heated particles removed from the metal with a high-speed grinding wheel. The test requires considerable personal skill and judgment. The test can be used for separation of high-carbon steel from iron and low-carbon steel.

Chemical nondestructive testing is a well-established technology for identifying materials. Three primary techniques: chemical spot testing, testing with ion-selective electrodes, and thin-layer chromatography, are available. There are several metal and alloy identification kits commercially available to do chemical spot testing. These kits are developed such that nonchemists in the metal working industries can use them. These kits have an advantage of immediate usefulness for the identification of industrial metals and alloys with simplified instructions.

For detailed discussion of the tests available for metal identification, the reader is referred to the nondestructive testing references, Goebbels, K., (1994), and Bray and McBride, (1992).

3.3.1.1 Wrought Iron Identification in Field

Depending on the age of the bridge, information in the literature is available on average properties of the material. In the United States, manufacturing of steel started somewhere around 1890. Hence, if the structure was built before 1890, then the metal may be either cast iron or wrought iron. The ability to cut out a corner of metal with the help of sharp knife without much effort suggests that the metal is wrought iron. In this case, detailed visual inspection may assist in the accurate identification of wrought iron. For detailed inspection, the metal surface has to be prepared. Grinding, sanding, and acid etching can be used to prepare the metal surface. After preparation, a magnifying glass can be used for inspection. If the metal is wrought iron, then laminations and inclusions of slag will be clearly visible. For further verification, an acid etch test can be performed in the laboratory on a sample of metal removed from the bridge. Further background information on wrought iron is provided in Appendix D.

3.3.2 Chemical Composition

For more detailed examination of the metal, chemical composition tests can be used. This will assist in exact identification of metal and to evaluate its quality. Several methods based on optical spectrometry and X-ray radiation are available to determine chemical composition in field. For further information on the tests, refer to Goebbels, K., (1994).

The methods based on optical spectroscopy require removal of a small material volume. As the quantity of the metal sample is very small, the accuracy of spectroscopy will depend on the purity of the collected sample. To get a

chemical composition that is representative of the actual metal, the collected sample should be free of any contamination. The main source of contamination of a collected metal sample is the method used for the collection of the sample. If the surface of metal is corroded, then the collected sample will be contaminated with oxides of metal elements. In this case, it is necessary to prepare the surface carefully. The method used for preparation of the surface may be a source of contamination. For example, the deposit of carbides from a grinder or from sandpaper will be collected along with the metal sample. Files used for preparation of surface will also contaminate the sample with its particles. Both the carbide and/or file particle content in the collected sample will change the results of spectroscopy. Hence, it is very important to prepare the surface carefully while using spectroscopy. The spectroscopy methods based on laser technique will allow collection of a metal sample without any contamination.

Analysis time for spectroscopy is about 30 seconds. The elements C, Si, Mn, P, S, Al, Cr, Cu, Mo, Nb, Ni, Ti, V, and Fe are analyzed simultaneously with the same accuracy and reproducibility as with the stationary equipment. Other mobile spectrometers burn the material at the surface and transport the light via glass fiber bundles to the spectrometer. A disadvantage of this technique is that the glass fibers cannot transport the whole spectrum, especially the low wavelength carbon lines.

Mobile X-ray fluorescence analysis system is available for non-destructive analysis for chemical composition. More than twenty elements can be identified within 30-seconds time. More elements can be identified by using longer

measurement time. Shorter identification time is generally used for identification of the metal.

3.3.3 Microstructure

Metallography is a standard technique for developing an image of a metal's microstructure. The properties of a material are a direct consequence of the microstructural features of the material. Grinding, polishing, and etching allow a detailed view of the material's composition under a microscope with more than 1000 times magnification. Grain size, grain shape, grain boundaries, inclusions, and segregates/precipitates are some of the parameters that can be studied with high resolution.

On-site metallography is comparable to conventional metallography with a need for grinding, polishing, and etching of the surface. The technique is sufficiently developed so that magnifications up to 10,000 times can be used. On-site metallography can be used to detect microstructure damage due to fatigue, creep, and incorrect heat treatment, prior to development of macrostructure damage. Microstructure Determination is discussed by Goebbels, K., (1994), Bray and McBride, (1992), and Kehl, G.L., (1949).

3.3.4 Macrostructure

Parameters which describe the macrostructure of a metal are homogeneity of the microstructure over the thickness and the lateral extension of a sample, texture for direction dependant behavior, and residual stresses. Density is an important property in considering macroscopic behavior.

Density measurements are useful, primarily, for describing the soundness of a material. Local density variations are indicative of an inhomogeneous material. Density correlates directly to nondestructive test measuring parameters such as velocity, sound impedance, and reflection coefficient of ultrasonic waves and x-ray absorption coefficient. By using appropriate measuring techniques, local densities can be obtained with satisfactory resolution. For density, homogeneity and texture determination of a metal sample, tests based on ultrasonic, x-ray, or Gamma-rays can be used.

3.3.5 Hardness Testing

Hardness testing is a descriptive term for a number of methods for the measurement of the resistance of a metal surface to the action of a body which is forced into it under pressure or by means of an impact. Care must be taken before conducting any hardness test on an unknown metal, especially when the metal is likely to be cast iron. Cast iron is very brittle, and the indentation created by hardness test may initiate a fracture in an otherwise sound member. Care must also be exercised when conducting field hardness tests in regions with cold temperatures as brittleness of cast iron increases as temperature goes down. Hence, it is important to identify the metal before doing a hardness test. If is the metal is wrought iron, then the hardness test will not harm the member.

The hardness of a metal can be determined using cutting hardness, abrasive hardness, tensile hardness, rebound hardness, indentation hardness, or deformation hardness. The hardness values measured will depend upon mechanical properties, homogeneity, and surface finish of the metal sample.

Furthermore, the geometry of the test body, the force of the test body and the velocity during the application of pressure or impact as well as the loading time will all affect the result. Hardness tests are often conducted to obtain an estimate of a metal's tensile strength. Correlation between hardness and tensile strength is possible because hardness is related to plastic deformation of metals. For a ductile material, hardness increases with yield and tensile strength and reduces with plasticity and ductility.

Portable Brinell hardness testing instruments are available. This instrument is calibrated to give equivalent results to those of a standard Brinell machine on a comparison test bar of approximately the same hardness as the material to be tested. For detail requirement of the portable test are available from the latest version of Test Method E 110 of ASTM Standards. Boving, K.G., (1989) discusses hardness test in more detail.

3.3.6 Detection of Defects

The most common methods used for defect detection in metal are X-ray radiography, magnetic particle test, eddy current test, dye penetration test and ultrasonic test. Other test methods are also available to estimate material degradation, plastic deformation and fatigue of metals. For a thorough discussion on these methods, refer to AASHTO "Manual for condition evaluation of bridge", [AASHTO, 1994].

Apart from the above methods, other devices are available for detecting cracks. These are the acoustic crack detector and magnetic crack definer. Both instruments are portable, fully contained devices, battery operated, and

commercially available. The acoustic crack detector is a survey device based on ultrasonic pulse echo techniques; the magnetic crack definer is a device based on magnetic field disturbance techniques. Both the devices can be used for determination of precise location and length of the crack.

3.4 STRUCTURAL TIMBER

The evaluation of wood structural members must identify the characteristics of the wood's strengths, such as density, knots, and moisture content, that define its structural performance.

Grade markings stamped on the lumber at the mill are valuable aids in evaluating structural members. These can be related to a recommended design value by reference to the National Design Specification for Wood Construction or other relevant documents. They determine the quality and strength properties of the timber. The difficulty is finding them. If grade marks are not discernible it may be necessary to engage a wood evaluator experienced in identifying and grading wood products.

It is necessary to determine the species of wood before starting to estimate unit weight, tensile, compressive, and shear strengths, or its moduli. Unit weight among softwoods can range from about 20 pcf to over 37 pcf depending on species and on moisture content. Even more variable is the range of some mechanical properties; for example, allowable fiber stresses in bending can range from 225 psi to almost 3500 psi depending upon species, moisture content, and grade. Even the modulus of elasticity can range from 600,000 psi to 2,000,000 psi. Within species, the variation of modulus of elasticity exceeds 20% for clear-

cut specimens. The in-place moisture content can vary within a given member. Grain pattern and knots can be extremely irregular and significantly affect the strength of individual members, although the impact of local irregularities on the strength of an assembly can be mitigated by their randomness.

Among the major construction materials, wood represents the most complex behavior. Biodegradability, directional properties, inelastic behavior, inherent variability, fibrous composition, porosity, combustibility, hygroscopicity, and inhomogeneity represent additional factors which need to be considered when developing nondestructive evaluation procedures for engineered structures built of wood or wood composites.

Several methods and instruments are available to estimate extent of decay, moisture content, and mechanical properties of a wood structural member in the field, such as manual inspection and probing, visual stress grading, various moisture meters, ultrasonic and radiography. A detailed discussion on various methods is presented in Wilson, F., (1984). The nondestructive methods presented in this handbook are useful for determination of extent of decay, moisture content, mechanical strength, modulus of elasticity, density, presence of defects, flaws and internal discontinuities of a wood structural member.

3.5 MASONRY

Masonry usually fails because of water intrusion through cracks, mortar joints, surface absorption and capillary action. Another cause of masonry failure is tension. If unreinforced, masonry performs poorly in tension. Supporting piers for historic metal truss bridge are sometime constructed of masonry.

Consequently, it is important to know how to evaluate the condition of the masonry and to determine whether it is capable of supporting the loads imposed by vehicular traffic. This evaluation will help to determine the response of the masonry to the applied loads and to define retrofit procedures, if needed. The fundamental purpose of structural assessment is to confirm that masonry is structurally safe for its existing or proposed use. The evaluation of the condition of masonry materials is not an exact science. It involves engineering judgment and an understanding of when physical and chemical tests; visual inspection or calculations are needed. The specific elements of an assessment include examination of written documentation; on-site survey; laboratory and field-testing; structural analysis; and load testing. The extent of investigation in each test may vary, based on the specific purpose of the assessment.

Several nondestructive evaluation methods have been used with various degree of success to determine the physical properties of the masonry unit and mortar. However, these methods have limited application and generally provide information only on the physical make-up of the masonry (continuity, locations of voids, reinforcement, etc.). Low frequency ultrasonics can provide an estimate of compressive strength by an experienced operator and evaluator, but it is prohibitively expensive to use in routine investigations. Determination of masonry material properties by destructive tests of specimens removed from the structure is often unsatisfactory because of the difficulty of handling such specimens without damaging them, the difficulty of obtaining such specimens with suitable geometrical accuracy for testing, and the limited number of such specimens which

may realistically be taken from a given structure without causing unacceptable damage.

In contrast to the limited choice and limited reliability of nondestructive methods for evaluating in-situ strength properties of masonry, there are a larger number of more developed destructive test methods available for this purpose, which require testing other than in-situ. Depending on the user's need for information, the practicality of performing these tests, funding availability, etc., these may be particularly applicable in rehabilitation projects. Nondestructive evaluation of masonry, perhaps combined with a limited number of destructive tests for calibration purposes, potentially is a method for relatively rapid and more comprehensive material evaluation. The selection of nondestructive evaluation methods for assessing the condition of masonry should be based on consideration of the important physiochemical and engineering properties which need to be measured.

A comprehensive discussion on available laboratory and in-situ test methods for masonry assemblages (units and mortar) and masonry is presented in Wilson, F., (1984). The test methods presented in this handbook are useful for determination of strength and durability properties, such as compressive, tensile and shear strength, permeability and water absorption, resistance to environmental changes, and structural soundness of masonry assemblages and masonry. The nondestructive test methods presented are ultrasonic tests, gamma radiography, flatjack test, Schmidt rebound hammer test, and in-place bedjoint shear test.

Additional discussion on test methods for masonry is presented by Fattal, S.G., (1975), Clifton, J.R., (1985), and Kingsley, G.R., (1988).

3.6 METAL EVALUATION FOR CASE STUDY BRIDGE

This section describes methods used for identifying and evaluating the metal of the case study bridge in Shackelford County, Texas. For a thorough understanding of this metal, it was decided to conduct both laboratory and in-situ tests. Laboratory testing involved identification of the locations from where the materials could be removed without hampering the strength or aesthetics of the bridge, removal of the materials and testing. The in-situ testing consisted of selecting the type of tests to be performed and selection of test locations. The main objectives of the material testing were to identify the material of construction and its mechanical properties. Each of these tasks is described in the following sections. Both the laboratory and in-situ testing results are documented in Appendix C.

3.6.1 Laboratory Testing

3.6.1.1 Selection of Location for Material Removal

The location of material removal should be selected in such way that the removal of material will not adversely affect the strength of the part of the bridge from which the material is removed, nor the strength of the overall bridge. While selecting the location, the aesthetics of the bridge should also be kept in mind. The selection of the location should be based on the properties to be determined. As far as possible the material should be removed from the members or parts, which are critical, or need to be rehabilitated.

Prior to choosing material sampling locations, a detailed structural analysis should be done. The analyses will determine the critical members as well as the least stressed members of the bridge. In the case study, it was found that the lower tension chord members were the critical members with respect to the load rating. The ideal location of material removal should be these members. However, since these members were eyebars, removal of any material may have adversely affected their strength. Structural analysis showed that the least stressed members were the vertical compression members located at mid-span of the trusses. These compression members are built-up sections with two channels connected back-to-back with lacing members. Several lacing members were removed for material testing. New lacings members were put in place of the removed lacings.

3.6.1.2 Removal of Material

Lacings from the compression members were removed by cutting the rivet heads by using a disc grinder. The grinding operation was carried out carefully to avoid grinding of the channel sections. After cutting the rivet heads, they were removed by hammering. Two lacing members were removed from each column. The lacing members were labeled for identification. Replacement steel lacing members were installed in place of the removed members, and structural bolts were installed in place of the removed rivets.

3.6.1.3 Test Conducted

For metal lacing samples, the following tests were conducted:

- Tension test;
- Chemical composition;
- Hardness test; and
- Metallography.

Test results are described in Appendix C. Average test results are listed in Table 3.1. Chemical composition and photomicrograph showed that the metal is of good quality wrought iron.

Table 3.1: Average test results for metal specimen

	Average
Static yield stress, ksi	36.3
Dynamic yield stress, ksi	39.5
Dynamic ultimate stress, ksi	53.9
Elongation, %	16
Hardness on Rockwell B scale	79

3.6.2 In-situ Testing

As described above, the critical members controlling the load rating of the case study bridge were the tension chord eyebars. However, material could not be removed from the eyebars without adversely affecting their strength. Consequently, lacing members were removed and tested. In order to determine if the lacing metal is similar to the metal used in the eyebars, hardness tests were conducted in the field. This was done using a portable mini-Brinell hardness tester.

The results of the hardness tests are listed in Appendix C. The average field hardness was found to be 78 on Rockwell hardness B scale. These results indicated similar hardness values for the lacing members and the eyebars, suggesting that strength of the lacing members and eyebars are similar.

Chapter 4

Analysis and Load Rating

4.1 INTRODUCTION

The main objective of this chapter is to illustrate the analysis and load rating of the Shackelford County case study bridge structure. This is a key step for evaluation of an existing bridge structure. In the following sections, a general discussion of load rating is provided, followed by analysis and load rating of the case study bridge. Detailed analysis and load rating results are summarized in Appendix E.

These calculations will provide a basis for determining the safe load capacity of the bridge according to AASHTO standards. The calculations should be based on the best available information on the current condition of bridge as described in Chapters 2 and 3. Per the AASHTO manual, [AASHTO, 1994], the load rating should be done for two different service levels: Inventory rating level and operating rating level. The load rating may be done by using either Allowable Stress or Load Factor methods, as per the AASHTO manual, [AASHTO, 1994].

4.2 RATING LEVELS

The inventory rating level is based on AASHTO specified design levels for stresses, but reflects the existing bridge and material conditions with regard to deterioration and loss of section. Load ratings based on the Inventory level allow

comparison with the capacity for new structures and, therefore, results in a live load which can safely utilize an existing structure for an indefinite period of time. Hence, the inventory rating relates to the load under which a bridge can perform safely indefinitely.

The operating load rating describes the maximum possible live load to which the structure may be subjected. Allowing unlimited numbers of vehicles to use the bridge at operating level may shorten the life of the bridge. The operating level rating relates to the maximum loads that may be permitted on the bridge.

4.3 RATING METHODS

In the load rating of bridge members, two methods for checking the capacity of members, Allowable Stress Design method and Load Factor Design method can be used. The nominal capacity to be used in the rating equation depends on the structural material, the rating method and the rating level used. The “Manual for Condition Evaluation of Bridges” [AASHTO, 1994] and Standard Specifications for Highway Bridges [AASHTO, 1996] can be used to calculate required capacities of each component of the bridge.

The allowable or working stress method constitutes a traditional specification to provide structural safety. The actual loadings are combined to produce a maximum stress in a member which is not to exceed the allowable or working stress. The latter is found by taking the limiting stress of the material and applying an appropriate factor of safety.

The load factor method is based on analyzing a structure subject to multiple of the actual loads (factored loads). Different factors are applied to each

type of load which reflect the uncertainty inherent in the load calculations. The rating is determined such that the effect of the factored loads does not exceed the strength of the member.

4.4 RATING EQUATION

As per AASHTO manual, [AASHTO, 1994], the following expression should be used in determining the load rating of the bridge structure:

$$RF = \frac{C - A_1 D}{A_2 L (1 + I)} \quad (4.1)$$

where:

RF = the rating factor for the live-load carrying capacity. The rating factor multiplied by the rating vehicle in tons gives the rating of the structure;

C = the capacity of the member;

D = the dead load effect on the member;

L = the live load effect on the member;

I = the impact factor to be used with the live load effect. The formula suggested in the AASHTO specifications (1996) can be used to calculate this impact factor;

A₁ = factor for dead loads; and

A₂ = factor for live load.

The rating factor, RF, may be used to determine the rating of the bridge member in tons as follows:

$$RT = (RF)W \quad (4.2)$$

where:

RT = bridge member rating

W = weight (tons) of nominal truck used in determining the live load effect, L.

For the allowable stress method, both the A_1 and A_2 load factors in the equation (4.1) should be taken as 1.0. The capacity, C, depends on the rating level desired. A higher value of capacity, i.e. a lower value of factor of safety, is used for the operating level.

For the load factor method, $A_1 = 1.3$ and A_2 varies depending on the rating level desired. For inventory level, $A_2 = 2.17$ and for operating level, $A_2 = 1.3$. The nominal capacity, C, is the same regardless of the rating level desired.

4.5 LOADINGS

The dead load effects of the structure should be computed in accordance with the condition existing at the time of analysis. Minimum unit weight of materials used in computing the dead load stresses should be in accordance with current AASHTO standard design specifications, [AASHTO, 1996]. Nominal values of dead weight should be based on the dimensions shown on the plans or on the recent field measurement.

The live load to be used in the equation (4.1) should be the HS20 truck and lane loading as defined in the AASHTO Design Specifications, [AASHTO, 1996]. In the analysis and load rating presented here, the H15 truck is also

considered. The load rating with trucks other than HS20 will be helpful for load posting the bridge, if needed.

4.6 ANALYSIS

Analysis of the bridge is divided between the truss analysis and the deck analysis. For analysis both hand methods and the SAP2000 structural analysis program [SAP2000, 1997] were used. Various types of analyses, under different loading conditions can be carried out using the software. Any commercially available structural analysis program can be used.

4.6.1 Truss Analysis

Four different structural models, with varying degree of complexity, were used to determine the member forces. This section describes the models and loadings used for the analysis of the truss.

Simple 2-D model

All the truss members are modeled as pin-ended truss elements. The supports were modeled as hinge support at one end of the bridge and roller support at the other end to represent the idealized support conditions for the actual bridge. The Figure 4.1 shows the model, the frame elements with end releases and the supports.

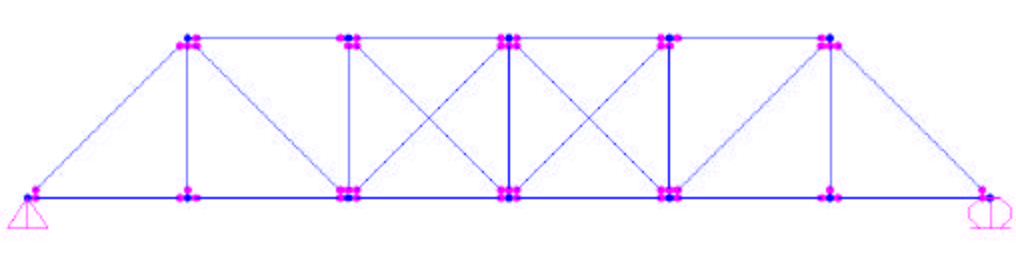


Figure 4.1: The simple 2-D model of the truss

Simple 2-D model with continuous top chord

The top compression chord of the truss was modeled continuous over the joints. All the other truss members were modeled as pin-ended truss elements. This model more accurately represents the actual truss top chord construction.

3-D model

All the members of both trusses were modeled. This included all the truss members, the top lateral bracing members, the lower lateral bracing members, and the metal floor beams. All the joints were modeled as pin joints except the portal-bracing joint at both ends of the bridge. The Figure 4.2 shows the model and the supports.

3-D model with continuous top chord

This model is same as the 3-D model described in section 4.8.1.3 except that the top chord of both the trusses were modeled as continuous over the joints.

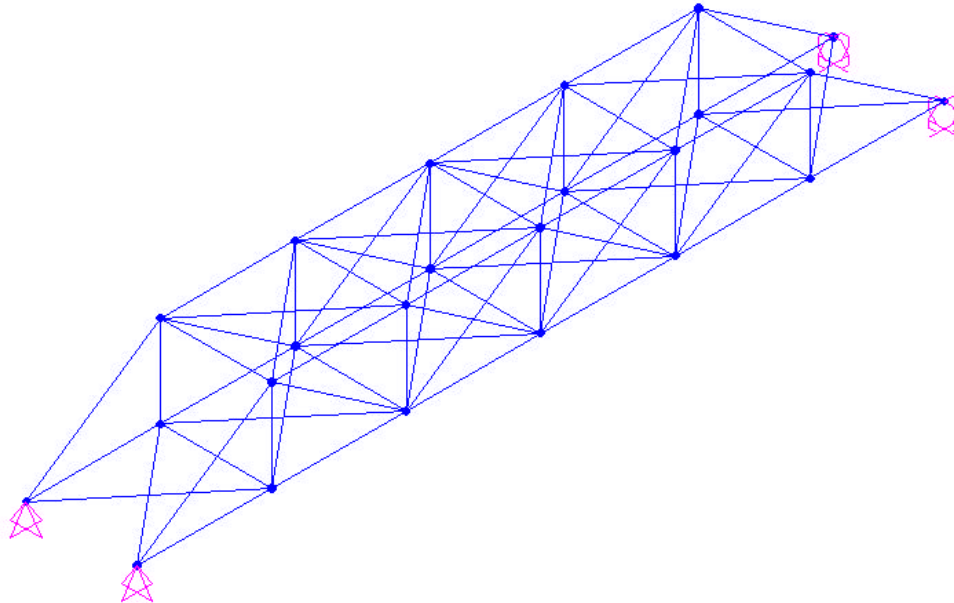


Figure 4.2: The 3-D model of both the trusses

Dead load

The dead load of the truss members, the lateral bracing, and the deck system was calculated based on the measured dimensions and standard unit weights of the metal and timber. The dead load was assumed to be acting as uniformly distributed loads. The dead load of the deck was distributed to different panel points of the truss according to the tributary area supported by that panel point. The dead load calculated based on the current condition of the deck.

Rating live load

Both HS20 and H15 trucks were used as live load in the bridge analysis. The size and weight distribution of the truck is as per AASHTO standard design specifications, [AASHTO, 1996]. As the bridge is only a single-lane bridge, the

truck was placed along the centerline of the bridge. The truck load is distributed to different panel points by assuming the timber stringers and the metal floor beams are simply supported. This assumption is representative of the actual geometry of the timber stringers and the metal floor beams as the end connections of these members are not capable of resisting moment.

4.6.2 Truss Analyses Comparison

Among all the mathematical models used, the two-dimensional simple truss model was the easiest to model and analyze. This model can also be analyzed by hand calculations very easily. This model captures the basic behavior of the truss. The model can easily be modified for different support conditions, e.g., the roller support behaving as a hinge support. The other mathematical models showed almost the same member forces as those shown by the simple two-dimensional model. The mathematical models with the continuous top compression chord did not show appreciable bending moments in the top compression chords. A second order analysis was also carried out on the simple two-dimensional model. This analysis also did not show any appreciable change in the member forces. Hence, using a very simple 2-D pin-connected truss model appears adequate to predict member forces. There appears to be little advantage in the use of more complex models for the trusses. Analysis results are shown in the Appendix E, only for simple two-dimension truss model. These analysis results will be further evaluated and compared to field load test data in Chapter 5.

4.6.3 Deck Analysis

The bridge deck is made up of timber planks resting on several timber stringers. The stringers are supported on metal floor beams connected to lower panel joints of the trusses. Metal floor beams were analyzed manually by considering them as simply supported beams. These girders were analyzed for the reactions transferred to them from the timber stringers. The dimension and layout of the timber stringers are shown in Figure 2.2. For deck analysis, different mathematical models with varying degree of complexity were used. The AASHTO, [AASHTO, 1996], load distribution factors are also used for comparison with the computer models. The models used are described in the following sections.

2-D models with spring supports

A timber plank, either at mid-span or near-supports, was modeled using frame elements. The stringers were modeled as spring supports. The spring stiffness for a particular stringer was calculated based on the moment inertia, assumed modulus of elasticity, and location of the plank. These models are simple to develop and analyze. The analysis gives the force in the each spring support. From this force in the spring, bending moments developed in a stringer can be calculated considering it as simply supported at both ends. Figure 4.3 shows the model with the spring supports.

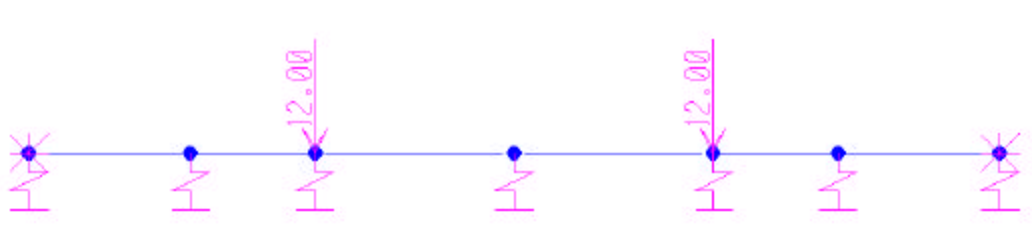


Figure 4.3: The 2-D model of bridge deck with spring supports

3-D models

All the timber planks and stringers were modeled using frame elements. The stringer supports were modeled as hinged at one end and as a roller at the other end. All the sectional properties were based on the actual measured dimensions. All the material properties were based on the AASHTO standard design specification, [AASHTO, 1996]. Three different models were studied. All the three models were identical in all respects except for the torsional rigidity used for different frame elements. In the first model, torsional rigidity for all the planks and the stringers was considered, in the second model, torsional rigidity was considered only for planks, and in the third model, torsional rigidity was neglected for both the planks and the stringers. Figure 4.4 shows the model and the supports.

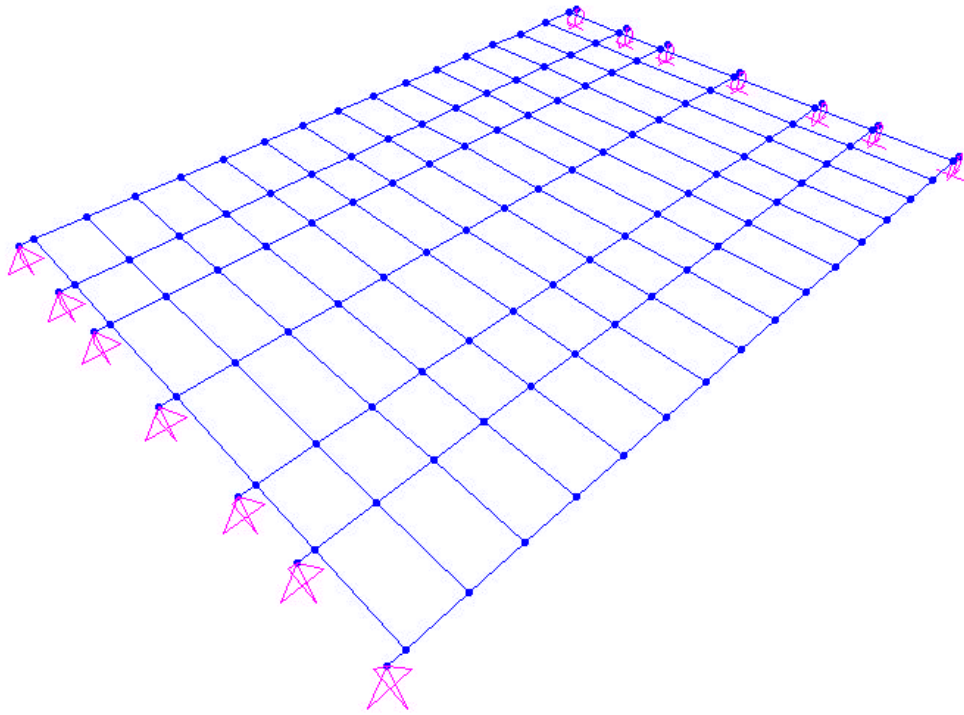


Figure 4.4: The 3-D model of the bridge deck

Manual calculation

In this calculation, it is assumed that none of the smaller stringers, (3" x 12" deep), is participating in resisting the truck load. Hence, the entire truck load is supported by the two main/stronger stringers (8" x 16" deep). The bending moment due to the truck is divided between the two stringers equally. This is the simplest and fastest way to analyze this type of deck system.

The 3-D computer analysis showed that these main timber stringers are supporting about 85% of the total bending moment. This is due to the fact that the bending stiffness of these stringers is much higher than that of the remaining

smaller stringers. To take in to account that the smaller timber stringers are also contributing to transfer some of the load, the 6% of the total load was used to analyze each smaller timber girder. The value of 6% is conservative for this type of bridge decks. This value varies from 2% for the outermost timber stringer to 6% for the central timber stringer with 4.5% for the second outermost timber stringer. These distribution factors were derived from the 3-D analysis of the bridge deck. Using same value of distribution factor for all the smaller stringers is simple, conservative and easy to use for manual calculations.

AASHTO load distribution

In addition to use of different mathematical models, AASHTO load distribution factors given in AASHTO standard design specification, [AASHTO, 1996], were also used to analyze the deck system. The total bending moment is distributed to different stringers based on the distribution factors given in the specifications. The total bending moment is calculated considering the stringers are simply supported.

4.6.4 Deck Analyses Comparison

The bridge floor deck was analyzed for dead load, and a H15 truck load. These were described in section 4.8.1.5. The HS20 truck was not considered, as preliminary load rating for the deck was quite smaller than HS20. The two-dimensional model with spring supports was simple to construct and to analyze. The results obtained matched well with the results obtained from the three-dimensional model.

The three-dimensional model is fairly complex and hence care is required in constructing the model. The output from this model is quite large and hence time consuming to evaluate. The results obtained from this model are likely more reliable as compared to the other models. The better results can be obtained when the torsional constant for all the planks and the timber stringers is set to 0. This is due to small torsional rigidities of timber planks and stringers. It is observed that the maximum bending moment in the stringer will develop when the rear wheel of the H15 truck is at mid-span. It was also observed that the maximum shear force in different stringers developed at different rear wheel positions. For the stronger stringers, placing the rear wheel near the end of the span produced the maximum shear force. For the remaining stringers, placing the rear wheel at approximately three-quarters of the span produced maximum shear force.

The manual method of analysis is same as that given in the AASHTO specifications, [AASHTO, 1996], except that the distribution factors were obtained from the analyses of the 3-D model of the bridge deck. This method is very simple, fast and conservative for this particular type of decking system. The total load was distributed to both the stronger stringers equally and additional 6% of the total load was assign to each smaller stringer. These distribution factors are applicable to the bending moment calculations only. For shear force calculation, the distribution is 50% to each stronger stringer, 20% to the central stringer, and 6% to each remaining stringers.

The AASHTO load distribution factors do not provide an accurate prediction of load distribution for this type of timber deck system. The deck is

made up of different sized timber stringers and hence the vehicle load will be distributed to different stringers according to their relative bending stiffness. The AASHTO load distribution factor is 54% of the total weight for all of the stringers based on an average spacing of 26" and using average spacing divided by a factor four specified by AASHTO, (1996) for this type of deck system. The three-dimensional analyses show about 42% distribution to the two stronger stringers and 2% to 6% distribution to the remaining smaller timber stringers. Hence, the AASHTO load distribution factors are conservative.

Evaluation of structural models of varying degrees of complexity for the metal trusses of this bridge indicated that the very simplest model (2-D pin-connected truss) predicted essentially the same member forces as the most complex model (3-D model with continuous top chord). Consequently, the use of more complex structural models provides little or no advantage in developing a more accurate load rating. This, however, was not the case for the timber floor system of the bridge. More complex models, such as the 3-D model developed for the floor deck of this bridge, gave significantly different predictions of bending moments and shear forces in the timber stringers than the simple hand calculations using AASHTO distribution factors. The simple hand calculations appear to give quite conservative results. Consequently, for the analysis of the floor system, the use of a more complex structural model may lead to an improved load rating, and may serve to reduce or even eliminate the need to strengthen or replace the timber floor deck.

4.7 NOMINAL CAPACITY CALCULATIONS

The calculation of nominal capacity, C , of the truss members and the deck members is described in the following sections. The capacity was calculated for two different level of service i.e. inventory level and operating level. For each service level the capacity was calculated based on the Allowable Stress Method, and the Load Factor Method.

4.7.1 Truss

The capacity of the truss members were calculated based on the measured dimensions and material properties obtained from AASHTO manual, [AASHTO, 1994]. The cross sectional properties, such as cross sectional area, moment of inertia, and radius of gyration were calculated based on the measured dimensions. The metal properties were obtained from the AASHTO manual, [AASHTO, 1994].

The design yield stress given in the manual is much less than what was measured in the laboratory on the samples taken from lacings. The measured yield stress of lacings could be higher than the yield stress of truss members. This may be attributed to more exposure of lacings to cold working during fabrication processes. The effect of cold working was implied by the smaller measured percentage elongation of the tension coupon test specimen than the average percentage elongation found in literature on wrought iron. The load rating obtained using design yield stress from AASHTO manual is conservative.

4.7.1.1 Inventory

The member capacity calculations were done as per AASHTO manual, [AASHTO, 1994]. The allowable stress for tension members was taken as 0.55 times the yield stress. The allowable stress for compression members was calculated based on the slenderness ratio (KL/r_{\min}) with the safety factor of 2.12. The K factor for columns was taken as 0.875 for pinned connected members and 0.75 for the continuous top chord members. These K factors are listed in the AASHTO manual, [AASHTO, 1994], for different end conditions and lacing or battens configurations.

For the load factor method, the design stress for tension members was taken as the yield stress. The design stress for compression members was calculated based on the slenderness ratio (KL/r_{\min}) with the safety factor of 1.0. The K factors were the same as for the allowable stress method.

4.7.1.2 Operating

The allowable stress for tension members was taken as 0.75 times the yield stress. The allowable stress for compression members was calculated based on the slenderness ratio (KL/r_{\min}) with the safety factor of 1.7. The K factors were the same as above.

The capacity calculation for the load factor method is independent of the service level. Hence, the calculations are identical for both Inventory and operating service levels.

4.7.2 Timber Deck

The bending moment and shear capacities of all the timber stringers were calculated based on measured dimensions and assumed timber properties. The allowable bending stress and allowable horizontal shear stress values were taken from the AASHTO standard design specifications, [AASHTO, 1996]. For both allowable stresses, the minimum of all the listed values was used. These were 550 psi for allowable bending stress and 70 psi for allowable horizontal shear. The minimum values were selected, as no other details were available about the timber. Based on visual inspection of the new timber stringers, they appear to be in good condition and do not show any major sign of deterioration or decay. Hence, the selected values of allowable stresses are appropriate and conservative. If the timber species and the timber stress grading were available then higher values of allowable stresses can be used from the AASHTO specifications. This shows the need of detailed mechanical properties evaluation for the timber members.

For operating level load rating, the above mentioned allowable stress values were increased by 33% as per AASHTO manual, [AASHTO, 1994].

4.7.3 Metal Floor Beams

The capacity of the metal floor beams at different sections was calculated based on the AASHTO manual, [AASHTO, 1994]. The maximum unsupported length of the compression flange was assumed to be the span length of the floor beam. However, lateral torsional buckling was not controlling the capacity. Any

lateral restraint from the timber stringers was neglected as they are not physically connected to the floor beam but are resting on them.

The capacity calculations were also done by considering the bracing effect of the timber stringers. For these metal floor beams, the bracing effect shows no influence on the capacity. For more information on lateral bracing effects of deck on steel stringers, refer to Vegesna, S., (1992) and Webb, S.T., (1992).

The results of capacity calculations for the truss members, the deck system and the floor beams are presented in Appendix E.

4.8 LOAD RATING

The load rating of both the trusses and the deck was carried out based on the analysis results, and the calculated nominal capacities. The load rating was done for two different level of service i.e. inventory level rating and operating level rating. The load rating was done per the procedure described in section 4.5. An impact factor of 0.22 was used in the general rating equation based on the AASHTO standard design specifications, [AASHTO, 1996]. The calculations are shown in the Appendix E.

4.8.1 Discussion on Load Rating Results

The central bottom tension chords control the load rating of the truss under H15 and HS20 truck loads. For H15 load rating, all other members of the truss were load rated above H15. For HS20 load rating, in addition to the central bottom tension chords, the remaining bottom tension chords, vertical hangers, and diagonal members were rated below HS20. A summary of the controlling load rating for the truss is listed in Table 4.1.

Table 4.1: Summary of controlling load rating for the truss

Truck	Inventory load rating		Operating load rating	
	ASD*	LFD**	ASD*	LFD**
H15	H 16.6	H 17.0	H 27.3	H 28.3
HS20	HS 9.6	HS 9.9	HS 15.9	HS 16.5
* Allowable Stress Method				
** Load Factor Method				

The difference between the load rating obtained using the allowable stress method and the load factor method was small for this bridge.

The load rating of the timber deck is controlled by the shear capacity of the stringers. The shear capacity of the stringers is less than the shear developed in them due to dead load of the structure. The load rating of the stringers was done only for an H15 truck and only using the allowable stress method. The load rating based on bending capacity of the stringers was H3.2 and H4.6 for inventory and operating load rating, respectively.

The load rating of the metal floor beam is controlled by the sections at which main stringers are supported on them. The metal floor beam is tapered along its length and the bending moment distribution along the length of the floor beam is constant between the two wheel loads. Consequently, the mid-span section of the floor beam is rated higher than the other sections. A summary of the controlling load rating for the metal floor beam is listed in Table 4.2.

Table 4.2: Summary of controlling load rating for the floor beam (beam section under the wheel load)

Truck	Inventory load rating		Operating load rating	
	ASD*	LFD**	ASD*	LFD**
H15	H 9.4	H 8.3	H 13.5	H 13.9
HS20	HS 6.3	HS 5.6	HS 9.1	HS 9.4
* Allowable Stress Design				
** Load Factor Design				

The load rating of the main bridge span is the lowest load rating of the truss, stringers and metal floor beams. Hence, the load rating of the main span is controlled by the load rating of the stringers. The load rating of the stringers is controlled by their shear capacity. The shear capacity of the timber stringers is calculated based on the lowest allowable shear stress given in the AASHTO standard design specification, [AASHTO, 1996]. To improve the load rating, a thorough testing on timber is required to determine its mechanical properties. In addition to this, a field load test may be carried out, which may give some insight into the behavior of the bridge under the action of a moving vehicle.

The field load testing was carried out on the case study bridge. Since, the timber stringers are controlling the bridge rating, the aim of the load testing should be to study them in detail. However, the timber members are difficult to instrument with strain gages. In addition, the results collected are highly dependent on the local climatic condition, and moisture content of timber. Hence, only truss members and metal floor beams were instrumented with strain gages. The aim of the load testing was to study the behavior of the truss and to verify the mathematical models used to analyze the truss. Complete details of the load testing are presented in Chapter 5 and Appendix F.

Chapter 5

Field Load Testing

5.1 INTRODUCTION

A field load test was conducted on the case study bridge in Shackelford County, Texas. The truss members and a metal floor beam were instrumented with strain gages. The field test was carried out by driving a loading vehicle along the bridge centerline. The strain gage data were collected, analyzed and compared to predictions of member response obtained from the structural models described in Chapter 4. This chapter presents only an overview and summary of the load test. A detailed listing of gage location and field load test results are provided in Appendix F.

5.2 OBJECTIVE

The primary objective of the field load test was to determine if the strains, stresses and forces developed in the members of the bridge are accurately predicted by the structural model. Field load tests on other types of bridges [Bakht, B., 1990] have shown that the stresses measured during a test are often significantly lower than predicted by structural analysis. The field load test can provide a more accurate assessment of the structural response and the strength of a bridge, and can sometimes, be used to justify an improved load rating. The field

load test can also sometimes be used as a diagnostic tool to uncover problem areas with the bridge.

For the case study bridge, the objectives of the field load test were as follows:

- Develop an improved understanding of the overall behavior of the bridge;
- Evaluate the accuracy of the structural models of the bridge;
- Study the load distribution between the two trusses of the bridge;
- Evaluate the behavior of the metal floor beams;
- Evaluate the effect of the damaged bridge roller bearing on bridge response; and
- Develop an improved load rating of the bridge, if justified.

5.3 OVERVIEW OF FIELD LOAD TESTING

Two separate field load tests were conducted on the Shackelford county bridge. These test were conducted on 6th May 1999 and on 7th September 1999. In the first test, a large number of members were instrumented to evaluate the overall response of the trusses under the applied truckload. In the second test, only a few members of the upstream truss were instrumented. The objective of the second test was to address questions raised by the data collected in the first test. In the following section, the details of each field test are described.

5.3.1 Strain Gage Layout

Forty-five strain gages were used to instrument the bridge for both load tests. This limitation was imposed by the number of available channels of the data

acquisition system. A detailed description of the location of the strain gages is presented in Appendix F.

To mount the gages on steel members, standard procedures and chemical listed in a bulletin published by Vishay Measurements Group, [Vishay, 1992], were used. Precautions were taken to align the strain gages along the axis of the member.

5.3.2 Description of Test Equipment

Temperature compensating electrical resistance strain gages with a 10 mm gage length and about 120-ohm electrical resistance were used for both the tests. A Campbell Scientific CR9000C data logger and Windows PC9000 software were used to collect the digital data. A complete discussion on the data acquisition system is presented elsewhere [Jáuregui, D.V., 1999]. A calibration check was done on all gages.

5.3.3 Loading Vehicle

The vehicle used for the first field load testing was a Ford van. The dimensions and weight of the vehicle are as shown in the Figure 5.1. The total weight of the vehicle was 5660lb. The vehicle used for the second test was different than the one used for the first test and is shown in Figure 5.2. The dimension of the vehicle for the second test was 168" x 66" with the front axle weight of 3255lb and rear axle weight of 2845lb. These vehicles were selected based on the bending moment load rating of the timber stringers for inventory service level. Axle weights were determined using a public truck scale near the bridge site.

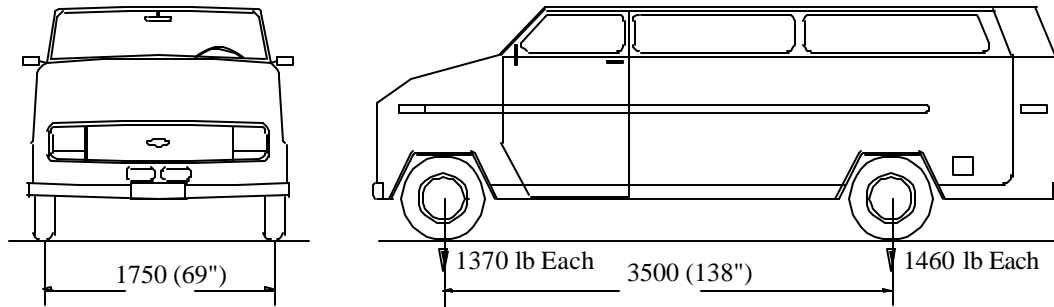


Figure 5.1: The details of the loading vehicle used for the first test

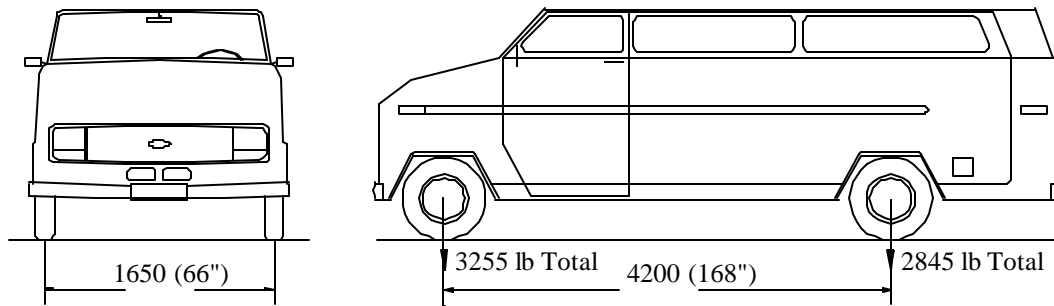


Figure 5.2: The details of the loading vehicle used for the second test

5.3.4 Field Load Testing

Load tests were carried out by driving the loading vehicle along the bridge centerline. Due to the restricted geometry of the bridge and the position of the stronger timber stringers, it was decided to align the vehicle only along the centerline of the bridge. The loading vehicle was run over the bridge ten times and the data was collected for each run. The details of each run are listed in Table 5.1 for the first test and in Table 5.2 for the second test. For the first load test, two

vehicle speeds: slow, i.e., about 5 miles per hour, and fast, i.e., about 20 miles per hours, were used. For the second load test only slow vehicle speed was used.

Table 5.1: Details of first load testing runs

Test Run #	Data #	Direction	Description
1	0	South to North – Forward	Vehicle speed – Slow
2	1	North to South – Reverse	Vehicle speed – Slow
3	2	South to North – Forward	Vehicle speed – Slow
4	3	North to South – Reverse	Vehicle speed – Slow
5	4	South to North – Forward	Vehicle speed – Slow
6	5	North to South – Reverse	Vehicle speed – Slow
7	6	South to North – Forward	Vehicle speed – Slow with stops at panel joints of the truss
8	7	North to South – Reverse	Vehicle speed – Slow with stops at panel joints of the truss
9	8	South to North – Forward	Vehicle speed – Fast
10	9	South to North – Forward	Vehicle speed – Fast

Table 5.2: Details of second load testing runs

Test Run #	Data #	Direction	Description
1	0	South to North – Forward	Vehicle speed – Slow
2	1	North to South – Reverse	Vehicle speed – Slow
3	2	South to North – Forward	Vehicle speed – Slow
4	3	North to South – Reverse	Vehicle speed – Slow
5	4	South to North – Forward	Vehicle speed – Slow
6	5	North to South – Reverse	Vehicle speed – Slow
7	6	South to North – Forward	Vehicle speed – Slow with stops at panel joints of the truss
8	7	South to North – Forward	Vehicle speed – Slow with stops at panel joints of the truss

5.4 ANALYSIS OF THE FIELD LOAD TEST DATA

The results of the field load tests are presented in a series of plots in Appendix F. Each plot shows the stress measured at a particular gage location versus the position of the front wheel of the test vehicle. Graphs F.1 through F.44 represent test data for the first test. Graphs F.45 through F.86 represent test data

for the second test. Graphs F.87 through F.98 represent average test data for the second test. The strain measured at each gage location was converted to stress by multiplying the modulus of elasticity, which was taken as 29,000 ksi.

5.5 THEORETICAL ANALYSIS OF LOAD TEST VEHICLE

Analysis of the truss was carried out by using SAP2000 software [SAP2000, 1997]. The model used for the analysis was the simple two-dimensional model described in Chapter 4. All the truss members were modeled as pin-ended truss elements. The supports were modeled as a hinge support at one end of the bridge and as a roller support at the other. Different load cases were used to simulate the movement of the load test vehicle on the bridge. As the loading vehicle was run along the centerline of the bridge, it was assumed that both the trusses were sharing equal load. The timber stringers were assumed to be simply supported on the metal floor beam for calculating the panel point loads. The results of this analysis are graphically presented for each member in the Appendix F together with the field data.

5.6 FIELD LOAD TEST ISSUES

In this section, several key issues related to field load testing are presented. Structural analysis of a truss gives member forces. The field load test gives stress at a particular location in the member. Consequently, it can be difficult to directly compare the results of analysis and testing. Often, it is assumed that the stress distribution over the cross section of a axially loaded member is uniform. From this assumption, uniform stress in the member can be calculated from the forces obtained from the structural analysis. However, this

assumption of uniform stress distribution may not be accurate for all member geometries. Individual elements of built-up sections may not act as a unit, which can cause large variations of stresses across the entire cross-section. Eccentric connections and initial crookedness of the member may result in bending moment, causing stress distribution to be non-uniform. To eliminate the effect of bending moment, a larger number of gages can be mounted on the members.

The variation of stresses measured among a large number of gages mounted on a built-up member is often difficult to interpret. The individual elements may not be acting as a single member and each element may bend about different axes. The interpretation of the data gets complicated for such cases. Hence, even a large number of gages may sometimes fail to give an accurate estimate of member forces.

5.7 COMPARISON OF THE TEST DATA AND THEORETICAL ANALYSIS

For comparison of test and analysis results, graphs of stress versus the position of the front wheel of the loading vehicle were prepared for each strain gage location. Each graph shows the theoretical results in the form of a line. The field test results are presented in the form of minimum value, maximum value, and average value of the stress measured among the slow test runs. All the graphs are presented in Appendix F. It can be observed from the graphs presented in Appendix F that the stress level in the members was very low. The highest compression and tension measured was about 2 ksi.

5.7.1 First Field Load Test

The measured stresses for different members are presented in Graphs F.1 through F.44. The following observations were made from comparison of the first field load test and corresponding analysis results:

- a) Significantly lower stresses were measured in the bottom tension chords, i.e., members L0L1, L1L2, L2L3, L3L4, L4L5, and L5L6, than predicted by analysis. This is clearly indicated by Graphs F.1 through F.14. The gage locations are as shown in Figures F.1 through F.3. It was also observed that the distribution of stresses among each element of these members was not uniform. This is indicated by the difference in measured stresses on each element of the same bottom tension chord. The difference in measured stresses can be observed by comparing Graph F.1 with Graph F.2, Graph F.4 with Graph F.5, Graph F.7 with Graph F.8, Graph F.10 with Graph F.11, and Graph F.13 with Graph F.14. This indicates that the tension chords are subjected to some amount of bending moment. In this test, only one face of each element was instrumented. Mounting gages on both sides of the element will assist to evaluate the amount of bending moment.
- b) Significantly higher stresses, about 50% higher, were observed in the inclined compression chords (L0U1 and U5L6). This is indicated by Graphs F.15, F.16 and F.25. These members are rigidly connected to portal braces. This rigid connection may be a source of bending moment in the member. These members were instrumented with a single gage.

These members are built-up sections made from two-channel sections connected back-to-back by a cover plate and battens. As discussed above, a built-up section may not be acting as a single member. The measured stress by a single gage may not give an accurate indication of the state of stress in this member. More gages should be mounted to evaluate the response of a built-up member.

- c) Higher stresses, about 10% higher, were observed in the top compression chords (U1U2, U2U3, U3U4, and U4U5). This was clearly indicated by Graphs F.17 through F.24. These members are similar to those discussed above and hence more gages should be used to evaluate member forces.
- d) Significantly higher stresses, about 50% higher, were observed in the vertical hangers (L1U1 and L5U5). This was clearly indicated by Graphs F.26, F.27 and F.33. Based on the construction details, higher stresses in these members are difficult to justify. The hanger system is determinate and non-redundant; hence, the reasons for higher stresses are difficult to evaluate. However, possible reasons for the higher stresses may be a lower cross-sectional area as compared to that used in the analysis and the effect of any initial crookedness of the hangers. These members were instrumented with a single gage; hence, more gages should be mounted to estimate an accurate state of stress.
- e) Mixed responses in stresses were observed in the vertical compression members (L2U2, L3U3, and L4U4). This was clearly indicated by Graphs F.28 through F.32. These members are built-up section made from two-

channel section connected back-to-back by lacings. In addition, the stress level in these members is very low. Low stress levels are generally difficult to measure accurately due to limitations of the sensitivity of the data acquisition system.

- f) Good agreement between test and analysis results was found for members U1L2 and L4U5. These are diagonal members at both the ends of the truss. This is shown by Graphs F.34 and F.39.
- g) Mixed responses in stresses were observed in the remaining diagonal members (L2U3 and U3L4; and U2L3 and L3U4). This is shown by Graphs F.35 through F.42. These members are made up of long and very slender elements, either of rectangular section or of circular sections. Even a small amount of bending moment in these members will change the state of stress. Hence, more gages should be used to eliminate the component of bending stress from the measured stress.
- h) Good agreement between test and analysis results was found for the metal floor beam. This is seen in Graphs F.43 and F.44. The analysis of these metal floor beams was done assuming that they are simply supported at both the ends. Test results support this assumption and also support assumptions regarding load distribution from the stringers.
- i) The stresses measured in the identical members of the two trusses were not the same. This indicates that the distribution of stresses in two trusses is not equal. The analysis of the truss was carried out assuming that equal load is shared by the trusses. However, the test results contradict this

assumption. As discussed above, the metal floor beams are acting as simply supported beams and hence, there is no reason to justify that the trusses are sharing load unequally. More test data is required to investigate this in detail.

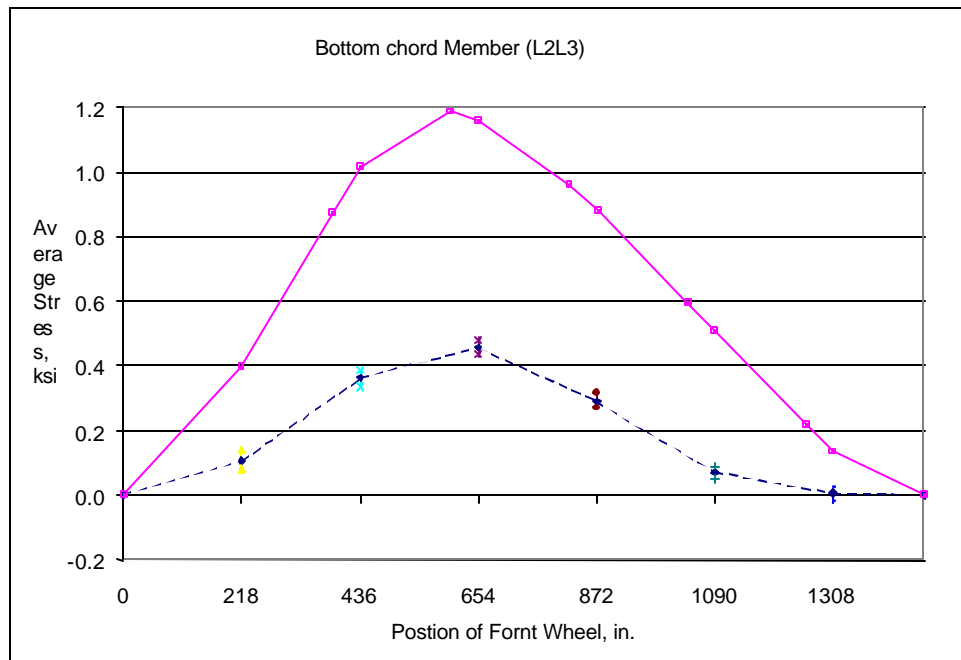
- j) The test runs carried out at the higher vehicle speed showed about 10% to 15% higher stress values when compared to the slow test runs. AASHTO standard design specification, [AASHTO, 1996], specifies an impact load factor equal to 22%. Hence, the AASHTO impact factor appears to be conservative in this case.

It is clear from the above discussion that even for a simple determinate truss system, it is difficult to correlate test results with analysis results. The questions raised by the first test about lower stresses in bottom tension chords and higher stresses in top compression chords, vertical hangers and almost all diagonal members need to be addressed by thorough instrumentation and more tests. This was the main objective of the second field load test. For the second field load test, only a few members of upstream truss were instrumented with more gages.

5.7.2 Second Field Load Test

The measured stresses for different members are presented in Graphs F.45 through F.86. The average stresses calculated for different members are presented in Graphs F.87 through F.98. The following observations are made from the comparison of the second field load test and corresponding analysis results:

a) Significantly lower stresses in the bottom tension chords, i.e., L0L1 through L5L6, were found. The stresses measured on opposite faces of each element were different. These differences in stresses strongly indicate that the bottom tension chord members are subjected to bending moment. This is clearly indicated by Graphs F.45 through F.49. The average stresses are presented in Graphs F.87 and F.88. Graph F.88 is reproduced here as Graph 5.1.

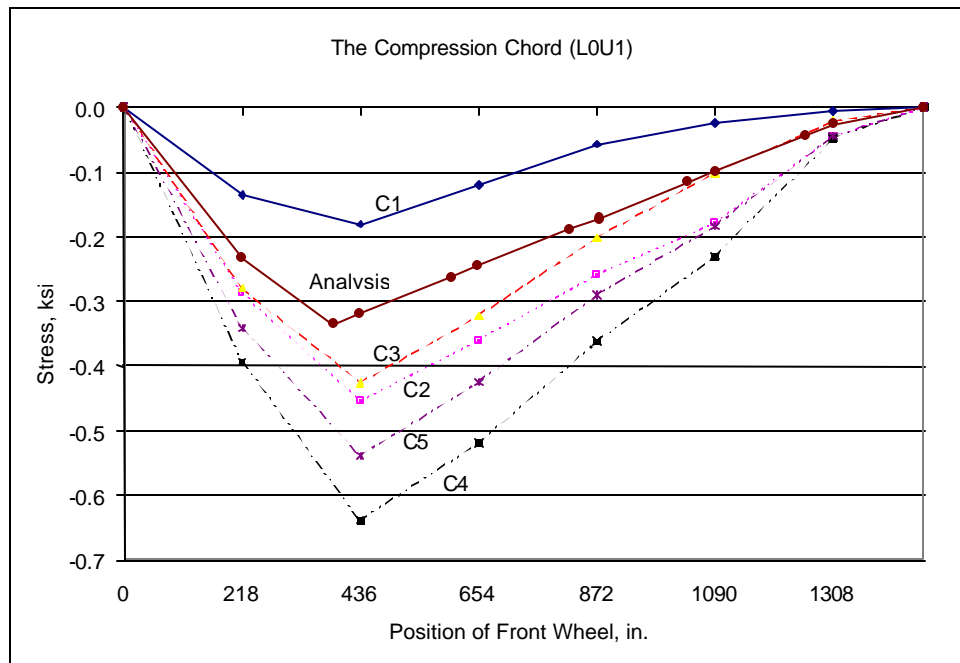


Graph 5.1: Average stress: Bottom chord (L2L3)

The average stresses in the bottom tension chord members were lower, about half, as compared to stresses obtained from analysis. The lower stresses in the tension chord members can likely be attributed to the locked roller supports. The roller supports for both trusses are dislocated.

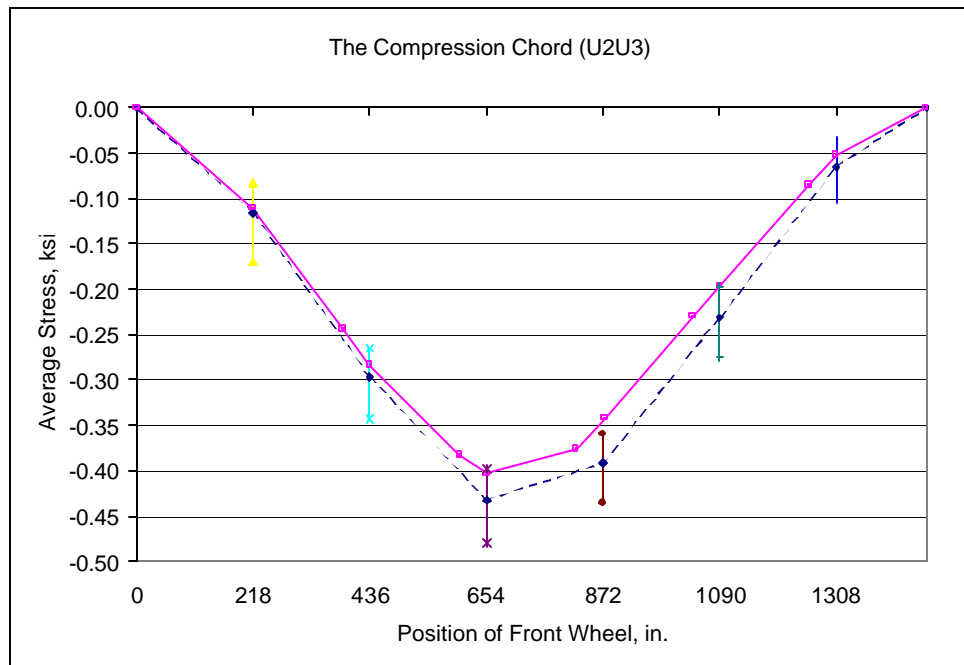
Due to accumulation of debris they are likely not functioning as a true rollers. The locking of the rollers leads to the reduction of forces in the bottom tension chords. However, one should not count on this mechanism in the analysis for reduction on the forces. This is due to fact that the behavior may not be same at higher load levels, and after rehabilitation the rollers will function as the true rollers and will not provide this type of resistance. This type of behavior can be taken into account by modifying the support conditions in the analysis model, by modeling the roller as a pin. This analysis was done with simple 2-D truss model. The analysis also showed a reduction, 50% to 80%, or reversal in the bottom tension chord member forces.

- b) Five gages mounted on inclined compression chord, LOU1, showed a highly variable stress distribution across the section. This is shown by Graphs F.50 through F.54. The comparison of these measured stresses is presented in Graphs 5.2 and F.98. This graph indicates non-uniform stress distribution across the cross-section. The average measured stress is presented in Graph F.89. The average measured stress was found to be higher than the analysis result. A closer look at the stresses revealed that the individual elements of this built-up section were bending about different axes. This made data interpretation very difficult. It can be concluded that even with five gages it is difficult to estimate an accurate state of stress for built-up sections.



Graph 5.2: Stress variation: Top Chord (L0U1)

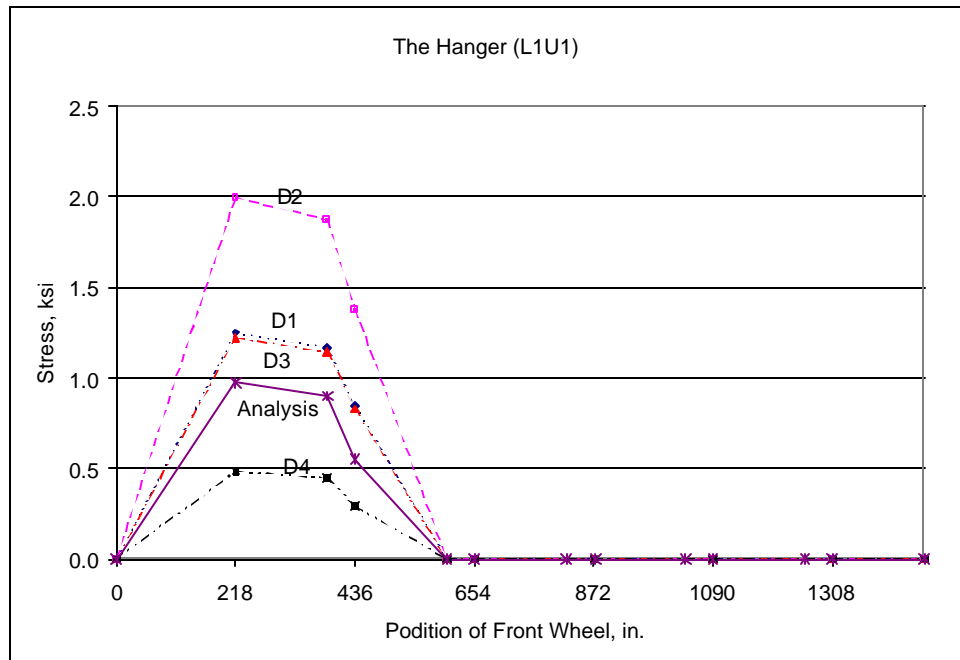
- c) Five gages mounted on each of top compression chords U1U2 and U2U3, showed some variation of stresses across the cross-section. This is indicated by Graphs F.55 through F.63. The average stresses for members U1U2 and U2U3 are presented in Graphs F.90 and F.91 respectively. Graph F.91 reproduced here as Graph 5.3. The average measured stresses for these members were found to be in good agreement with the analysis results.



Graph 5.3: Average stress: Top Chord (U2U3)

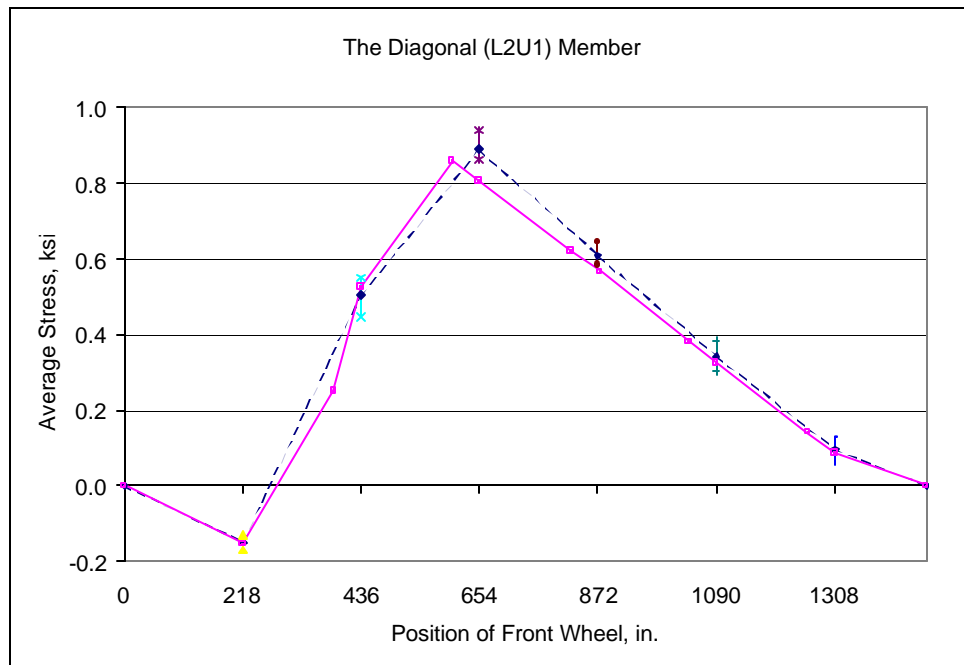
d) Eight gages mounted on vertical hanger, L1U1, showed variation in the measured stresses across the cross-section. This is shown by Graphs F.64 through F.72. The variation in the measured stresses is presented in Graphs 5.4 and F.97. The average measured stress is presented in Graph F.92. The average measured stress was found to be higher than the analysis result by about 25%. From the first test results, it was higher by about 50%. After eliminating bending component from the measured stresses, it is higher by 25%. This indicates that these hangers are subjected to a significant amount of bending stresses. However, the reason for the 25% higher measured stresses is unclear and needs more

evaluation. As discussed above, a possible reason is a lower cross-sectional area.



Graph 5.4: Stress variation: Vertical Hanger (L1U1)

- e) The measured stresses in vertical compression member (L2U2), and diagonal members (L2U3, L2U1, and L3U2), were found to be non-uniform. This was clearly indicated by Graphs F.73 through Graph F.86. However, the average stresses calculated for these members were found to be in good agreement with the analysis results, as showed by Graphs F.93 through F.96. Graph F.93 reproduced here as Graph 5.4.



Graph 5.5: Average stress: Diagonal member (L2U1)

5.8 CONCLUSIONS DERIVED FROM FIELD LOAD TESTS

From the above discussion of both field load tests, the following conclusions are derived:

- a) All the truss members were subjected to varying amounts of bending moment;
- b) The built-up sections may not act as a single member.
- c) The dislocated and non-functioning roller supports were the likely reason for the lower measured stresses in the bottom tension chord members.
- d) From reasonable agreement of measured stresses, with analysis results, for top compression chords, vertical compression members and diagonal member, it may be concluded that both the trusses share equal load.

- e) The overall behavior of simple determinate truss, like this case study bridge truss, can be adequately predicted by simple 2-D truss analysis.
- f) Field load tests may prove helpful for diagnosing problems with the bridge structure. For example, in this case study, it was found that the dislocated roller had an effect on member forces and that additional investigation is required to understand behavior of vertical hangers.
- g) Careful interpretation of test results showed that the load rating of the bridge can not be increased, as the field data does not indicate appreciable difference in truss behavior from that predicted by structural analysis.

The above conclusions are applicable to the trusses of the bridge. For the timber deck system, the following conclusion can be made:

- a) The rating of timber stringer based on shear capacity is zero. However, during the field load test, a truck load of 5.66 kips (2.6 tons) and 6.10 kips (2.8 tons) were used for first and second field load tests, respectively. This indicates that the rating of timber stringers done for this case study is conservative.
- b) Additional work is necessary to evaluate strength properties of these timber stringers. Possible alternatives for further evaluation are: thorough mechanical properties evaluation of the timber, or performing proof load testing, [Saraf, V.K., 1996], for the bridge; or replacement of the timber deck, if possible.

Going through material evaluation, detailed structural analysis, and field load tests have revealed deficiencies of the case study bridge structure. Based on

the deficiencies, different rehabilitation options available can be studied. In Chapter 6, some of the rehabilitation options that may be used for case study bridge are described.

Chapter 6

Rehabilitation Options

6.1 INTRODUCTION

Previous chapters addressed issues and techniques involved with the evaluation of older metal truss bridges. These included data collection, material evaluation, structural analysis, and field load testing. These techniques are intended to provide the most realistic load rating possible for the bridge and to identify problem areas and deficiencies in the bridge. For older metal truss bridges, the evaluation process will often indicate the need for some type of repair or rehabilitation in order to keep the bridge in vehicular service. This chapter discusses some options available to engineers to address common deficiencies in older metal truss bridges.

In the following section, common deficiencies found in older metal truss bridges are reviewed. This is followed by a discussion of repair or rehabilitation options that may be useful in dealing with these deficiencies. At the end of this chapter, deficiencies found in the case-study bridge will be discussed along with possible rehabilitation measures.

6.2 COMMON DEFICIENCIES IN OLDER METAL TRUSS BRIDGES

This section briefly reviews deficiencies and problems commonly found in older metal truss bridges, particularly in off-system bridges. The discussion focuses primarily on problems with the truss bridge superstructure.

6.2.1 Inadequate Load Capacity of Truss

The load rating process for a bridge may indicate that the load capacity is insufficient for the intended use of the bridge. For typical older off-system truss bridges, achieving an HS-20 load rating will often prove difficult, and will frequently not be a realistic goal. For example, the inventory load rating determined for the truss portion of the Shackelford County case study bridge was approximately HS10 (see Section 4.10.1). However, many off-system bridges can likely remain in service with lower load ratings, although load posting may be required. Nonetheless, in a number of cases, the load rating for the bridge may still be inadequate for the intended service, even though the required capacity may be well below HS-20.

Inadequate load capacity in off-system metal truss bridges can result from two causes. The first cause is inherent lack of strength due to initial low design loads for the bridge. That is, even in the absence of damage or deterioration, the bridge members are simply too light to carry the required loads. Many older off-system truss bridges were supplied by private bridge companies and were not designed for any specific load standard. Further, many of these bridges were not originally designed for automobile or truck loads.

The second cause for inadequate load capacity is damage or deterioration to the bridge. If in good condition, many off-system truss bridges may have adequate load capacity for their intended service. However, due to either damage and/or deterioration to bridge components, the load rating may be reduced below a level where the bridge can remain in service.

If the cause of an inadequate load rating is damage or deterioration, then repair of the damaged or deteriorated bridge components will be the primary focus of a bridge rehabilitation plan. On the other hand, if the cause of an inadequate load rating is inherent lack of strength, then more significant and costly strengthening measures may be called for.

6.2.2 Damage and Deterioration to Truss

Older off-system metal truss bridges commonly exhibit a variety of different types of damage or deterioration. Following is a brief list of typical problem areas.

- Corrosion

Due to their age, off-system metal truss bridges exhibit corrosion problems in varying degrees. These problems are typically exacerbated by the member fabrication techniques used in these bridges. Many truss bridge members are built-up cross-section in which plates, structural shapes and lacing members are riveted together to form a single member. These types of members collect water and debris between the elements that make up the cross-section. Moisture and debris also commonly accumulate at truss joints.

- Fatigue Cracks

Typical off-system metal truss bridges were constructed prior to the common use of welding in bridge construction. Instead of welding, members are joined by rivets, bolts and pins. Consequently, many of the fatigue prone details associated with welding are not present. Nonetheless, because of their age, fatigue cracking can still be a concern in these bridges. Areas of severe corrosion or pitting, or areas where members have been dented or bent can act as stress riders to initiate fatigue cracks.

Although welding was not normally used in the original construction of off-system truss bridges, welded components are sometimes found on these bridges. In some cases, welds may have been used as part of a repair for a damaged member. In other cases, brackets can be found welded to bridge members to carry pipes or other utilities across the bridge. In many of these instances, such welds may have been done by unqualified welders, without proper evaluation of the weldability of the metal, without approved welding procedures, without proper preheat, etc. Such uncontrolled welds represent a potential source of fatigue cracking. Defects at these welds, such as undercuts, act as notches that can cause fatigue cracks. Uncontrolled welding may also adversely affect the toughness of the base metal, which may exacerbate fatigue problems or initiate a brittle fracture.

- Impact Damage

Bridge members with various types of damage from vehicle impacts are frequently found in off-system truss bridges. The very light (or sometimes nonexistent) railings found on these bridges provide little protection to the truss members. Consequently, dented or bent members are a common occurrence. In the case of through-trusses, damage to the portal bracing can sometimes be found due to impact with over-height vehicles.

- Damaged or Nonfunctional Bridge Bearings

One end of a truss bridge is normally provided with roller bearings. In many cases, these bearings are found to be deteriorated, damaged or filled with debris. In such cases, the bearings are not likely functioning as intended, i.e., they are no longer permitting free horizontal movement. When these bearings become “locked,” additional stresses can be developed in the truss members due to restrained thermal expansion, due to certain live load cases, or due to bridge pier movements, as discussed below.

- Bent Bottom Chord Members

In some cases, eyebars in the bottom chord of a truss are found to be bent out of the plane of the truss. This bending does not appear to be impact damage, as the eyebars are located in an area where vehicle impact is unlikely. Rather, it appears that these eyebars have buckled due to compressive loads in the members. Since they are in the bottom chord,

these members would normally be expected to be under tension and therefore not subject to buckling. It appears this buckling of bottom chord members may be related to failure of the bridge roller bearings to function properly. If the roller bearings cease to function due to damage or debris accumulation, then compressive forces can, in fact, develop within the bottom chord. Structural analysis of a truss, with the roller bearings locked, will show small compression forces in the bottom chord members for certain live load cases. The field load test of the Shackelford County case study bridge, for example, showed compressive strains in the bottom chord eyebars for some loading cases. Restraint of thermal expansion due to locked bearings could also produce compression in the bottom chord. Perhaps a more likely cause for buckling of the bottom chord eyebars may be failure of the roller bearings combined with small movements of the bridge piers. If the roller bearings are locked, and the bridge piers move inward even a small amount, sufficient compression may be developed in the eyebars to cause buckling. The buckling capacity of eyebars is quite small, so even a small compressive load can cause the members to buckle.

- Deteriorated Timber Decks

Portions of timber decks in truss bridges are often found with varying degrees of deterioration due to rot and decay, splitting, etc.

6.2.3 Geometrical Deficiencies

Restricted horizontal clearance and/or vertical clearance, inadequate vertical and horizontal alignment, and limited vehicle sight distance are a

common problem in older truss bridges. Similar to the Shackelford County case study bridge, many off-system trusses are narrow single lane bridges. In many cases, however, these bridges serve lightly traveled rural roads where a single lane bridge does not pose a serious traffic problem. However, when located on more heavily traveled roads or city streets, the restricted clearances of an older truss bridge can pose more significant traffic and safety problems.

6.2.4 Deficiencies in Substructure

Piers and foundations of older truss bridges may also be subject to damage and deterioration. A variety of different types of piers are found on these bridges. In the case of the Shackelford County case study bridge, large masonry piers were provided. As described in Chapter 2, these piers exhibited considerable deterioration, with a number of loose or missing stones. For some older truss bridges, the piers are large circular metal columns, also frequently deteriorated. The foundation for the piers may have also deteriorated, settled or moved laterally. In some cases, the foundation and piers may have experienced considerable lateral movement or tilting over the years, producing distortions of the superstructure.

6.3 REHABILITATION TECHNIQUES

This section describes a number of options for addressing common deficiencies in older off-system metal truss bridges.

6.3.1 Bridge Floor and Deck System

A common type of rehabilitation for older truss bridges is replacement of the bridge deck. The life of a bridge deck is often considerably less than that of

the bridge, particularly for timber decks. Consequently, due to deterioration, the deck may be replaced several times during the life of the bridge. The existing deck of the bridge may also be replaced with a lighter deck system, in order to reduce the dead load on the bridge. Reduction of dead load, in turn, will permit an increase in the live load capacity of the bridge.

Several options are available to the designer when replacing a bridge deck. The most common approach is to replace the existing deck with the same type of decking. For example, a deteriorated timber deck is frequently replaced with a new timber deck of the same basic design. However, as noted above, an existing deck can sometimes be replaced with a lighter weight system in order to increase the load rating of the bridge. Three options for a lighter weight replacement deck are: (1) open grid steel or fiberglass grating; (2) cold formed corrugated metal decking; and (3) laminated timber decking. Steel or fiberglass grating may become slippery when wet.

Steel or fiberglass grating can provide high load capacities at low weight. This is particularly true for fiberglass grating, where very high strength to weight ratios can be achieved. However, skid resistance of grating can be a concern when wet. Further, fiberglass grating can be quite costly compared to other options. The corrugated plate system can be placed over existing stringers and some supplemental floor beams. The corrugated plate is normally covered with concrete or asphalt to provide a wearing surface. Glue laminated or prestressed timber deck is a recent innovation. Prefabricated panels are normally clamped or bolted to

existing stringers. Laminated panels can offer good resistance to deicing chemicals.

The metal floor beams that support the floor deck of the truss bridge may also need repair, replacement or strengthening. If severely deteriorated or if significant strengthening is needed, girder replacement is an option. Existing metal floor beams can be strengthened by the addition of cover plates. Attachment of cover plates by bolting is generally preferable to welding to avoid fatigue prone welding details. For older metal trusses, weldability of older steels or wrought iron may also be questionable, and must be carefully investigated prior to welding.

If the deck of the bridge is reinforced concrete, strengthening of the metal floor beams may also be possible by the addition of shear connectors, in order to develop composite action between the deck and the beams.

Metal floor beams can also be strengthened by the use of post-tensioning. Steel cables are connected the ends of the tension flange, and are tightened by turnbuckles or other tensioning devices. This induces a bending moment in the beam that counteracts the dead and live load moment, thereby increasing the capacity of the beam.

If adequate clearance is available under the bridge, metal floor beams can also be strengthened by the addition of a kingpost truss system. This requires the installation of a truss with one or more posts to the bottom flange of the beam. Threaded end connections are provided so that proper tension can be induced in the system.

6.3.2 Damage and Deterioration

As discussed in Section 6.2, a variety of different types of damage or deterioration may be found in older truss bridges. Bridge members that exhibit impact damage or other geometric distortions can frequently be repaired by flame straightening. Information on repair techniques for a variety of different types of distress in bridge members is available in NCHRP Report No. 271 [NCHRP #271, 1984].

Corrosion of truss bridges can be reduced by repainting the bridge, and addressing drainage problem areas. This includes repairing or replacing expansion joints that permit water to infiltrate the bridge floor system.

Repair of fatigue damaged details is case specific and is generally dependent on the size and location of cracks. Repair techniques include hole drilling and peening. Fatigue crack repair methods are described in [Fisher, J.W., 1990].

Nonfunctional bridge bearings can be replaced, or cleaned and adjusted to the proper alignment.

6.3.3 Truss Strengthening

Several techniques are available for increasing the load capacity of existing trusses, as follows:

- Addition of Supplemental Members

Additional chord or diagonal members can be added to increase truss capacity. These are typically added parallel to existing members. For example, if the tension chord is made of a pair of eyebars, an additional

member can sometimes be added between the two eyebars. Connections between the new members and the existing truss requires careful consideration.

- **Post-Tensioning**

Post-tensioned steel cables can be used to increase the load capacity of tension members in the truss. Cables are attached to the member ends and tensioned with turnbuckles or other devices. A similar procedure can be used along the entire tension chord of a truss. In this case, the cables are attached to the end bearing points and then tensioned. Post-tensioning can also be used for floor beams, as discussed earlier. Section 6.3.4 provides a more detailed description of post-tensioning.

- **Supplemental Truss Supports**

In some cases, it may be feasible to add supports to a truss bridge. By placing these supports under the first interior panel point, the truss span can be reduced significantly. Connections to the truss should be designed to provide vertical support without changing the expansion characteristic of the bridge.

6.3.4 Truss Strengthening by Post-Tensioning

Post-tensioning truss bridges is a means of strengthening and creating redundancy in the structural system. Post-tensioning increases strength, fatigue resistance, and redundancy, and reduces deflections and member stresses. Thus, the remaining life of a truss bridge can be increased by this technique.

The post-tensioning forces needed to strengthen the deficient members are a function of the tendon layout, tendon cross-sectional area, and truss type. The effect of post-tensioning forces on the members is dependent on the truss type, connectivity of the members, and tendon layout within the group of members.

The analyses of a post-tensioned truss can be carried out in three stages. In the first stage, an analysis of the truss is carried out under dead load only. The second stage of analysis is performed using the post-tensioning loads as applied to the truss joints. In the third stage, an analysis is performed using live, impact, and any additional loads. The stiffness of the tendons is considered only in the third analysis stage. The final solution is obtained by superimposing the solutions of all the three analyses.

For a statically determinate truss, if the tendon layout coincides with one or more truss members, then these members are the only ones affected by post-tensioning; all other members are unaffected. On the other hand, for a statically indeterminate truss, no matter how the tendons are arranged, a group of redundant members is affected by post-tensioning if the tendon passes within that group.

The relation between the cross-sectional area, the post-tensioning force of the tendon, and the desired final member stress, after post-tensioning can be easily derived for the statically determinate truss, see for example [Troitsky, M. S., 1990].

For statically indeterminate trusses, the stiffness analysis can be based on the three-stage solution. However, the design, which involves the selection of the magnitude of the post-tensioning force for a specified tendon profile, requires an

iterative trial-and-error solution. The equations presented in the above reference can be used as a guide to start the iterative solution scheme.

Other design considerations requiring special attention include post-tensioning losses, detailing end anchorages, pulleys for draped tendons, buckling of compression elements, members' stress level before and after post-tensioning, initial and final fatigue conditions, corrosion and construction feasibility.

The post-tensioning losses include tendon relaxation, structural steel creep, and anchorage set. The creep of structural steel is relatively small and hence can be neglected. Losses due to tendon relaxation and anchorage set can be determined with the currently used method in post-tensioned concrete elements. End anchorages for post-tensioned trusses can be of the same type as those used in post-tensioned concrete elements.

The effect of the sequence of post-tensioning on the stress level and the stability of all truss members need to be evaluated and checked. Adequate safety against yielding of tension and compression members, and buckling of compression members at the end of each post-tensioning stage should be provided.

Other considerations related to post-tensioning include corrosion protection of the tendons, tendon anchorages, and the effect of post-tensioning on the fatigue strength of the truss. All these factors should be properly investigated prior to finalizing details of post-tensioning.

6.3.5 Substructures

Abutments and piers in older bridges can sometimes be subject to considerable movement or settlement. Longitudinal movements of abutments can be stabilized with the use of tiebacks to anchor the abutment to soil or rock anchors. Devises should be used to distribute the tieback load over the abutment.

Settlement is often a difficult and costly problem. Underpinning of abutments can be used to prevent continued settlement. Providing a supplemental support for the approach span can also reduce settlement. This can be accomplished by constructing a pile bent or other support at the rear face of the backwall to support the approach span. An additional support can also be provided in front of the abutment to help support the bridge superstructure. Soil stabilization procedures can also aid in reducing settlement.

Where lateral earth pressure is causing movement of an abutment or pier, a cutoff structure can be constructed to resist lateral forces. Sheet piling driven behind and abutment is an example of this technique.

Proper drainage can often be effective in addressing abutment stabilization problems. Reducing hydrostatic pressure behind abutments, preventing saturation of supporting soils, and preventing erosion in front of the abutment can reduce stability problems.

Masonry piers supporting older truss bridges often exhibit deteriorated mortar. This can be address by repointing. Repointing is the process of removing deteriorated mortar from the joints of a masonry wall and replacing it with new mortar. Repointing can restore the visual and structural integrity of the masonry.

Scour can also be a problem at bridge piers. The placement of riprap is the most common technique for protection against local scour. Alternatives to riprap include grout bags, extended footings, tetrapods, cable-tied blocks, anchors and high density particles.

6.4 CASE STUDY BRIDGE: REHABILITATION OPTIONS

The previous sections of this chapter provided a general discussion of typical deficiencies found in older metal truss bridges and some possible repair and rehabilitation options. This section discusses problem areas and possible rehabilitation approaches for the case study bridge in Shackelford County, Texas. The discussion is separated into three areas: the timber deck, the metal floor beams, and the trusses.

6.4.1 Timber Deck

The timber floor system consists of longitudinal timber stringers resting on top of metal floor beams. Timber floor planks are placed transversely over the stringers, and are nailed to the stringers. There are a total of seven stringers running between adjacent metal floor beams, as shown in Fig. 2.2. Five of these seven stringers are 3" wide ×12" deep timbers. The remaining two stringers are 8" wide ×16" deep timbers. In order to provide the same top elevation for all stringers, the 16" deep stringers are notched at their ends where they sit on the metal floor beam. That is, the 16" deep stringers essentially have dapped ends.

As described in Chapter 2, several additional older stringers are located between the seven stringers described above. These appear to have been left in place from previous deck rehabilitation. One of the simplest things that can be

done to improve the load rating of this bridge is to remove these old stringers. These old stringers add substantial dead load to the bridge, but contribute little to the floor capacity as indicated by the structural analysis described in Chapter 4. Removing these old stringers will reduce the total dead load on the bridge by 22-percent, thereby permitting an increase in live load capacity. The load rating presented in section 4.10 already presume that the old timber stringers have been removed. In absence of the old timber stringers, inventory load rating, based on allowable stress method, of the metal floor beams was increased from H7.1 to H9.4.

The load rating conducted for this bridge (Chapter 4) indicated that the timber stringers controlled the load rating. Because of uncertain material properties, the load rating process indicated that the seven floor stringers had a load rating essentially of zero. Clearly, this load rating is not an accurate assessment of their true load carrying capacity, since the bridge floor system supported the load test vehicles during the field load tests described in Chapter 5. One option to address this problem is to attempt to improve the load rating of the stringers through further materials evaluation. Additional testing and inspection of the stringers by a wood specialist will assist in identifying the species and provide further information on condition and strength. This, in turn, may justify the use of substantially higher allowable stresses for the stringers. The use of an improved model for structural analysis of the timber floor deck, as described in Chapter 4, can provide a better assessment of the forces in each stringer. These forces will often be lower than those predicted by the more conservative simplified analysis

methods typically used for load rating. Combining improved material strength evaluation with improved structural analysis may well lead to a substantially increased load rating for the stringers. Further detailed evaluation of the dapped stringer ends would also be required to assure that notches cut into the ends of the stringer do not adversely affect their strength.

An alternative approach for addressing the low load rating for the timber stringers is replacement. This would entail removing all existing timber stringers and planks and providing a new system of stringers. The new stringers could be, for example, glue-laminated timbers, steel-timber composite sections, or new steel wide flange sections. Glue laminated or solid timber stringers can be used depending on the availability and cost. Once the new stringers are placed, it would be possible to reuse many of the existing timber planks, replacing only those that are in poor condition. Alternatively, all new planks could be provided, or some other type of surface can be provided such as corrugated deck, or steel or fiberglass grating. Numerous options are available for replacement of the stringers and deck.

To illustrate some of the possibilities for deck replacement, several new stringer designs will be considered. It is assumed that timber planking (new or reused) will be placed over and attached to the new stringers.

For the design of the new stringer system, it was assumed that seven new stringers will be provided for each span, and will be located at the same positions as the existing stringers. All stringers will sit on top of the metal floor beams. Further, all seven stringers will be 12" deep in order to maintain the same top of

deck elevation as the existing deck and to avoid the need for dapped ends. Making all seven stringers the same depth will also provide for a more uniform distribution of live load among the stringers.

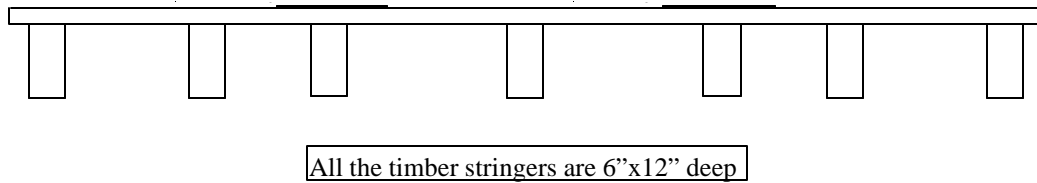


Figure 6.1: New timber deck layout with all timber stringers

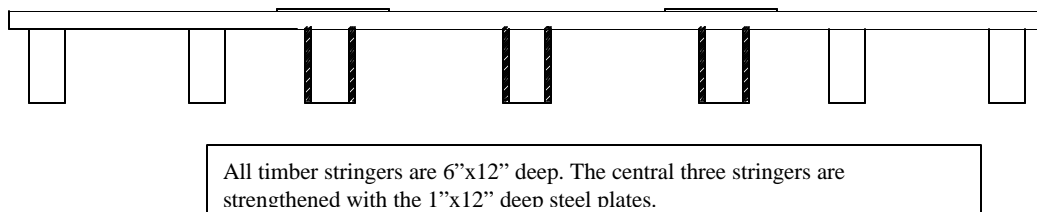


Figure 6.2: New timber deck layout with the steel-timber composite stringers

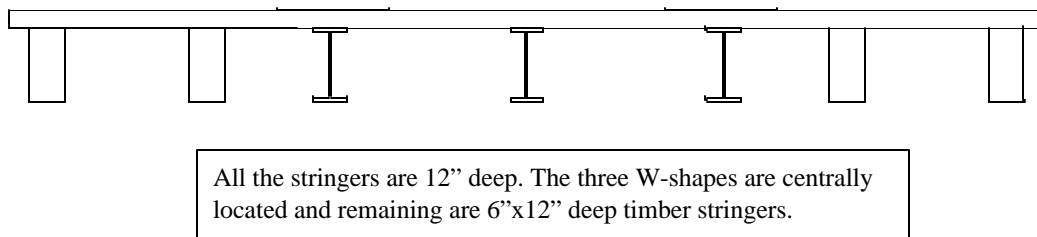


Figure 6.3: New timber deck layout with W-shape stringers

Figures 6.1 to 6.3 shows three possible options for stringer replacement. There are, of course, many other suitable options. For each layout preliminary analysis was carried out to determine load distribution between different stringers.

Figure 6.1 shows the case where all seven new stringers are 6" wide \times 12" deep timbers. Based on assumed 6" width of the timber stringers, the load rating

of the new stringer system was evaluated. The load rating of this new stringer system was found to be less than H15 loading. However, this option can be considered if load posting is needed. Treated glue-laminated timber or solid timber stringers can be used depending on availability and cost.

An additional option is the use of steel-timber composite sections, as illustrated in Figure 6.2. Steel plates are attached to the sides of timber sections. Placing the steel plates on the sides enhances both the bending and shear strength of the composite section, and leaves the top free to accept nails for attaching planks. For economy, it may be possible to only provide steel plates in the center three stringers, as shown in the figure. For preliminary design, 1"x12" deep A36 steel plate was selected. The composite steel-timber stringer sections can be designed based on the procedure presented in [Ryder, G.H., 1957]. The load rating for this stringer system was found to be less than H15 loading. However, this option can be considered in detail if load posting is needed.

A third option is shown in Figure 6.3, where the central three stringers are steel wide flange sections, and the remaining outer stringers are timber. The steel sections could be simply supported between metal floor beams, or could be made continuous over the metal floor beams. Steel wide flange stringers that are continuous would provide greater strength, but may pose problems with transporting, handling and placing very long members. A particular W-shape can be selected based on the desired load rating level. Various connection details to attach timber planks to steel stringer are presented in [Vegešna, S., 1992 and Webb, S. T., 1992].

Whatever new deck system is chosen, if its weight is substantially different than the existing deck, the bridge should be reanalyzed considering the new deck weight.

6.4.2 Metal Floor Beams

The metal floor beams are tapered sections, as shown in Figure 2.4. The inventory load rating for the floor beams (Section 4.10, Table 4.2) was H9.4, based on allowable stress design. Based on this low rating, strengthening of the floor beam may be necessary. For nominal capacity calculations of these metal floor beams, the unsupported length of the compression flange was taken as span of the floor beam, i.e., 180". The nominal capacity can be increased if the unsupported length of compression flange is reduced. The reduction in the unsupported length of the compression flange can be achieved by providing lateral restraint to the flange. Lateral restraint may be available from the timber stringers resting on the metal floor beam, as discussed in [Vegešna, S., 1992 and Webb, S. T., 1992].

The nominal capacity of the metal floor beams was calculated considering this lateral restraint of the timber stringers. However, for this case study bridge, the capacity could not be increased, as allowable stress based on lateral torsional buckling was higher than the maximum allowable stress. Other options for increasing nominal capacity of these metal floor beams are attaching cover plates or structural shapes at top and bottom of the floor beams or providing post-tensioning. The preliminary design for attaching cover plates is presented in

sections 6.5.2 and 6.5.3. Detailed discussion on cover plating is presented in [NCHRP #293, 1987 and NCHRP #222, 1980].

6.4.3 Truss

As indicated in Section 4.10, the inventory load rating for the truss superstructure (not including metal floor beams) based on allowable stress design, was H16.6 for an H-loading, or HS9.6 for an HS-loading. This relatively high rating may be adequate, depending on the intended future service of the bridge. Should this rating be inadequate, some approaches for strengthening the truss will be presented in the following section.

Even if it is deemed that the current load rating for the truss is adequate for continued vehicular service, some repair and maintenance of the truss is recommended, as follows:

- Bracing and tension rods with turnbuckles should be tightened to remove slack from the rods.
- There is a bent hanger, L1U1, on the downstream truss. Since this is a tension member, the kink in this member should have little impact on member capacity, and it is likely acceptable to leave this bent hanger as is. Nonetheless, the kink in this tension member could potentially lead to a fatigue crack. Consequently, if the member is not repaired, this area should be examined in future routine inspections. If repair of this member is desired, heat straightening techniques can likely be used.

- The original railing is still in good condition, except that the railing supports are disconnected from the deck in a number of locations. The railing supports should be reconnected to the new deck.
- The truss members, despite being in service, exhibit remarkably little corrosion. No paint is currently visible. It appears that the truss can likely be left unpainted, and just inspected periodically for the development of any corrosion problems. Although not essential, painting the bridge will help mitigate future corrosion, and will enhance the aesthetics of the bridge.
- The roller bearings are dislocated from their original position and are filled with debris. The rollers should be cleaned, lubricated and properly aligned.
- There are several brackets welded to the bottom tension chord eyebars of the truss. It appears that these welds were likely made with unqualified procedures. Poorly made welds can initiate a fatigue crack. Since these bottom chord eyebars are fracture critical members, these welded brackets represent a potential safety problem. The brackets and welds should be removed from the eyebars. This can be done by carefully grinding off the welds, taking care not to remove material from the eyebars and without introducing nicks or gouges. The area should then be inspected for any cracks using a method such as dye penetrant. Ultrasonic examination of the eyebars in the region of the removed welds can provide further assurance against the presence of cracks.

6.4.4 Substructure and Approach Spans

The masonry piers for the truss should be repaired. This will require regrouting and repointing of open masonry joints. Stone masonry units which have become dislocated or have fallen out of the pier should be repositioned or replaced as needed. Some scour protection, such as the placement of riprap, is recommended at the base of the piers.

The approach spans of the truss bridge were not included in the scope of this study. However, the approach spans are in considerably poorer condition than the truss, and would need to be addressed as part of an overall rehabilitation plan, either by repair or replacement.

6.5 CASE STUDY BRIDGE: REHABILITATION PLAN

To further illustrate options for rehabilitating the case study bridge, three overall rehabilitation plans were considered, as follows:

- I) Do nothing;
- II) Rehabilitate the bridge for H15 loading;
- III) Rehabilitate the bridge for HS20 loading.

6.5.1 Plan I: Do Nothing

In this plan, minor repairs can be carried out as described in section 6.4.3 and the bridge can be kept for pedestrians.

6.5.2 Plan II: Rehabilitate the Bridge for H15 Loading

The truss is already adequate for H15 loading, and would only require the repair items noted in section 6.4.3. The timber deck and metal floor beams,

however, will require strengthening to an H15 level. For the timber deck, the options suggested in Section 6.4.1 can be used. The new timber deck can be easily designed for an H15 load rating.

The metal floor beams can be strengthened by attaching top and bottom cover plates. Calculations show that cover plates of 6½” width x 0.3” thickness of A36 steel will be sufficient to bring the metal floor beam to H15 load rating. The cover plates can be attach to the floor beams during replacement of the timber stringer system. Timber deck dead load and truck load will act on the composite section of the metal floor beam and hence overall sectional properties can be used for load rating calculations. The cover plates can be easily bolted to the existing floor beam during the timber deck replacement.

6.5.3 Plan III: Rehabilitate the Bridge for HS20 Loading

The trusses, metal floor beams and timber deck would all require strengthening to achieve an HS20 load rating. For the timber deck, the options suggested in the Section 6.4.1 can be used, with the new timber deck designed for an HS20 load rating.

The truss tension chord, hangers and all diagonal members are currently rated below HS20. Hence, major strengthening measures would be needed. For rehabilitation of the tension chord, addition member can be added as shown in Figures 6.4 and 6.5. This detail is presented in a paper by Bondi, [Bondi, R.W., 1985]. The hangers need to be replaced with new hangers as the geometry of the cross-section will not allow any suitable means of rehabilitation. The diagonal members can be strengthened either by addition of new member or by post-

tensioning. The analysis of post-tensioned trusses is described in the Section 6.3.4. The other details of the truss i.e. pins, joint details, and the U-bolt connection details at the metal floor beam ends must also be properly evaluated for the higher load levels.

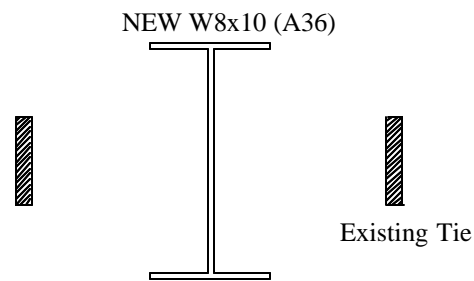


Figure 6.4: Addition of member to tension chord

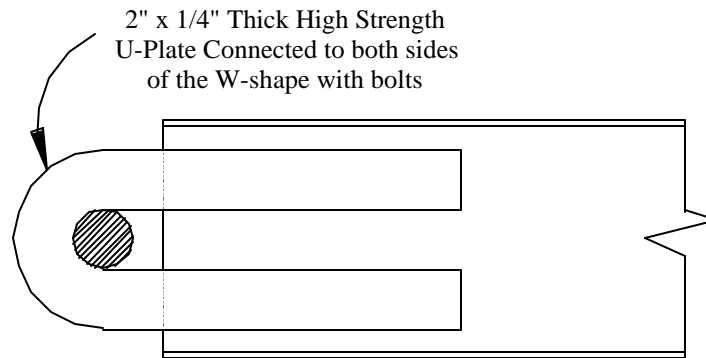


Figure 6.5: Connection details for the added member

The floor beam will require 6½” wide x 1.15” thick top and bottom A36 steel cover plates to increase the capacity to HS20 live load. Bolting 1.15” thick plates to the 0.3” thick existing angle is not a practical solution. The width required for the thinner cover plates is much larger than the 6½” and hence also not a practical solution. In addition, the floor beam is deficient for shear

developed by HS20 truck. The only reasonable solution is to replace the floor beams either with W-shape beams or with fabricated tapered beams with the required capacity. This plan will require major and costly modifications to the main trusses, and hence does not appear practical. The reasonable load rating is H15 and hence the bridge should be load rated at H15.

Chapter 7

Summary and Conclusions

7.1 REVIEW OF PROJECT SCOPE AND OBJECTIVES

This report has documented a study on the structural evaluation and rehabilitation of historic metal truss bridges. More specifically, this study focused on historic “off-system” metal truss bridges in Texas. The term “off-system” indicates that these bridges are not on the state highway system. Rather, off-system bridges are typically located on county roads or city streets. The term “metal” is used to describe these bridges, as they may be constructed using wrought iron, cast iron or steel. There are a large number of older off-system metal truss bridges still in vehicular service in Texas. A number of these are of significant historical interest due to their age and other unique features, and are either listed or eligible for the National Register of Historic Places.

Many of the historic off-system metal truss bridges in Texas were constructed in the late 1800’s and early 1900’s by private bridge companies located in Texas and elsewhere. They were not designed to modern highway bridge loading standards using “H” or “HS” truck loading criteria. In fact, a number of these bridges predate the automobile, and were initially intended to carry horses, livestock, farm vehicles, etc.

Considerable interest exists in maintaining historic metal truss bridges in continued vehicular service. However, achieving this goal is often problematic due to structural and functional deficiencies found in these bridges. The structural load rating can often be very low due to the initial low design loads used for the bridge combined with damage and deterioration that has occurred over the very long service life of the bridge. In addition to structural problems, off-system truss bridges also frequently suffer from functional deficiencies due to narrow widths and constricted vertical clearances. Most off-system historic metal truss bridges in Texas are single lane bridges.

The primary objective of the study reported herein was to address structural issues involved with historic off-system metal truss bridges. More specifically, the objectives were to examine methods that can be used to develop an accurate and realistic load rating for an old metal truss bridge, to examine methods that can be used to strengthen the bridge, if needed, and to address problems of damage and deterioration.

7.2 SUMMARY OF MAJOR PROJECT TASKS AND FINDINGS

In order to investigate structural issues involved with historic metal truss bridges, a case study bridge was chosen as the focus of this study. The case study bridge was used to provide a real-world example of the types of problems encountered in an old metal truss bridge, and to provide a model of evaluation and rehabilitation techniques that can be applied to other off-system truss bridges.

The case study bridge chosen for this investigation is located in Shackelford County, Texas. The bridge is on County Road 188 near Fort Griffin,

and crosses the North Fork of the Brazos River. It is located in a rural area on an unpaved road used primarily by local ranchers, farmers and residents. The bridge was originally constructed in 1885 by a private bridge company, and remained in vehicular service for over one hundred years. It was only recently closed to traffic due to a low structural sufficiency rating. The bridge is a pin-connected Pratt through truss with a span of 109-feet and is the oldest surviving Pratt through truss in Shackelford County and one of the oldest in the state of Texas. The truss is made of metal members. Bottom chord members are eyebars and top chord members are riveted built-up sections. The floor system is made of transverse metal floor beams attached to the bottom chord panel points of the truss. The floor beams are tapered in depth, a unique feature found in many older off-system bridges. The remainder of the deck is timber. Longitudinal timber stringers are supported by the metal floor beams. Transverse timber planking is placed over the stringers. The entire truss bridge is supported on two tall stone masonry piers.

The investigation of the case study bridge was divided into several tasks, as follows:

- collection of data on the bridge;
- evaluation of materials;
- structural analysis and load rating;
- field load testing; and
- development of rehabilitation options.

7.2.1 Data Collection

The first task in this case study was data collection. This involved collecting information needed to conduct a structural analysis and load rating for the bridge. The required data includes the length, cross-sectional dimensions and condition of all structural members in the bridge, in addition to information on connection details. Information on the cross-sectional shapes and dimensions for a bridge can usually be obtained from the original construction drawings. For the case study bridge, no drawings were available. This is likely a common situation for older off-system bridges. Consequently, every member of the case study bridge was measured, and a set of bridge drawings was prepared. A complete photographic record of the bridge and its components was also prepared.

In addition to recording the basic bridge geometry and member dimensions, an inspection of the bridge is needed to identify any damage or deterioration to the structural members. An inspection of the case study bridge indicated that its overall condition was reasonably good. Although all members exhibited surface corrosion, there was no apparent significant loss of cross-section on any member. Some members exhibited bent areas, likely due to vehicle impacts. Further, several of the bottom chord eyebars had brackets welded to them to carry a pipe across the bridge. These welds were not part of the original construction, as structural welding was not yet available in 1885. These welds were likely made using unqualified welding procedures, and are a potential source of fatigue cracking and a potential fracture initiation site. The presence of such unqualified welds on the eyebars, which are fracture critical members, was an

area of concern. The inspection also revealed that the roller bearings for the bridge were dislocated from their original position, were filled with debris, and were likely no longer functioning as rollers. The portion of the case study bridge which exhibited the greatest degree of deterioration was the timber deck. A number of the timber stringers were in rather poor condition.

The case study bridge exhibited problem areas typical of many older off-system metal truss bridges: corrosion, impact damage, presence of unqualified welds, nonfunctional bearings, and a deteriorated timber deck.

7.2.2 Evaluation of Materials

The second major task in this study was materials evaluation for the bridge. Since no original construction records were available for the bridge, the type and properties of the metal used in the bridge were unknown. Based on the age of the bridge, the material of construction was most likely wrought iron, although this was not completely certain. For evaluation of older bridges, AASHTO (1994) provides a recommended yield stress for metals, based on the age of the bridge. Consequently, these AASHTO specified values could be used for load rating, with no additional materials evaluation or testing required.

For the case study bridge, additional testing was conducted on the bridge metal. The purpose of this testing was to determine if the AASHTO specified material properties were appropriate for the bridge, and to provide additional information that would be useful in evaluating the bridge and addressing problem areas. As part of this evaluation, the material was first examined in the field. Small areas of various members were polished, etched and examined under a

magnifying glass. This visual examination revealed the presence of lines of slag, suggesting the material was wrought iron.

As a next step in the materials evaluation process, several small lacing members were removed from the bridge and subjected to laboratory testing. Lacing members were used for this purpose as these could be removed without endangering the safety of the bridge. The critical members of the bridge were the bottom chord eyebars and the metal floor beams. However, a sufficient amount of material to permit laboratory testing could not be removed from these members without adversely affecting their strength.

Laboratory tests conducted on the lacing members included tension testing, hardness testing, chemical analysis, and metallographic examination. These laboratory tests indicated that the material was in fact a high quality wrought iron. The material showed a yield stress approximately 10 ksi higher than the values specified by AASHTO, and also showed good elongation. High quality wrought iron exhibits a number of desirable properties, including resistance to fatigue and fracture, good corrosion resistance, and good weldability. The slag inclusions characteristically found in wrought iron serve as natural barriers to the propagation of cracks and corrosion, and the very low content of carbon and other alloys make most types of wrought iron quite weldable. This type of information is useful when evaluating the potential consequences of various types of damage and for the development of appropriate repair or strengthening procedures.

As a last step in the materials evaluation process for the case study bridge, field hardness tests were conducted on a number of bridge members. The purpose

of these tests was to compare the hardness of the lacing members with that of other members. These tests indicated that the bridge members showed hardness values very similar to that of the lacing members. This suggested at least some degree of similarity between the laboratory tested lacing members and the other, more critical bridge members such as the eyebars.

Ultimately, when load rating the bridge, the AASHTO specified values of yield stress were used rather than the significantly higher measured values from the lacing members. Despite the similarity of hardness values, there was not complete certainty that the mechanical properties of the lacing members were the same as that of the other members. Nonetheless, the material tests provided confidence that the AASHTO specified values for material yield strength was safe, and likely quite conservative. Further, the data provided by the materials tests provided valuable information to aid in the overall evaluation of the bridge.

The materials evaluation tests conducted on the case study bridge were all standard tests that can be performed inexpensively by most testing laboratories. Further, these tests provided a great deal of useful information on the bridge. The use of such simple material testing techniques appears to be a highly useful and cost-effective measure for evaluation of historic off-system metal truss bridges.

7.2.3 Structural Analysis and Load Rating

The next major task in this study was structural analysis and load rating. This task was separated into three analyses: the trusses, the metal floor beams, and the timber deck. The trusses were analyzed with simple classical analysis methods that can be done by hand, as well as with computer models. Several

computer models were examined, including two and three-dimensional models, as well as models that included fixity at some truss joints. All models predicted essentially the same member forces. This work suggested that the use of advanced computer models offered no significant advantages for the trusses. Simple hand methods of analysis or simple computer models of the truss appear quite adequate. The trusses of the case study bridge, typical of many off-system trusses, are simple structures with a low degree of redundancy. Consequently, there are few alternate load paths within the truss, and simple methods of analysis are appropriate.

Very simple analysis methods were also used for the metal floor beams. These members were analyzed as simply supported beams, with loads applied at the location of the timber stringers. The floor beams were non-prismatic members, with the depth varying over the length of the member. The variable depth was considered in the analysis of the members, but posed no particular complication. The accuracy of this very simple model for the metal floor beams was later confirmed in the field load test of the bridge.

The final analysis conducted for the bridge was for the timber stringers. A key issue in this analysis was the distribution of wheel loads to the stringers. The stringers were first analyzed using simple hand methods of analysis with AASHTO (1996) specified distribution factors. Various computer models were also developed of the floor system, including a three dimensional model. The computer models showed significantly lower forces in the timber stringers than the simple AASHTO procedures. Consequently, while the use of advanced

computed models did not appear to be of value for the trusses or for the metal floor beams, they appear to offer some advantage in obtaining a better estimate of member forces in the floor stringers. Further, while these computer models require more effort than the simplified AASHTO procedures, these models are still relatively simple, and can be developed using commonly available commercial structural analysis software.

After completion of the structural analysis, load ratings were developed for the bridge using AASHTO procedures. Inventory and operating level ratings were developed using both the allowable stress design (ASD) and load factor design (LFD) procedures in AASHTO. Further, the bridge was rated for both an “H” truck and for an “HS” truck. Results of the load rating were essentially the same using the ASD or LFD procedures.

The inventory load rating for the truss was about H15, and was controlled by the bottom chord eyebars. The inventory rating for the metal floor beams was just under H10. Interestingly, for the timber stringers, standard load rating procedures using conservative AASHTO specified timber strength estimates, resulted in a load rating of zero. That is, the load rating calculations indicated that the timber stringers were inadequate to even carry the dead load of the timber deck, and therefore had no live load capacity. This was obviously an overconservative rating for the timber stringers, as they were clearly carrying dead load.

7.2.4 Field Load Testing

The next major task undertaken in the case study was field load testing. Two field load tests were conducted on the bridge. In each test, a number of bridge members were instrumented with strain gages. A vehicle with known axle weights was then passed over the bridge, and readings were taken from the gages. The measured strains were converted to stresses, and then compared to the stresses predicted by a structural analysis of the bridge for the same vehicle. The purpose of the field test was to evaluate the accuracy of the structural analysis and to help identify any potential problem areas in the bridge. Only the metal truss members and metal floor beams were instrumented. Although the timber stringers were critical for the load rating, these were not instrumented in the load test, as interpreting strain data for a timber member would have been difficult and likely inconclusive. Further, it was assumed that the timber would be replaced as part of any bridge rehabilitation plan.

The field load tests were conducted using vehicles that weighed approximately 3 tons. Even though the load rating for the stringers indicated no live load capacity whatsoever, it was the judgment of the researchers that a 3-ton vehicle could be safely accommodated. Both field load tests were, in fact, successfully completed without any apparent distress in the timber stringers or any other bridge member.

Several observations were made from the field load test. First, it was found that interpretation of the field data was quite difficult for truss members with built-up cross-sections. Members made of various shapes and plates that are

riveted together exhibited very complex distributions of stress among the elements of the cross-section. It was found that even with a large number of gages on the cross-section, it was quite difficult to reliably estimate the axial force in the member from the strain gage data.

The field load test data for the simpler, single element members such as eyebars, rods, and hangers could be interpreted more clearly. Although all of these members exhibited bending in varying degrees, the axial force in the members could still be accurately estimated by using a sufficient number of gages over the cross section of the member.

Evaluation of the reliable field load data indicated that the truss behaved essentially as predicted by a simple structural model. One notable exception was for the bottom chord eyebars. The field-measured stresses were typically considerably smaller than those predicted by structural analysis. Interestingly, for some loading cases, the field data showed compressive stresses in the bottom chord eyebars. This anomaly was ultimately attributed to the bridge's nonfunctional roller bearings. To examine this hypothesis, the structural model for the bridge was modified to restrict horizontal movement at the roller. For this model, the analysis showed similar trends in the bottom chord forces as seen in the field data. It was deemed that these lower measured stresses in the bottom chord could not be used to increase the load rating of the bridge, as the roller bearings may move at large loads or after receiving maintenance.

The metal floor beams were also instrumented in the field load test. The stresses measured in the beams showed very close agreement with those predicted from the simple analysis model used for the beams.

Overall, the field load test confirmed that the structural analysis models used for the truss and floor beams were reasonable and appropriate. Consequently, the load ratings developed previously for the truss and floor beams were not altered as a result of the field load test. Nonetheless, the field load test was useful in developing confidence in the analysis approach.

The field load test was also useful for diagnosing the problem with the nonfunctioning roller bearings. Interestingly, the field test data indicated that the nonfunctioning roller bearings were not detrimental to the live load capacity of the bridge, and were even somewhat beneficial by reducing tension stress levels in the critical bottom chord members. Ultimately, however, frozen roller bearings can cause other problems associated with the development of additional stresses due to constrained thermal movements of the bridge or due to substructure movements. An interesting phenomenon observed in a number of off-system truss bridges are buckled eyebars in the bottom “tension” chord of the truss. This appears to be due to compressive stresses in the eyebars developed when the roller bearings have frozen, and the bridge piers have moved or tilted slightly inwards. Due to the very low buckling capacity of an eyebar, only very small movements of the piers are needed to cause buckling of the bottom chord if the roller bearings are not properly functioning.

Based on the experience of this case study, it appears that field load testing is not likely justified for most historic off-system metal truss bridges. Field load testing can be a difficult and costly undertaking, requiring specialized equipment and expertise. Further, interpretation of the field data requires considerable experience and judgment, and can be quite difficult and time consuming. While very useful in the context of a research project, field load testing is not likely a cost-effective measure for routine evaluation purposes. Nonetheless, for particularly critical or complex bridges, field load testing can provide very useful insights into the behavior of the bridge, and may be justified in some cases.

7.2.5 Development of Rehabilitation Options

The final task of this study was to evaluate options to rehabilitate the case study bridge so that it can be returned to vehicular service. The required rehabilitation measures depend, in part, on the desired load rating of the bridge. For new bridges or for bridges on the state highway system, a load rating of HS20 is generally required. However, for many historic off-system metal truss bridges, developing an HS20 load rating is not practical, and is not likely needed. For the traffic demands on these bridges, a lower HS or H rating may be quite acceptable, combined possibly with a load posting on the bridge. The desired load rating depends on local traffic conditions and the types of vehicles expected to use the bridge, and must be established on a case by case basis.

For the case study bridge, several possible load rating scenarios were investigated. All of the scenarios had several items in common. In all cases, it was assumed that the existing timber stringers would be replaced due to their rather

poor condition and uncertain load capacity. It was also assumed that damaged truss members would be repaired. For the case study bridge, this would require straightening of bent members and removal of the welds holding pipe brackets on the bottom chord eyebars. These repairs can likely be accomplished quite easily and inexpensively. Finally, the roller bearings should be realigned and cleaned.

Beyond the repair items noted above, rehabilitation techniques were investigated to achieve three load rating levels: H10, H15 and HS 20. For an H10 rating, only replacement of the timber stringers is needed, as the metal floor beams and truss already satisfy this rating. New timber stringers can be easily designed to achieve an H10 rating.

To achieve an H15 rating would require replacement of the timber stringers as well as strengthening of the metal floor beams. Larger timber stringers would be needed to achieve an H15 rating. Alternatively, composite timber-steel stringers could be used, or steel wide flange stringers could be used. The metal floor beams would need to be strengthened from their current H10 rating up to H15. This could be accomplished by a variety of methods, including the addition of thin cover plates bolted to the existing member. No strengthening would be required of the truss, as it already satisfies an H15 rating.

The final option evaluated was rehabilitating the bridge to achieve an HS20 rating. Substantial strengthening would be needed for the stringers, metal floor beams, and a number of truss members. The metal floor beams would require the addition of very thick cover plates or other strengthening measures, or replacement with new steel floor beams. The truss itself would also require major

strengthening. This could be accomplished by replacing understrength members, supplementing understrength members with additional members, post tensioning of the bottom chord, and a variety of other techniques. Developing an HS20 rating is likely to require very major and costly modifications to the bridge.

In summary, the results of the investigation of the case study bridge indicate that the bridge can likely be returned to vehicular service with an H10 or H15 rating, with only minor repairs, replacement of the timber stringers, and minor strengthening measures. With continued inspection and maintenance, this bridge should be capable of providing many more years of service. The investigation also indicated that returning the bridge to service with an HS20 rating will require major strengthening measures, and is not likely a practical option.

7.3 CONCLUSIONS

The results of this investigation and the detailed evaluation of the case study bridge have demonstrated a number of techniques useful for load rating, repairing and strengthening of historic off-system metal truss bridges. While these bridges typically exhibit a number of apparent structural deficiencies, many of these deficiencies can be addressed using simple and cost effective remedies. As demonstrated by the case study bridge, only minor repair and strengthening measures may be needed to allow continued use of the bridge in vehicular service. Of course, not all historic metal truss bridges can be saved. In some cases, the deterioration, damage or inherent lack of strength will be so severe as to practically preclude structural rehabilitation. However, in many other cases, only

a small additional effort may be all that is required to save an important historical resource.

Appendix A

Photographs of Case Study Bridge

This appendix presents a series of photographs of the case study bridge in Shackelford County, Texas. All photos were taken during spring 1999. Designations for bridge components referred to in these photographs are identified in the bridge drawings shown in Appendix B.



Photograph A.1: Case study bridge – looking towards south



Photograph A.2: Side view of the south approach span



Photograph A.3: Side view of the main truss span of the bridge



Photograph A.4: Side view of the north approach span



Photograph A.5: Details of the upstream truss



Photograph A.6: Details of the downstream truss



Photograph A.7: Details of the southwest roller support



Photograph A.8: Details of the northwest hinge support



Photograph A.9: Details at bottom chord joints L1 and L5



Photograph A.10: Details at bottom chord joints L2, L3, and L4



Photograph A.11: Connection details at bottom chord joint L1



Photograph A.12: Connection details at bottom chord joint L1



Photograph A.13: Details of tension rod L2U3 and L4U3, turnbuckle connection



Photograph A.14: Details at upper chord joints U1 and U5



Photograph A.15: Details at upper chord joints U2, U3, and U4



Photograph A.16: Details of top bracing connection



Photograph A.17: Details of bridge deck



Photograph A.18: Details of bridge deck



Photograph A.19: Details of the north stone masonry pier and the main span deck



Photograph A.20: Details of the south stone masonry pier and the main span deck



Photograph A.21: Details of the top lateral bracing system



Photograph A.22: Details of the turnbuckle of the top bracing tension rods



Photograph A.23: Details of metal railing



Photograph A.24: Details of metal railing connection to truss member



Photograph A.25: Details of the timber deck of the south approach span



Photograph A.26: Details of the metal bent of the south approach span



Photograph A.27: Details of the timber deck of the north approach span



Photograph A.28: Details of the connection between timber stringers in the north approach span



Photograph A.29: Details of the timber stringers of the main span resting on the south pier



Photograph A.30: Details of the ground slope at the base of the south pier



Photograph A.31: Details of the metal wing wall at the north abutment



Photograph A.32: Details at base of pipe column of metal bent for north approach span



Photograph A.33: Details of base of pipe column of metal bent for north approach span



Photograph A.34: Deteriorated foundation of metal bents for north approach span



Photograph A.35: Deteriorated abutment at south end of south approach span



Photograph A.36: Details of metal bent for north approach span



Photograph A.37: Details of the metal retaining wall at the north abutment



Photograph A.38: Details of the metal retaining wall at the north abutment

Appendix B

Drawings of Case Study Bridge

This appendix presents a series of drawings of the case study bridge in Shackelford County, Texas. All drawings are based on field measurements and observation of the bridge made in August 1998. Dimensions shown on the drawings are in millimeters, with equivalent dimensions in inches shown in parenthesis.

Figure B.1 provides an overall view of the bridge, and identifies the three major components: the main truss span, the north approach span and the south approach span. Figures B.2 to B.16 show details of the main truss span. The remaining figures show details of the approach spans and the bridge piers.

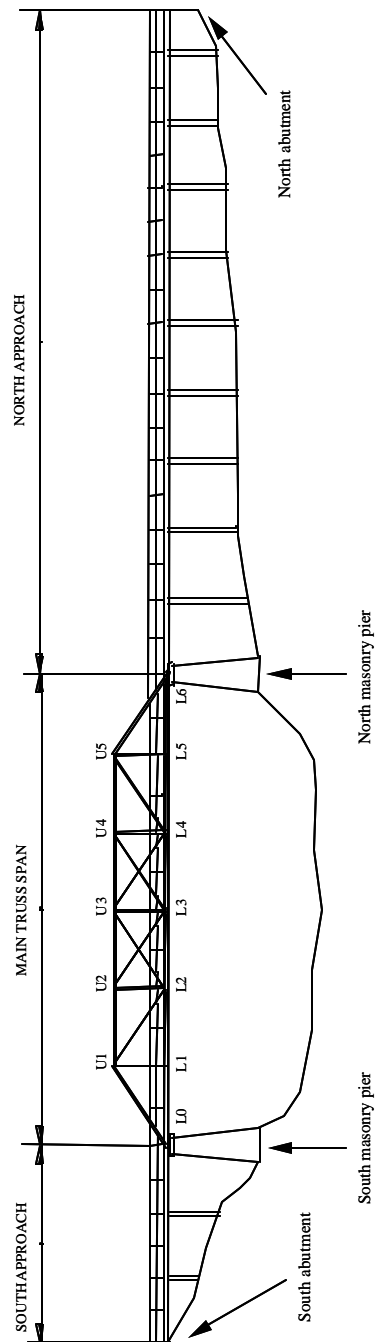


Figure B.1: Overall view of case study bridge

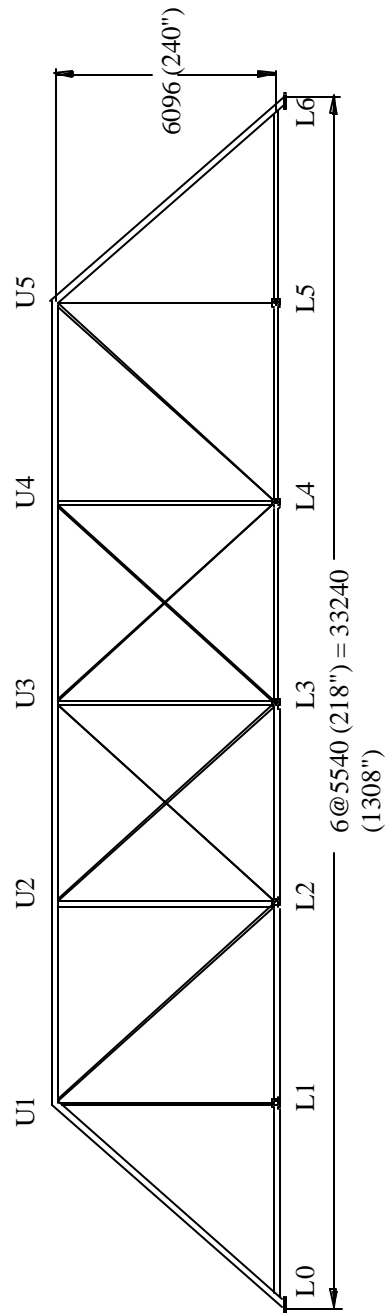


Figure B.2: Details of the metal truss

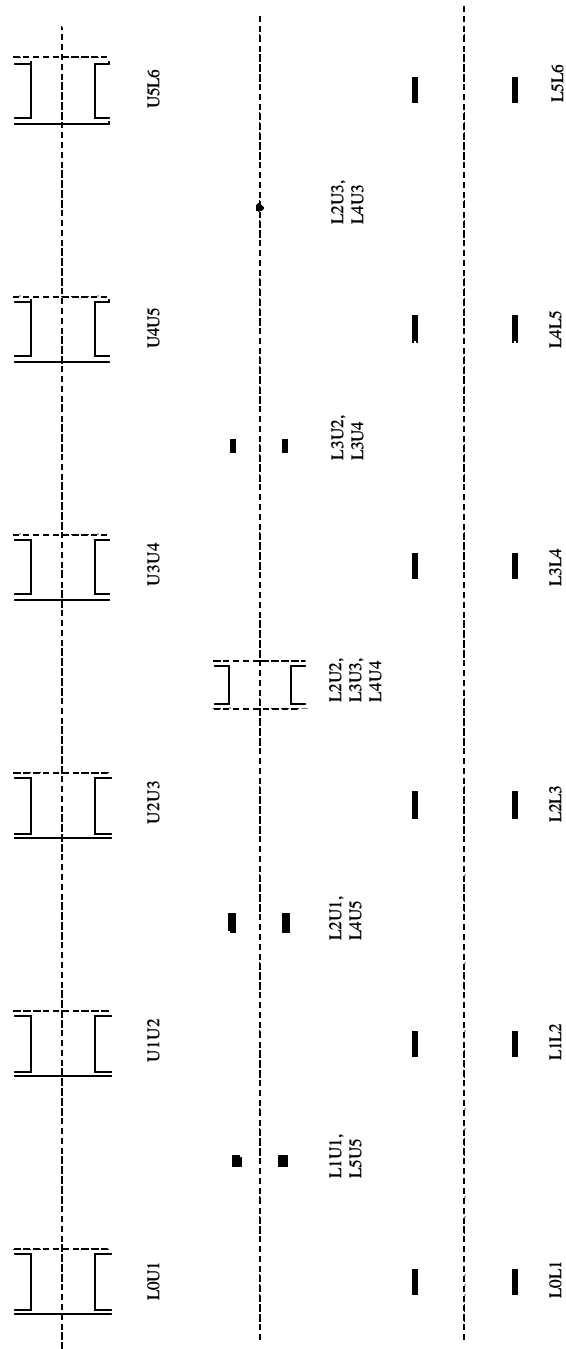


Figure B.3: Cross-sections of the truss members

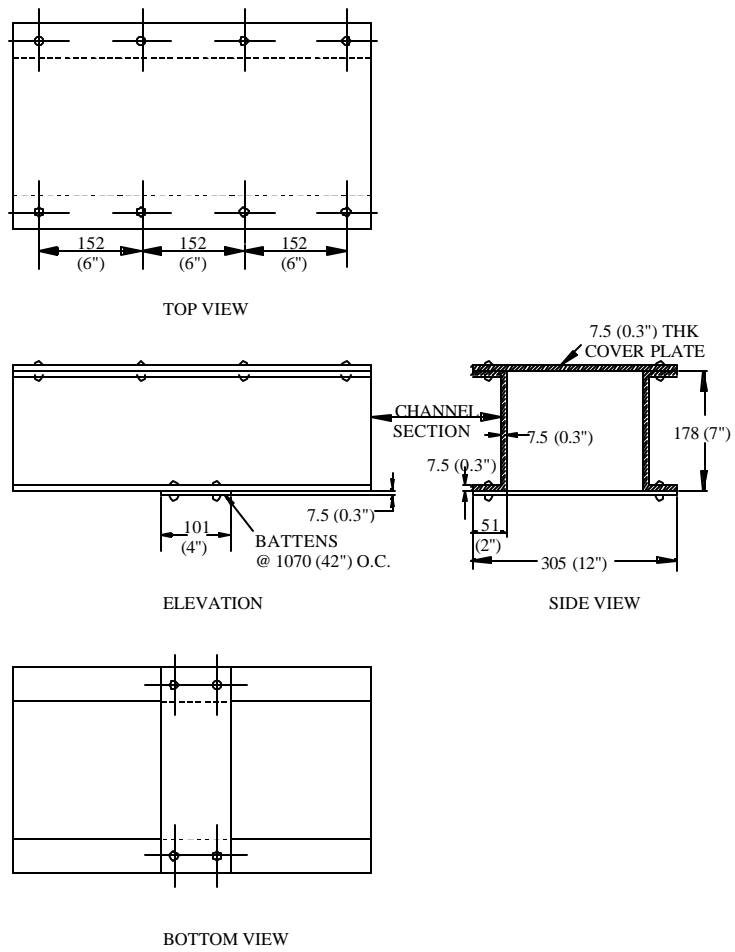


Figure B.4: Details of the top compression chord

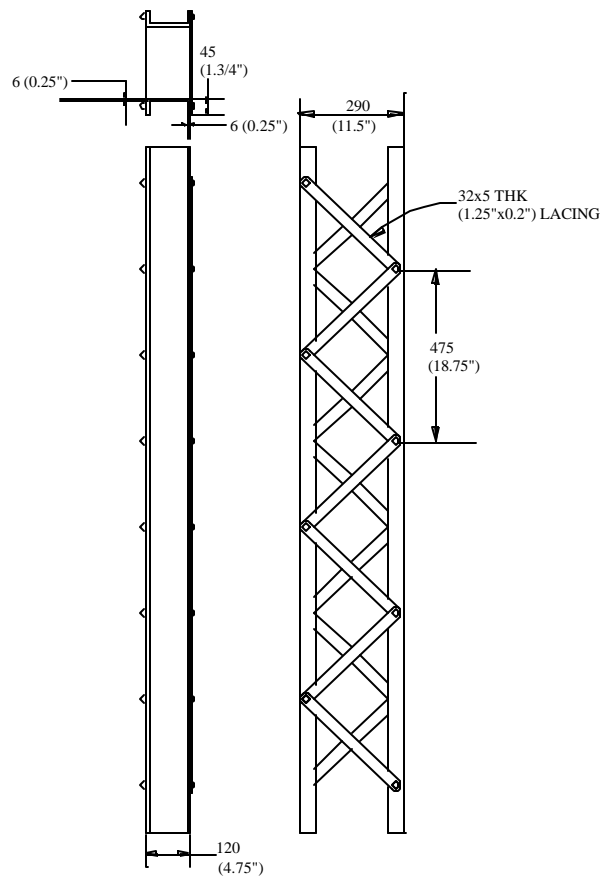


Figure B.5: Details of the vertical members (L2U2, L3U3 and L4U4)

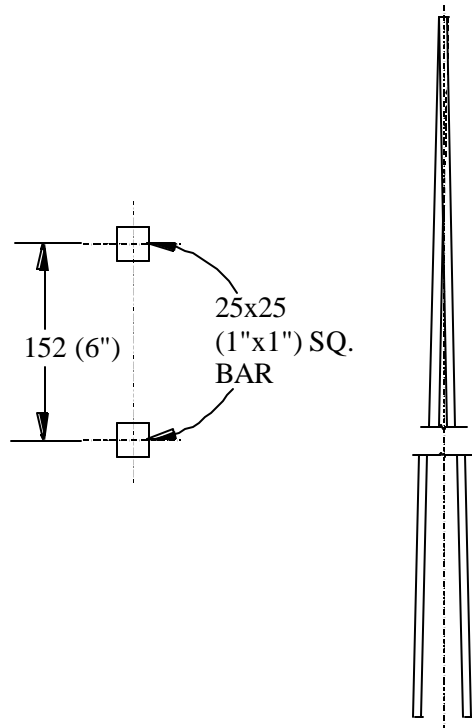


Figure B.6: Details of the hangers (L1U1 and L5U5)

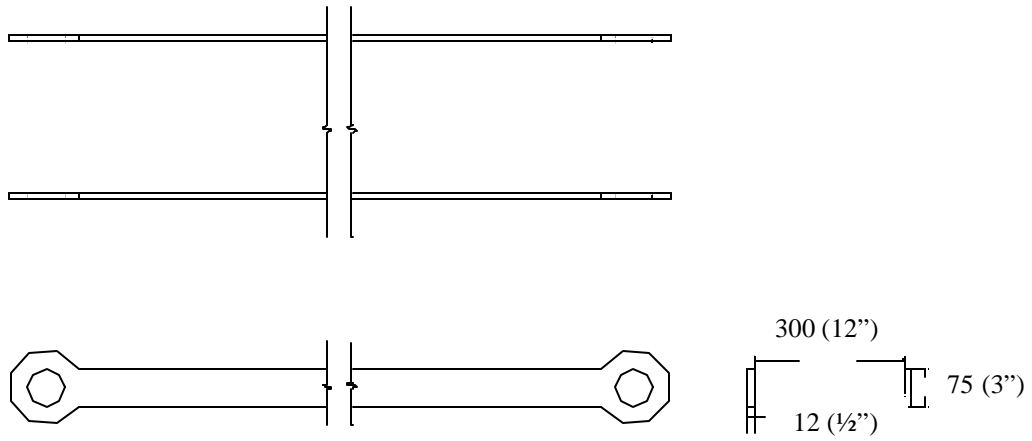


Figure B.7: Details of the bottom chord members (L0L1, L1L2, L2L3, L3L4, L4L5 and L5L6)

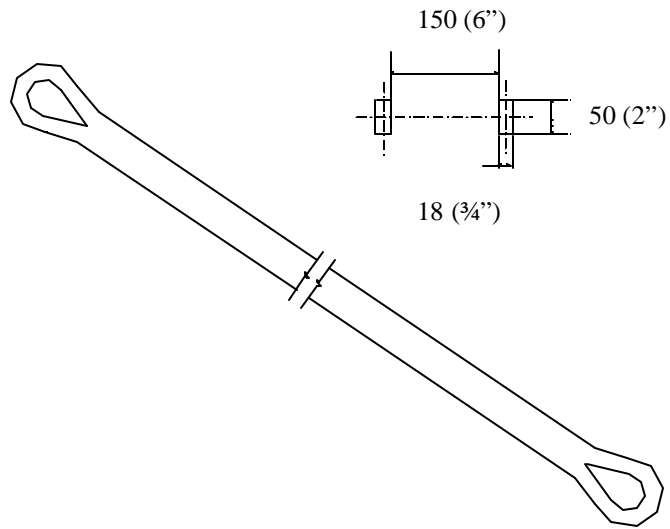


Figure B.8: Details of the diagonal members (L2U1 & L4U5)

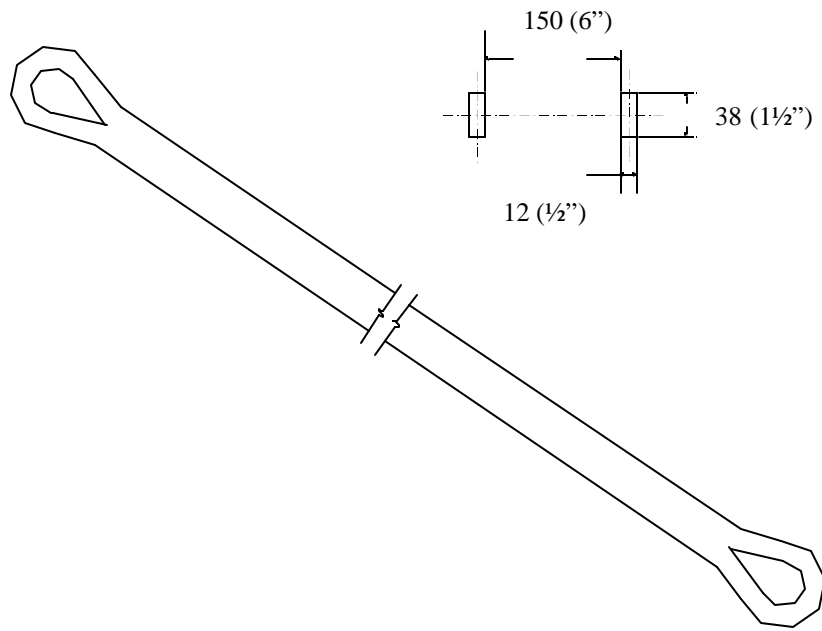


Figure B.9: Details of the diagonal members (L3U2 & L3U4)

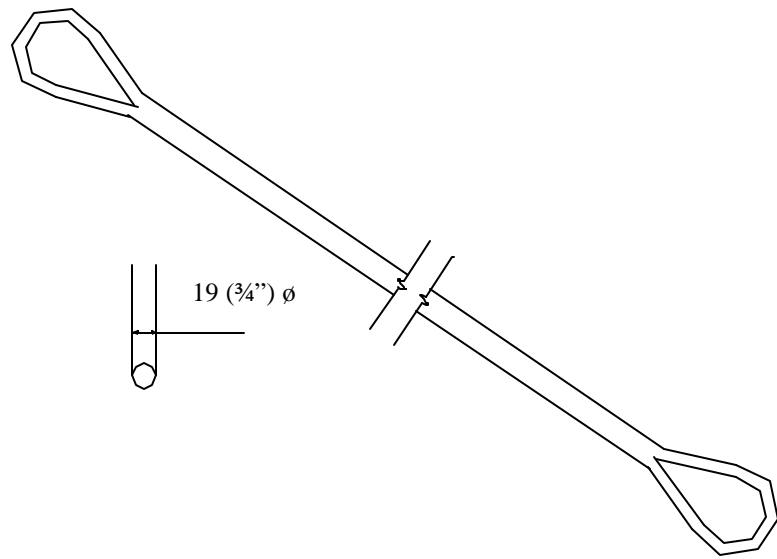


Figure B.10: Details of the tension rods (L2U3 & L4U3)

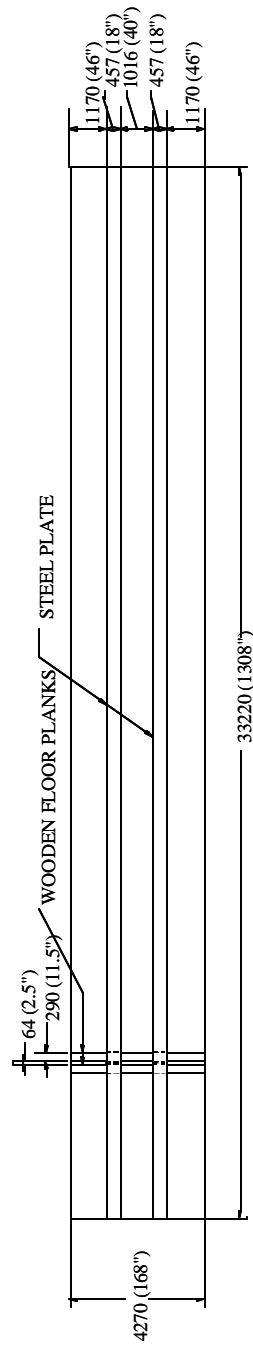


Figure B.11: Details of the timber bridge deck – Plan view

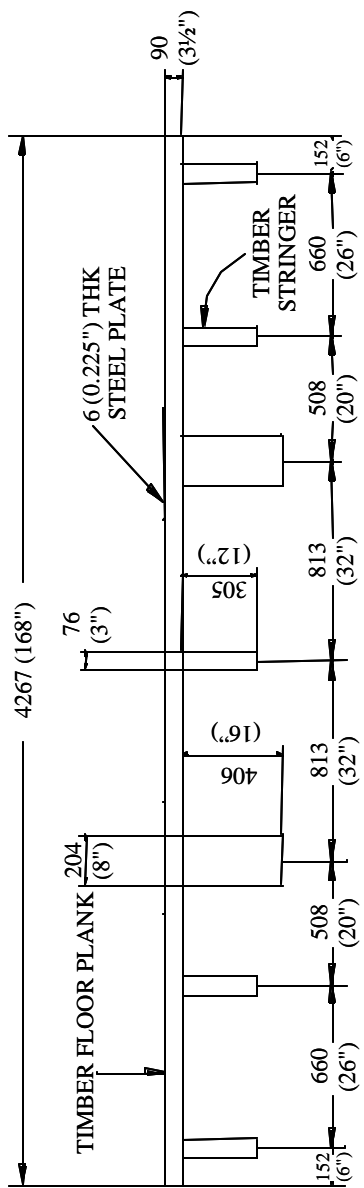


Figure B.12: Details of the cross-section of timber bridge deck

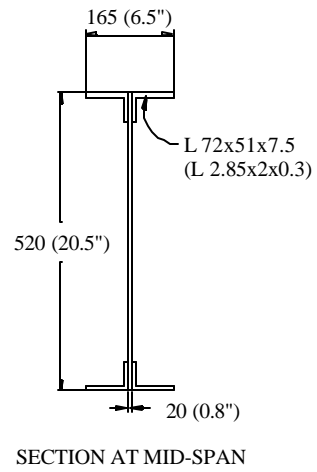
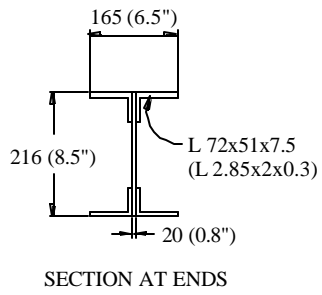
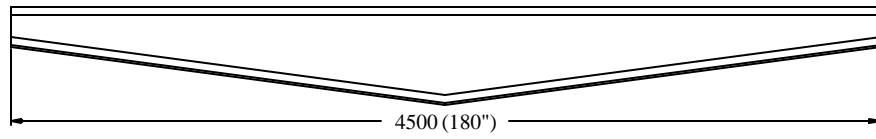


Figure B.13: Details of the metal floor beam

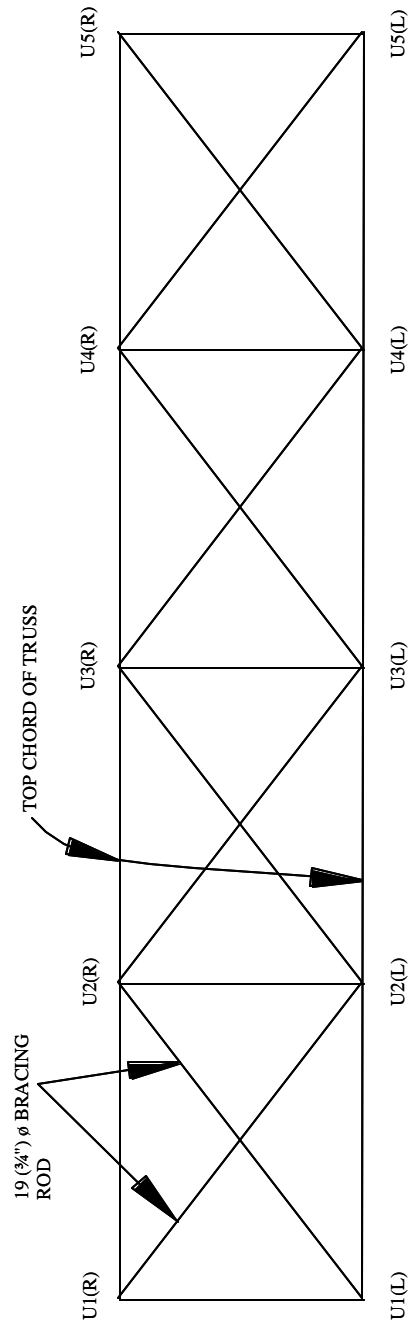


Figure B.14: Details of top lateral bracing

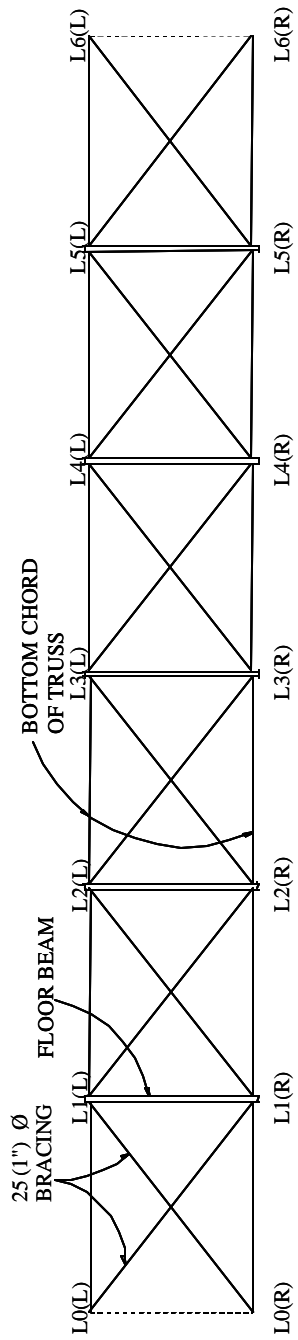
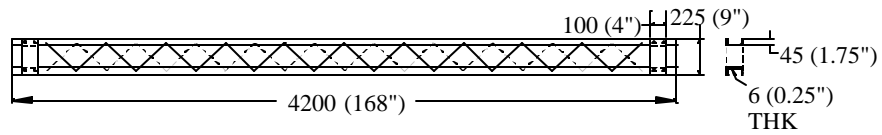
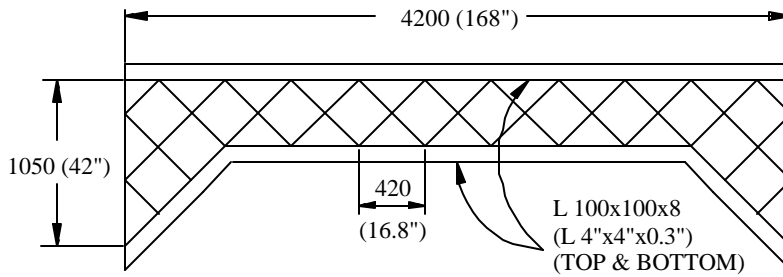


Figure B.15: Details of bottom lateral bracing



DETAILS OF INTERMEDIATE BRACING
(Located between trusses at U2, U3 and U4)



DETAILS OF PORTAL BRACING
(Located between trusses at U1 and U5)

Figure B.16: Details of portal bracing and intermediate bracing

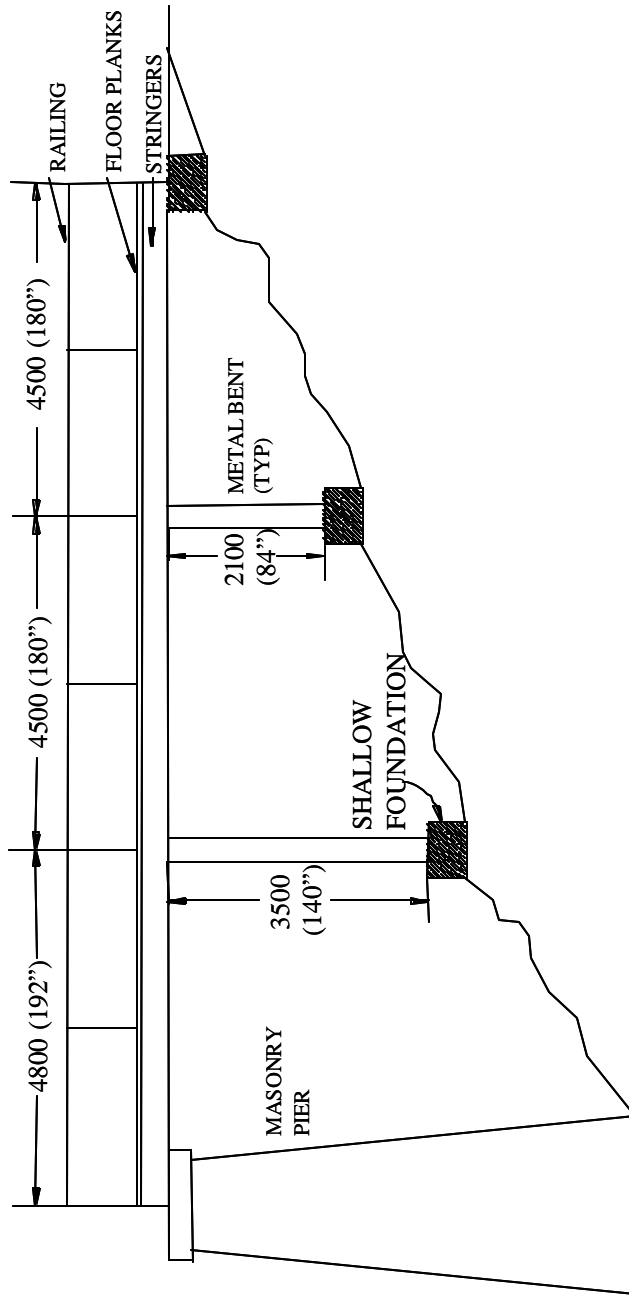


Figure B.17: Details of the south approach spans

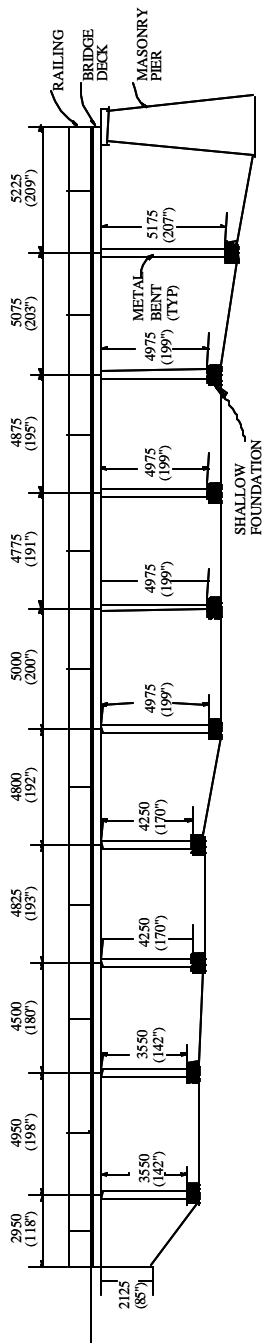


Figure B.18: Details of the north approach spans

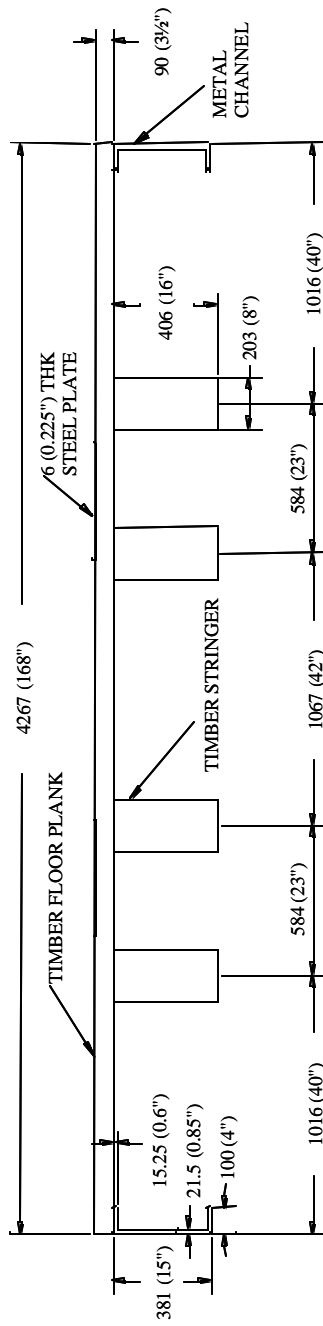


Figure B.19: Details of the timber deck of the approach spans

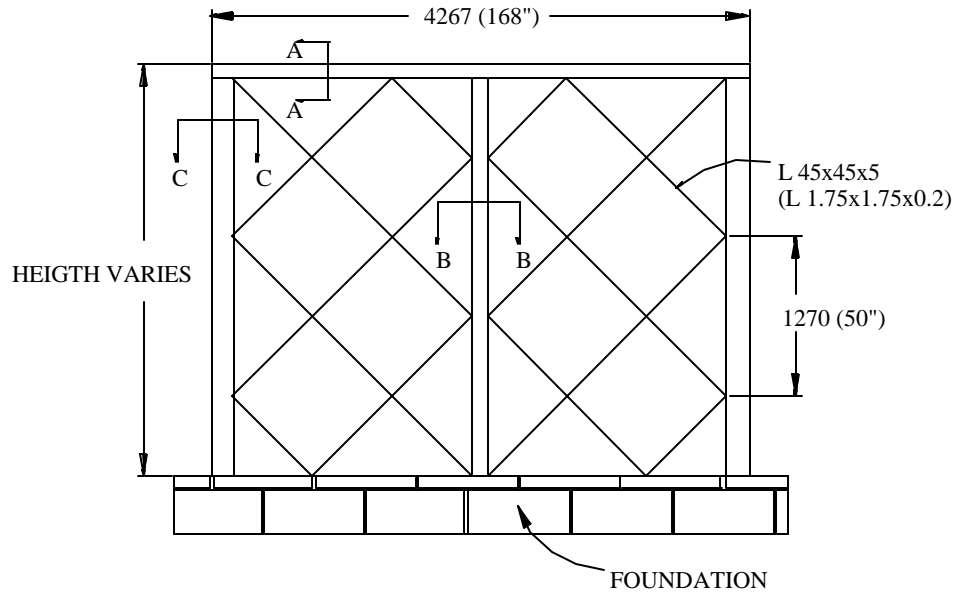


Figure B.20: Details of metal bent for approach spans

(For sections AA, BB, and CC refer Figure B.21)

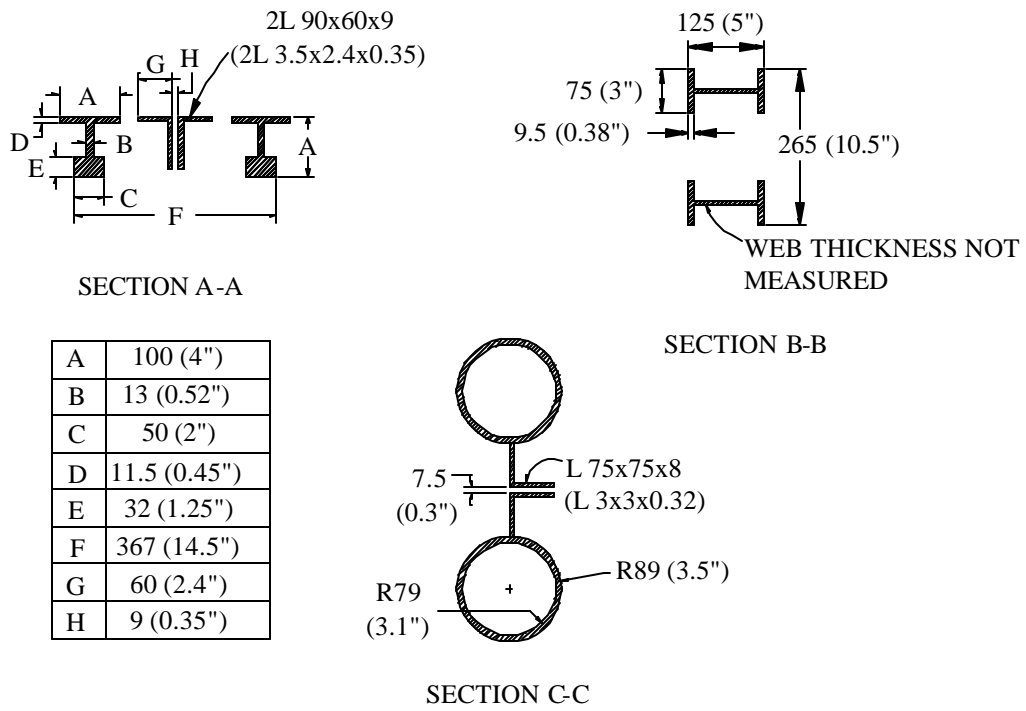


Figure B.21: Details of metal bent for approach spans

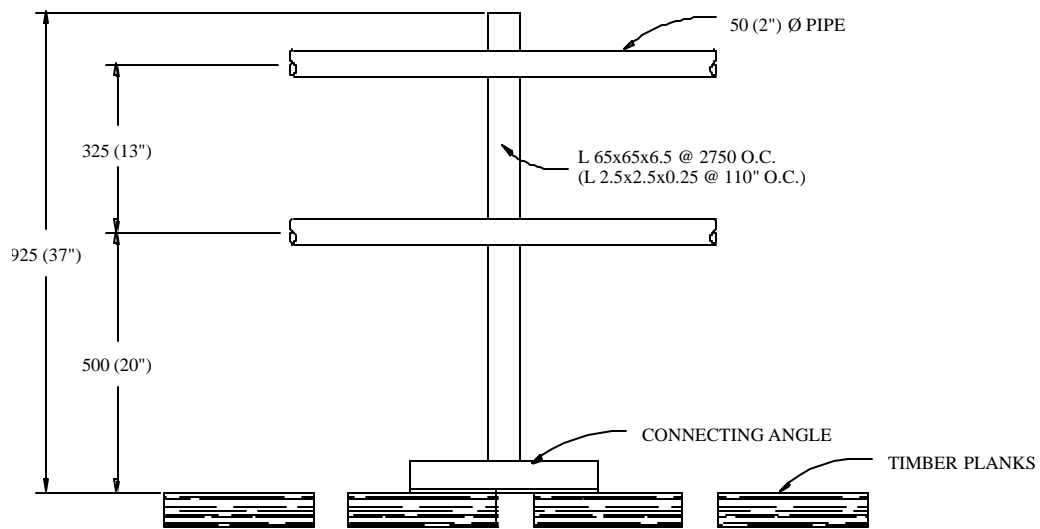


Figure B.22: Details of metal railing

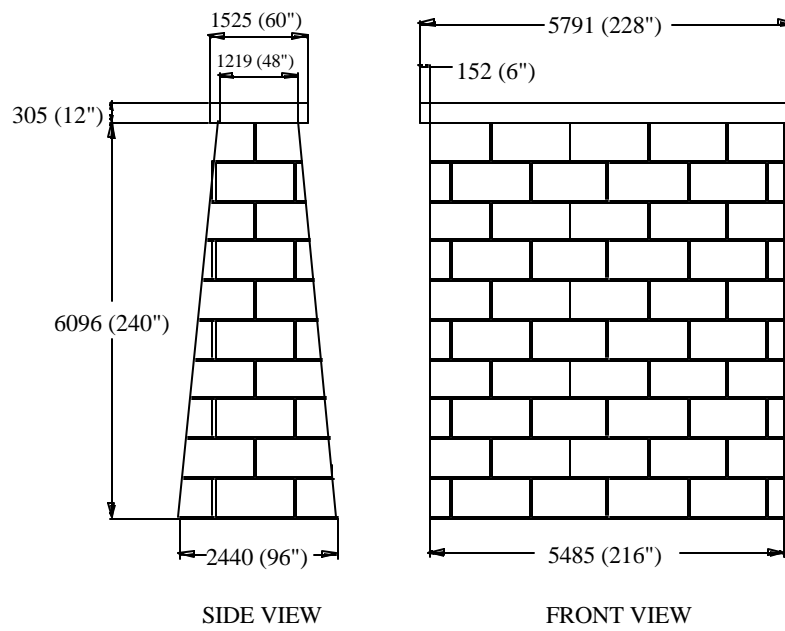


Figure B.23: Details of the stone masonry piers

Appendix C

Material Testing Results for Metal Samples of Case Study Bridge

As described in Chapter 3, samples of metal were removed from the case study bridge and subjected to several laboratory tests, including tension testing, hardness testing, and chemical analysis. In addition, photomicrographs were prepared. The purpose of these tests was to confirm that the metal in the case study bridge was wrought iron, and to obtain information on the mechanical properties and overall quality of the wrought iron. All samples of material were lacing members removed from truss members. The lacing members were removed from the bridge in May 1999. Tension and hardness tests were conducted at the University of Texas Ferguson Structural Engineering Laboratory in Austin. Chemical analysis and production of photomicrographs were done by An-Tech Laboratories, Inc., a commercial materials testing laboratory located in Houston. The results of all laboratory testing are documented in Section C.1 below.

In addition to laboratory testing of lacing members removed from the truss, field hardness measurements were made on several truss members. The purpose of these measurements was to establish whether or not the material for the lacing members (on which laboratory tests were conducted) was similar to the material used for the other truss members. The results of the field hardness tests are provided in Section C.2 below.

C.1 RESULTS OF LABORATORY TESTING

The metal samples removed from the bridge were labeled as listed in the Table.C.1.

Table.C.1: Metal sample identification

Sample Identification	Location
1	Downstream truss – Central column, L3U3 – North face – lacing
2	Upstream truss – Central column, L3U3 – South face –lacing
3	Downstream truss – Central column, L3U3 – North face –lacing
4	Upstream truss – Central column, L3U3 – South face –lacing

Tension coupons were prepared from lacing sample Nos. 1 and 2. Typical sheet type tension coupons with a reduced section were machined from the lacing members. Standard sheet-type, ½” wide specimen as per ASTM 370 was used. The length of the reduced section was about 2½ inches and the width of the reduced section was ½ inches. The thickness of the specimen was equal to the thickness of lacing.

The coupons were tested in a screw-driven test machine. An extensometer with an initial 2-inch gage length was used. Testing was done using a constant test machine crosshead rate of 0.02 inches/minute. Once the material reached the yield plateau during the test, the crossheads were stopped and held stationary for 3 minutes. The load after a 3-minute load hold was used to compute a static yield stress. The value of load at the yield plateau measured with the machine crossheads in motion was used to compute the dynamic yield stress. Finally, the ultimate load on the coupon was measured with the machine crossheads in motion to determine the ultimate yield stress. After fracture of the coupon, the distance

between gage marks on the coupon, initially at 2-inches apart, was measured to determine the %-elongation. Results of the tension tests are listed in Table C.2. Note that the “dynamic” yield and ultimate stress correspond to the values measured using standard test procedures per ASTM A370. Yield stress of steel is strain rate dependent. Consequently, the “static” yield stress was measured to characterize the yield stress at a zero strain rate. The static yield stress reflects the resistance of the steel under static loads.

Table.C.2: Results of tension test

	Sample 1	Sample 2	Average
Static yield stress, ksi	35.8	36.8	36.3
Dynamic yield stress, ksi	38.8	40.2	39.5
Dynamic ultimate stress, ksi	54.2	53.6	53.9
Elongation, %	16	16	16

A hardness test was also carried out on sample Nos. 1 and 2. The Rockwell B scale was used for the hardness testing. The average hardness of the metal was 79 on the Rockwell B scale. The result of these tests are listed in the Table C.3.

Table C.3: Results of hardness measurements

	Sample 1	Sample 2
1	79.5	75
2	79	78
3	75.5	78
4	79	85
5	79	85
6	76.5	79.5
Average	78	80

A chemical analysis of a metal sample was carried out. The elements and their percentage content found in the metal sample are listed in the Table C.4.

Table C.4: Chemical analysis

Element	Percentage content
Carbon	0.005
Sulfur	0.025
Manganese	0.025
Phosphorous	0.38
Silicon	0.20
Chromium	0.006
Molybdenum	<0.001
Nickel	0.007
Copper	0.007
Vanadium	0.007
Columbium	0.000
Titanium	0.007
Aluminum	0.044
Cobalt	0.004
Tin	<0.001
Tungsten	0.008
Arsenic	<0.005
Boron	0.0004
Calcium	0.0068
Magnesium	0.011
Zirconium	0.000
Nitrogen	0.0072
Iron	Balance

Photomicrographs were prepared from one sample of metal. Three different directions were examined as shown in Figure C.1. The photomicrographs are as shown in the Photograph C.1 to Photograph C.3. All three photomicrographs are taken on the unetched surface with 100X magnification. The slag laminations are clearly visible in the photomicrograph in the longitudinal direction, i.e., in the Photograph C.1. The metal can easily identified as wrought iron from the chemical analysis and the photomicrographs.

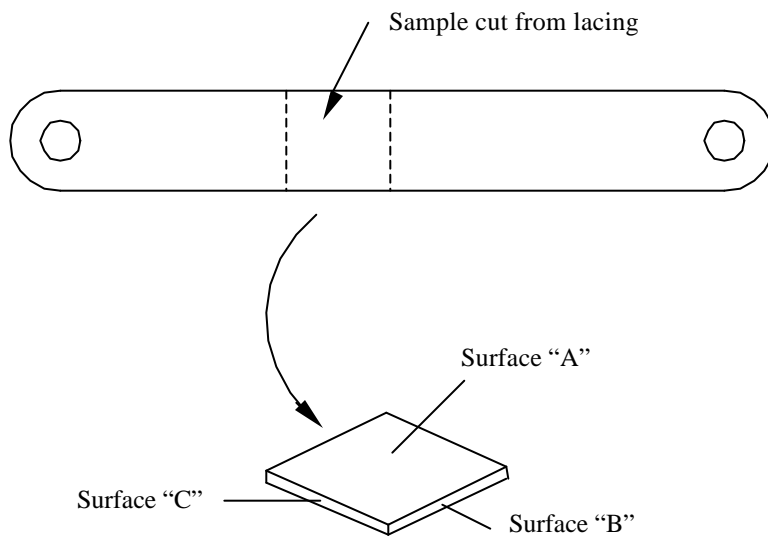
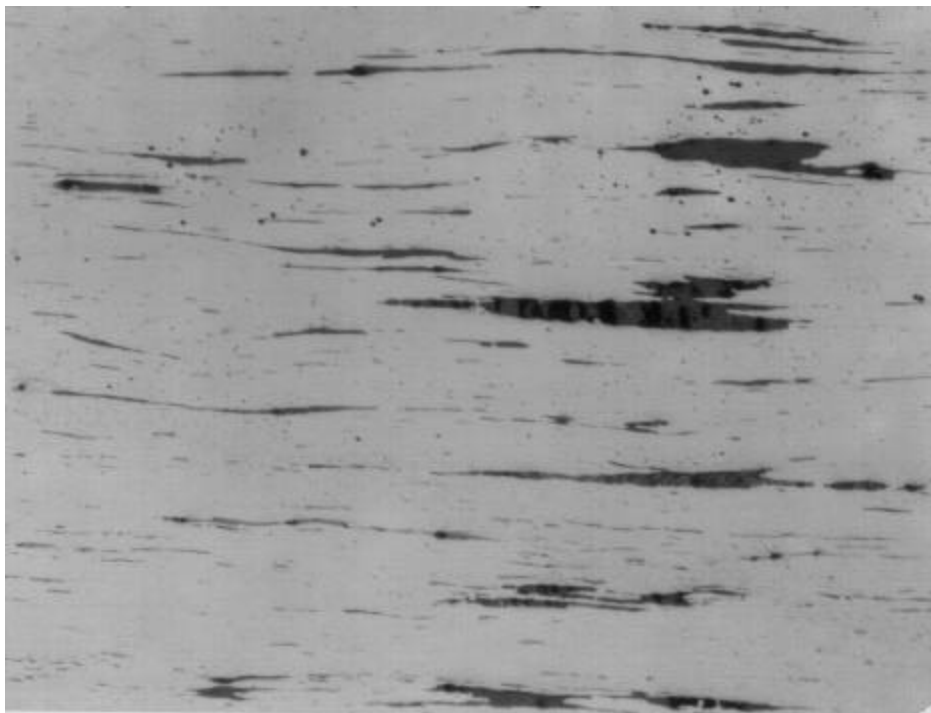
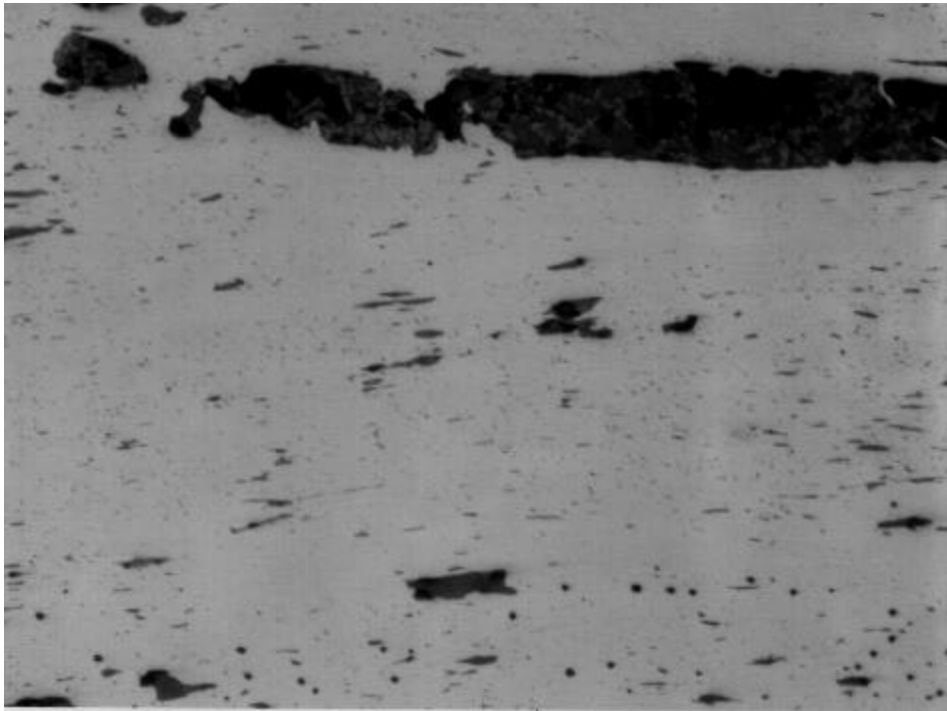


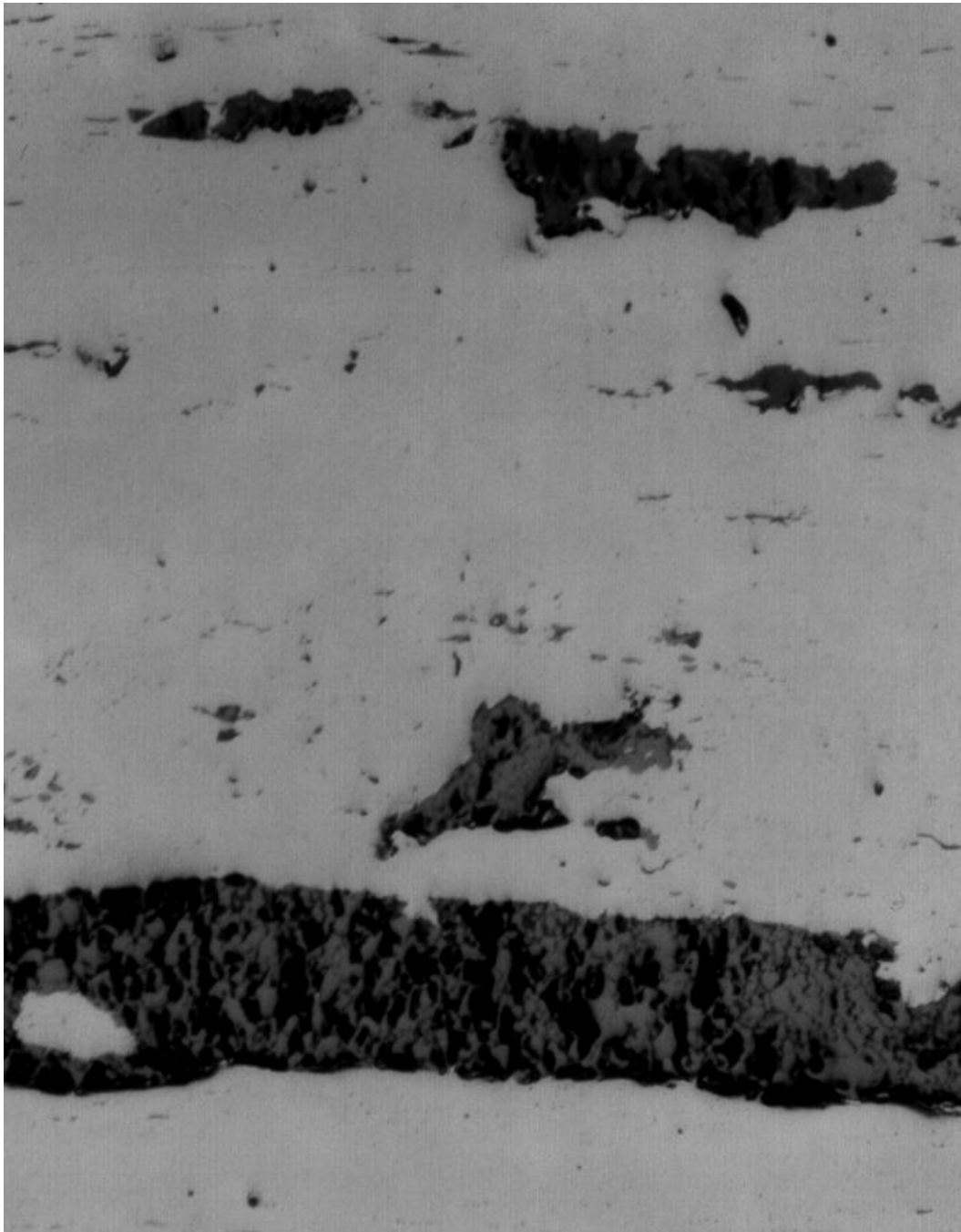
Figure C.1: Locations of photomicrographs



Photograph C.1: Photomicrograph on surface "A"



Photograph C.2: Photomicrograph on surface "B"



Photograph C.3: Photomicrograph on surface "C"

C.2 FIELD TESTING

Field hardness tests were carried out using a Mini-Brineller. Mini-Brineller is a hand held device which can be used on-site to determine hardness of a metal. To use this device, an indentation on metal sample and calibrated metal piece is made by a stroke of hammer. Hardness of the metal sample is determined by correlating diameter of the indentations made on the sample and calibrated metal piece. The test results are as shown in the Table C.5 and Table C.6.

Table C.5: In-situ hardness values measured on members of upstream truss

Location	Description	Hardness
1	L0U1	169.0
2	L1U1 - LEFT	128.4
3	L1U1 - RIGHT	137.3
4	L2U1	138.8
5	L2U2	139.2
6	L2U3	134.2
7	L3U2	155.6
8	L3U3	183.0
9	L3U4	117.1
10	L4U3	115.3
11	L4U4	136.3
12	L4U5	133.7
13	L5U5 - LEFT	145.1
14	L5U5 - RIGHT	137.4
15	L6U5	144.0
16	L0L1	122.9
17	L0L1	122.9
18	L1L2	126.4
19	L1L2	128.3
20	L2L3	148.4
21	L2L3	164.0
22	L3L4	129.6
23	L3L4	129.3
24	L4L5	140.6
25	L4L5	149.0
26	L5L6	138.5
27	L5L6	139.2

Table C.6: In situ hardness values measured on members of downstream truss

Location	Description	Hardness
28	L0U1	136.3
29	L1U1 - RIGHT	137.7
30	L2U1	145.5
31	L2U2	144.4
32	L3U2	155.9
33	L3U3	152.1
34	L3U4	141.3
35	L4U4	143.6

The average hardness of the bridge metal is 140 on the Brinell hardness scale which is equivalent to a hardness of 78 on Rockwell hardness B scale [NDTech]. The laboratory hardness test average value is 79 on the Rockwell hardness B scale. Standard correlation [Chapter 10, Boving, K.G., 1989] between hardness and ultimate stress does not match with the laboratory test values. Hence, hardness test may not give an accurate range of ultimate stress for certain metal. Based on both the laboratory and in situ hardness tests, it appears that the metal used in the bridge construction has the similar strength properties as the tested lacing members.

Appendix D

Wrought Iron

This appendix provides details of wrought iron found from several sources. The information available from the following references has been reproduced in the following paragraphs; [Aston, J., 1936], [Cain, J.R., 1924], [Clauser, H.R., 1963], [Frank, K.H., 1974], [Kent, W., 1916], [Mark, L.S., 1930], [Mills, A.P., 1939], [Miner, D.F., 1955], [Rawdon, H.S., 1924], and [Rawdon, H.S., 1917].

D.1 INTRODUCTION

The definition of wrought iron given by the American Society for Testing Materials is: “A ferrous material, aggregated from a solidifying mass of pasty particles of highly refined metallic iron, with which, without subsequent fusion, is incorporated a minutely and uniformly distributed quantity of slag”.

Wrought iron is one of the oldest forms of ferrous metal made by man. It is a tough, ductile, and easily malleable metal. These properties are due to its low carbon content, usually less than 0.12 percent, and absence of impurities. It can be forged and welded, and has a high capacity to withstand the action of shocks and vibrations; but it cannot be tempered so as to form cutting tools. Wrought iron melts at white heat, but is pasty at lower temperatures, and in this condition can be easily worked and welded. It is ductile when cold. Wrought iron differs from

all other metals in that it is produced in a pasty, rather than a molten condition and it contains a large percentage of iron silicate slag distributed throughout the mass. There is no chemical combination between the two materials. For this reason, wrought iron is called a “two component” metal, in contrast to the chemical or alloy relationship that generally exists between the constituents of other metals. Hence wrought iron is a two-component metal composed of high-purity iron and iron silicate, which is an inert non-rusting glasslike slag. The slag content varies from about 1 to 3 percent in finished wrought iron. The slag is distributed throughout the iron in the form of threads or fibers which extend in the direction of rolling and are so thoroughly distributed throughout the iron that there may be 250,000 or more per square inch of cross-section. The slag content is responsible for the laminated or fibrous structure which characterizes wrought iron, and which serves to differentiate it from steel.

Wrought iron may be graded as Charcoal iron, Puddle iron, and Busheled iron. The first is the purest grade of wrought iron. The second is classified as staybolt (grade A) and merchant iron (grades B and C). The third grade is made from iron scrap, with which steel sometimes is mixed. It is irregular in quality.

D.2 THE MANUFACTURING OF WROUGHT IRON

There are two processes by which wrought iron can be manufactured. These are the puddling process and the Aston process or new Byers process. Both the methods are described in the following sections.

D.2.1 The Puddling Process

Iron ore, consisting essentially of Fe_2O_3 or Fe_3O_4 with silica, phosphorous, sulfur, manganese, etc., as impurities, is heated in a blast furnace at a high temperature resulting in molten product called pig iron. This iron contains about 3.5 percent Carbon and considerable Silica, Manganese, Phosphorous, and Sulfur which have been reduced with the iron. The pig iron is then heated in a puddling furnace at a temperature somewhat above its melting point, with the addition of fettling material in the form of iron ore or iron oxides. The puddling furnace is a reverberatory furnace and the oxidizing flame plays over the bath of molten metal. Air is allowed to enter the furnace, which further promotes the oxidization. The impurities are gradually burnt out of the iron, and its melting point is thereby raised so that the resulting pure metal forms in globules which are collected together by means of long iron rods manipulated by the puddler. This pure iron is not molten, but comes from the furnace in a pasty condition in the form of balls and contains semi-molten slag (silicate of iron) mechanically included. The ball is then put through a squeezer or hammered with a steam hammer to remove a large portion of the slag and is now called a bloom. It finally passes through a rolling mill and is then known as muckbar. Muckbar contains too much slag to render the metal useful. The bars are therefore sheared, piled crosswise and the pile is reheated and re-rolled, the purer iron product being called refined bar iron. This is the wrought iron of commerce. When refined bar iron is sheared, piled and rolled in a similar manner, the resulting material is called double-refined iron. If a charge of iron scrap or of pig iron is heated in a so-called “knobbling” furnace

with charcoal, and air is forced into the furnace through tuyeres, the product, after being subjected to the mechanical treatment describe above is known as knobbed charcoal iron. Common iron is made from re-rolled scrap, no attempt being made to separate the iron and steel scrap.

D.2.2 Aston Process or New Byers Process

In another method of manufacturing wrought iron, known as the Aston Process or New Byers Process, a very low-carbon ferrous metal is prepared in a suitable furnace, preferably an electric furnace, open-hearth furnace or Bessemer converter. The metal is finished in the usual way but no recarburizer or ferromanganese is added. The relatively pure molten iron is poured into a ladle containing slag of the proper composition. The melting point of ferrous silicate slag is considerably lower than that of nearly pure iron, so that the liquid slag acts as a quenching agent for the purified iron. An instantaneous and violent action with profuse gas liberation occurs upon solidification of the metal and the latter becomes a pasty mass of disintegrated iron particles thoroughly mixed with slag. This pasty ball of iron is similar to the old puddled ball except that it is six or seven times as heavy. The ball is then taken to a squeezer and compacted into a 1000 lb. bloom which can be rolled directly into muckbar, slabs, rods, skelp or any other desired form.

D.3 CHEMICAL COMPOSITION OF WROUGHT IRON

The composition of wrought iron approaches that of pure iron very closely. The typical chemical composition of wrought iron is as listed in the Table D.1. The usual impurities – carbon, silicon, phosphorous, sulfur, and

manganese – are always present in small amounts, in addition to the slag which is invariably present. The slag content of wrought iron varies from about 1 to 3 percent by weight. Wrought iron is a composite material consisting of an intermingling of high-purity iron base metal and siliceous slag, and the impurities are distributed between the metal and the slag. Hence, it is desirable to know the distribution of the impurities between them. A typical chemical analysis, showing the distribution of the impurities between the base metal and the slag, is shown in the Table D.2.

Table D.1: Typical chemical composition of wrought iron

	High-quality Wrought iron, Upper Limit, Percent	High-quality Wrought iron, Typical Analysis, Percent	Very pure Swedish Charcoal iron, Percent
Carbon	0.10	0.04	0.050
Silicon	0.20	0.10	0.015
Phosphorous	0.25	0.10	0.055
Sulfur	0.05	0.03	0.007
Manganese	0.10	0.05	0.006
Slag	3.2	2.75-3.25	0.610

Table D.2: Distribution of impurities between the base metal and the slag

	Total Content Percent	In the base metal Percent	In the slag Percent
Carbon	0.02	0.02	
Manganese	0.03	0.01	0.02
Phosphorous	0.12	0.10	0.02
Sulfur	0.02	0.02	
Silicon	0.15	0.01	0.14
Total	0.34	0.16	0.18

Quality wrought iron is distinguished by its low carbon and manganese contents. Carbon in well-made wrought iron seldom exceeds 0.035%. Due to

specifications, manganese content is held at 0.06% maximum. Phosphorous in wrought iron usually ranges from 0.10% to 0.15% depending upon property requirements. Sulfur content is normally low, ranging from 0.006% to below 0.015%. Silicon content ranges from 0.075% to 0.15% depending upon the siliceousness of the entrapped iron silicate. Silicon content of base metal is 0.015% or less. Residuals such as Cr, Ni, Co, Cu, and Mo are generally low, totaling less than 0.05%. In the following paragraphs, a brief description of role of each impurity in wrought iron is provided.

D.3.1 Carbon

The carbon content is usually lower in wrought iron than in steel and cast iron, but it is not lower than in the class of open-hearth product known as ingot iron. Quality wrought iron is usually associated with a carbon content of 0.02% or 0.03%. However, in some cases good wrought iron may have a carbon content of 0.08% to 0.10%. Higher amounts may be an indication of imperfect or incomplete refining or may suggest that steel scrap has been used in bushelling or piling.

D.3.2 Manganese

In well-made wrought iron, the manganese content is usually below 0.06%. High manganese may result from imperfect refining or it may indicate adulteration by the use of some steel in bushelling or piling.

The virtual absence of manganese in wrought iron and its almost universal presence in steel has resulted in the manganese determination being used as means of identification and differentiation.

D.3.3 Phosphorous

The phosphorous content of wrought iron is almost invariably higher than that of steel. It is in part alloyed with the base metal and in part associated with the slag. In well-made wrought iron the phosphorous content ordinarily ranges from 0.10% to 0.15%. In general, the lower range of phosphorous is advisable for products where high ductility is desirable; where shock is a service factor, or where high heat effects might result in brittleness.

D.3.4 Sulfur

The element sulfur is always undesirable and is a promoter of “red-shortness” and corrosion. In well-made wrought iron it is usually less than 0.03%.

D.3.5 Silicon

The element silicon is quickly removed in the refining of iron. In wrought iron, the usual silicon content is between 0.10% to 0.20%. Practically all of this is in the siliceous slag component.

D.3.6 Influence of Chemical Composition upon the Welding Properties

It has been believed that slag would facilitate welding, but the work by Holley, [Mark, L.S., 1930] does not bear this out, his conclusion being that, while “slag should theoretically improve welding like any flux, its effect in these experiments could not be definitely traced”. The iron highest in slag (2.26 percent) “welded less soundly than any other bar of the same iron, and below average as compared with the other irons”. He concluded that “although most of the irons under consideration are alike in composition, the hardening effects of

phosphorous and silicon can be traced, and that of carbon is obvious. Phosphorous, up to 0.20 percent, does not harm and probably improves iron containing Silica not above 0.15 percent and Carbon not above 0.03 percent. Non of the ingredients, except Carbon in the proportions present, seem to very notably affect welding by ordinary methods”.

D.3.7 Influence of Chemical Composition on the Properties of Wrought Iron

Back in 1877, forty-two chemical analyses were made of different brands of wrought iron, with a view to determine what influence the chemical composition had upon the strength, ductility, and weldability. The following information is taken from the report of these tests by A.L.Holley. Table D.3 shows average tensile strength of different brands of wrought iron with their chemical composition. Where two analyses are given, they are the extremes of two or more analyses of the brand. Where one is given, it is the only analysis. Brand L is puddled steel. Table D.4 shows the order of quality of tested brands of wrought iron on the scale of 1 through 19. The reduction of area varied from 54.2 to 25.9 percent, and the elongation from 29.9 to 8.3 percent.

Table D.3: Influence of chemical composition on the properties of wrought iron

Brand	Average Tensile strength, psi	Chemical composition, percent					
		S	P	Si	C	Mn	Slag
L	66598	Trace	0.065	0.080	0.212	0.005	0.192
			0.084	0.105	0.512	0.029	0.452
P	54363	0.009	0.250	0.182	0.033	0.033	0.848
		0.001	0.095	0.028	0.066	0.009	1.214
B	52764	0.008	0.231	0.156	0.015	0.017	-
J	51754	0.003	0.140	0.182	0.027	Trace	0.678
		0.005	0.291	0.321	0.051	0.053	1.724
O	51134	0.004	0.067	0.065	0.045	0.007	1.168
		0.005	0.078	0.073	0.042	0.005	0.974
C	50765	0.007	0.169	0.154	0.042	0.021	-

Table D.4: Order of qualities graded from no. 1 to No. 19

Brand	Tensile Strength	Reduction of Area	Elongation	Weldability
L	1	18	19	Most imperfect
P	6	6	3	Badly
B	12	16	15	Best
J	16	19	18	Rather badly
O	18	1	4	Very good
C	19	12	16	-

Brand O, the purest iron of the series, ranked 18 in tensile strength, but was one of the most ductile; brand B quite impure, was below the average both in strength and ductility, but was the best in welding power; P, also quite impure, was one of the best in every respect except welding, while L, the highest in strength, was not the most pure, it had the least ductility, and its welding power was most imperfect. The evidence of the influence of chemical composition upon quality is therefore quite contradictory and confusing. The iron differing remarkably in their mechanical properties, it was found that a much more marked

influence upon their qualities was caused by different treatment in rolling than by differences in composition.

In regards to slag Mr. Holley says: "It appears that the smallest and most worked iron often has the most slag. It is hence reasonable to conclude that an iron may be dirty and yet thoroughly condensed".

D.4 STRUCTURE OF WROUGHT IRON

In view of the fact that wrought iron is a composite material, methods of examination which reveal the distribution of slag throughout the base metal are of paramount importance in identification and determination of quality. Such evidence may be visible to the naked eye through a macro-etch or may be apparent only through the use of the microscope. The microscopic and macroscopic structures of the wrought iron are described in the following sections.

D.4.1 Microscopic Examination

Structurally, the base metal and the slag are in physical association, in contrast to the chemical or alloy relationship that generally exists between the constituents of other metals. The appearance of a longitudinal section of wrought iron under high magnification is as shown in the Figure D.1. The slag appears as many irregular black lines of varying thickness and the crystalline nature of the pure iron can also be plainly seen. The photomicrograph of the appearance of the transverse section of wrought iron can be seen in the Figure D.2. The structure is in every way similar to that seen in the longitudinal section except that the slag

here appears as irregular dark areas corresponding to the cross-section of the slag fibers.

The grain size of hot-worked wrought iron may be controlled by continuing the working until the temperature has decreased to about 1300°F (704°C). The fibrous structure of wrought iron is exhibited in a tensile test by a jagged, fibrous fracture and in a nickbend test by a longitudinal fibrous fracture. If there is any appreciable amount of carbon in the iron, it shows at the junctions of the ferrite polyhedra as dark, irregular particles of pearlite, the amount of this constituent varying from zero to about 12 percent of the area as the carbon content varies from zero to 0.1 percent.

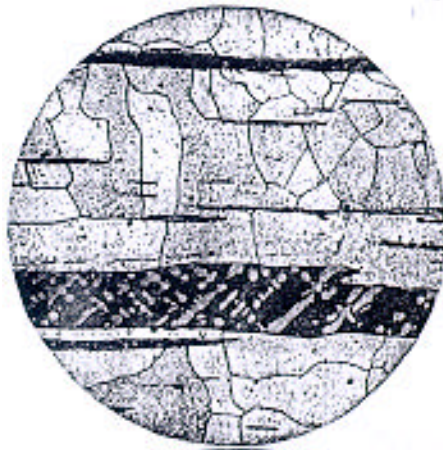


Figure D.1: Longitudinal section of wrought iron

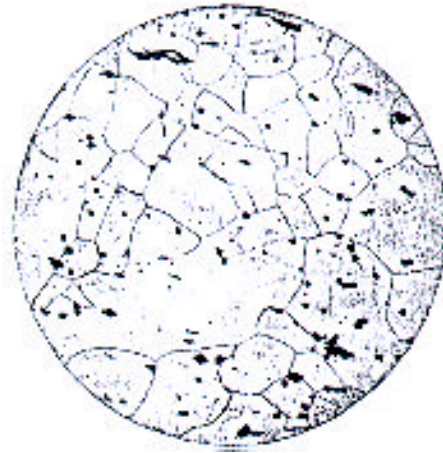


Figure D.2: Transverse section of wrought iron

The form and distribution of the iron silicate particles may be stringerlike, ribbonlike, or platelets. Practically, the physical effects of the incorporated iron-silicate slag must be taken into consideration in bending and forming wrought iron pipe, plate, bars, and shapes, but when properly handled – cold or hot – fabrication is accomplished without difficulty.

The microscopic examination will disclose:

- Pearlitic areas due to carbon and resulting from incomplete refinement in prevalent methods of manufacturing of wrought iron or from adulteration with steel scrap of even moderate carbon content.
- Type of slag and its distribution; such as coarse slag pockets, fine textures resulting from heavy rolling reductions, or the absence of normal slag content.

- Unusual characteristics of structure; such as coarsened grain caused by over-heating, high phosphorous “ghost line” or other abnormalities.

In connection with any examination under the microscope it should be borne in mind that the area under observation is very small – pinhead size at one hundred magnifications. All of these test methods for determining the quality of the material are useful, but in applying them it is important that conclusions should be reached by weighing the evidence developed from the various ones employed. In determining the finer points of quality, experience in the interpretation of test results and knowledge of the material’s characteristics is essential.

D.4.2 Macroscopic Examination

The nick bend, or fracture test, has long been a favorite way of quickly distinguishing wrought iron from steel. The former exhibits a well-known fibrous fracture as contrasted with the crystalline break of the latter. The fracture of wrought iron depends to a very great extent upon the method employed in breaking the metal. A sudden break causes the production of a so-called “crystalline” or “granular” fracture, while a gradual rupture produces a “fibrous” fracture. At times there may be confusion, since dirty steel may show a semblance to fiber, while on other occasions good wrought iron may, if broken suddenly, exhibit some crystalline structure which may be due to high carbon, high phosphorous or prolonged heating. Where the material is in question because of

suspicion of scrap adulteration, a fracture test is of doubtful value and is liable to be misleading if it is the sole reliance for basing judgment.

Deep etching with acid is a prevalent inspection method in the selection of wrought iron products; particularly (1) as a means of disclosing method of piling, and (2) for the detection of adulteration with steel scrap. Wrought iron etches deeply, with a roughened, stringy or woody surface, whereas steel will show a comparatively smooth surface. Consequently, a mixture of wrought iron with steel will exhibit a mixed type of surface if the distribution is sufficiently coarse to be discernible.

D.5 MECHANICAL PROPERTIES

The mechanical properties and physical properties of wrought iron are essentially the same as those of pure iron. The strength, ductility, and elasticity are affected to some degree by small variations in the metalloid content and even greater degree by the amount of incorporated slag and the character of its distribution. The longitudinal mechanical properties are, however, decidedly superior to the transverse properties. This anisotropic behavior, amounting to 20% or more, is due to the characteristic fibrous structure of wrought iron, brought about by the elongation of the slag particles in the direction of rolling. The design of most structures is such, however, that the members are stressed in a direction parallel to the longitudinal axis (direction of rolling of material), and the somewhat lower transverse properties do not cause serious objection. The properties are only slightly changed by heat treatment. The yield point of wrought iron is unaffected by the slag component and is of the same magnitude in both the

longitudinal and transverse directions. The ultimate strength of good wrought iron is not well defined. The yield point ranges from 2-4 ksi higher than the elastic limit. Up to certain limits, ductility increased by extra working, due to its effect in causing a finer distribution and more thread-like character of the incorporated slag. This is accomplished through the large reduction of section obtained in rolling or forging large initial blooms into proportionately small final sections; or it may be obtained by rolling smaller initial masses to bar sections, which in turn are built into piles, heated to welding temperature and rolled to desired forms. In common practice this is done once for single-refined wrought iron and twice for double-refined wrought iron products.

The development of rolling procedures affected an equalization of the normal ultimate strength and ductility in the two directions. This important advance in technique has had a marked influence in making possible the use of wrought iron plates for applications where severe fabrication requirements must be met.

D.5.1 Tensile Strength

The tensile properties of wrought iron are largely those of ferrite plus the strengthening effect of any phosphorous content which adds approximately 1000 psi for each 0.01% above 0.10% of contained phosphorous. Strength, elasticity, and ductility are affected to some degree by small variations in the metalloid content and in even greater degree by the amount of the incorporated slag and the character of its distribution. Nickel, molybdenum, copper and phosphorous are

added to wrought iron to increase yield and ultimate strengths without materially detracting from toughness as measured by elongation and reduction in area.

The tensile strength of a given wrought iron depends to a considerable extent upon the direction of stress with respect to the “grain” of the iron. The tensile strength of wrought iron, in the direction of rolling, ranges from about 45 to over 50 ksi. The size of cross-section of a tensile specimen affects the strength to some extent and this fact can be taken into consideration by decreasing the minimum limit of tensile strength of specimens above certain sizes when full-size sections of bars are employed for testing. The yield point of wrought iron is strongly indicated in testing by the “drop of the beam” or “halt of the gage” of the testing machine, and occurs at from 50 percent to somewhat over 60 percent of the tensile strength. The ductility of wrought iron undergoing tension is less than that of very low carbon steel, owing to the presence of the slag. The elongation in the direction of rolling will vary from about 20 percent to about 30 percent. The typical physical properties of wrought iron in the longitudinal and transverse direction are given in the Table D.5.

Table D.5: Longitudinal and transverse tensile properties of wrought iron

Property	Longitudinal	Transverse
Tensile strength, ksi	48-50	36-38
Yield point, ksi	27-30	27-30
Elongation in 8 in., %	18-25	2-5
Reduction of area, %	35-45	3-6

The tensile strength and ductility of wrought iron at right angles to the direction of rolling are considerably less than the longitudinal strength and ductility. This is to be expected, since the continuity of the metal in a direction

transverse to the direction of rolling is interrupted by numerous strands of slag, which are comparatively weak. The tensile strength of wrought iron in a transverse direction has usually been found to be between 0.6 to 0.9 of the strength in the longitudinal direction. The ductility is also appreciably greater in a longitudinal direction than in a transverse direction, but the yield point is practically the same in either direction. The transverse tensile strength and ductility are important when wrought iron plates must withstand severe treatment in the fabrication. A special rolling procedure, developed for plates, tends, to a large extent, to equalize the strength and ductility in both directions. Plate so manufactured is designated as “special forming plates”. This development has an important bearing on the use of wrought iron for applications where the metal must be formed in more than one direction, as in flanged and dished tank heads.

Average tensile properties of plain and alloyed wrought iron for different product forms are tabulated in the Table D.6. Physical properties of different varieties of wrought iron are as shown in the Table D.7.

D.5.2 Shear Strength

The ratio of shearing strength across the thickness of a wrought iron plate, either with or across the grain, is about 80% of tensile strength. If the shearing forces are applied on the planes perpendicular to the plane of the plate, the shearing strength is about the same as the tensile strength. Shearing resistance on a plane parallel to the plane of the plate is about half the shearing strength across the thickness of the plate.

The resistance of the material to shearing stresses will be less on a plane parallel to the direction of the “grain” than on that cuts the fiber of the iron transversely. The actual shearing strength shown by the test is variable, but in general it will be from 20 to 35 ksi on a longitudinal plane and from 30 to 45 on a transverse plane.

Table D.6: Average tensile properties of plain and alloyed wrought iron

	Tensile Strength, Ksi	Yield point, Ksi	Elongation in 8 in., %	Reduction of Area, %
Plain Wrought iron				
Bars ($1/8$ in. Round)	50	30	32	55
Pipe ($1\frac{1}{4}$ in. std.)	48	28	25	-
$3/8$ in. Plate	48 ^a	30	20	-
(Standard)	42 ^b	30	4	-
$3/8$ in. Plate	45 ^a	30	10	-
(special forming)	45 ^b	30	10	-
Alloyed Wrought iron				
Iron 3.5 % Ni (1 in. Round)	60	45	25	50
0.30% P, 0.30% Cu $3\frac{1}{2}$ in o.d. tubing	60	40	25	-
1.3% Cu ($1/8$ in. Round)	60	45	25	40
1% Mn, 0.10% P (6 in. Pipe)	60	40	25	-
^a Longitudinal				
^b Transverse				

Table D.7: Physical properties of different varieties of wrought iron

Variety of iron	Quality	Form	Tensile strength, lb/sq.in.	Elastic limit, lb/sq.in.	Reduction of area, %	Elongation, %
Swedish charcoal	Very good	1 in. square	43904	27440	72.18	56.0 on 31/8
Best Yorkshire (Bowling)	Very good	1 ¹ / ₈ in. round	50848	30688	55.00	29.0 on 10
Very common	Very bad	1 in. square	46995	30800	5.29	4.5 on 31/8
Puddled iron	Very bad	¼ in. plate	41664	30912	4.50	3.0 on 10

The specifications of the American Society for Testing Materials prescribe the tensile properties as given in the Table D.8.

Table D.8: ASTM Specifications for tensile properties of wrought iron. Longitudinal properties – minimum requirements

Property	Pipe	Refined Bars	Double Refined Bars	Forgings	Rivet rounds	Plates	Special forging plates (maximum transverse ductility)	Rolled shapes and bars
Tensile Strength, ksi	40	45-48	46-54	45	47	48	39	46-48
Yield point, ksi	24	25	23-32.4	22.5	28.2	27	27	23-28.8
Elongation in 8 in., %	12	16-20	22-28	24*	22-28	14	8 (either direction)	20-25
Reduction of area, %			35-45	33				30-40
* Four-inch gage length								

Table D.9 is based on the British standard specifications, which are also representative of American iron.

Table D.9: British standard specification of wrought iron

Shapes	Rounds and squares							Flats, angles and tees	Plates
	$\frac{3}{8}$	$\frac{9}{16}$	$\frac{3}{4}$	$1\frac{1}{2}$	2	$3\frac{1}{2}$	4		
Dimension, in								All size	$\frac{1}{4}$ - $\frac{1}{8}$ in. thick
Tensile strength, ksi	49- 56	49- 56	47- 54	47- 53	47- 53	47-53	47- 53	47-54	47-54**
Yield point as a % of tensile strength	56	56	56	56	56	50	50	50	
Elongation on 8 in., Percent	27	28	29	29	26	23-35	22	24-26*	17***
* 24 for angles and tees									
** Parallel to grain; 45(minimum) perpendicular to grain									
*** Parallel to grain; 12 perpendicular to grain									

D.5.3 Torsion Strength

Shafts of fibrous materials such as wrought iron, with the fiber parallel to the axis and along which fibers the shearing strength is relatively low, fail by shearing longitudinally. A hollow shaft, such as a thin-walled tube or pipe made of wrought iron and subjected to torsional failure, first flattens and then fails at a transverse section similar to a low carbon-steel pipe, which also has a shearing strength less than its tensile strength.

D.5.4 Impact Strength

Impact strength, in ft-lb, for wrought iron at 68°F, using various types of impact specimens, is listed Table D.10.

Table D.10: Impact strength of wrought iron

Standard Charpy (keyhole notch)	24 to 28
Standard Izod (Izod V-notch)	50 to 60
Modified Charpy (Izod V-notch) ^a	70 to 85
Modified Charpy (Izod V-notch) ^b	40 to 44
^a Specimens machined from double refined wrought iron rounds	
^b Longitudinal specimens machined from wrought iron plates – notch in the plane of the plate, transverse to fiber direction	

D.5.5 Compressive Strength of Wrought Iron

The properties shown by wrought iron in compression do not differ materially from its tensile properties. Its elastic limit, ultimate strength, and modulus of elasticity are about the same in compression as in tension, provided that the ratio of length to radius of gyration of the cross-section of the test specimen does not approach the point where lateral flexure occurs.

The compressive strength of wrought iron is between 45 and 60 ksi if the length is short in proportion to the radius of gyration. Usually, however, this proportion is too great to make it possible to disregard flexure, and the ultimate compressive strength must be taken to be only equal to the stress at the yield point, or from 25 to 35 ksi, according to the character and condition of the iron. Hence, the useful compressive strength of wrought iron is assumed equal to the yield point which, also, generally is assumed equal in tension and compression.

D.5.6 Modulus of Elasticity

The modulus of elasticity of wrought iron in both tension and compression ranges from 25.5×10^6 to 30×10^6 pounds per square inch. An average value of 28×10^6 pounds per square inch is probably representative of wrought iron of good quality. Some authorities however recommend an average value of 29×10^6

pounds per square inch for design purposes. The modulus of elasticity in torsion shear is approximately 11×10^6 pounds per square inch.

D.5.7 Fatigue Resistance

Wrought iron shows good resistance to fatigue fracture, or progressive failure of the crystals. Its ability to resist fatigue fracture explains the reason for its extensive use, particularly in the railroad and marine industries. The slag fibers which confer on the metal a tough, fibrous structure somewhat analogous to that of stranded wire cables, are responsible for this desirable property. These strands serve to minimize the stress concentration and deflect the path of the slip planes that develop in a metal under the influence of conditions that would ordinarily result in fatigue failure. For this reason wrought iron has a much longer life than other commonly used metals when subjected to conditions where sudden shocks and vibrations are encountered.

D. 5.8 Hardness

Hardness of wrought iron is, to a large extent, a reflection of the hardness of the base metal. The hardness will range from 97 to 105 by the Brinell method and from 55 to 60 on the “B” scale of the Rockwell hardness-testing machine.

D.5.9 Machinability

Wrought iron ranks high in machinability; the base metal is soft and short chips, resulting from the presence of the slag, produce clean, sharp threads on pipe or bars.

D.5.10 Specific Gravity

The specific gravity of wrought iron usually is taken to be 7.70. The unit weight corresponding to this specific gravity is 480 pounds per cubic foot.

D.5.11 Coefficient of Linear Expansion

The thermal coefficient of linear expansion of wrought iron has been determined to be 0.00000673 per degree Fahrenheit.

D.6 EFFECT OF HIGH AND LOW TEMPERATURES ON THE PHYSICAL PROPERTIES

Extreme cold increases the elastic limit of the wrought iron, but does not affect the tensile strength appreciably. It increases the ductility very slightly, and decreases the resistance to impact by 3%. The tensile strength increases with temperature from 0° F up to a maximum at from 400 to 600° F, the increase being from 8 to 10 ksi, and then decreases steadily until the strength of only 6 ksi is shown at 1500° F. The comparative strength, taking strength at 68° F as 100, are shown in Table D.11.

Table D.11: Effect of temperature on the physical properties of wrought iron.

Temp. Degree, F	300	500	700	900	1100	1300	1500
Tensile Strength, (comparative)	108	116	103	79	43	34	15

D.7 EFFECT OF ROLLING TEMPERATURE

Tests on a high grade of staybolt iron of two sizes and finished at various rolling temperatures showed that bars rolled considerably colder than usual in both $1\frac{3}{8}$ in. and $\frac{7}{8}$ in sections gave higher tensile strengths than those rolled at a usual temperature or higher, while with the large bars the low rolling temperature

gave the highest elastic limit, and also the greatest elongation and contraction. The greatest difference in elastic limit in either size, however was only 5 percent., in tensile strength 2 percent., in elongation about 4 percent., and in contraction about 3 percent. of the average figures. There was a marked increase in the elastic limit and tensile strength and a slight decrease in elongation, with a slight increase in contraction in the case of smaller bars, as compared with the large ones.

D.8 EFFECT OF REPEATED HEATING

Puddled iron is much improved in quality by being cut up, piled, reheated, and rolled or hammered, but indefinite repetition of this is detrimental. In practice it is advantages only in special cases to reheat puddled iron more than once. The Table D.12 given below shows the effect of repeated working. The metal began to deteriorate seriously after six workings, and no advantage is seen after the third working when the extra fuel and labor expended and the waste incurred are taken into account.

Table D.12: Effect of repeated heating

Working	Original bar	2nd	4th	6th	8th	10th	12th
Tensile strength, lb./sq.in.	43900	52900	59600	61800	57300	54100	43900

D.9 EFFECT OF WORK UPON WROUGHT IRON

The Table D.13 shows the results obtained from plates rolled in a three-high train, and in a 25-in. universal mill. The better figures for the latter mill are said to be due to the continuous rolling in one direction. The width was alike for

similar thicknesses and no difference was found in the universal plates whether they were 9 or 42 in. in width.

Table D.13: Physical properties of wrought iron plates from shear and universal mills

Thickness, in.	Sheared plates from three-high train				
	Number of tests	Elastic limit, lb/sq.in.	Ultimate strength, lb/sq.in.	Elongation in 8 in., percent.	Reduction of area, percent.
1/4	1	32400	51800	11.2	18.9
1/2	5	31180	49760	14.2	22.0
3/8	4	30775	50200	15.5	22.5
3/4	3	30400	49050	16.0	22.4
Plates from 25 in. universal mill					
1/4	1	32100	51000	13.0	19.9
3/8	2	31050	50650	14.6	21.6
1/2	3	31100	50530	17.3	26.2
3/8	3	30500	50830	17.2	24.6
3/4	3	31470	52570	19.0	26.2

Good iron, when drawn into No. 10 wire (0.134 inch diameter), has a strength of about 90,000 lb., and Nos. 15 and 20 (0.072 and 0.035 inch) have a tensile strength respectively of about 100,000 and 111,000 lb. per sq. inch [Mark, L.S., 1930].

D.10 INFLUENCE OF REDUCTION IN ROLLING FROM PILE TO BAR ON THE STRENGTH OF WROUGHT IRON

The tensile strength of the iron used in Beardslee's tests ranged from 46,000 to 62,700 lb/sq.in., brand L which was really a steel not being considered.

Table D.14 shows a few figures from one of the brands.

Table D.14: Effect of rolling on the tensile strength of wrought iron

Diameter of bar, in.	4	3	2	1	1/2	1/4
Tensile strength, psi	46322	47761	48280	51128	52275	59585
Elastic limit, psi	23430	26400	31892	36467	39126	-

D.11 EFFECT OF OVERSTRAIN AND COLD WORK

The effect of previous straining of wrought iron upon the elastic limit and ultimate strength, as revealed by subsequent test, is to raise the elastic limit and increase the ultimate strength provided the metal has been allowed to rest after strains.

Cold working of wrought iron, i.e., deforming it by rolling, hammering, or pressing, at temperatures below about 690°C (1274°F), affects the structure and the mechanical properties of iron in much the same way as straining beyond the elastic limit. The elastic limit is considerably raised, the ultimate strength is slightly raised, and the elongation or ductility is usually lowered.

D.12 FABRICATION

From the standpoint of practical application and installation problems the important characteristics of wrought iron include – durability when subjected to corrosive conditions, resistance to fatigue caused by shocks or constant vibration, ability to take on and hold protective coatings, weldability, and good forming, machining and threading qualities.

D.12.1 Forming

Wrought iron products can be formed to meet practically any requirements using standard equipment. In any forming operation the physical characteristics of the metal must be taken into account and this, of course, is true in working with wrought iron. Forming may be done either hot or cold with wrought iron, depending on the severity of the operation.

D.12.2 Threading and Machining

Threading and machining operations are easily accomplished with wrought iron. The fibrous structure of the material and the softness and uniformity of the base metal are responsible for these desirable qualities. The machinability or free-cutting characteristics of most ferrous metals are adversely influenced by either excessive hardness or softness. Wrought iron displays almost ideal hardness for good machinability, and the entrained silicate produces chips that crumble and clear the dies. Standard threading equipment which incorporates minor variations in lip angle, lead and clearance is usually satisfactory with wrought iron.

D.12.3 Forging

Wrought iron is an easy material to forge using any of the common methods. The temperature at which the best results are obtained lies in the range of 2100 to 2400° F. Ordinarily, “flat and edge” working is essential for good results. Limited upsetting must be accomplished at “sweating to welding” temperatures.

D.12.4 Bending

Wrought iron plates, bars, pipe and structurals may be bent either hot or cold, depending upon the severity of the operation, keeping in mind that bending involves the directional ductility of the material. Hot bending ordinarily is accomplished at a dull red heat (1300 to 1400° F) below the critical “red-short” range of wrought iron (1600 to 1700° F). The ductility available for hot bending is

about twice that available for cold bending. Forming of flanged and dished heads is accomplished hot from special forming, equal property plate.

D.12.5 Welding

One of the valuable properties of wrought iron is the comparative ease with which it may be welded. Its superiority is due largely to its comparative purity, since all impurities, especially carbon, silicon, and sulfur, reduce weldability in a marked degree. The general use of welding as a means of fabrication makes this an important characteristic. Wrought iron can be welded easily by any of the commonly used processes, such as forge welding, electric resistance welding, electric metallic arc welding, electric carbon-arc welding, hammer-welding and gas or oxyacetylene welding. The iron silicate or slag included in wrought iron melts at a temperature below the fusion point of the slag gives the metal surface a greasy appearance. This should not be mistaken for actual fusion of the base metal; heating should be continued until the iron reaches the state of fusion. The high degree of purity of the base metal in wrought iron makes its fusion temperature somewhat higher than that of other common ferrous metals, and for that reason it should be worked hotter for best results. The siliceous slag content provides a self-fluxing action to the material during the welding operation, thus serving as an important factor in producing a strong, uniform weld.

In gas welding, the procedure to employ with wrought iron is the same as that of mild steel, except that heating should be continued for a slightly longer period in order to attain the proper temperature. When using the electric-metal-arc

process, the best results are obtained when the welding speed is decreased slightly below that suitable for the same thickness of mild steel. In welding light sections where there is a possibility of burning through the material, it also may be necessary to employ a slightly lower current value. Excessive penetration should be no greater than that required to secure a sound bond between the deposited metal and the parent metal. The slight modifications in the procedure for electric fusion welding that have been indicated fall well within the normal operating range of standard equipment. Any good quality welding rod, either coated or bare, can be used in welding wrought iron.

Welding is employed extensively in making wrought iron installations and any experienced welder who can produce satisfactory welds in mild steel can likewise produce satisfactory welds in wrought iron.

D.12.6 Protective Coatings

Wrought iron lends itself readily to such cleaning operations as pickling and sandblasting for the application of the protective coatings. Where protective coatings such as paint or hot-dipped metallic coatings are to be applied, the coating are found to adhere more firmly to wrought iron and a thicker coat will be attained compared with other wrought ferrous metals. This is because the natural surface of wrought iron is microscopically rougher than other metals after cleaning, thus providing a better anchorage for coatings. Weight of zinc taken on by wrought iron in hot dip galvanizing process averages 2.35 oz or more per square feet and shows excellent adherence.

D.12.6.1 Adherence and Weight of Protective Coatings

Under some conditions where corrosion is a factor, the useful life of metals can be increased to some degree by the application of a protective coating, such as paint or galvanizing. The added life due to the coating will be influenced by the adherence of the coating to the metal surface and its weight or thickness. It should be remembered that the length of service life obtained from an installation subjected to corrosion will depend primarily on the durability of the metal itself, because after the coating is destroyed, the relatively thicker metal must bear the brunt of the corrosive attack.

It has been found through experience that either paint or hot-dipped metallic coatings, such as galvanizing, will adhere better and last longer on wrought iron than on the other commonly used metals. The answer lies in the fact that the natural surface of wrought iron is microscopically rougher than that of other metals and, therefore, provides a better tooth, or anchorage for paints. In the case of galvanizing, the natural roughness of a wrought iron surface is accumulated by the acid pickling operation used to clean metal before it is dipped in the molten zinc. The slag fibers are responsible for this increase in the roughness. Thus, a coat of zinc is given an even better anchorage than paint on wrought iron. As a result, wrought iron will take on a natural zinc coating which is 25% to 40% heavier than that on other metals and this makes the coating itself longer lived.

D.12.7 Corrosion Resistance

The resistance of wrought iron to corrosion has been demonstrated by long years of service life in many applications. Some have attributed successfully performance to the purity of iron base, the presence of considerable quantity of phosphorous or copper, freedom from segregation, to the presence of the inert slag fibers disseminated throughout the metal, or to combinations of such attributes.

One point definitely established, namely, that the slag fibers in wrought iron are present in such a great numbers that they serve in one capacity as an effective mechanical barrier against corrosion and, under most conditions, force it to spread over the surface of the metal rather than pit or penetrate. There is also a reason to believe that they have a definite influence upon the chemical composition, density, and adherence to the metal surface of any corrosion products that might be formed. As a result, the film or layer of corrosion products on the surface, although of microscopic thickness in many cases, affords a high degree of protection to the underlying metal. This, of course, is highly desirable because it tends to make the corrosion uniform rather than to permit it to localize, thereby causing premature failure.

The record for durability that wrought iron has established over a long period of years, subjected to a wide variety of actual operating conditions, provides a sound engineering basis for its use in the many services. Lacking imperishability in a metal, it is obviously safe and economical to employ one that has definitely proved its durability.

Laboratory corrosion testing has shown that wrought iron has very definite directional corrosion properties; that is, transverse and longitudinal sections faces shows significantly higher corrosion rates than rolled surfaces or faces.

In actual service the corrosion resistance of wrought iron has shown superior performance in such applications as radiant heating and snow-melting coils, skating-rink piping, condenser and heat exchanger equipment, and other industrial and building piping services. Wrought iron has long been specified for steam condensate piping where dissolved oxygen and carbon dioxide present severe corrosion problem. Cooling water cycles of the once-through and open-recirculating variety are solved by the use of wrought iron pipe.

D.13 USE OF WROUGHT IRON

The general uses of wrought iron are very numerous. Wrought iron is well suited to certain applications because of such properties and characteristics as softness, fibrous structure, ease of welding, and resistance to vibratory and fatigue stresses. It is important to keep in mind that wrought iron may be produced to obtain high fatigue strength or high corrosion resistance, or, sometime, a good combination of both of these properties. High fatigue strength requires much more rolling than high corrosion resistance and extensive rolling decreases corrosion resistance. In the manufacture of wrought iron, for stay bolt, engine bolt, sucker rods, and coupling rods, a high endurance ratio is the most important physical property.

D.13.1 Forms Available

Wrought iron is available in forging blooms and billets, in all types of hammered bars and forms, hot-rolled shapes, sheets, plates, structurals, rivets, chain, tubular products including pipes, tubing and casing, cold-drawn tubing, nipples, welding fittings and in the form of wire for nails, barbed wire, and general manufacture.

D.13.2 Applications

Wrought iron was formerly used to a great extent for making crucible steel and also used in the form of staybolt, rivets, water pipes, steam pipes, boiler tubes, rolled rods, bars, wire and by blacksmiths for horseshoes and general forging purposes, especially where welding plays a part. Bars and plates are made of single-refined iron, staybolt of double-refined iron and boiler tubes of knobbed charcoal iron. The applications include engine bolts, stay bolts, heavy chains, blacksmith iron, drawbars, and various other parts of locomotive and machines.

For about 25 years prior to the introduction of the Aston process in 1930, the principal uses of wrought iron were for standard pipe, tubular products, bars, and forging stocks; since then wrought iron has been used for structural shapes, plates, sheets, welding fittings, rivets, and special pipes and tubes. Wrought iron products are used in building construction, public works construction, and for the railroad, marine, and petroleum industries. Some of the application areas of wrought iron include building construction, industries, public works, railroad and marine works, structural works, etc.

D.14 WROUGHT IRON VERSUS STEEL

The fibrous character of wrought iron is often used as a basis for differentiating wrought iron from low-carbon steel in the nick-bend test, wherein the bar to be tested is nicked with a sharp chisel and bent cold with the nick at the outside of the bend. Steel snaps sharply after a small bend, but wrought tears gradually with a distinctly fibrous or “woody” fracture.

Wrought iron may also be distinguished from steel by means of the fact that steel nearly always contains an appreciable amount of manganese whereas wrought iron usually contains very little of this element. The presence of slag in its characteristic lines also distinguishes wrought iron, as steel should contain practically no slag. The presence of slag can also be determined by a deep acid etch since the slag fibers cause the surface to become black.

D.14.1 Test for Distinguishing Wrought Iron from Steel

A section ground flat and polished with two grades of emery paper is immersed in a bath containing 9 parts water, 3 parts of H_2SO_4 (concentrated) and 1 part of HCl, added in the order named. After 20 to 40 min. immersion, remove the piece and wash off the acid. If the piece is steel, the section will present a bright, solid, unbroken surface, while if made of wrought iron, it will show faint ridges (or, in a pipe section, rings like the age rings in a tree) showing the different layers of iron and streaks of cinder. The test will also show on a section of welded metal whether it has been lap welded or butt-welded.

The cold bend test for wrought iron is an important one for judging of general quality. A bar, perhaps $\frac{3}{4}$ x $\frac{3}{4}$ inches and 15 inches long, is bent when

cold either by pressure or by blows of a hammer. Bridge iron should bend, without cracking through an angle of 90 degrees to a curve whose radius is twice the thickness of the bar. Rivet iron should bend, without showing signs of fracture, through 180 degree until the sides of the bar are in contact. Wrought iron that breaks under this test is lacking in both strength and ductility.

D.15 THE NICK-BEND TEST FOR WROUGHT IRON

In nearly all the specifications, the material is judged by the character of the fracture of a nicked bar. A coarsely crystalline fracture is generally considered as indicative of inferior material. The testes were carried out on different grades of wrought iron and by using different methods of fracturing by research workers. All the tests were carried out under different condition and character of fracture was studies for each specimen. The “crystallinity” of the fracture depends upon the size and distribution of slag threads in the wrought iron and is a maximum in open-hearth wrought iron, which contains no such slag inclusions. The rate at which the specimen is fractured also affects the character of the break, and when broken by severe impact crytallinity usually results. The same material broken by bending shows a fibrous fracture. The results show that the test can not be depended upon to show the presence of steel in wrought iron or to give results by which the phosphorous content may be judged. The chemical composition of wrought iron specimens used for test series is shown in the Table D.15. The different physical properties of wrought iron specimen tested are as shown in the Table D.16 and Table D.17.

Table D.15: Chemical composition of wrought iron specimen used for test series

Specimen	C	Mn	P	S	Si
A1	0.04	0.046	0.136	0.025	0.265
A2	0.03	0.051	0.139	0.022	0.25
A3	0.04	0.114	0.132	0.027	0.027
B1	0.03	0.031	0.083	0.015	0.13
B2	0.01	0.030	0.126	0.016	0.16
B3	0.02	0.080	0.129	0.017	0.10
C	0.03	0.028	0.114	0.023	0.17
D	0.07	0.025	0.082	0.015	0.10
E	0.04	0.031	0.103	0.023	0.22
F	0.02	0.02	0.345	0.026	0.22
G	0.03	0.07	0.150	0.012	0.19
H*	0.02	0.02	0.004	0.020	0.003

* Open-hearth iron.

Table D.16: Physical properties of wrought iron tested

Material	Tensile properties			
	Yield point, psi	Ultimate tensile strength, psi	Elongation in 2 in., %	Reduction of area, %
A1	36500	51750	30.5	41.0
A2	31750	50350	32.0	37.0
A3	36500	51750	30.5	32.5
B1	33600	49350	36.0	50.0
B2	37000	50100	35.0	51.0
B3	34500	48000	19.5	26.5
C	37900	51250	38.5	55.0
D	33750	48500	40.5	57.0
E	28500	46750	11.0	15.0
F	34250	53350	29.0	29.5
G	32000	50500	36.0	39.5
H	27000	43250	51.6	76.5

Table D.17: Properties of wrought iron tested

Material	Notched bar tension test , ksi		Impact resistance (Izod), energy absorbed.	Repeated impact test, number of blows, 5 – pound hammer
	Yield point	Ultimate tensile strength		
A1	-	57000	35.5, 51.3, 38.5	21912, 3422
A2	-	-	48, 41, 46.5	-
A3	-	59000	37.5, 47.5, 42.5	3022, 1630
B1	50500	58500	46, 49.5, 47	7070, 10340
B2	-	-	44.5, 43.5, 45	-
B3	50000	56000	45.5, 45.5, 62	702, 700
C	55500	60500	55, 61, 45.5	1980
D	54500	65000	56.5, 63, 44.5	1468, 660
E	35500 36000	40500 42000	40, 30, 34.5, 31.5, 25.5, 35.5	306, 532, 1468, 726
F	47000	56000	24, 26, 35, 25, 29, 24	1952

To determine structure it is better to etch the surface with ammonium persulfate rather than using concentrated hydrochloric acid as it is not as convenient and successful as ammonium persulfate.

The rate at which the load is applied in fracturing the notched bars of wrought iron is of great importance and appears to be one of the predominant factors which determine the character of the fracture.

Another factor which appears to bear a close relationship to the size of the crystalline areas developed under impact is the relative size and distribution of slag threads. When the continuity of the metallic matrix is broken by large slag threads, the probability of a fibrous fracture being produced increased proportionally.

Crystalline areas in the fracture of wrought iron bars broken by the nick bend test are not to be interpreted as indicative of the presence of steel.

D.16 ALLOYED WROUGHT IRON

For a number of applications where wrought iron products are used, tensile properties higher of those of standard wrought iron would be desirable. It has long been recognized that the strength of wrought iron could be enhanced materially through the use of alloys, but, prior to the development of the modern manufacturing process now in use, this could not be accomplished successfully. However, the present day method lends itself readily to the production of alloy material and nickel alloy wrought iron can be produced for those services where high strength is necessary.

Wrought iron containing up to 5% nickel is possible, but for most purposes 1.5% to 3% has been found satisfactory. The following data will provide an indication of the comparative properties of unalloyed and 3% nickel wrought iron in the same class of product. The comparison of physical properties of unalloyed wrought iron and alloyed wrought iron is shown in the Table D.18.

Table D.18: Properties of Alloyed wrought iron

	Unalloyed wrought iron	3% nickel wrought iron
Tensile strength, psi	48000	60000
Yield point, psi	30000	45000
Elongation in 8 in., %	25	22
Reduction of area, percent.	45	40

From this data it is obvious that the alloy has a more marked effect on the yield strength than on the ultimate strength. These properties of the alloy material can be enhanced further by proper heat treatment. Of particular importance is the

effect of nickel on the impact strength at low temperatures. Charpy impact tests reveals that nickel alloy wrought iron retains to a high degree its impact strength at sub-zero temperatures. All of the other desirable characteristics and properties of unalloyed wrought iron are retained by the nickel-bearing material.

D.17 AVERAGE PROPERTIES OF WROUGHT IRON FROM VARIOUS REFERENCES

Table D.19 shows range of chemical composition of wrought iron from different references. Table D.20 shows the average properties of wrought iron collected from different references uncovered. The tables show the typical values or range. These values can be used for preliminary studies. For more accurate study, laboratory tests should be carried out to determine all relevant properties.

Table D.19: Chemical analysis of wrought iron

Phosphorous Content	Copper Content	C	Mn	P	S	Si	Slag	Cu
Normal	No	0.012	0.015	0.145	0.010	0.030	1.360	-
		0.056	0.141	0.192	0.034	0.280	6.220	
		0.046	0.043	0.166	0.023	0.173	3.420	
Normal	Varying amounts	0.020	0.019	0.081	0.014	0.056	2.310	0.051
		0.040	0.044	0.199	0.029	0.329	4.500	0.890
		0.032	0.029	0.151	0.021	0.179	3.640	0.192
High	No	0.007	0.011	0.216	0.017	0.144	2.920	-
		0.053	0.067	0.373	0.057	0.320	4.940	
		0.033	0.041	0.279	0.029	0.205	3.820	
High	Varying amounts	0.020	0.011	0.221	0.011	0.122	2.420	0.020
		0.042	0.070	0.479	0.045	0.235	5.300	0.290
		0.031	0.034	0.269	0.024	0.185	3.700	0.123

Table D.20: Average properties of wrought iron

Weight, lb/cu.ft.	486.7-493.0
Elastic Limit, ksi	24
Charpy impact – room temp, ft-lbs	40-44
Specific gravity	7.4 – 7.9
Melting point, °F	2730-2912
Specific heat	0.11 at 68 °F
Thermal coefficient of linear expansion	0.00000648 from 0 – 212 °F
Tensile strength, ksi	42-50
Yield point average, ksi	26-35
Elongation in 8 in., percent	25-40
Reduction of area, percent	40-45
Modulus of elasticity, ksi	25000 – 29000
Shear strength in single shear, ksi	38-40
Elastic limit in torsion, ksi	20.5
Modulus of elasticity in torsion , ksi	12.8
Brineell Hardness	95-107
Rockwell hardness	B55
Electric Resistance, 70 F, mo/cm/sq.cm	11.97
Shear modulus, ksi	11.8 at 80 °F
Poisson's ratio	0.30
Thermal conductivity K, btu/hr/sq.ft./in/°F	423 at 32 °F 360 at 400 °F
Specific heat, °F	59-212

Appendix E

Analysis and Load Rating of Case Study Bridge

Structural analysis and load rating of the case study bridge in Shackelford County, Texas is described in Chapter 4. This appendix documents details of the load rating calculations.

E.1 TRUSS MEMBER PROPERTIES

The Table E.1 lists computed truss member cross-sectional properties. These values were calculated from measured cross-sectional dimensions. Measured dimensions are shown in the drawings in Appendix B.

E.2 TRUSS MEMBER AXIAL FORCES

In the Table E.2 the maximum axial forces developed in each member are listed for different load conditions. The dead load was calculated based on the measured dimensions of the members and assumed unit weights. A dead load of 4.7 kips at all panel points was used to calculate the member axial forces. The value of 4.7 kips includes weight of the entire metal structure, all timber planks, the metal plate on the deck and only the seven primary timber stringers. The weight of the old timber stringers was not included, as it was assumed that these will be removed during rehabilitation. By removing the old timber stringers, the total dead load will be reduced by 22%. The live load considered for the analyses were AASHTO trucks. Live loads were placed so as to develop maximum axial

force in each member. AASHTO lane loading did not control for the case study bridge.

Table E.1: Truss member properties

Member	Length (L), in	Area (A), in ²	I _{xx} , in ⁴	I _{yy} , in ⁴	R _{xx} , in	R _{yy} , in	L/R _{min}
L0L1, L1L2, L2L3, L3L4, L4L5, L5L6	218	3	2.25	0.0625	0.866	0.144	1513.9
L0U1, L6U5	308	9.84	70.5	170.17	2.677	4.16	115.05
U1U2, U2U3, U3U4, U4U5	218	9.84	70.5	170.17	2.677	4.16	81.434
L1U1, L5U5	218	2	0.167	0.167	0.289	0.289	754.33
L2U2, L3U3, L4U4	218	3.875	78.2	12.07	4.5	1.765	123.51
L2U1, L4U5	308	3	1	0.14	0.577	0.216	1425.9
L2U3, L4U3	308	0.44	0.016	0.016	0.1875	0.1875	1642.7
L3U2, L3U4	308	1.5	0.28	0.031	0.432	0.144	2138.9

Table E.2: Maximum member forces due to dead and live load

Member	Axial force due to Dead load, kip	Axial force due to H15 Truck, kip	Axial force due to HS20 Truck, kip
L0L1, L1L2, L4L5, L5L6	+11.750	+12.115	26.9
L2L3, L3L4	+18.897	+17.974	41.0
L0U1, L6U5	-16.617	-17.133	-38.0
U1U2, U4U5	-18.800	-19.230	-41.8
U2U3, U3U4	-21.053	-20.426	-45.5
L1U1, L5U5	+4.700	+12.690	20.4
L2U2, L4U4	-2.253	-5.772	-12.0
L3U3	+0.193	-0.674	-1.3
L2U1, L4U5	+9.970	+13.597	29.5
L2U3, L4U3	-0.137	+2.271	4.4
L3U2, L3U4	+3.187	+8.163	17.0
+ve Tension			
-ve Compression			

E.3 TRUSS MEMBER CAPACITIES

The truss member capacities were calculated using both the Allowable Stress Design (ASD) and Load Factor Design (LFD) methods. The capacities for both inventory and operating levels are as shown in Table E.3.

E.4 LOAD RATING OF THE TRUSS

The load rating of all the truss members was calculated based on AASHTO manual [AASHTO, 1994]. The rating values are calculated for both inventory and operating service levels by using both Allowable Stress Design and Load Factor Design methods. The Table E.4 shows the load rating of all the truss members.

Table E.3: Truss member capacities in kips

Member	Allowable Stress Design (ASD)		Load Factor Design (LFD)
	Inventory	Operating	
L0L1, L1L2, L4L5, L5L6	+42.9	+58.5	+78.0
L2L3, L3L4	+42.9	+58.5	+78.0
L0U1, L6U5	-78.6	-98.0	-166.6
U1U2, U4U5	-90.0	-112.3	-190.9
U2U3, U3U4	-90.0	-112.3	-190.9
L1U1, L5U5	+28.6	+39.0	+52.0
L2U2, L4U4	-34.7	-43.2	-73.5
L3U3	-34.7	-43.2	-73.5
L2U1, L4U5	+42.9	+58.5	+78.0
L2U3, L4U3	+6.2	+8.5	+11.4
L3U2, L3U4	+21.4	+29.2	+39.0
+ve Tension			
-ve Compression			

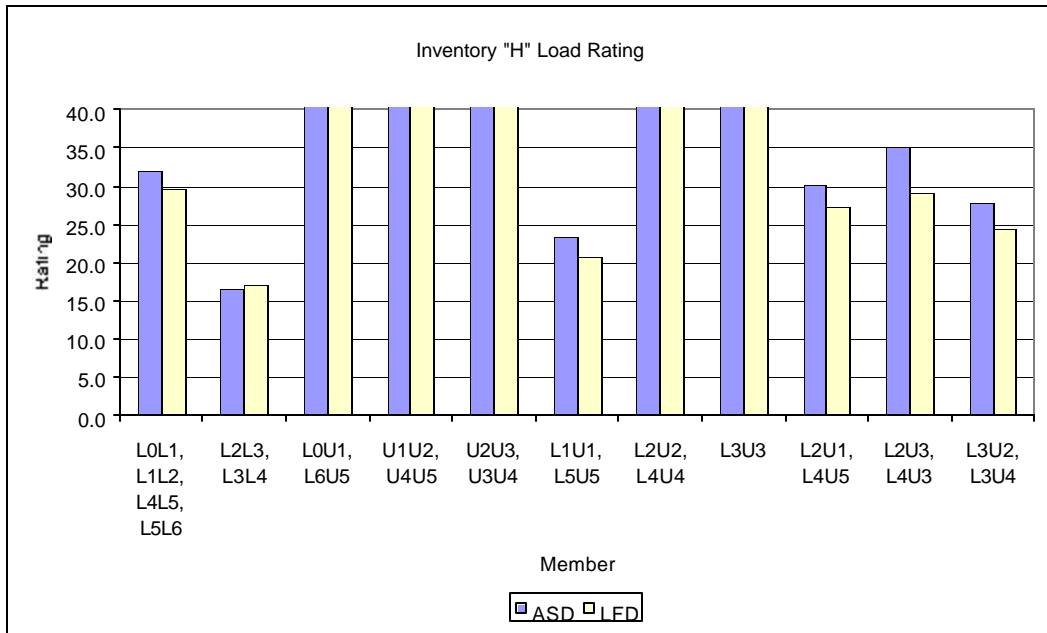
Table E.4: Truss member “H” load rating

Member	Allowable Stress Design (ASD)		Load Factor Design (LFD)	
	Inventory	Operating	Inventory	Operating
L0L1, L1L2, L4L5, L5L6	H 31.9	H 47.8	H 29.6	H 49.4
L2L3, L3L4	H 16.6	H 27.3	H 17.0	H 28.3
L0U1, L6U5	H 44.9	H 58.9	H 48.4	H 80.7
U1U2, U4U5	H 46.0	H 60.3	H 49.5	H 82.6
U2U3, U3U4	H 41.9	H 55.4	H 45.8	H 76.4
L1U1, L5U5	H 23.3	H 33.5	H 20.7	H 34.5
L2U2, L4U4	H 69.7	H 88.1	H 69.9	H 116.7
L3U3	H 641.8	H 799.4	H 625.6	H 1044.3
L2U1, L4U5	H 30.0	H 44.2	H 27.3	H 45.6
L2U3, L4U3	H 35.1	H 47.6	H 29.2	H 48.8
L3U2, L3U4	H 27.7	H 39.6	H 24.4	H 40.7

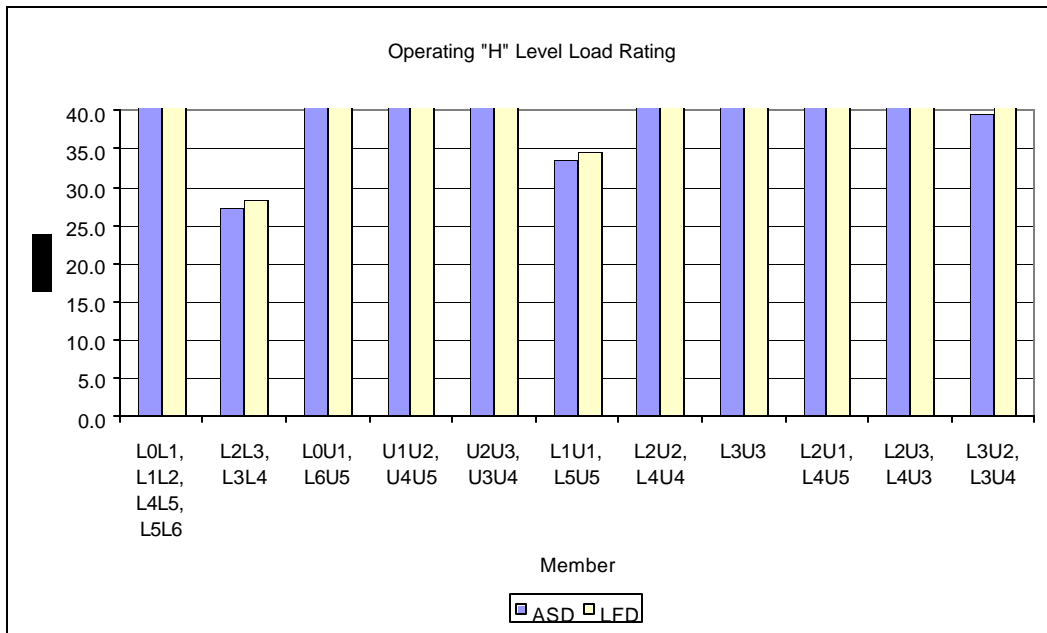
Table E.5: Truss member “HS” load rating

Member	Allowable Stress Design (ASD)		Load Factor Design (LFD)	
	Inventory	Operating	Inventory	Operating
L0L1, L1L2, L4L5, L5L6	HS 19.1	HS 28.7	HS 17.7	HS 29.6
L2L3, L3L4	HS 9.6	HS 15.9	HS 9.9	HS 16.5
L0U1, L6U5	HS 26.9	HS 35.4	HS 29.0	HS 48.5
U1U2, U4U5	HS 28.1	HS 36.9	HS 30.3	HS 50.6
U2U3, U3U4	HS 25.0	HS 33.1	HS 27.3	HS 45.6
L1U1, L5U5	HS 19.3	HS 27.7	HS 17.1	HS 28.6
L2U2, L4U4	HS 44.7	HS 56.5	HS 44.8	HS 74.8
L3U3	HS 443.6	HS 552.6	HS 432.4	HS 721.9
L2U1, L4U5	HS 18.4	HS 27.1	HS 16.7	HS 28.0
L2U3, L4U3	HS 24.3	HS 32.9	HS 20.2	HS 33.8
L3U2, L3U4	HS 17.7	HS 25.3	HS 15.6	HS 26.0

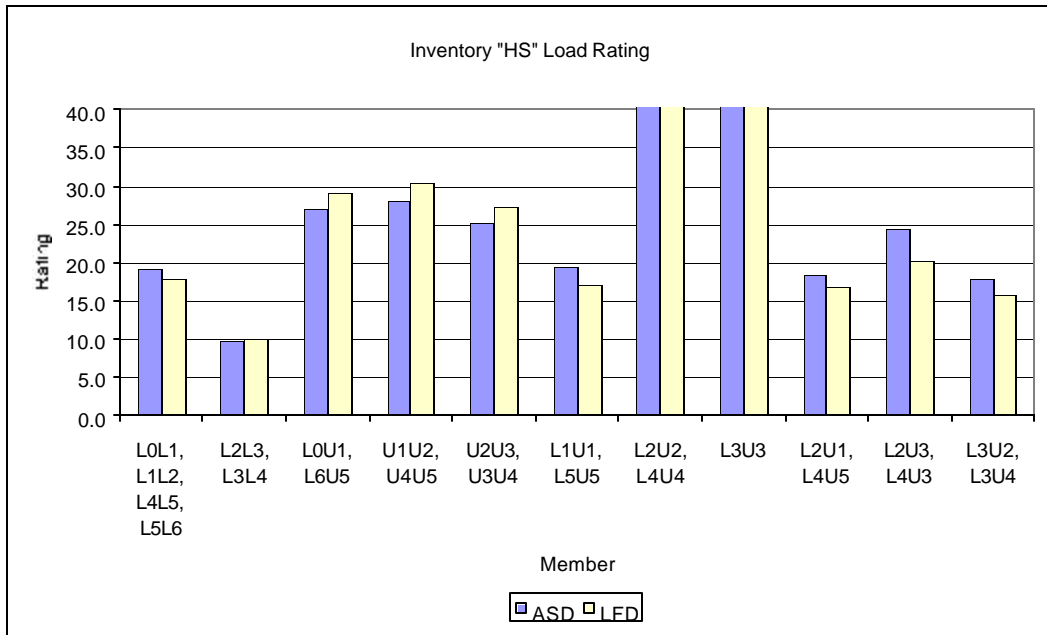
The above load ratings are graphically presented in the Graph E.1 through Graph E.4. The truss rating is controlled by the bottom chord members L2L3 and L3L4.



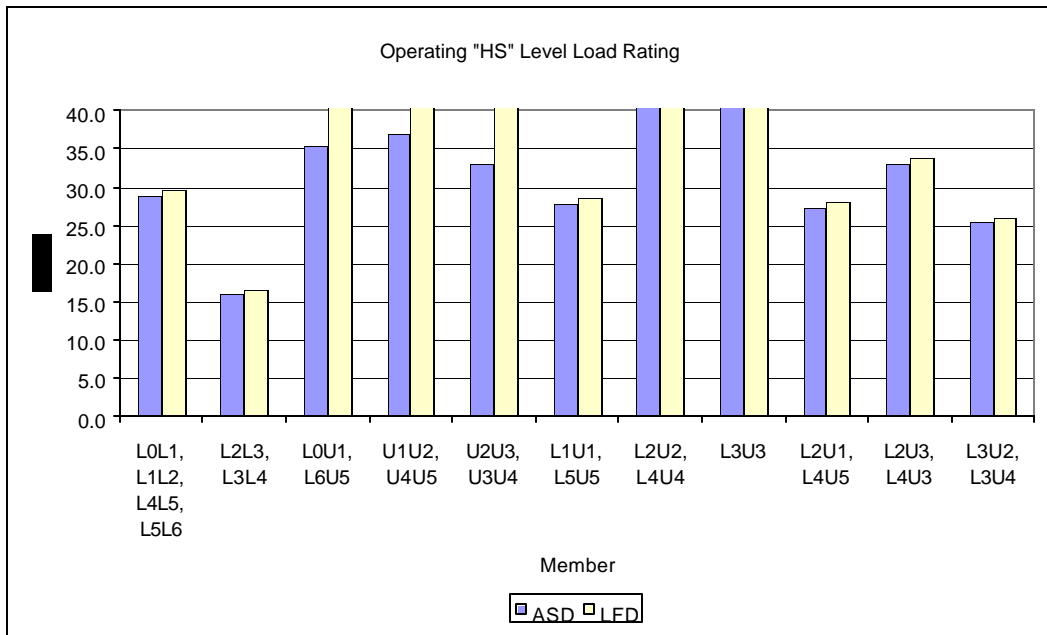
Graph E.1: Inventory "H" load rating of the truss



Graph E.2: Operating "H" load rating of the truss



Graph E.3: Inventory "HS" load rating of the truss



Graph E.4: Operating "HS" load rating of the truss

E.5 TIMBER DECK MEMBER PROPERTIES

The timber deck is made up of timber floor planks and timber stringers. For the dimensions and location of each stringer refer to Appendix B. The cross-sectional properties of the timber stringers are as shown on the Table E.6.

Table E.6: Timber stringer properties

Stringer Size		Span, L in	Area, A, in ²	Moment of Inertia. I _{xx} , in ⁴	Section Modulus, S _{xx} , in ³
Width, B, In	Depth, D, in				
8	16	218	128	2730	341
3	12	218	36	432	72

E.6 FORCES IN THE TIMBER DECK MEMBERS

From the various analyses conducted on the timber deck using various mathematical models (see Chapter 4), it was seen that most of the bending moment (about 80 to 85%) is carried by the two larger 8"x16" timber stringers. The remaining bending moment is distributed to the remaining smaller timber stringers. This distribution is dependant on the their stiffness, location and applied load. To simplify the analysis it was decided to divide the total wheel load between the two larger timber stringers. To take into account the fact that the smaller timber stringers will also carry some of the wheel load, it was decided to distribute 6% (see Chapter 4) of the total load to each of these stringers for bending moment. For shear force calculations, the total shear was distributed to the larger timber stringer, the central stringer and the outer stringer with distribution factors of 50%, 20% and 6% respectively (see Chapter 4). For calculation of the bending moment from the distributed load, the timber stringers

were considered as simply supported at both the ends. Table E.7 shows the forces developed in all the stringers due to an AASHTO H15 truck. Table E.8 shows the forces developed in all the stringers due to the dead load of the timber planks and timber stringers. The dead weight of the timber planks was distributed according to the tributary area supported by each timber stringer.

Table E.7: Forces in the timber stringers due to live load of AASHTO H15 truck

Stringer Size, in.	# of stringers	Load transferred from the wheel, kip	Maximum Bending moment, kip-in.	Maximum Shear Force, kip
8 x 16	2	12	654	12.69
3 x 12 (Central)	1	1.44	78.5	5.1
3 x 12 (Outer)	4	1.44	78.5	1.52

Table E.8: Forces in the timber stringers due to dead load

Stringer Size, in.	Self weight, Lb/ft	Weight of steel plate, Lb/ft	Weight of planks, Lb/ft	Total dead load, Lb/ft	Maximum Bending moment, kip-in.	Maximum Shear Force, kip
8 x 16	45	14	22	81	40	9
3 x 12	13	-	26	39	19.3	4.25

E.7 CAPACITY OF THE TIMBER DECK MEMBERS

The capacity of the timber stringers was calculated based on the lowest allowable bending stress, [AASHTO, 1996] as the species of the timber is not known. An allowable bending stress of 550 lb./in^2 and an allowable horizontal shear stress of 70 lb./in^2 were used for the capacity calculations. As the depth of the main stringers is more than 12 inches, the allowable unit stress in bending was modified for the size effect factor defined in the AASHTO specifications. For

operating level load rating all the capacities were taken as 1.33 times the capacities calculated as above. Table E.9 shows the calculated capacities for each stringer.

Table E.9: The capacity of the timber stringers

Stringer	Allowable bending stress, lb./in ²		Bending capacity, Kip-in		Allowable shear stress, lb./in ²	Shear capacity, kip	
	Original	Modified value	Inventory	Operating		Inventory	Operating
8 x 16	550	532	181	241	70	6	8
3 x 12	550	550	40	53	70	1.7	2.2

E.8 LOAD RATING OF THE TIMBER DECK

The load rating for the timber stringers was calculated for both the inventory and operating service level by using the allowable stress design method.

Table E.10 shows the load rating of the timber stringers.

Table E.10: The timber stringer load rating

Stringer	Inventory load rating based on		Operating load rating based on	
	Bending	Shear	Bending	Shear
8 x 16	H 3.2	-	H 4.61	-
3 x 12	H 3.9	-	H 6.4	-

The load rating based on shear capacity is less than zero as the dead load effect is more than the capacity. Hence, an HS load rating was not calculated.

E.9 METAL FLOOR BEAM PROPERTIES

The sectional properties of the metal floor beam were calculated based on the measured dimensions. Table E.11 shows the sectional properties at different sections of the floor beam.

Table E.11: Sectional properties of the metal floor beam

Section	Area, A, in²	Moment of Inertia, I_{xx}, in⁴	Section modulus, S_{xx}, in³
At mid-span	11.20	719.3	70.18
At end of the span	9.86	385.13	49.06
Under the wheel load (36" from mid-span)	7.84	91.91	21.63

E.10 FORCES ON THE METAL FLOOR BEAM

The bending moment and the shear force developed in the floor beam were calculated by considering it as a simply supported beam. The dead weight of the deck was calculated based on the tributary area supported by the each timber stringers. The dead weight of the deck from the stringers was considered to act as point loads on the floor beam. The wheel load transferred to the floor beam was maximum when the rear wheels were located directly above the floor beam. The Table E.12 shows the maximum bending moment developed in the floor beam at various sections due to dead load and live load.

Table E.12: Forces in the floor beam

Section	Bending Moment, kip-inch		
	Due to Dead load	Due to H15 truck	Due to HS20 truck
At mid-span	156.38	685.26	1107
Under the wheel load	135.82	685.26	1107

E.11 CAPACITY OF THE METAL FLOOR BEAM

The bending moment capacity of the floor beam was calculated based on the calculated sectional properties and the allowable bending compression stress based on the AASHTO guidelines [AASHTO, 1994]. In the calculations of

maximum unsupported length of the compression flange, no lateral support from the timber stringers was considered. Hence, the unsupported length of the compression flange was taken equal to the total span length of the floor beam. However, lateral torsional buckling was not controlling the capacity. The bending capacity was calculated at various sections by using both Allowable Stress Method and Load Factor Method. Table E.13 shows the calculated bending capacity of the floor beam at various sections.

Table E.13: The bending capacity of the floor beam

Section	Bending capacity of the floor beam, kip-inch		
	Allowable Stress Method		Load Factor Method
	Inventory	Operating	
At mid-span	1003	1368	1824
Under the wheel load (36" from mid-span)	701	956	1275

E.12 LOAD RATING OF THE METAL FLOOR BEAM

The load rating of the floor beam was calculated based on the forces developed and the capacity. Table E.14 shows the load rating of the floor beam.

Table E.14: The load rating of the floor beam

Section	Allowable Stress Method		Load Factor Method	
	Inventory	Operating	Inventory	Operating
At mid-span	H 15.3 HS 9.4	H 21.9 HS 13.5	H 13.5 HS 8.3	H 22.5 HS 13.9
Under the wheel load (36" from mid-span)	H 10.2 HS 6.3	H 14.8 HS 9.1	H 9.1 HS 5.6	H 15.2 HS 9.4

E.13 LOAD RATING OF THE BRIDGE

The bad rating of the bridge is taken as the minimum rating for any member of truss, the deck and the metal floor beams. The lowest load rating corresponds to the shear capacity of the timber stringers. The lowest rating of the bridge is less than zero. Hence, the bridge is not capable of taking any vehicular loads.

Appendix F

Field Load Testing of Case Study Bridge

As described in Chapter 5, two field load tests were conducted on the Shackelford County, Texas case study bridge. These tests were conducted on 6th May 1999 and on 7th September 1999. For each test, the bridge was instrumented with a total of 45 strain gages. Sections F.1 and F.2 of this appendix show the location of the strain gages for each test. Section F.3 presents a series of plots that compare the measured stresses derived from the strain gages, with the predicted stresses derived from a structural analysis of the bridge.

F.1 STRAIN GAGE LAYOUT FOR THE FIRST TEST

Out of the 45 strain gages used in this test, 31 were installed on the upstream truss, 12 were installed on the downstream truss, and remaining 2 were installed on a metal floor beam. The locations of strain gages were selected to obtain data on a large number of truss members, in order to evaluate the overall behavior of the trusses. All the members of upstream truss were instrumented with strain gages and one-half the members of downstream truss were instrumented. The locations of instrumented members are shown in Figure F.1. All strain gages mounted on the members were positioned away from the joints. Nearly all the strain gages were placed near the middle of the member length. This was done to eliminate any local variation of stress near the joints. An

identifier for each gage on the upstream and the down stream trusses are shown in Figures F.2 and F.3. The location of strain gages on the cross-section of each member are shown in Figures F.4. On these figures, “Inside” refers to the side of the member facing the bridge deck.

Since the bottom chord members were found to be critical from the load rating, it was decided to instrument as many of these as possible. All the six bottom chord members of the upstream truss were instrumented with two strain gages, one on each eyebar of each chord member as shown in Figure F.4(a). Top chord member U2U3 was instrumented with gages both at mid-span and at neat joint U3. These two sets of gages were provided to determine if any bending moment developed in these member.

The two strain gages on the metal floor beam were mounted on the top flange of the beam only. These gages were installed from the bridge deck. The bottom flange and the web of the floor beam were not easily accessible.

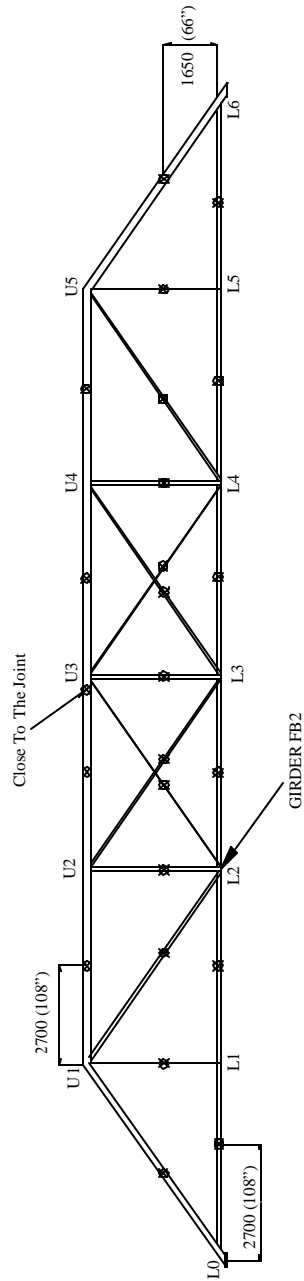


Figure F.1: Field load test No.1 – Locations of instrumented members

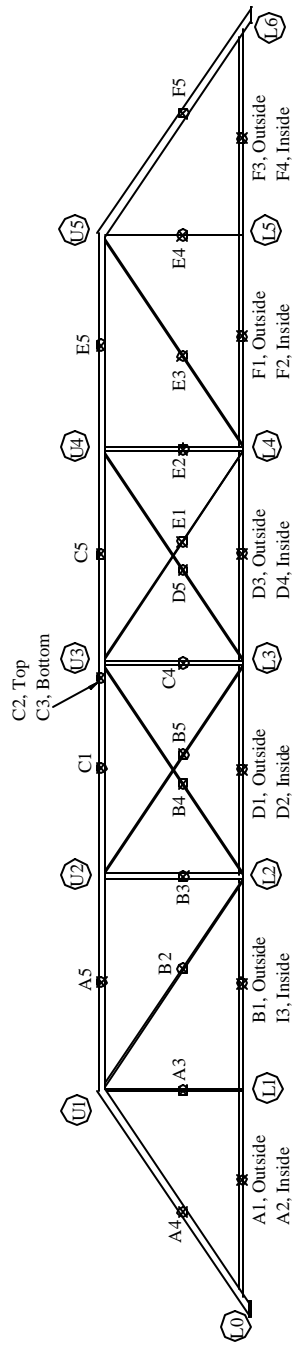


Figure F.2: Field load test No.1 – Gage identification for upstream truss

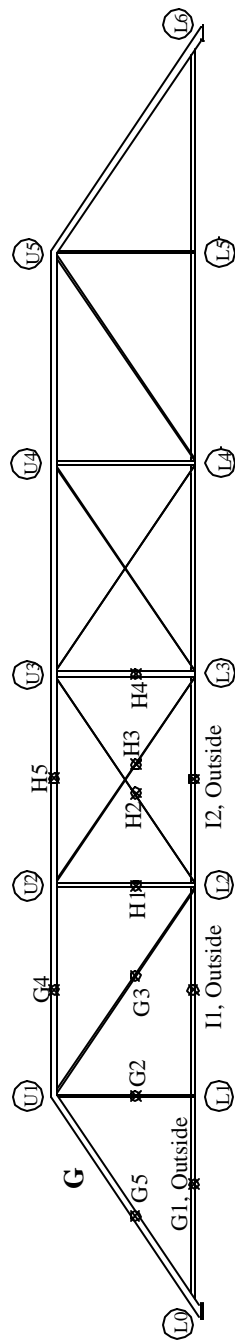


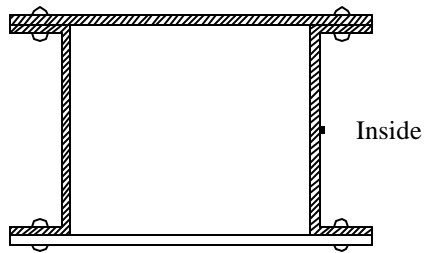
Figure F.3: Field load test No.1 – Gage identification for downstream truss



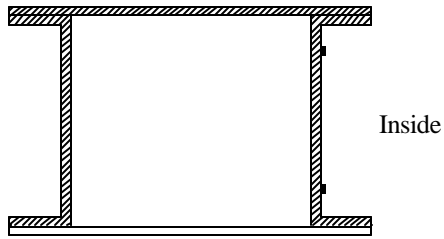
(a) Bottom chords of the upstream truss (members L0L1, L1L2, L2L3, L3L4, L4L5 and L5L6)



(b) Bottom chord of the downstream truss (members L0L1, L1L2 and L2L3)



(c) Top chord of the trusses (members L0U1, U1U2, U2U3, U3U4, U4U5 and U5L6 of upstream truss and members L0U1, U1U2 and U2U3 of downstream truss)



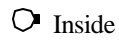
(d) Top chord near joint U3 (member U2U3 of Upstream truss)



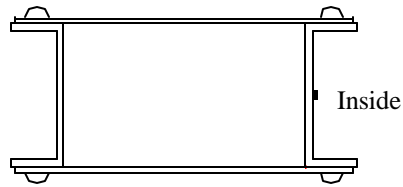
(e) Diagonal members of the trusses (members U1L2, U2L3, L3U4 and L4U5 of upstream truss, and U1L2 and U2L3 of downstream truss)



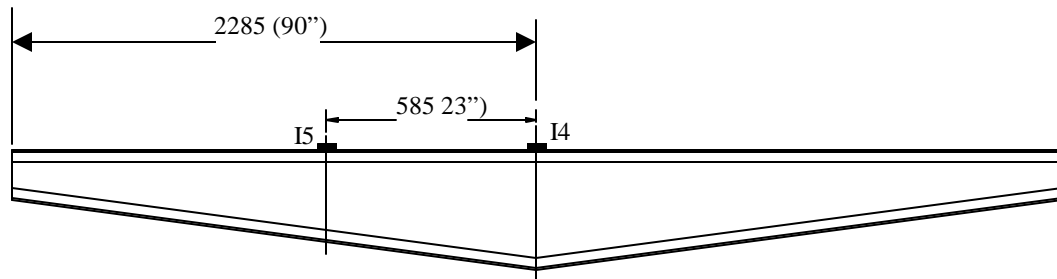
(f) Hangers of the trusses (members L1U1 and L5U5 of upstream truss, and L1U1 of downstream truss)



(g) Tension rods of the trusses (members L2U3 and U3L4 of upstream truss, and L2U3 of downstream truss)



(h) Vertical members of the trusses (members L2U2, L3U3 and L4U4 of upstream truss, and L2U2 and L3U3 of downstream truss)



(i) The metal floor beam (Girder FB2)

Figure F.4: Field load test No.1 – Location of strain gage on member cross-sections

F.2 STRAIN GAGE LAYOUT FOR THE SECOND FIELD LOAD TEST

Only a few members of upstream truss were instrumented with strain gages. A larger number of strain gages were installed at any particular section of the members to study the axial force distribution over the cross-section of the members. Figure F.5 shows the details of location of strain gages for the instrumented members.



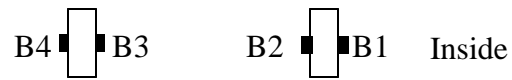
(a) Bottom chord L1L2



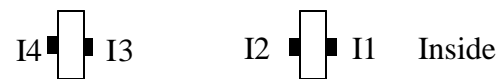
(b) Bottom chord L2L3



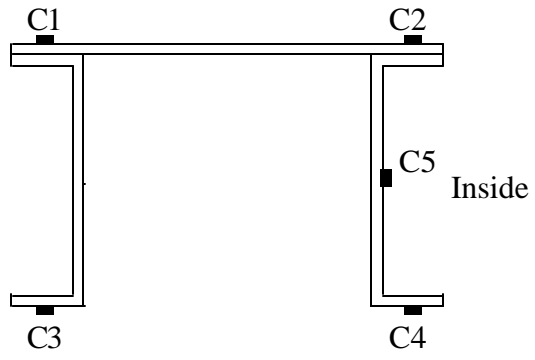
(c) Diagonal rod L2U3



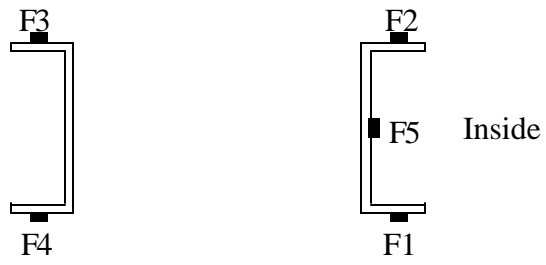
(d) Diagonal member L2U1



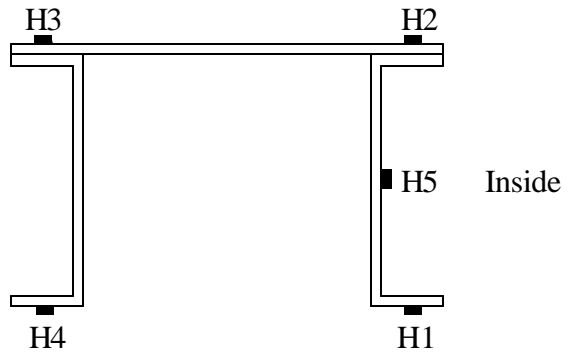
(e) Diagonal member L3U2



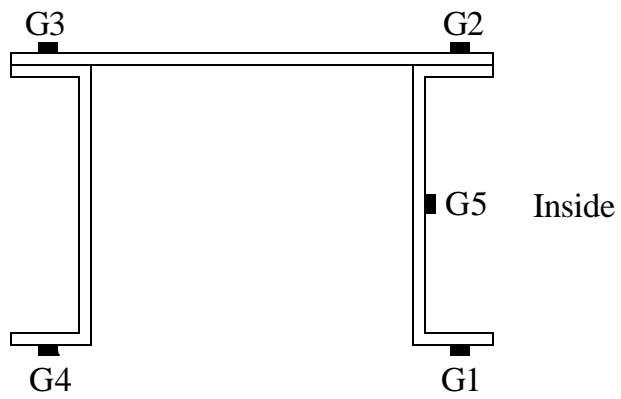
(f) Top chord L0U1



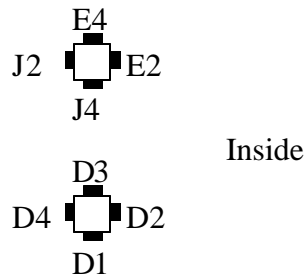
(g) Vertical member L2U2



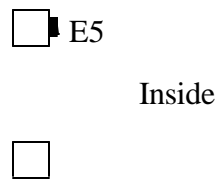
(h) Top chord U1U2



(i) Top chord U2U3



(j) Vertical hanger L1U1 (at 74" from the floor beam)

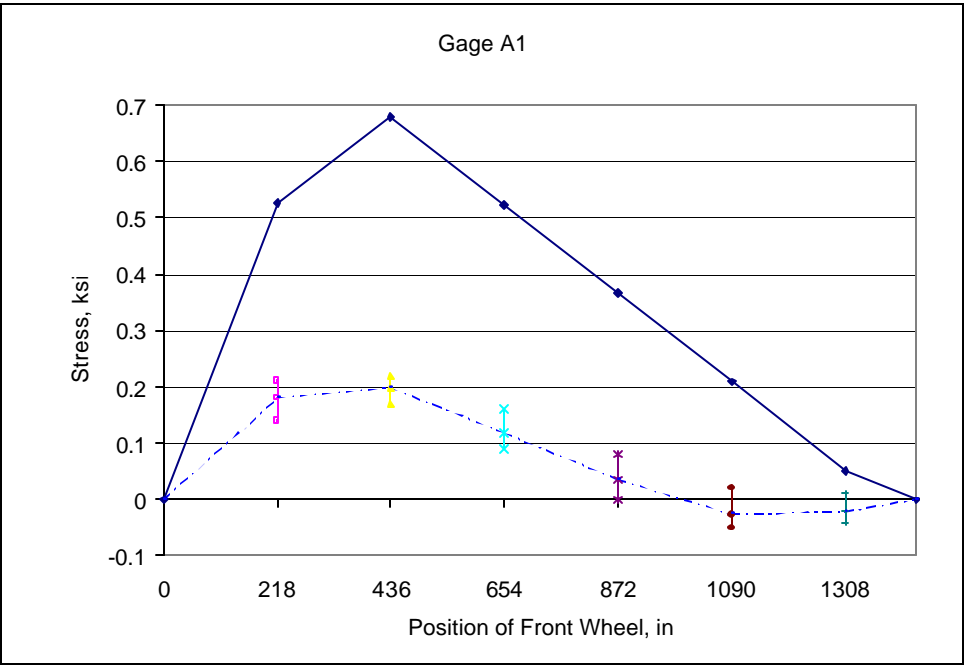


(k) Vertical hanger L1U1 (at 18" from the floor beam)

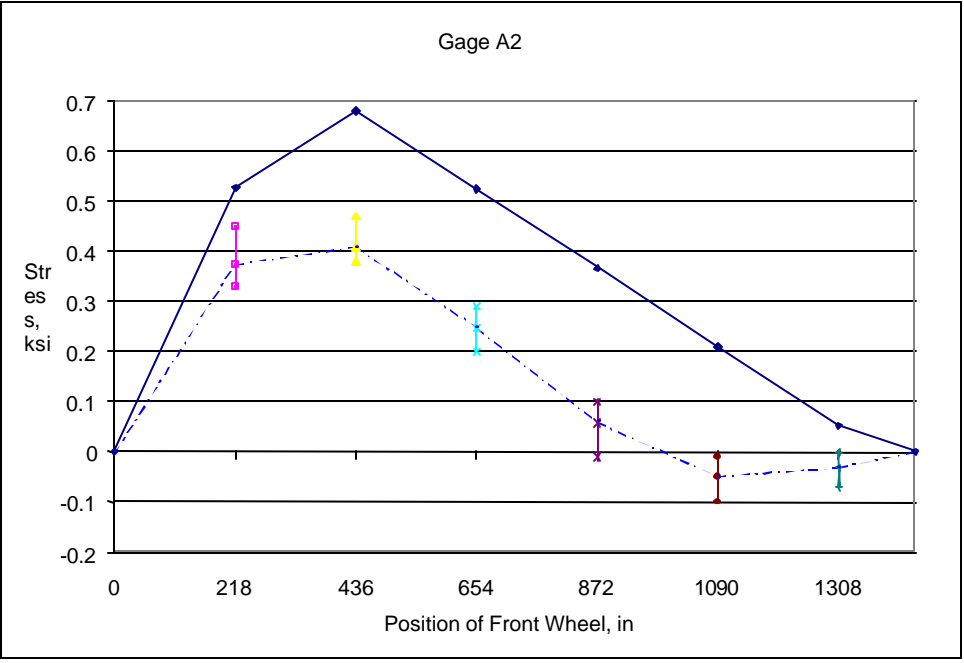
Figure F.5: Field load test No.2 – Location of strain gages

F.3 COMPARISON OF FIELD LOAD TEST DATA AND STRUCTURAL ANALYSIS RESULTS

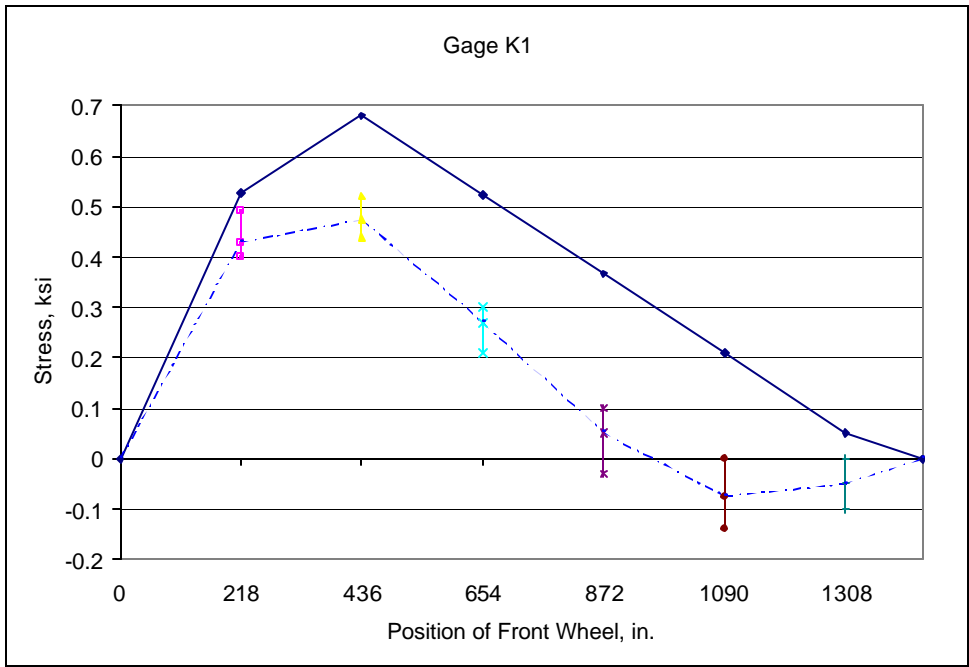
The collected data was analyzed and compared with theoretical analysis results predicted by structural analysis. In this section, graphs of Stress versus position of the front wheel of the loading vehicle are presented for all the gages. No results are presented for gage F2, as the gages malfunctioned during first field load test. Each graph shows the theoretical stress value in a solid line and the average test value in a dotted line. The field test results are presented in the form of minimum value, maximum value, and average value of the stress at different vehicle location. Graphs F.1 to F.44 are of field load test No.1 and the remaining graphs are of field load test No.2.



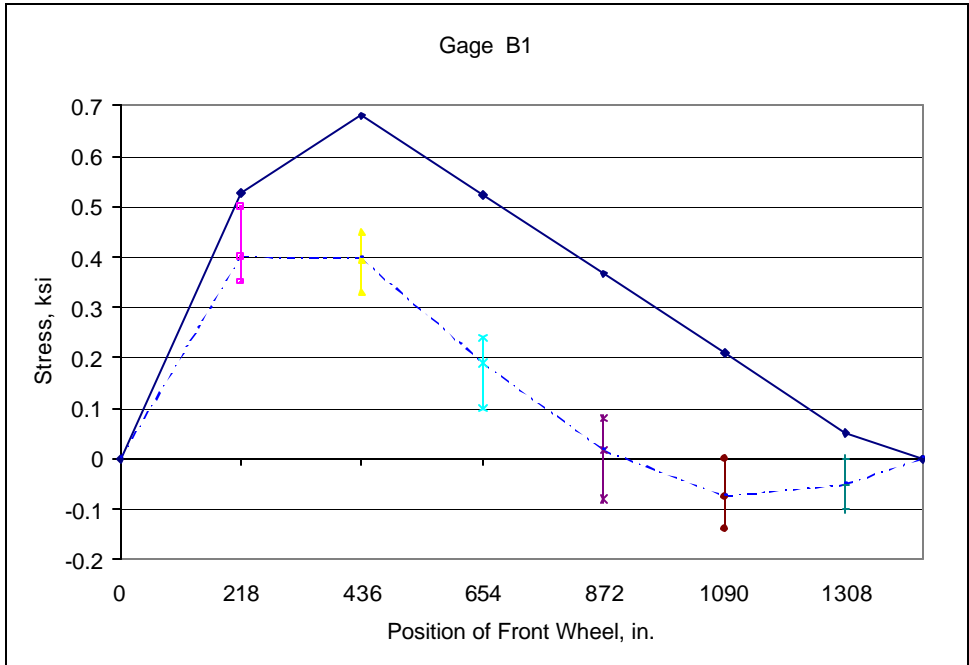
Graph F.1: Member L0L1 (Outside) of the upstream truss



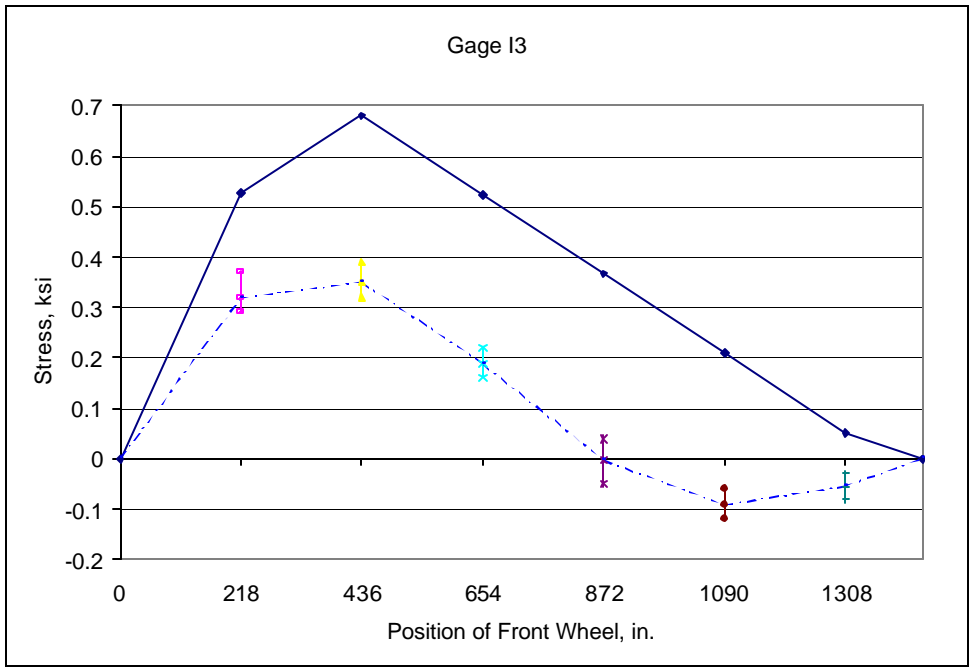
Graph F.2: Member L0L1 (Inside) of the upstream truss



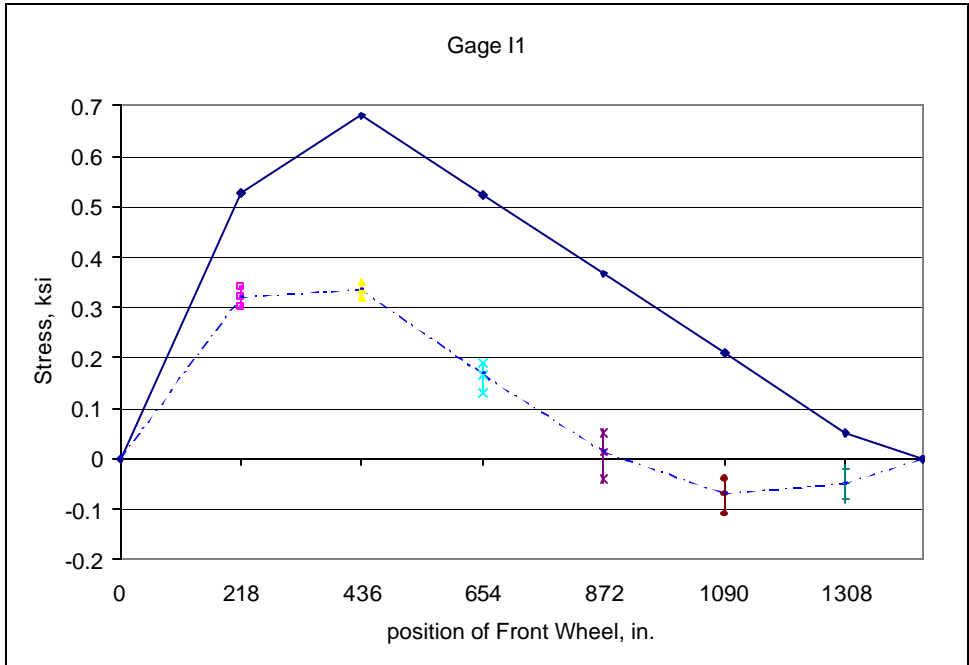
Graph F.3: Member L0L1 (Outside) of the downstream truss



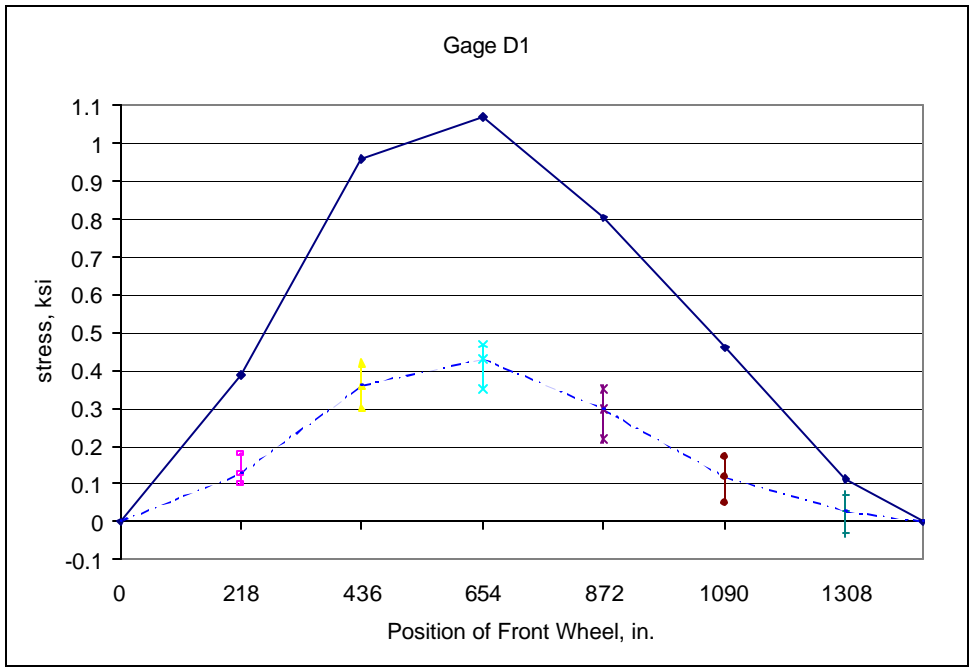
Graph F.4: Member L1L2 (Outside) of the upstream truss



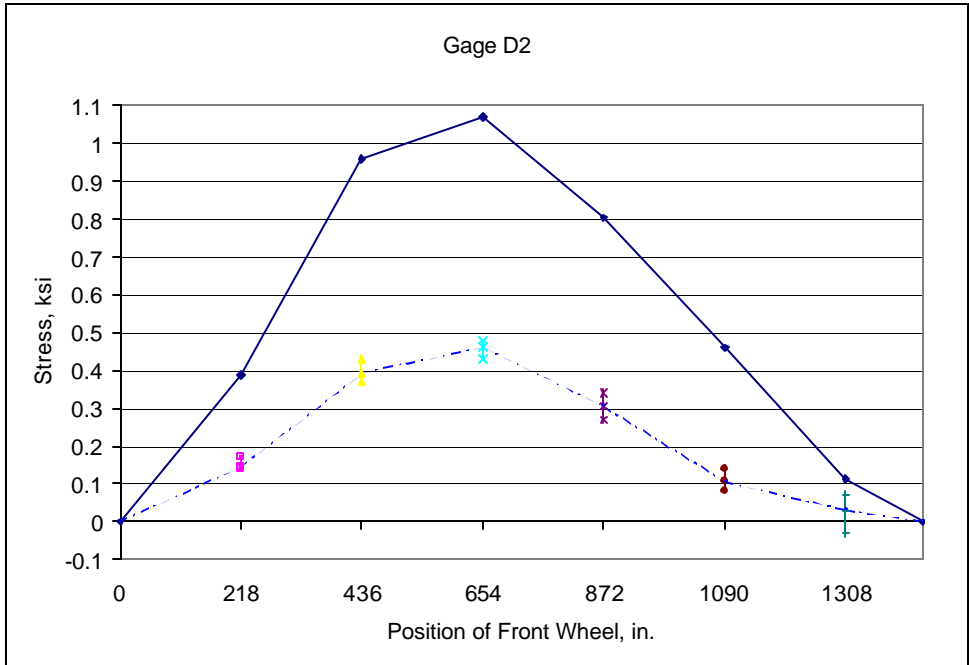
Graph F.5: Member L1L2 (Inside) of the upstream truss



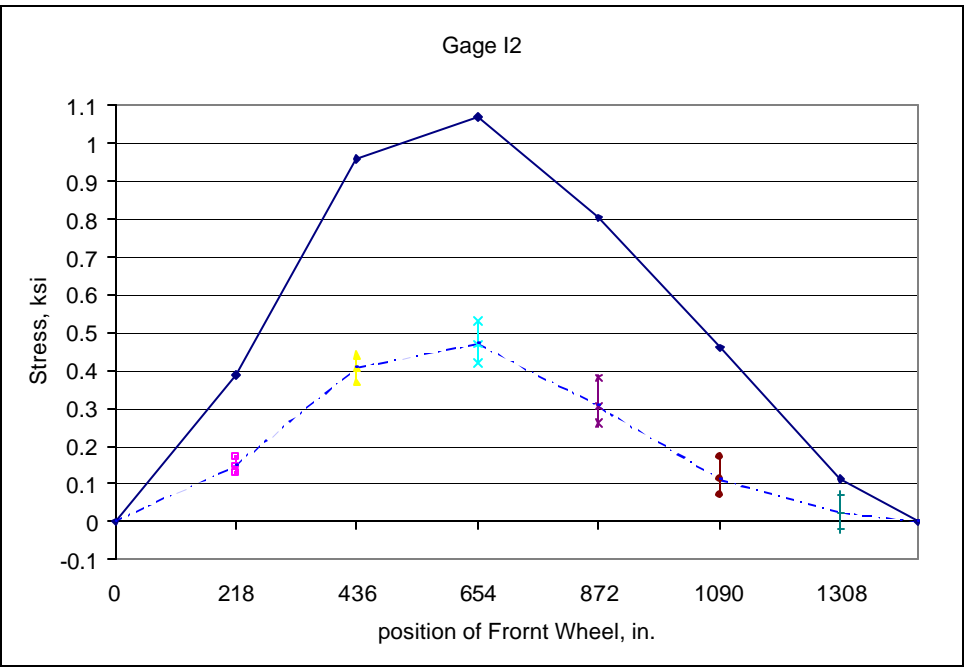
Graph F.6: Member L1L2 (Outside) of the downstream truss



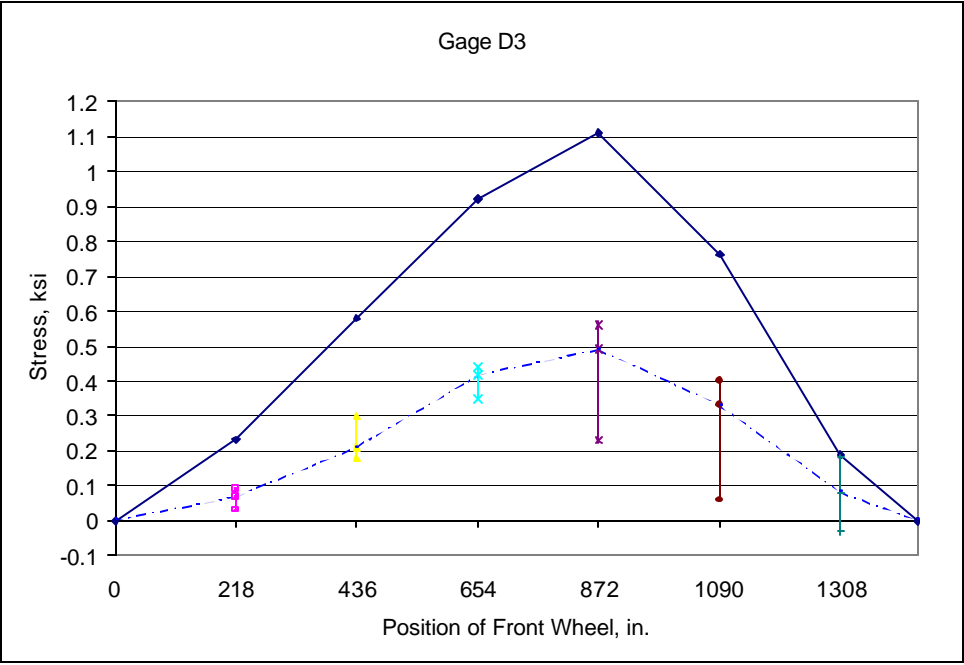
Graph F.7: Member L2L3 (outside) of the upstream truss



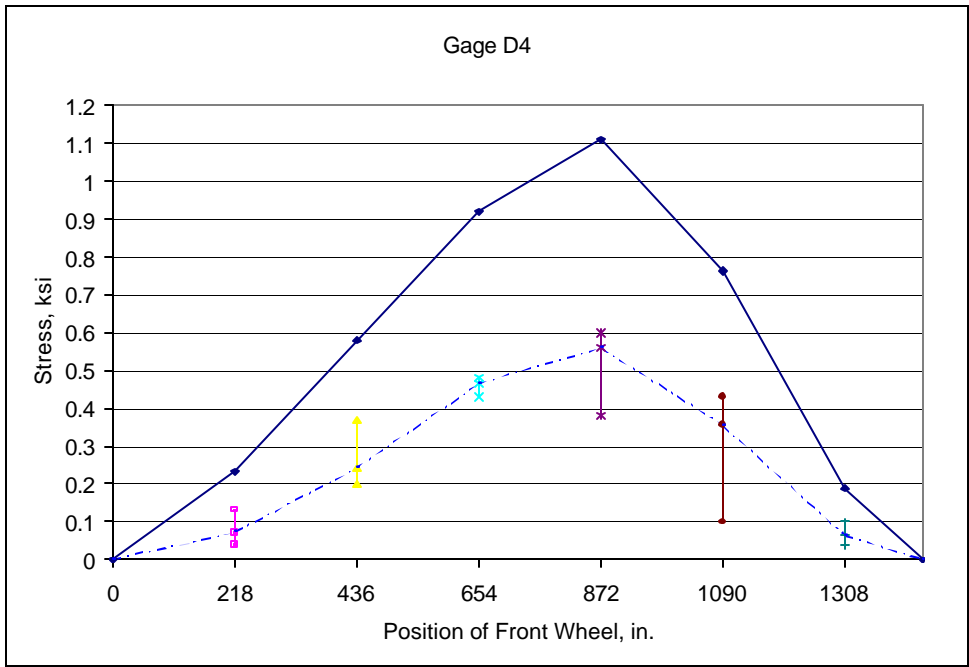
Graph F.8: Member L2L3 (Inside) of the upstream truss



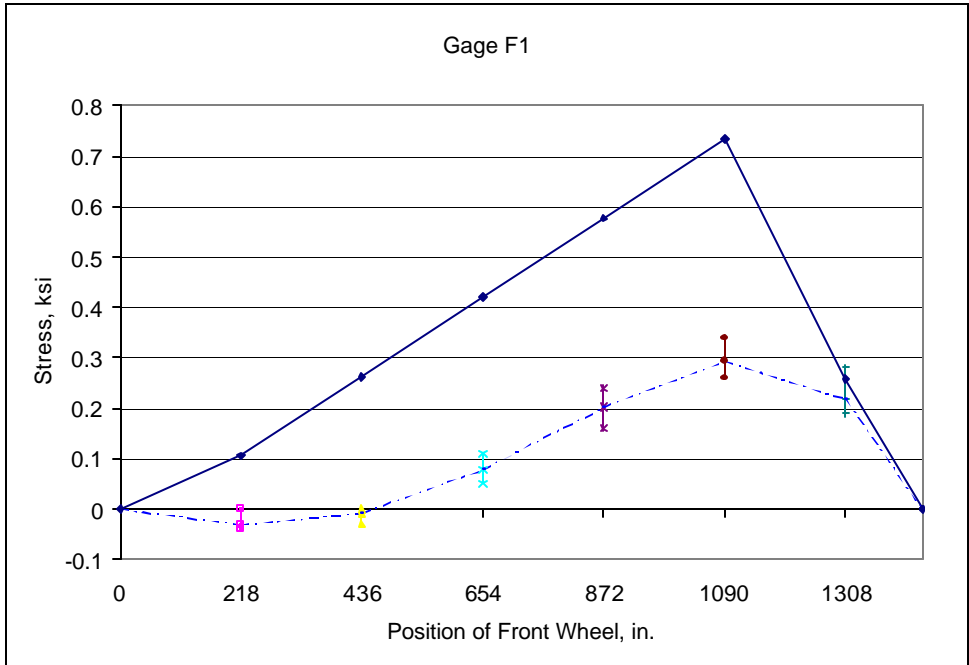
Graph F.9: Member L2L3 (Outside) of the downstream truss



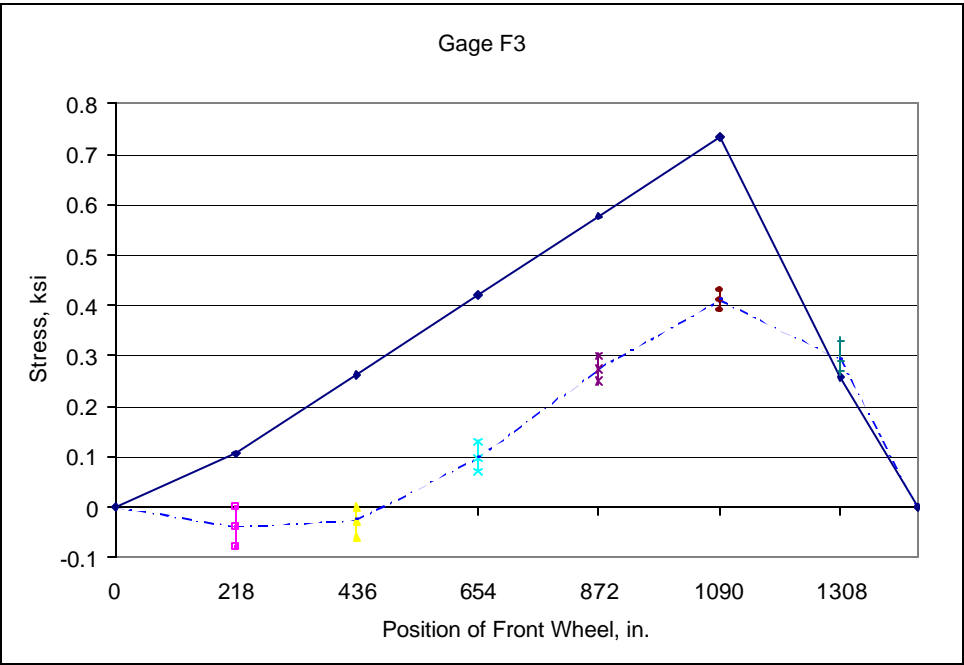
Graph F.10: Member L3L4 (Outside) of the upstream truss



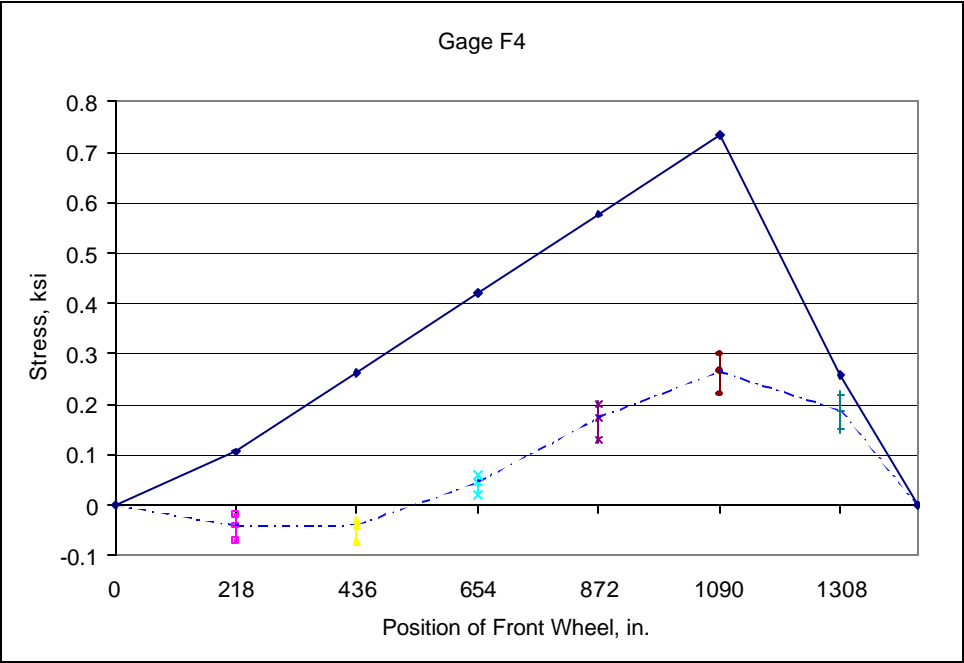
Graph F.11: Member L3L4 (Inside) of the upstream truss



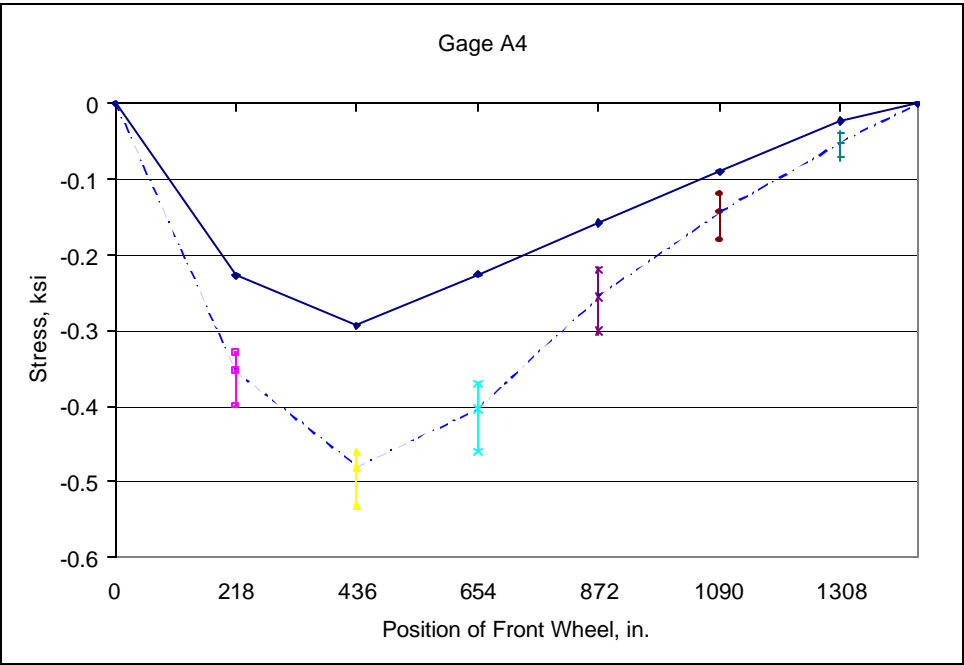
Graph F.12: Member L4L5 (Outside) of the upstream truss



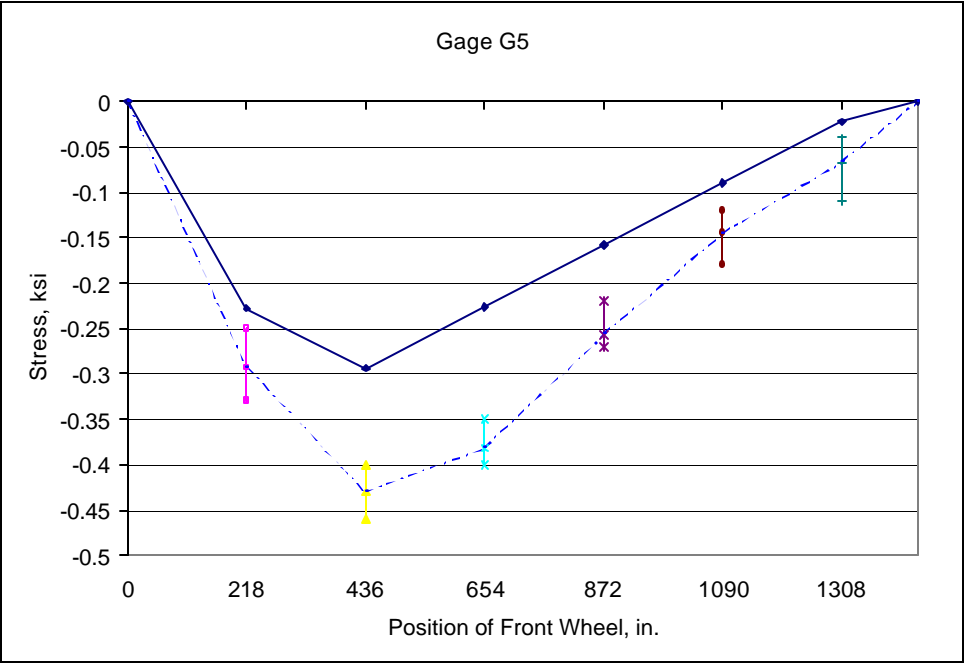
Graph F.13: Member L5L6 (Outside) of the upstream truss



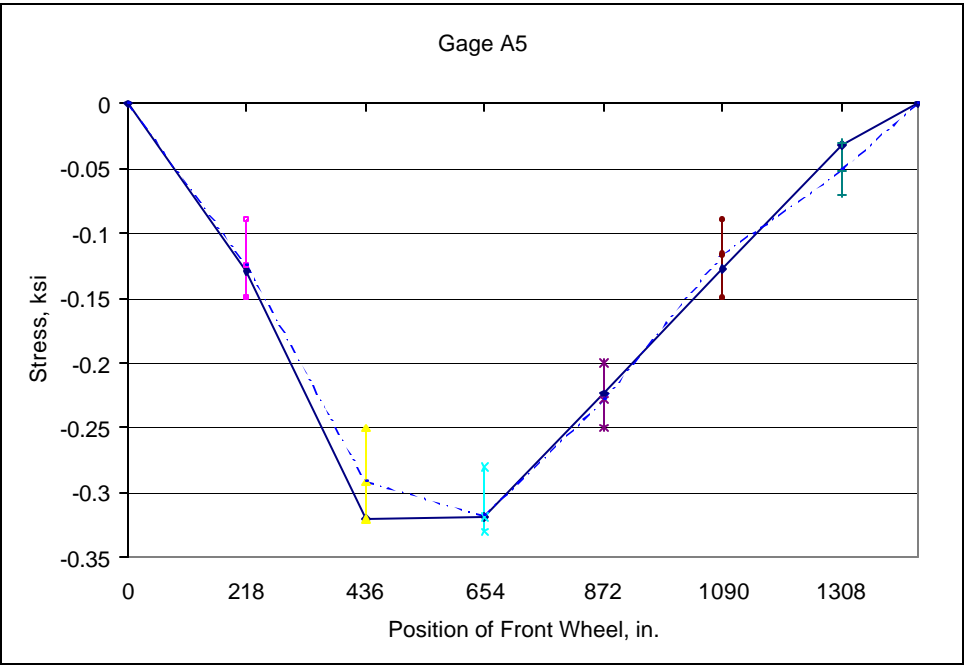
Graph F.14: Member L5L6 (Inside) of the upstream truss



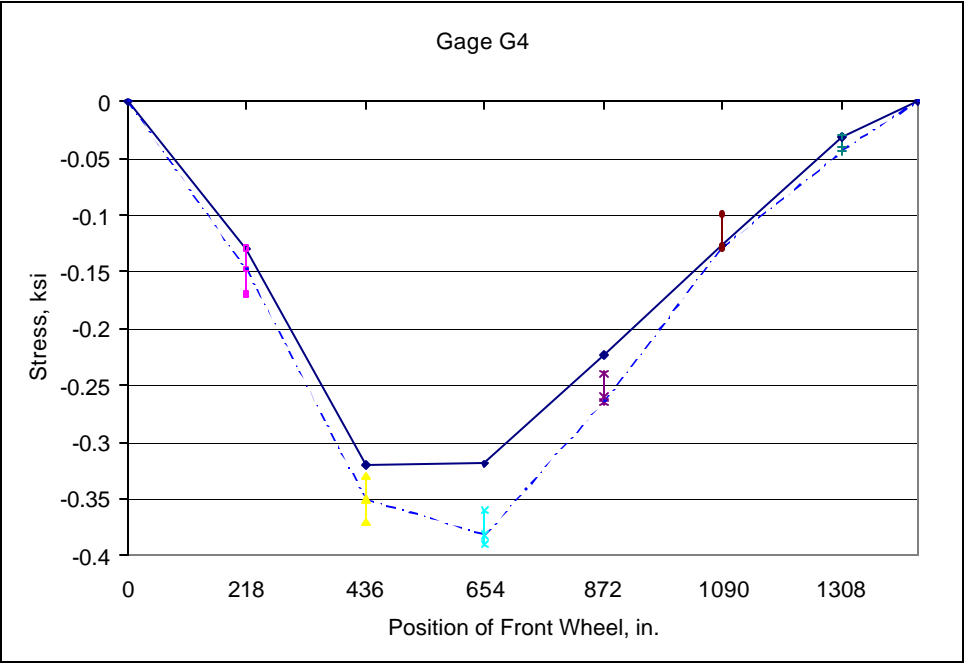
Graph F.15: Member LOU1 of the upstream truss



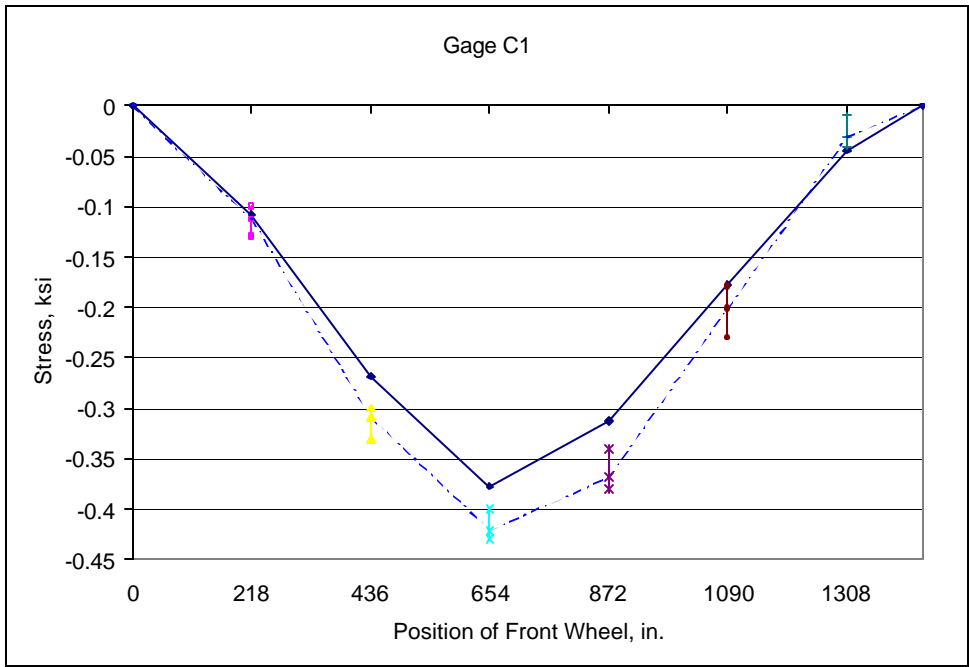
Graph F.16: Member LOU1 of the downstream truss



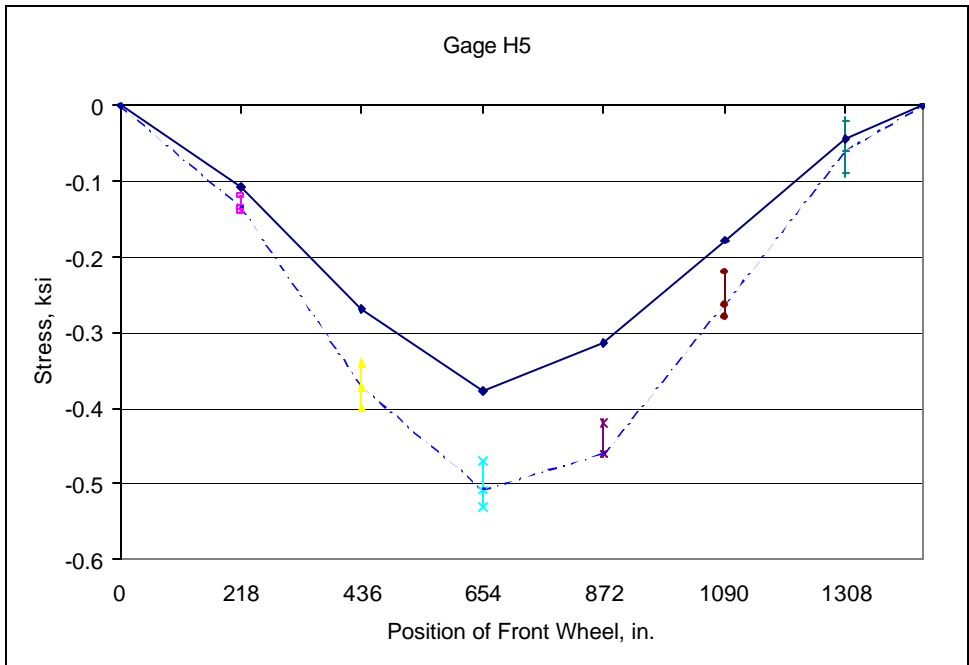
Graph F.17: Member U1U2 of the upstream truss



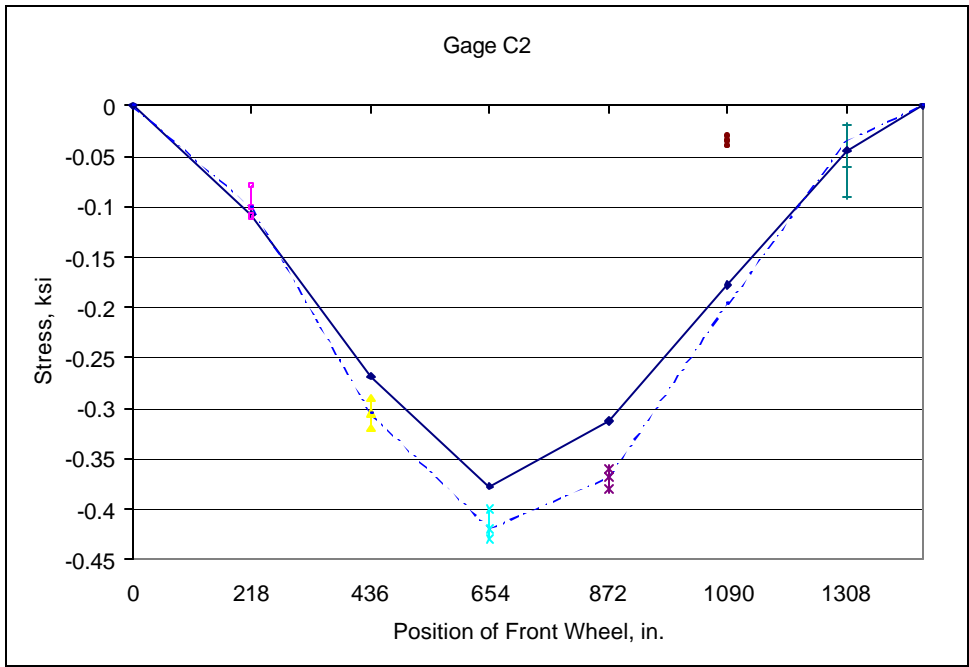
Graph F.18: Member U1U2 of the downstream truss



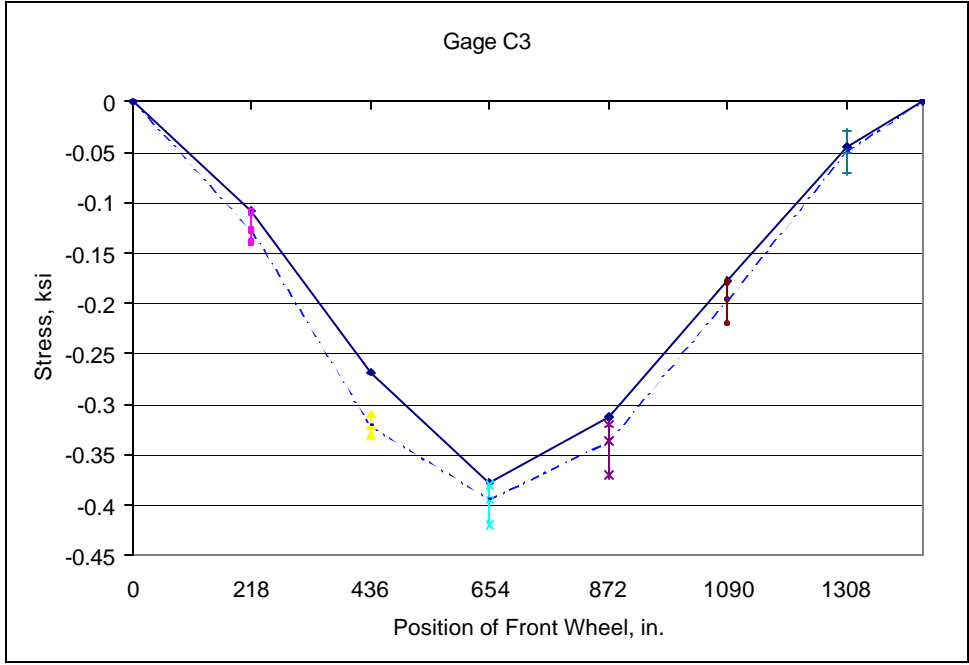
Graph F.19: Member U2U3 of the upstream truss



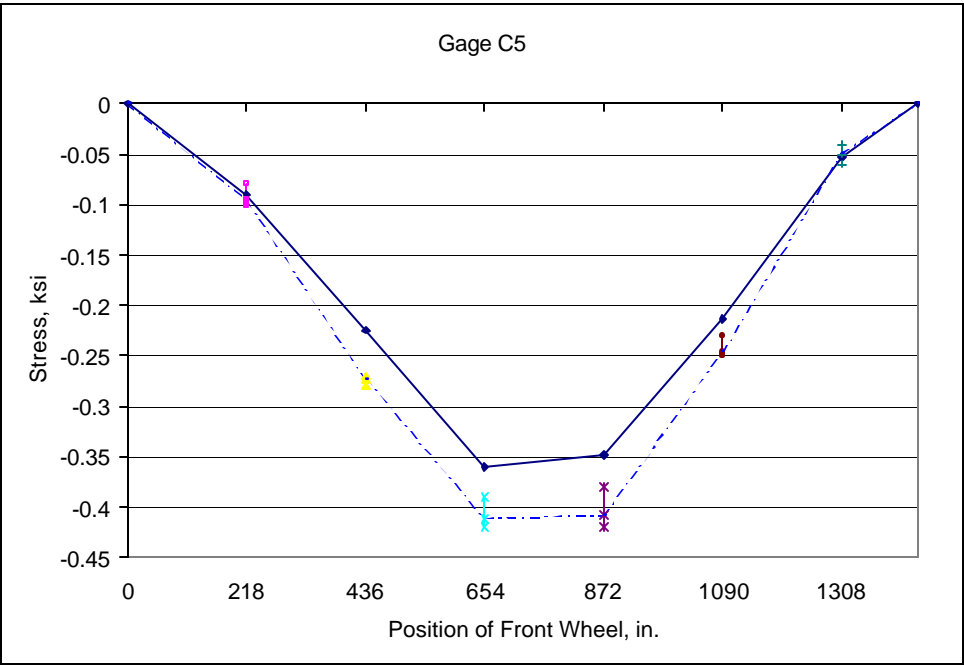
Graph F.20: Member U2U3 of the downstream truss



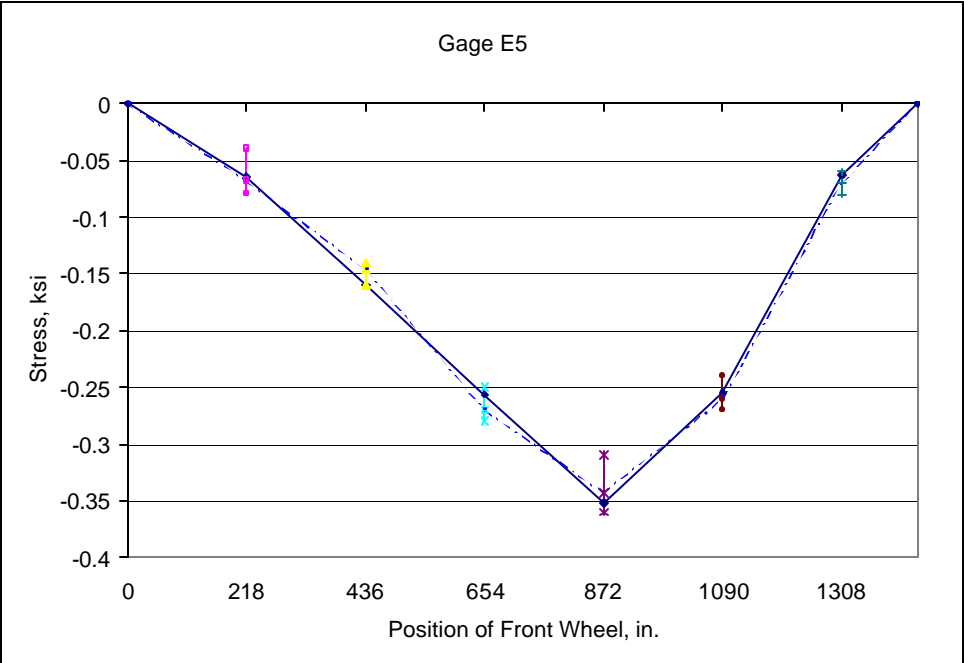
Graph F.21: Member U2U3 of the upstream truss (Near U3 joint, Top)



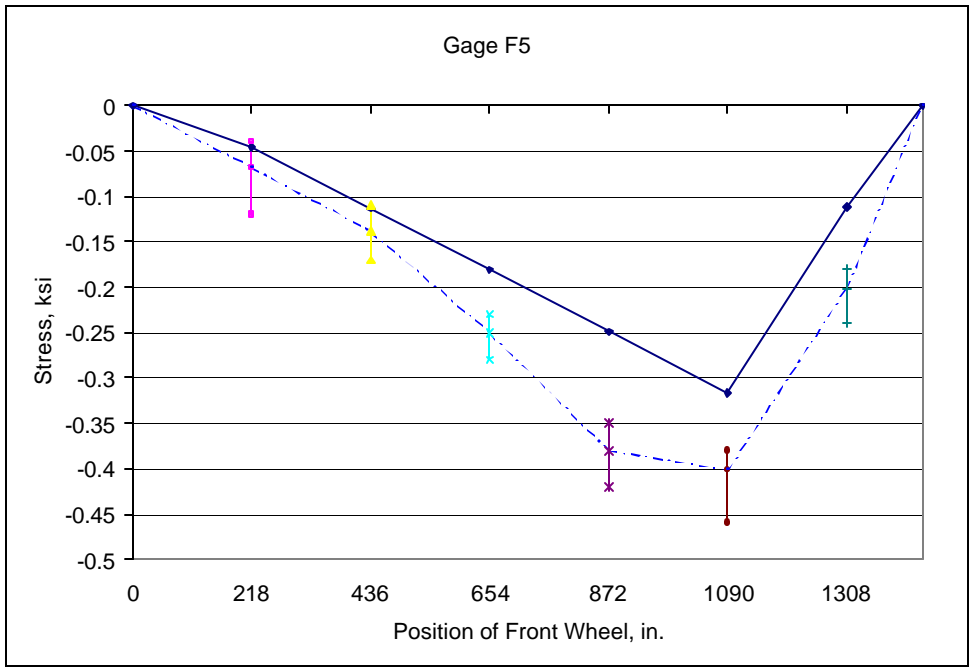
Graph F.22: Member U2U3 of the upstream truss (Near U3 joint, Bottom)



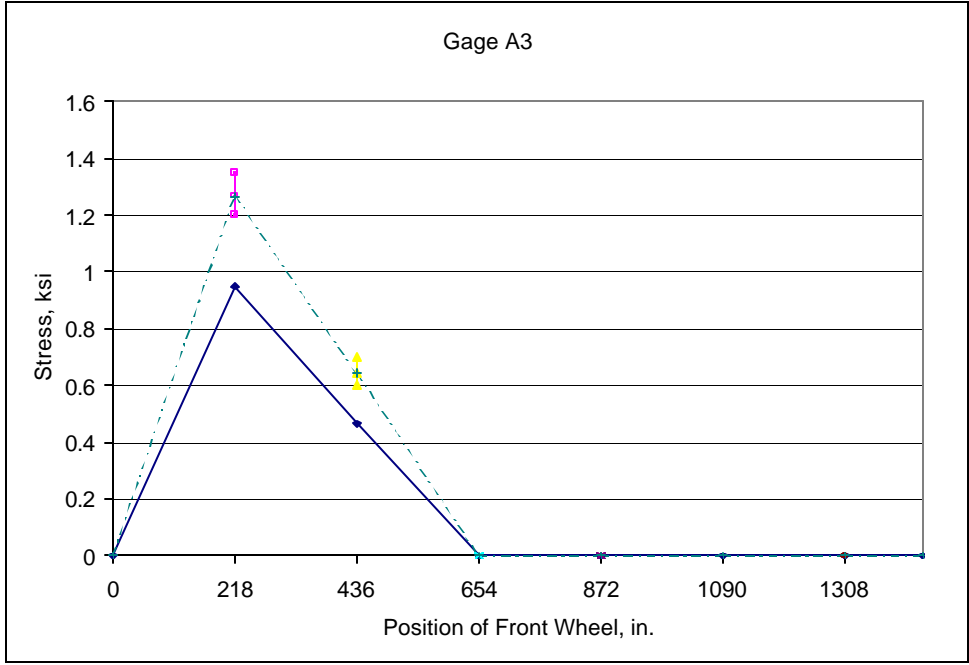
Graph F.23: Member U3U4 of the upstream truss



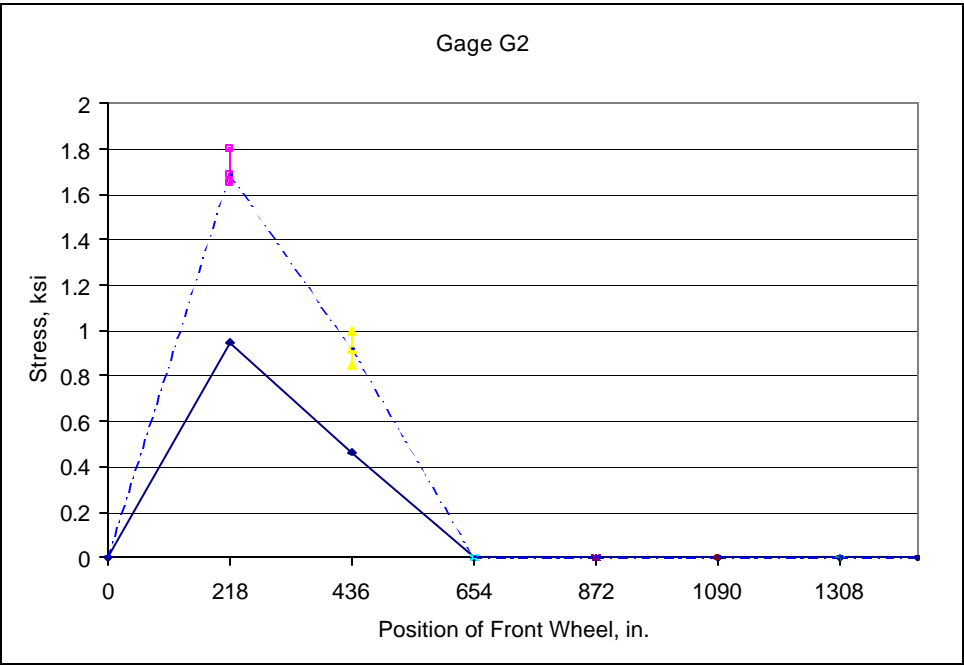
Graph F.24: Member U4U5 of the upstream truss



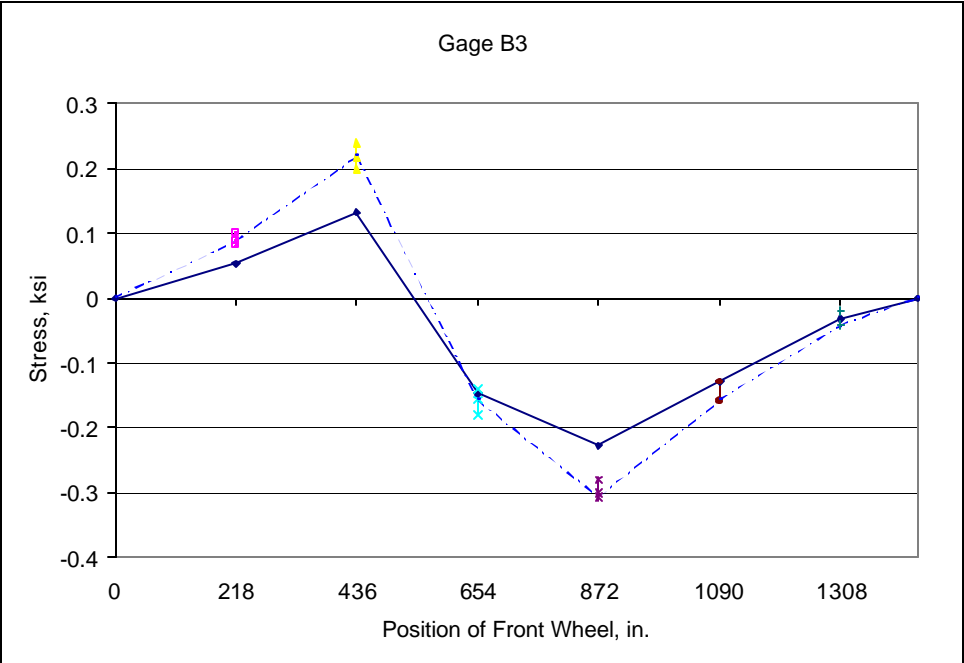
Graph F.25: Member L6U5 of the upstream truss



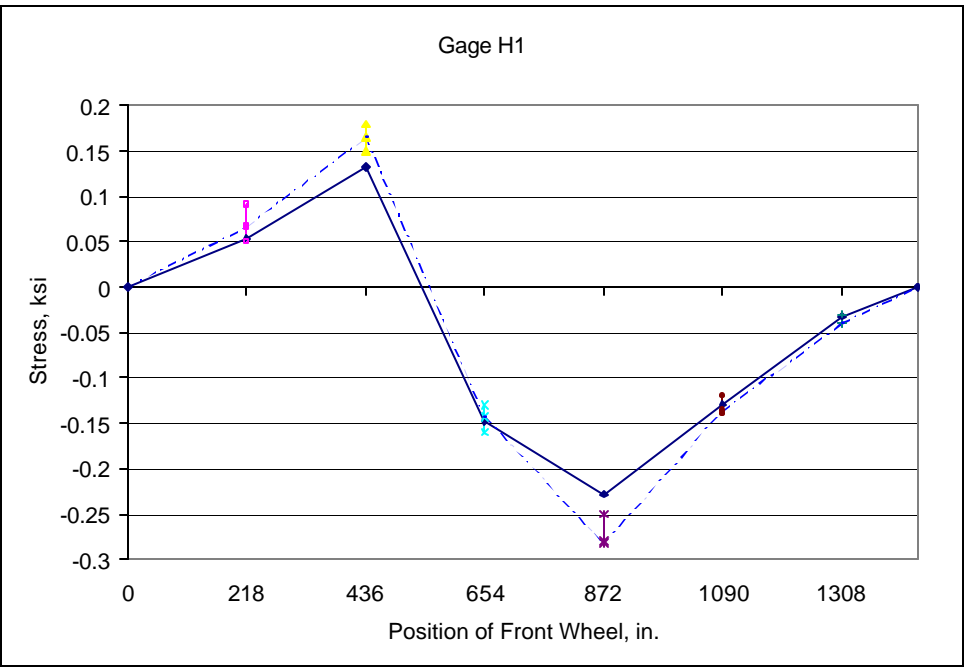
Graph F.26: Member L1U1 of the upstream truss



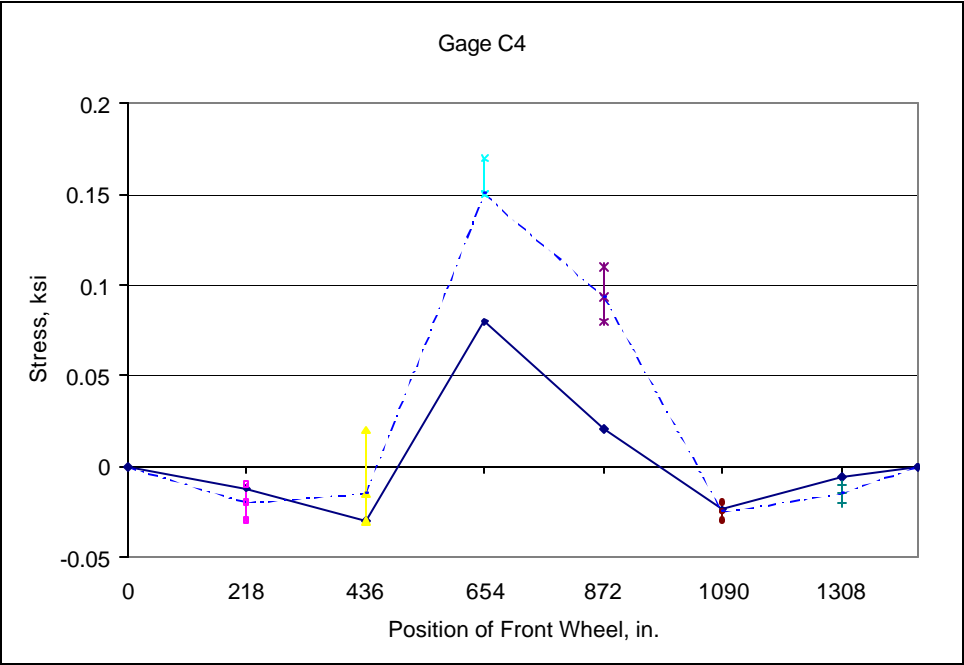
Graph F.27: Member L1U1 of the downstream truss



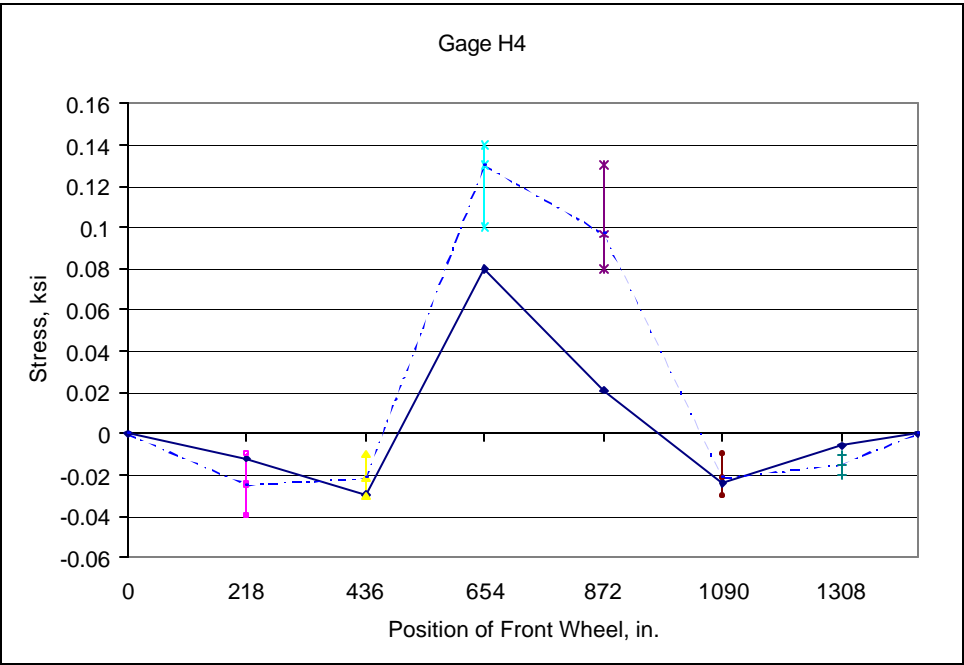
Graph F.28: Member L2U2 of the upstream truss



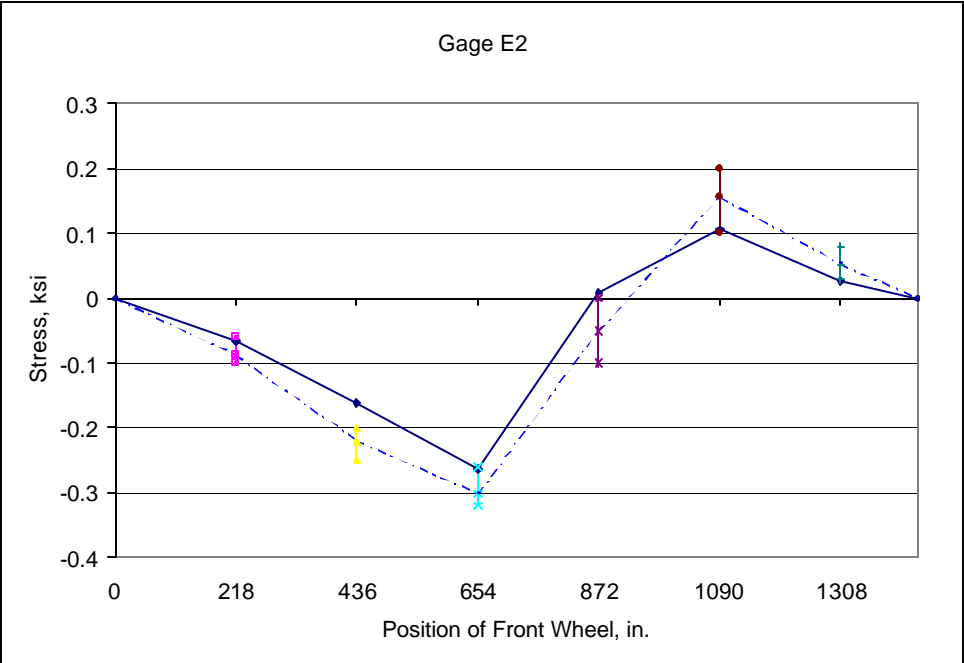
Graph F.29: Member L2U2 of the downstream truss



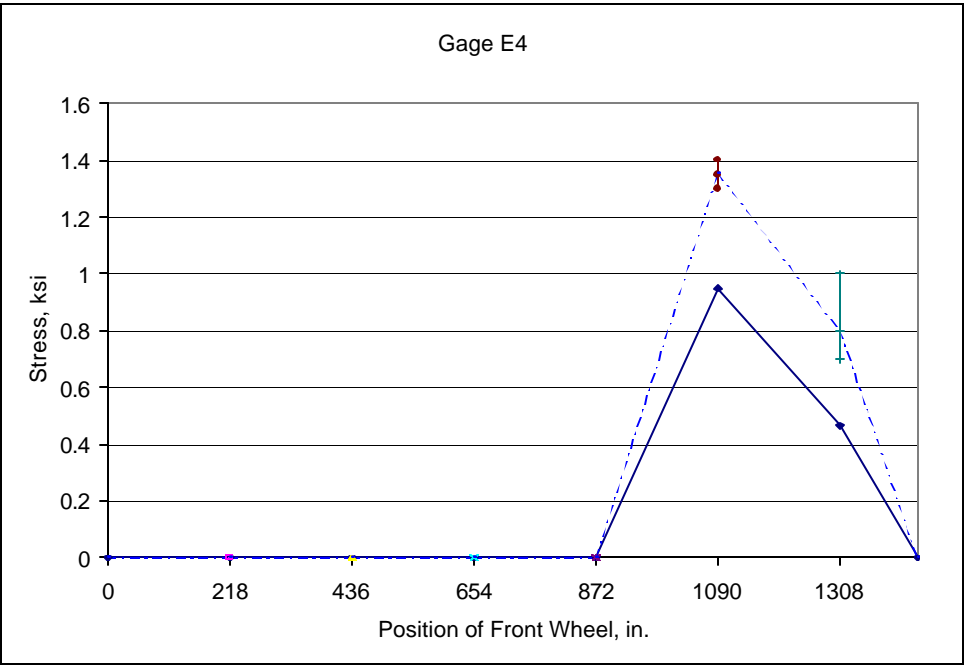
Graph F.30: Member L3U3 of the upstream truss



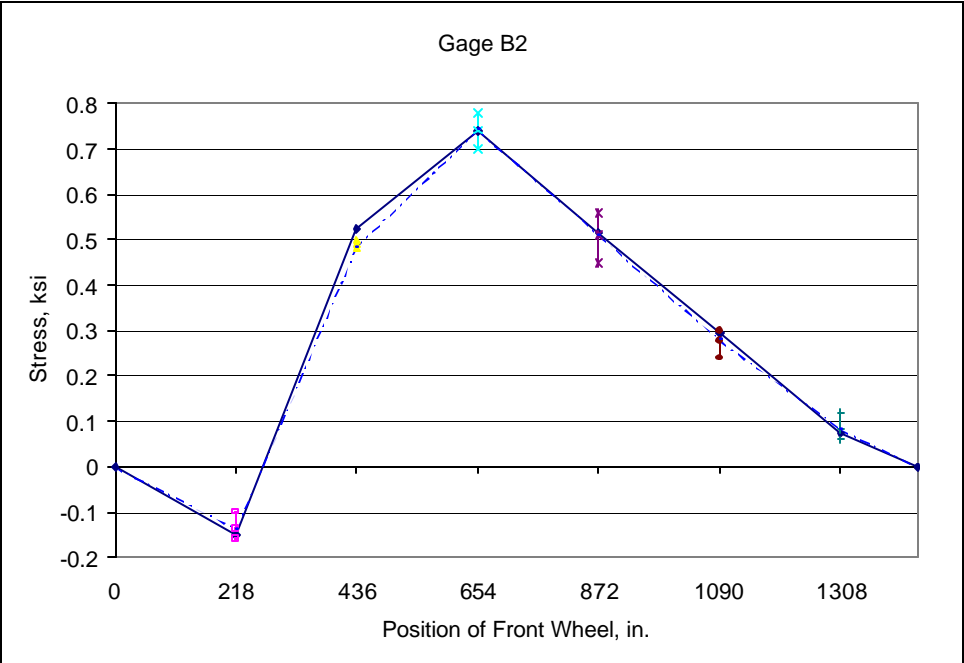
Graph F.31: Member L3U3 of the downstream truss



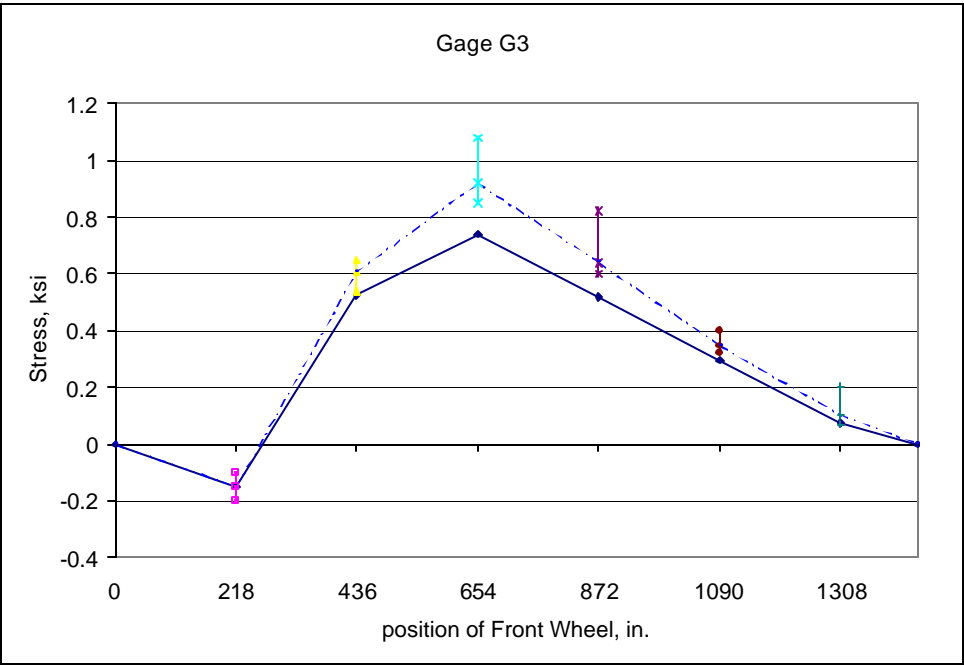
Graph F.32: Member L4U4 of the upstream truss



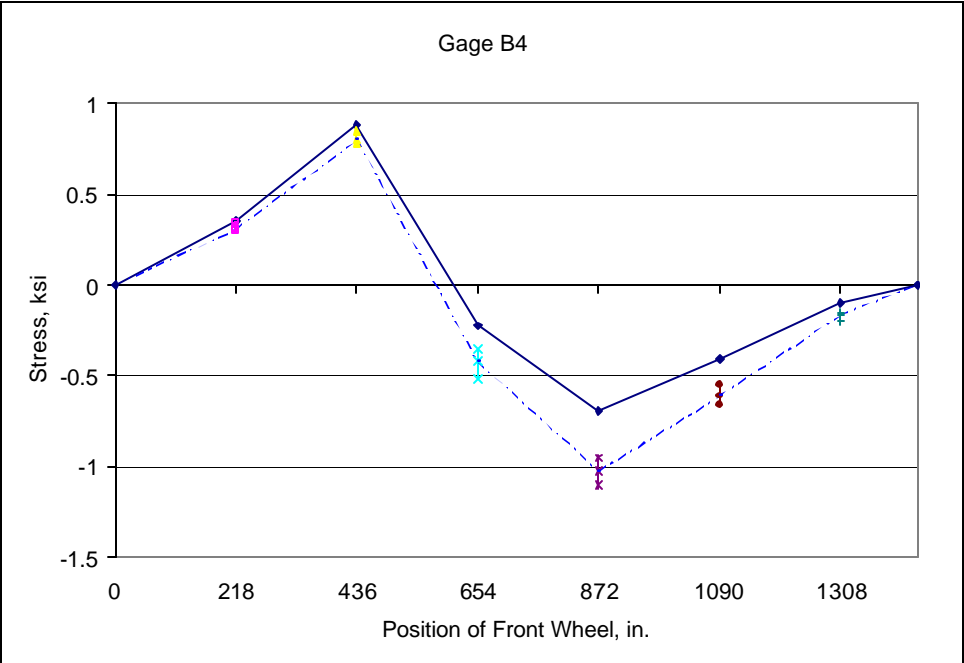
Graph F.33: Member L5U5 of the upstream truss



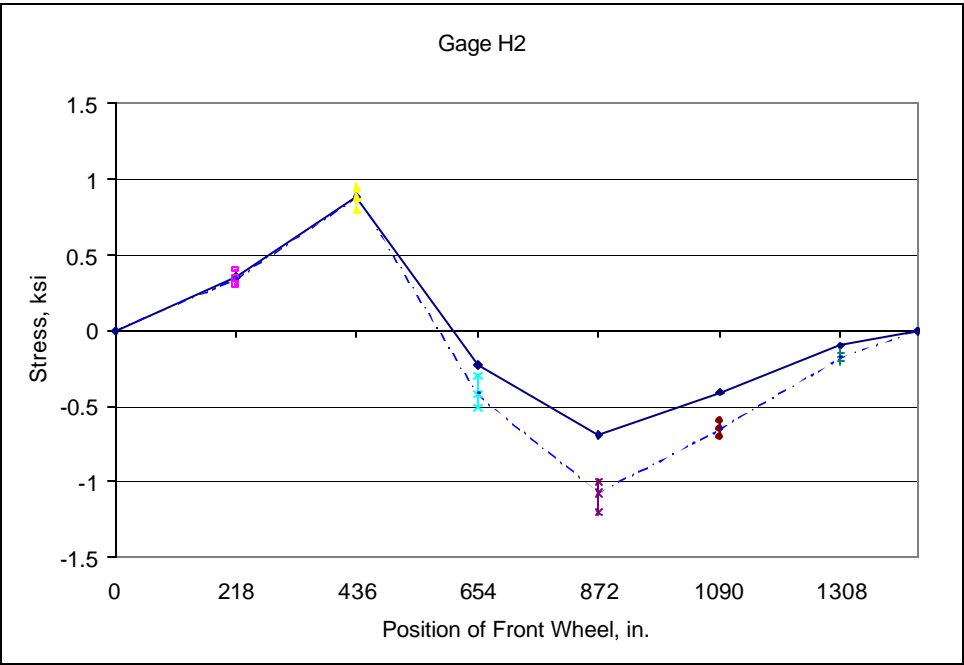
Graph F.34: Member L2U1 of the upstream truss



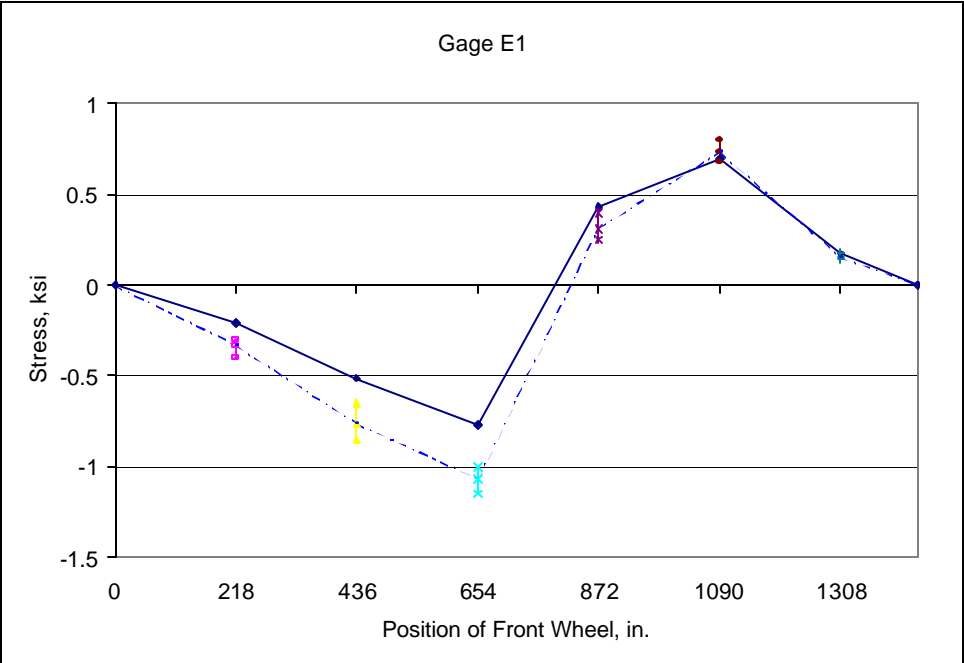
Graph F.35: Member L2U1 of the downstream truss



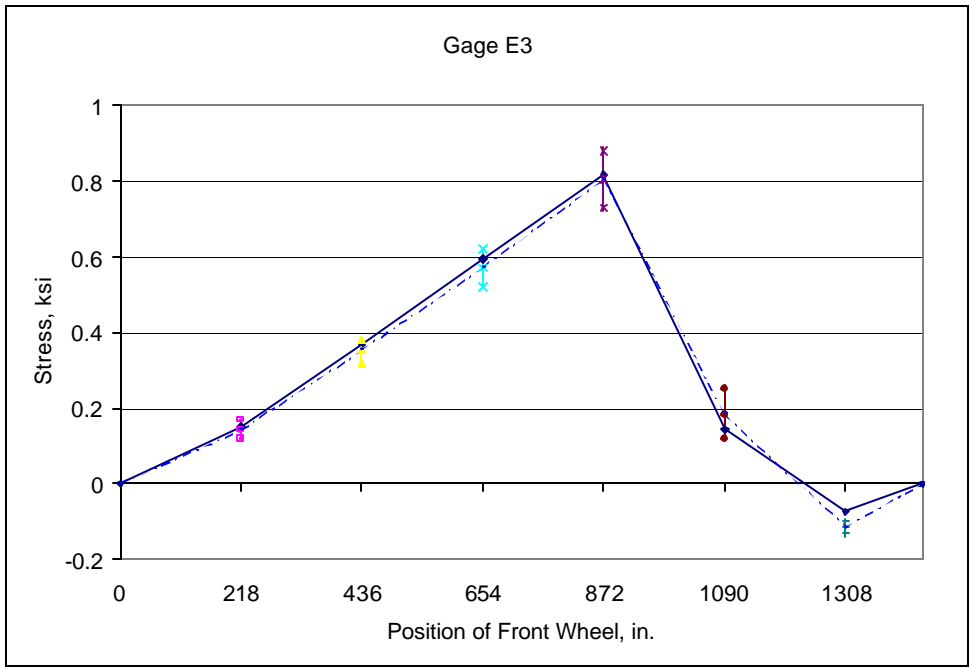
Graph F.36: Member L2U3 of the upstream truss



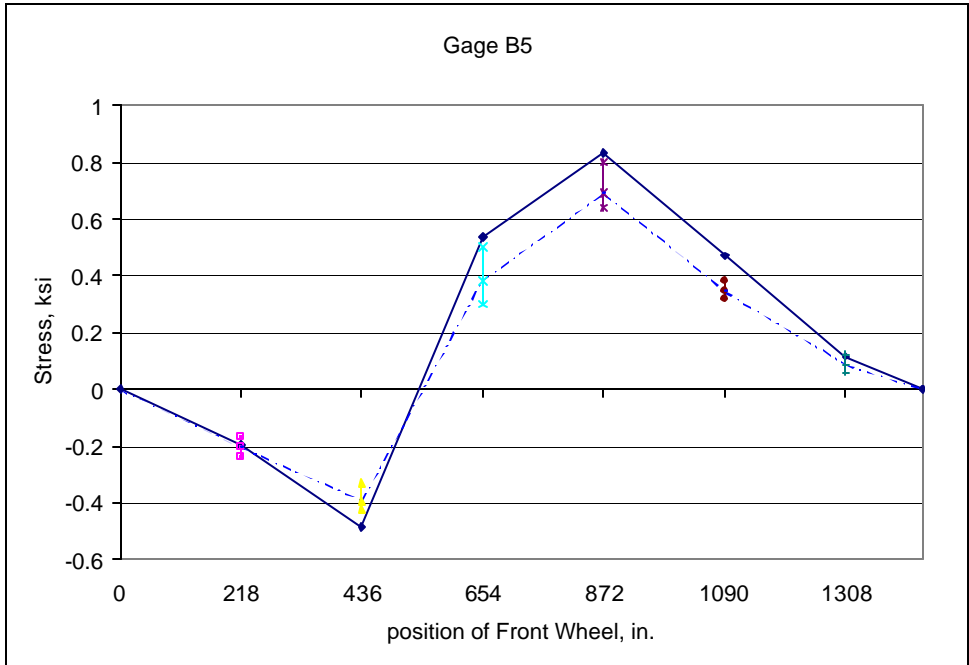
Graph F.37: Member L2U3 of the downstream truss



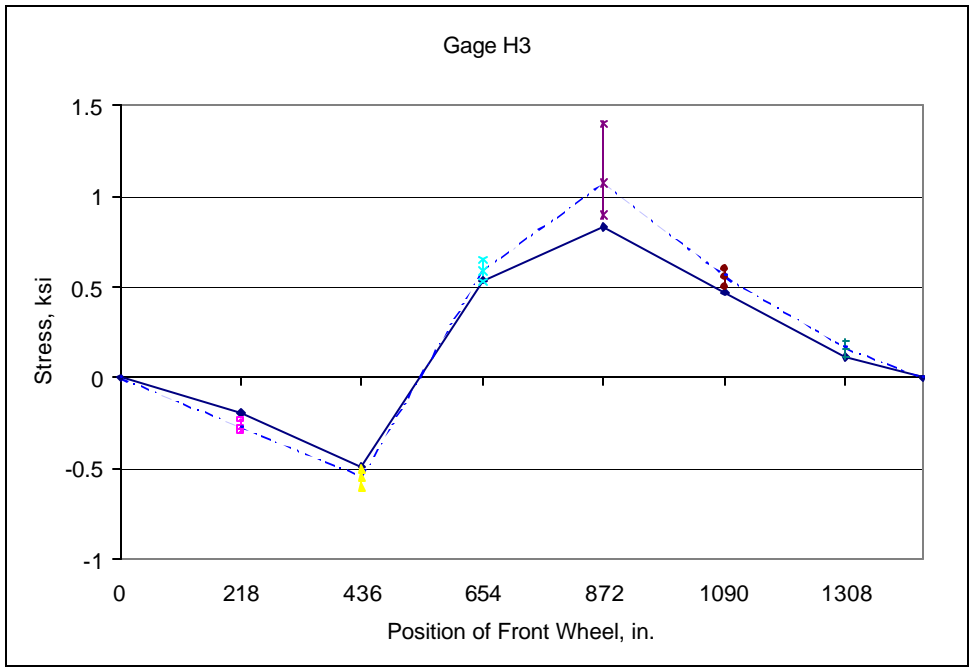
Graph F.38: Member L4U3 of the upstream truss



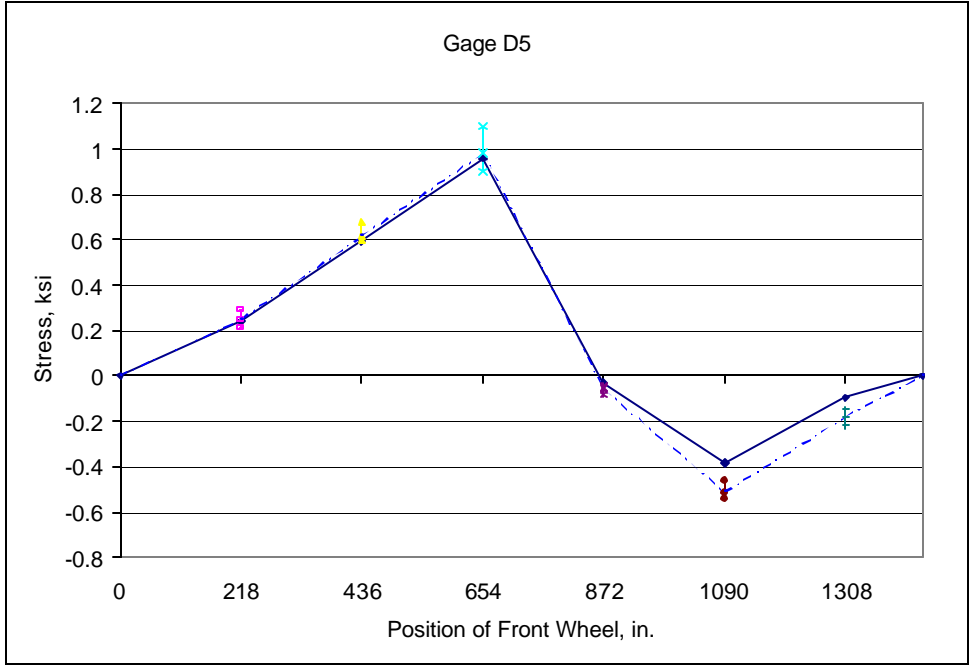
Graph F.39: Member L4U5 of the upstream truss



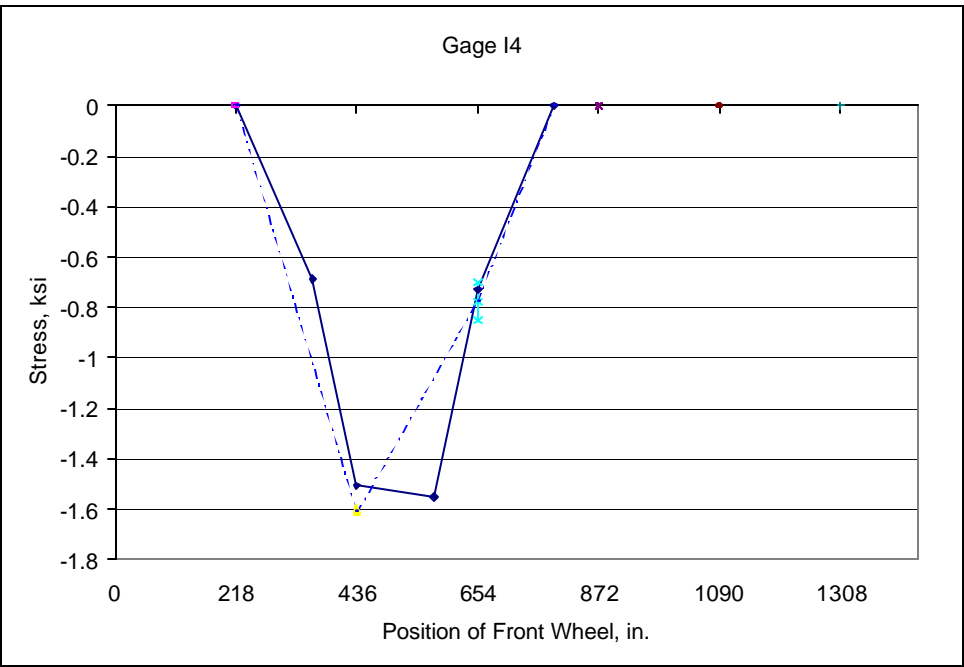
Graph F.40: Member L3U2 of the upstream truss



Graph F.41: Member L3U2 of the downstream truss



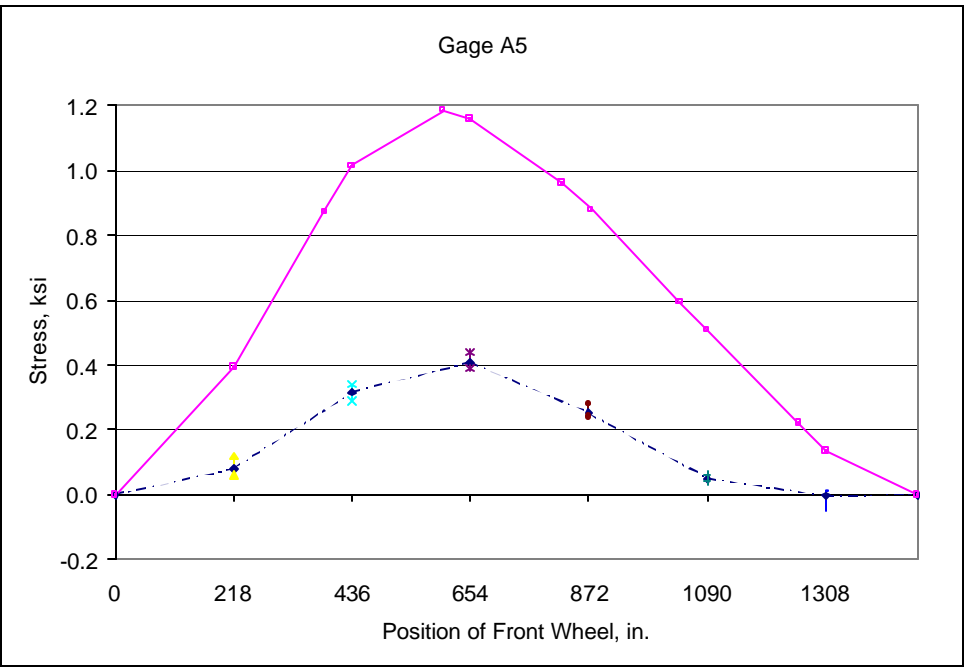
Graph F.42: Member L3U4 of the upstream truss



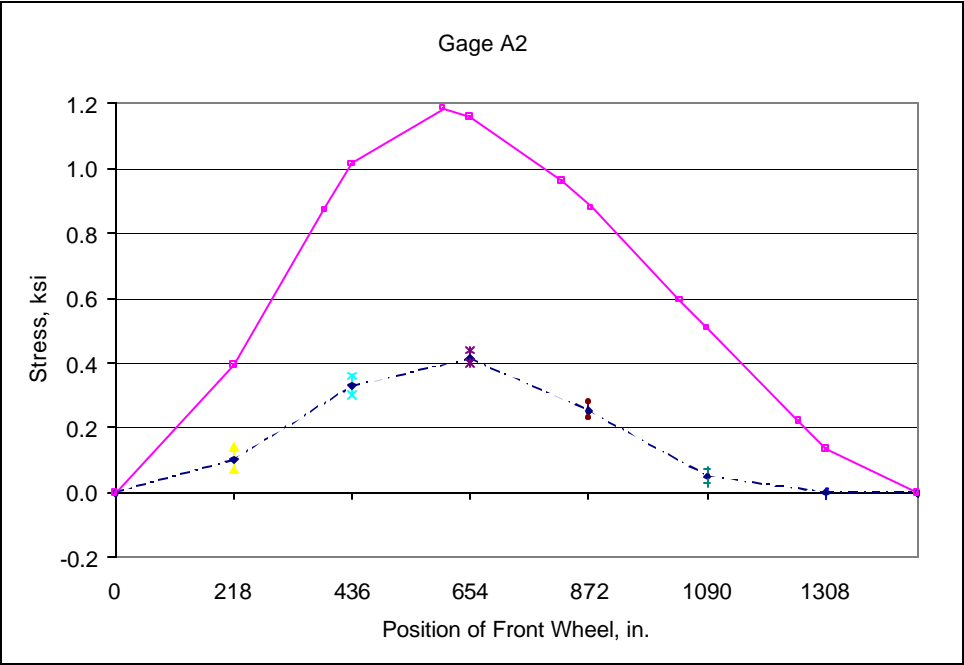
Graph F.43: Member mid-span section of the metal floor beam



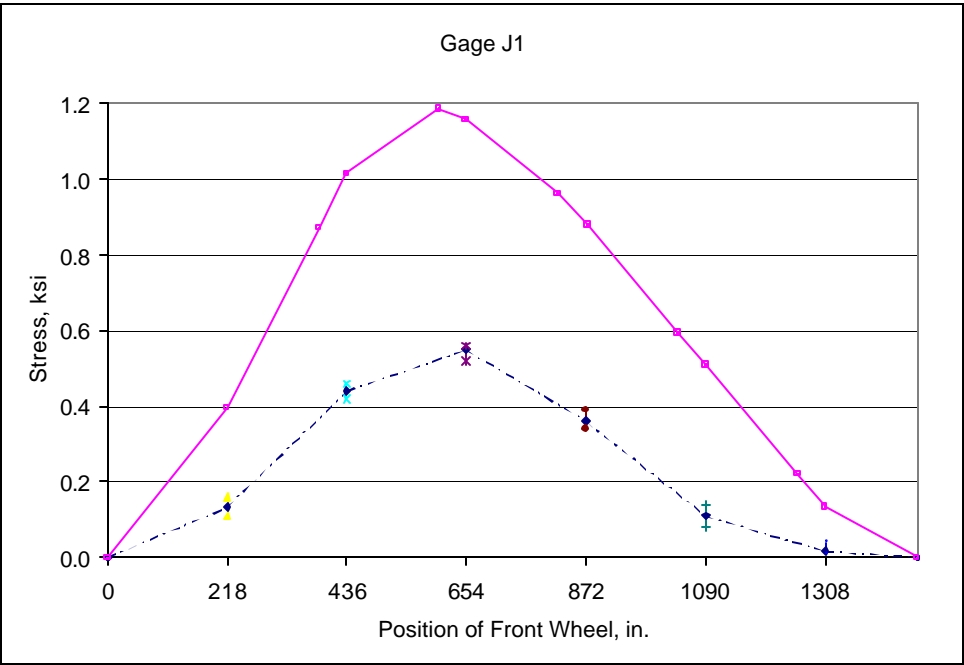
Graph F.44: Section at 23" away from the mid span of the metal floor beam



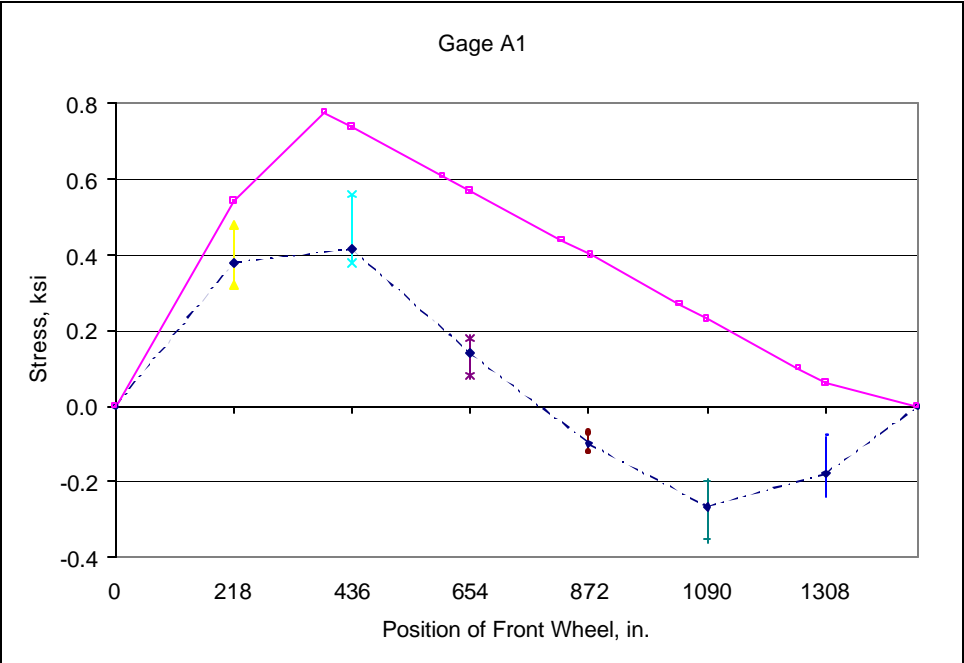
Graph F.45: Bottom chord L2L3 (Inside)



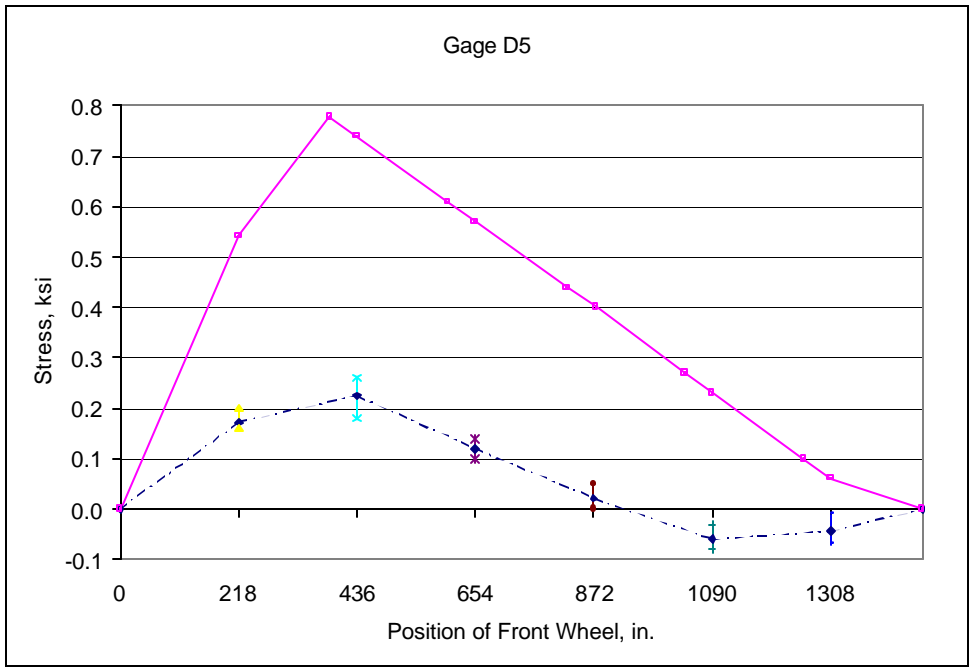
Graph F.46: Bottom chord L2L3 (Outside)



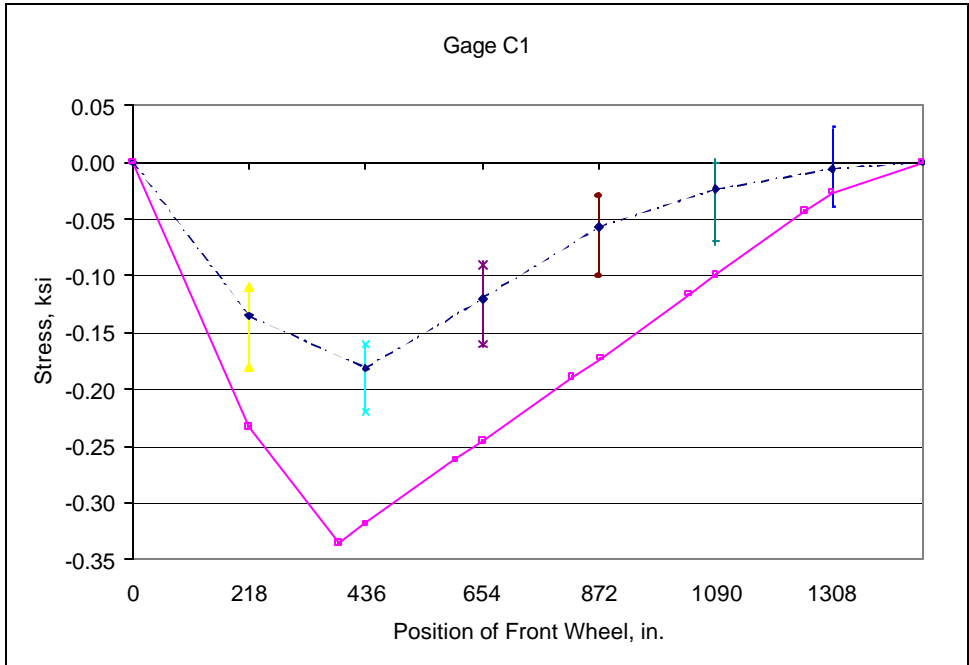
Graph F.47: Bottom chord L2L3 (Outside)



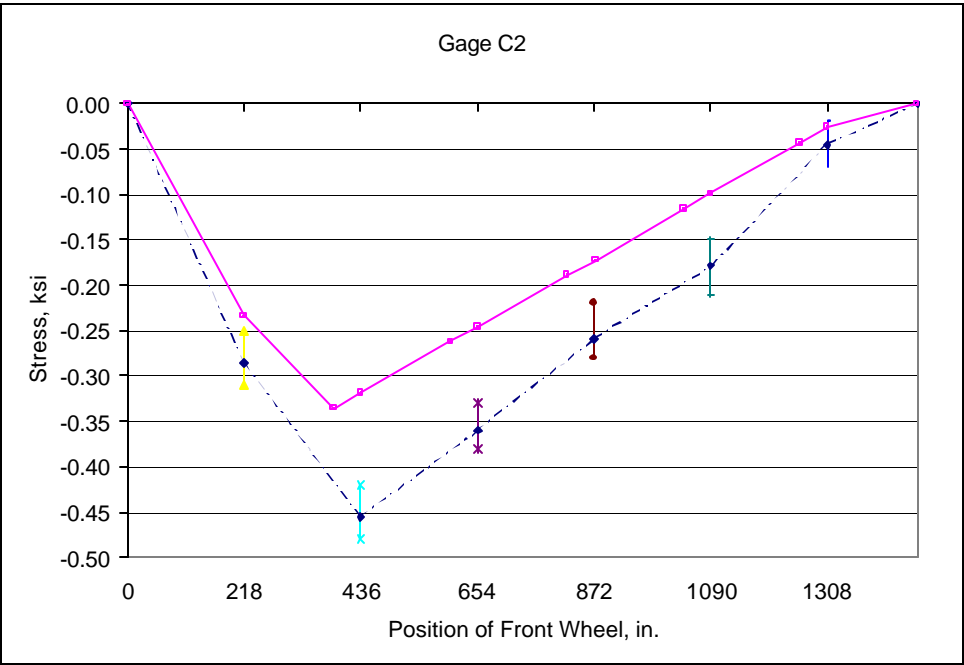
Graph F.48: Bottom chord L1L2 (Outside)



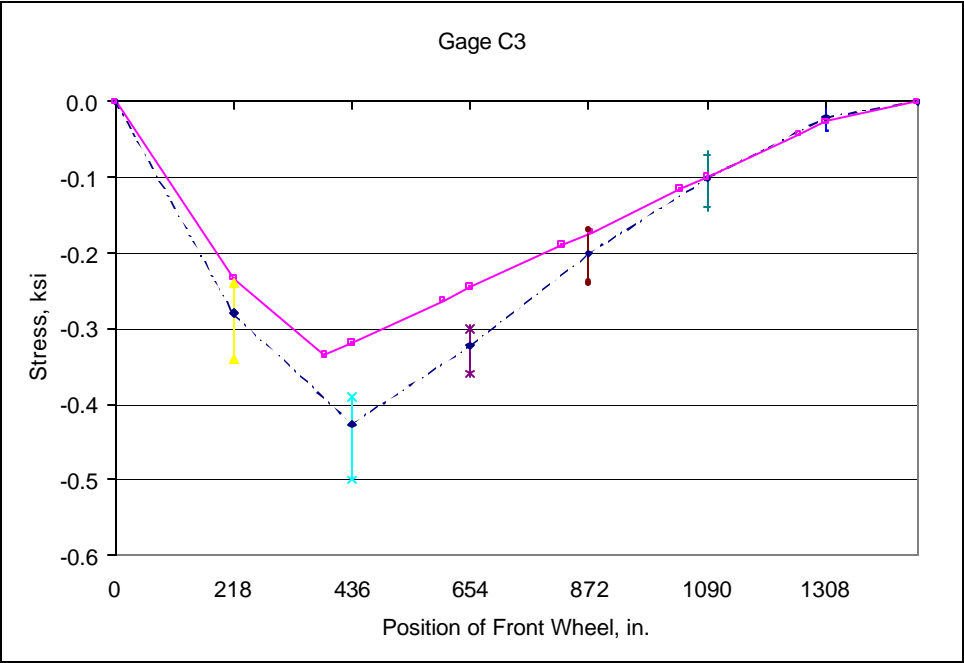
Graph F.49: Bottom chord L1L2 (Outside)



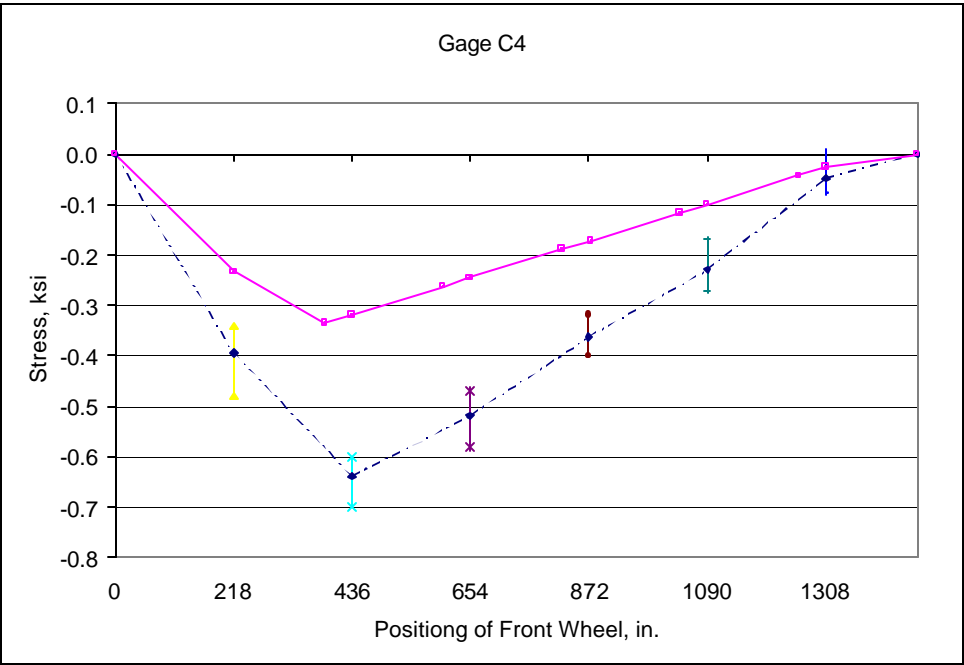
Graph F.50: Top chord LOU1



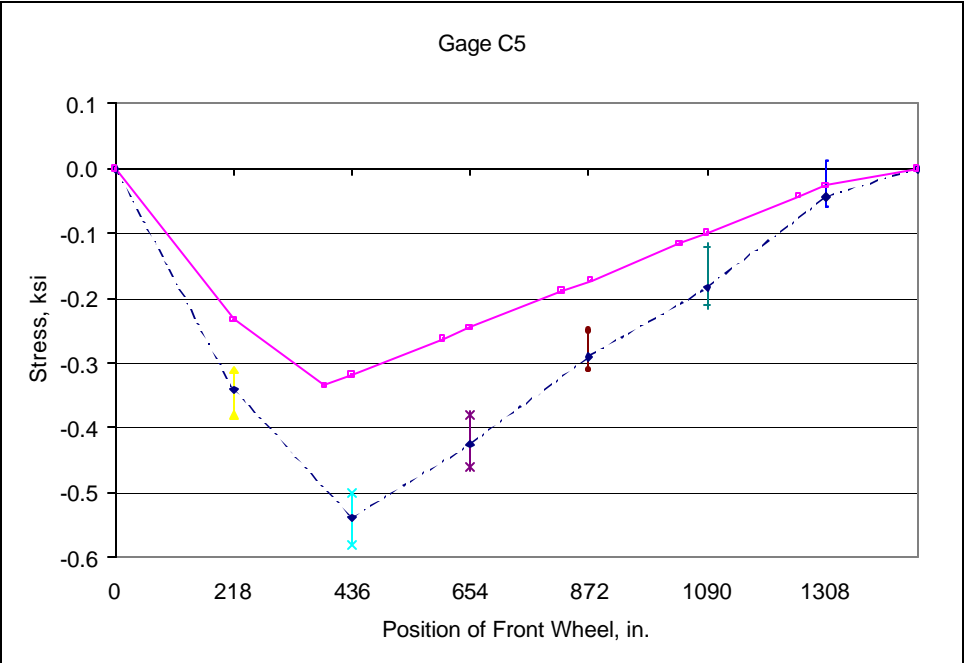
Graph F.51: Top chord LOU1



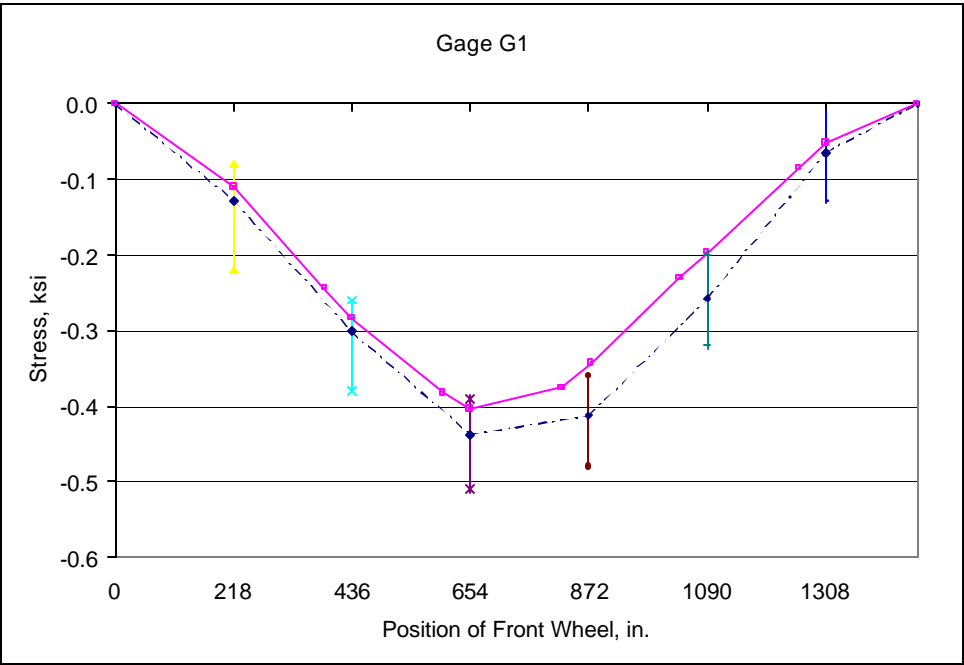
Graph F.52: Top chord LOU1



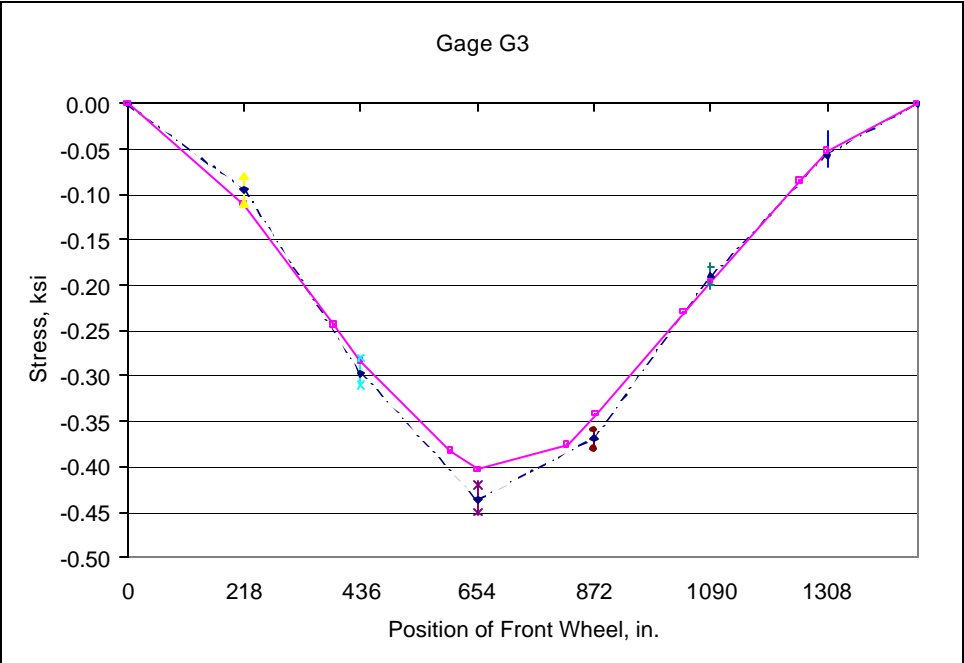
Graph F.53: Top chord LOU1



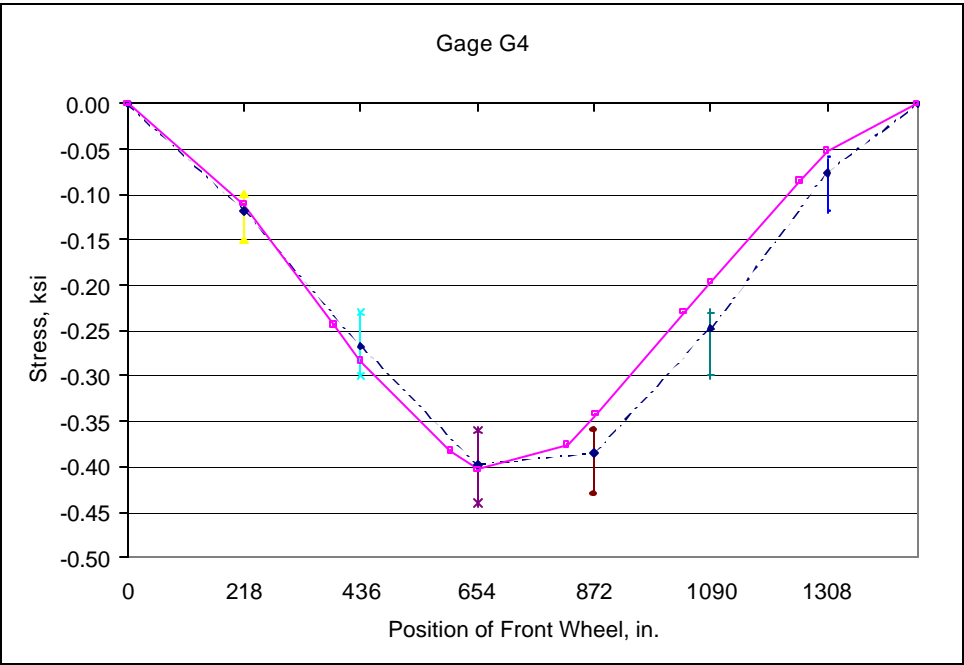
Graph F.54: Top chord LOU1



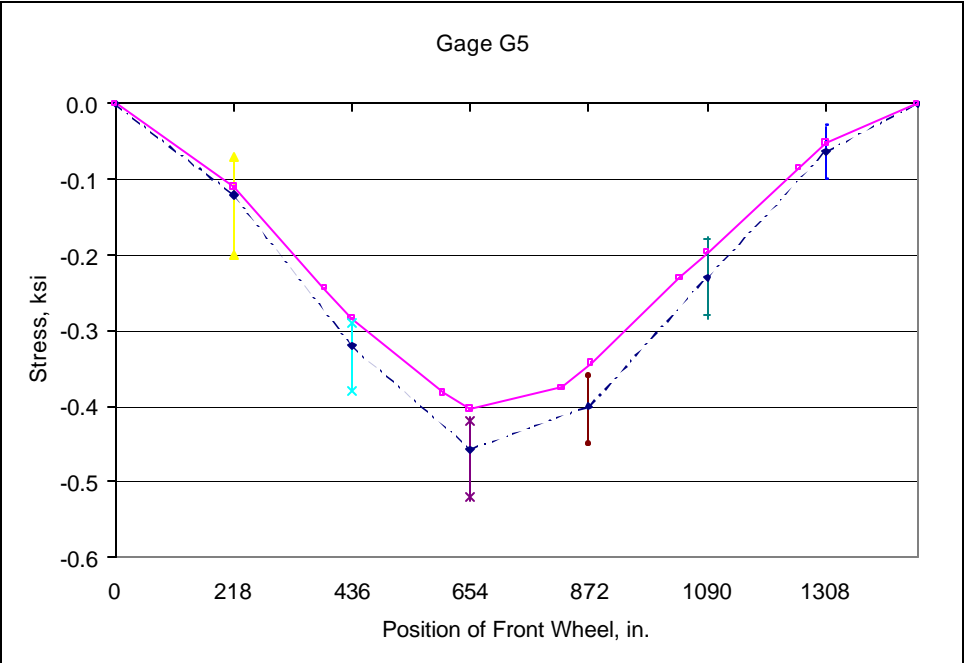
Graph F.55: Top chord U1U2



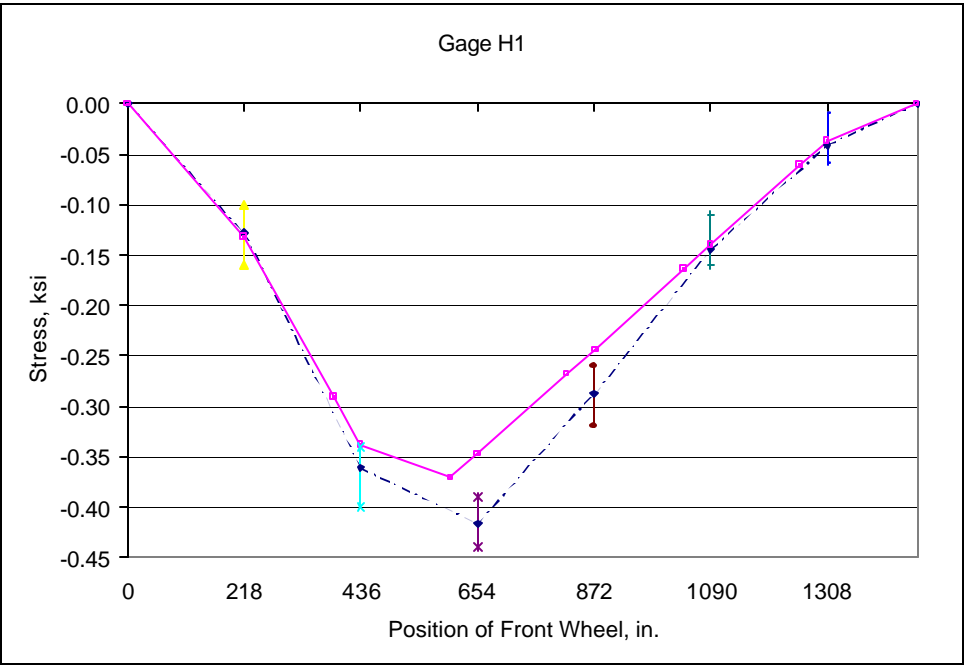
Graph F.56: Top chord U1U2



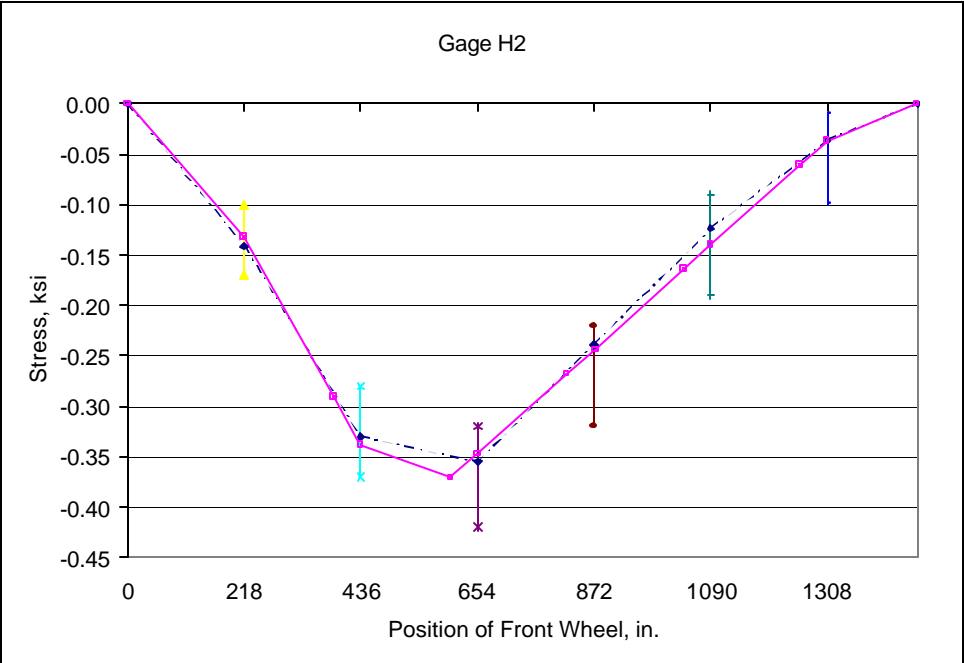
Graph F.57: Top chord U1U2



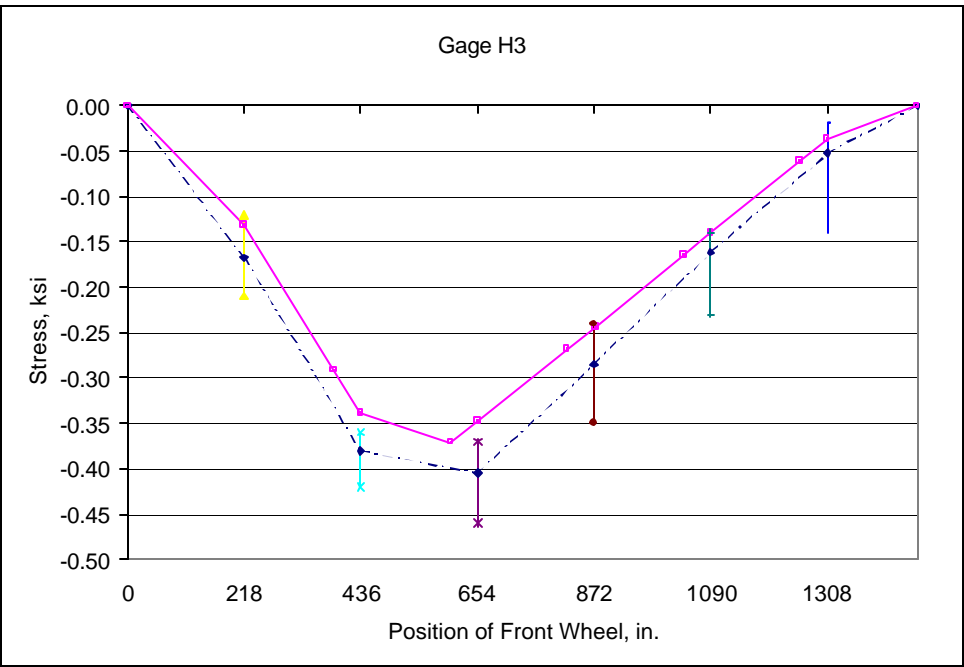
Graph F.58: Top chord U1U2



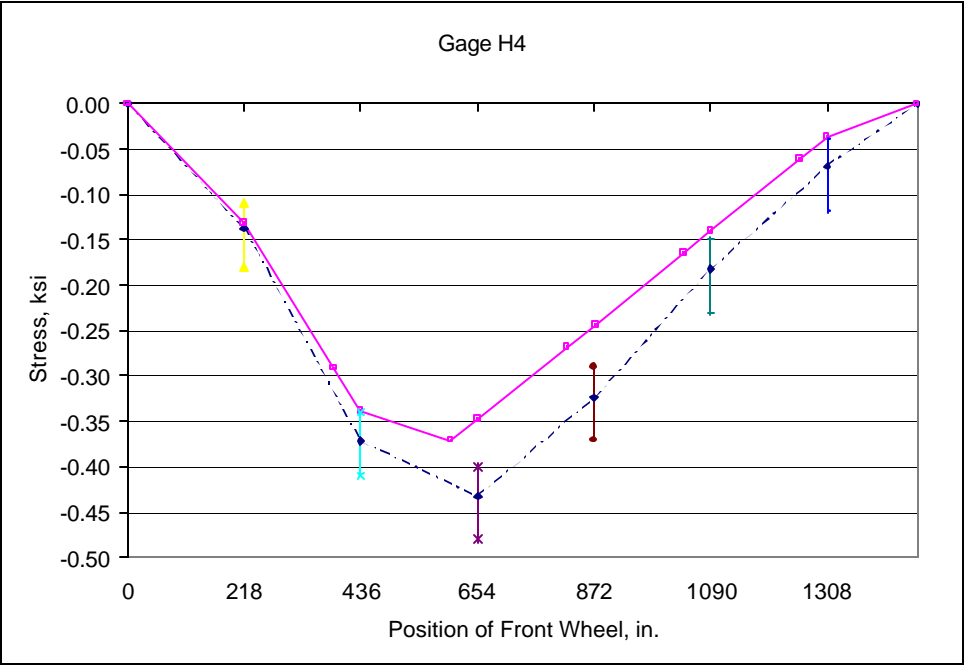
Graph F.59: Top chord U2U3



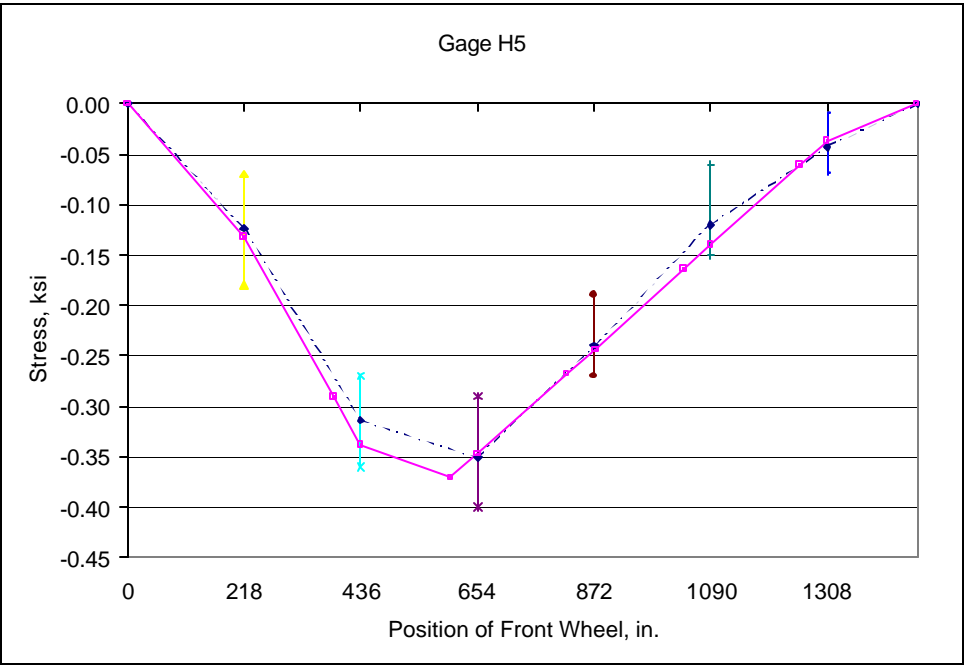
Graph F.60: Top chord U2U3



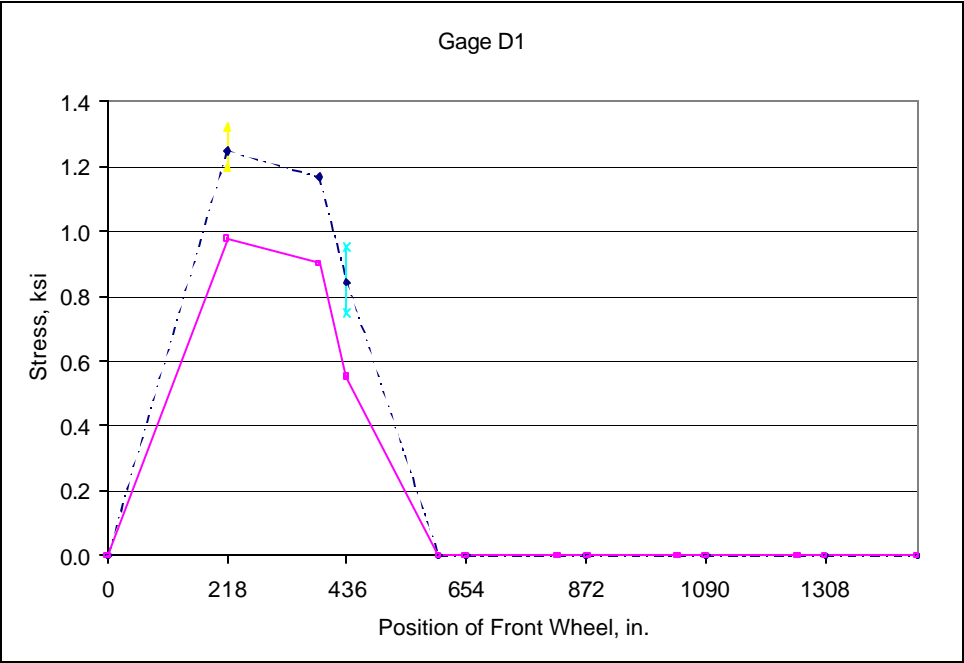
Graph F.61: Top chord U2U3



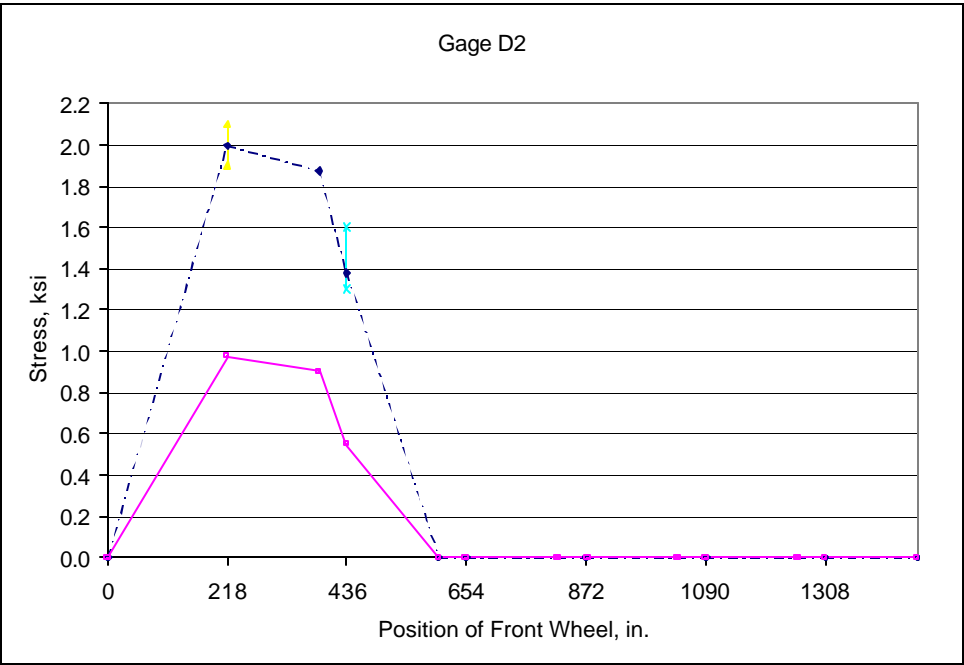
Graph F.62: Top chord U2U3



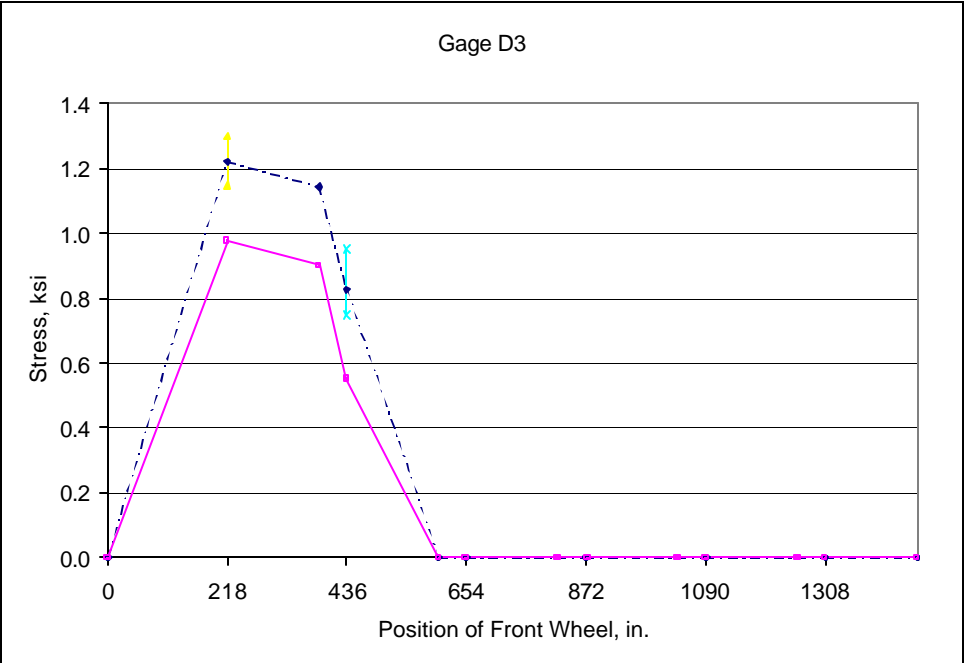
Graph F.63: Top chord U2U3



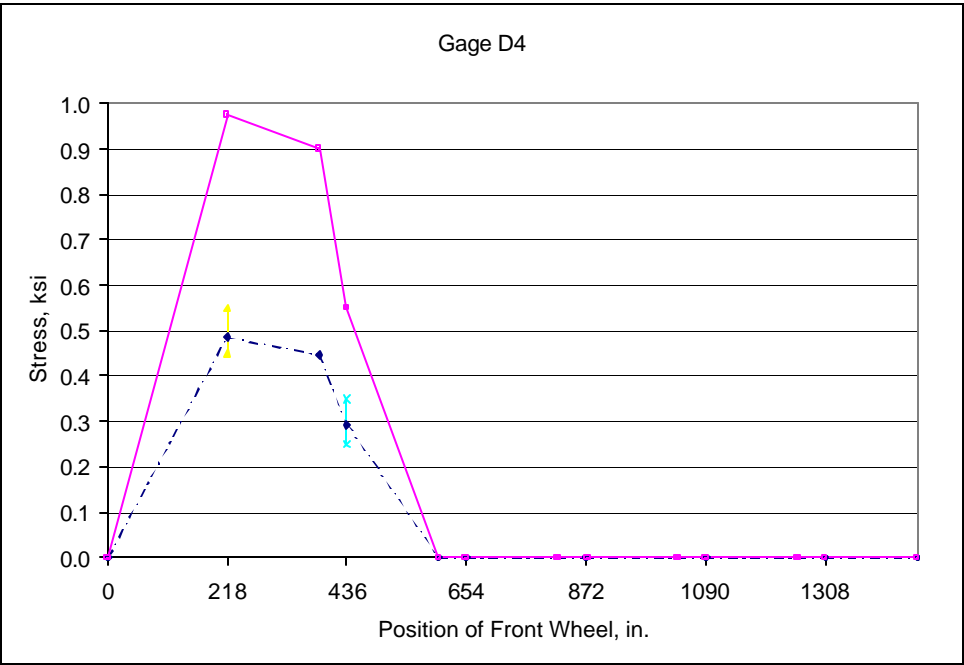
Graph F.64: Vertical hanger L1U1



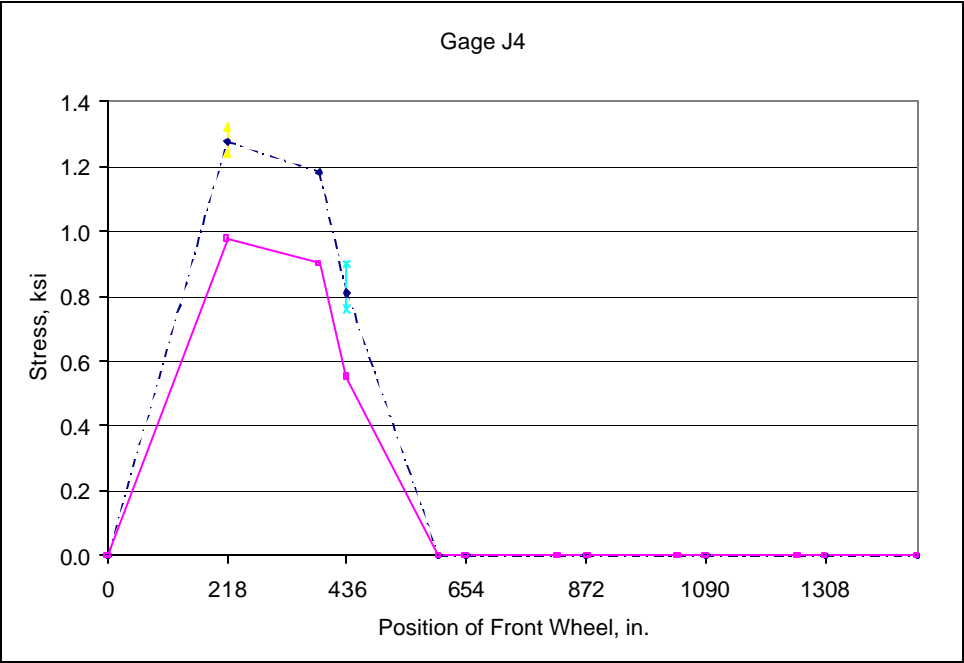
Graph F.65: Vertical hanger L1U1



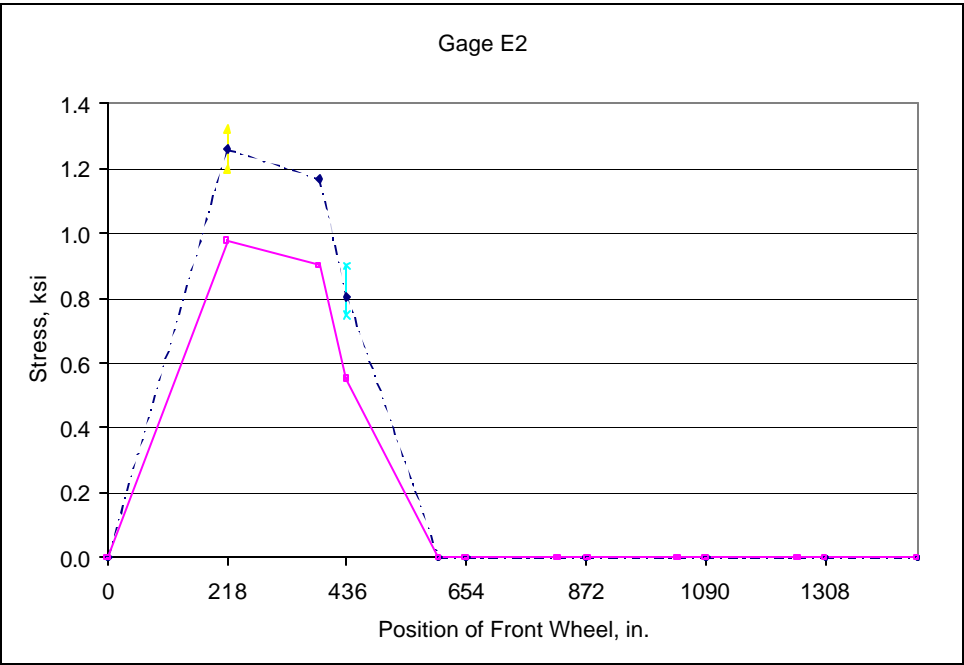
Graph F.66: Vertical hanger L1U1



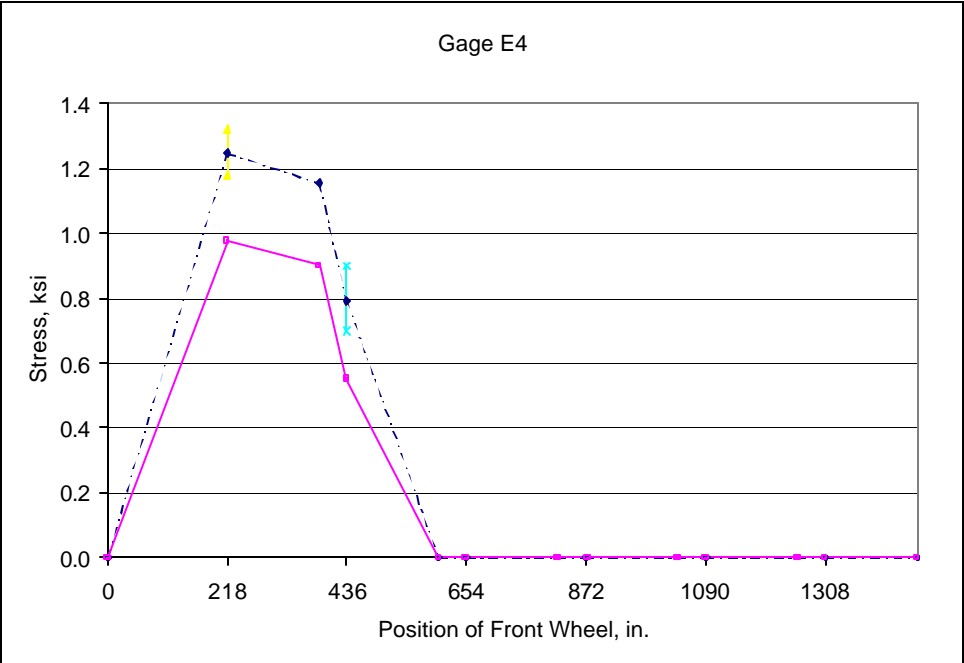
Graph F.67: Vertical hanger L1U1



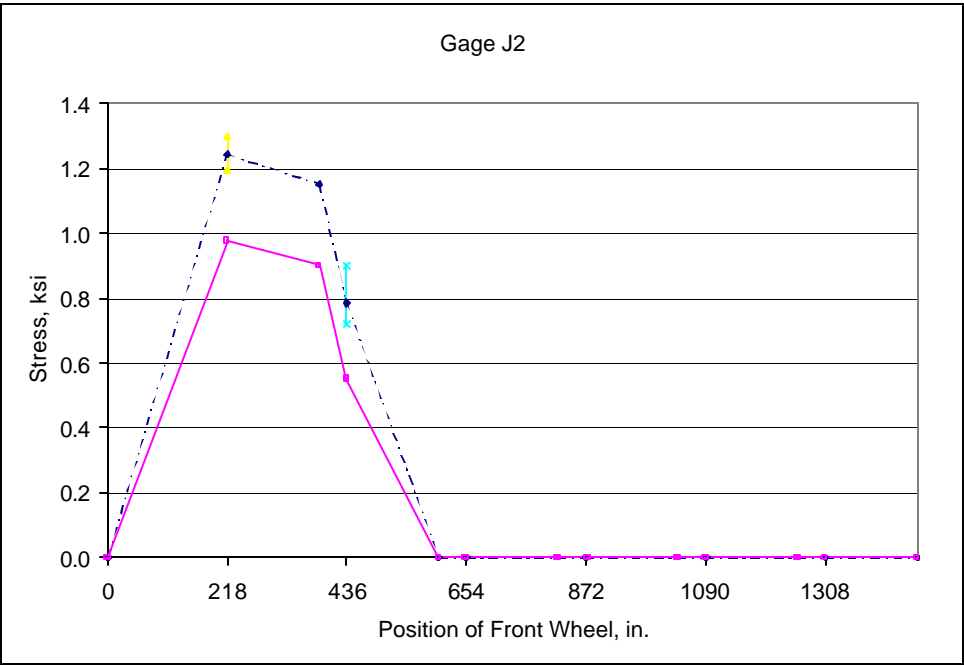
Graph F.68: Vertical hanger L1U1



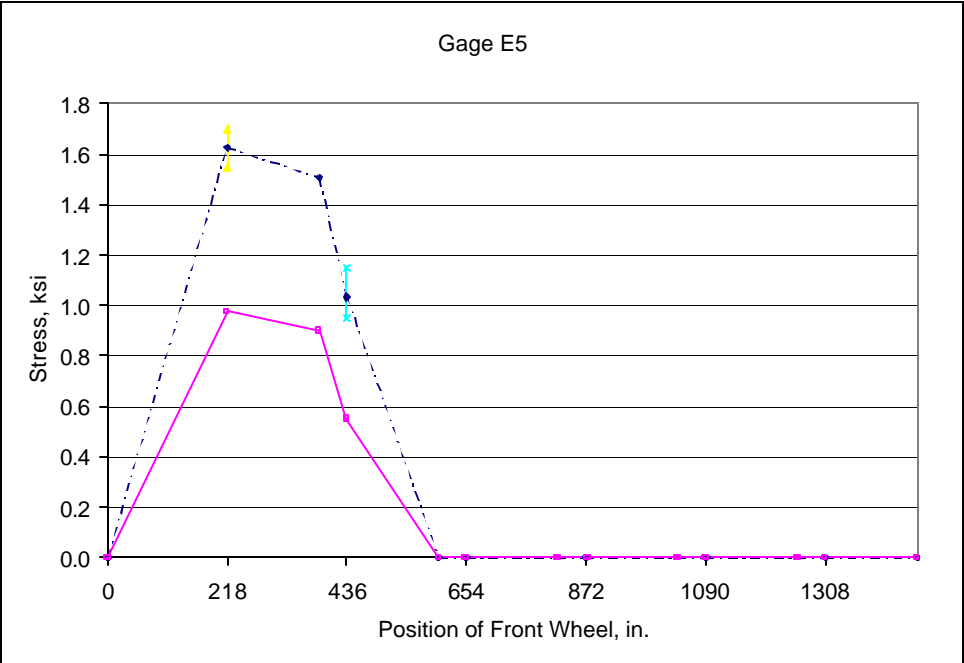
Graph F.69: Vertical hanger L1U1



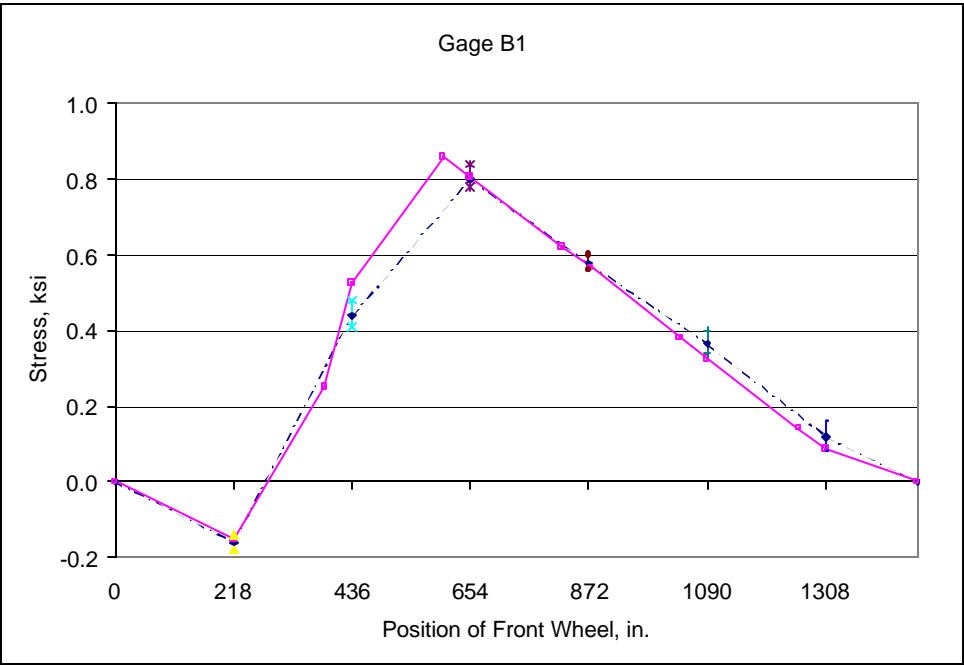
Graph F.70: Vertical hanger L1U1



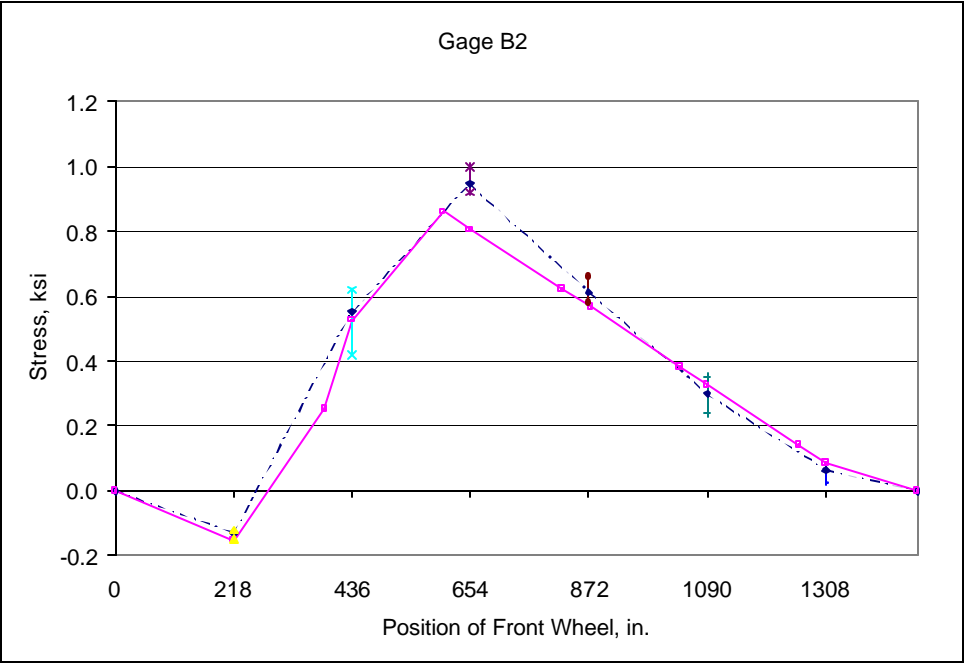
Graph F.71: Vertical hanger L1U1



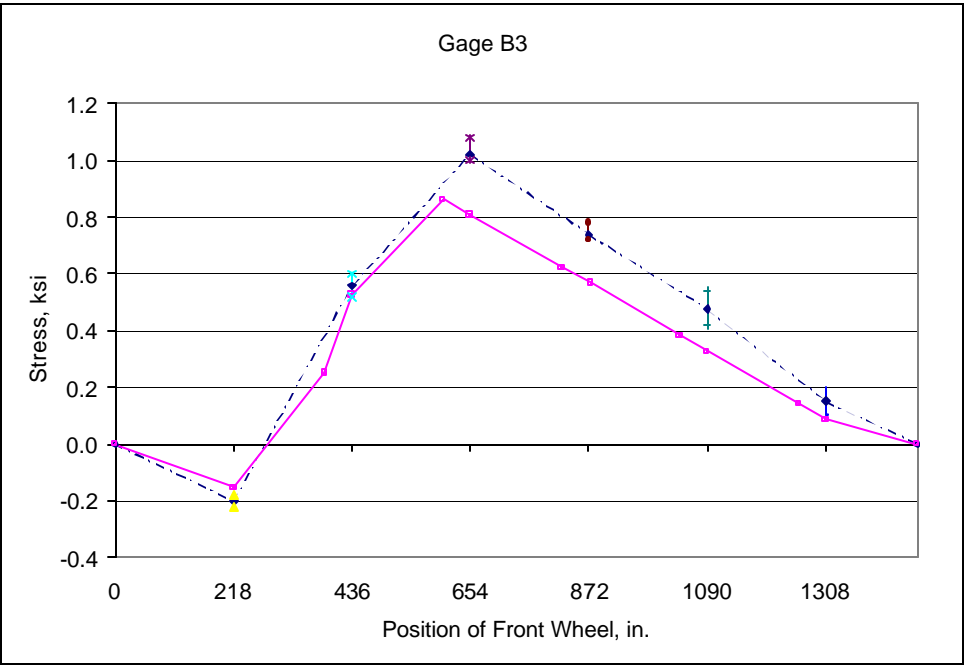
Graph F.72: Vertical hanger L1U1



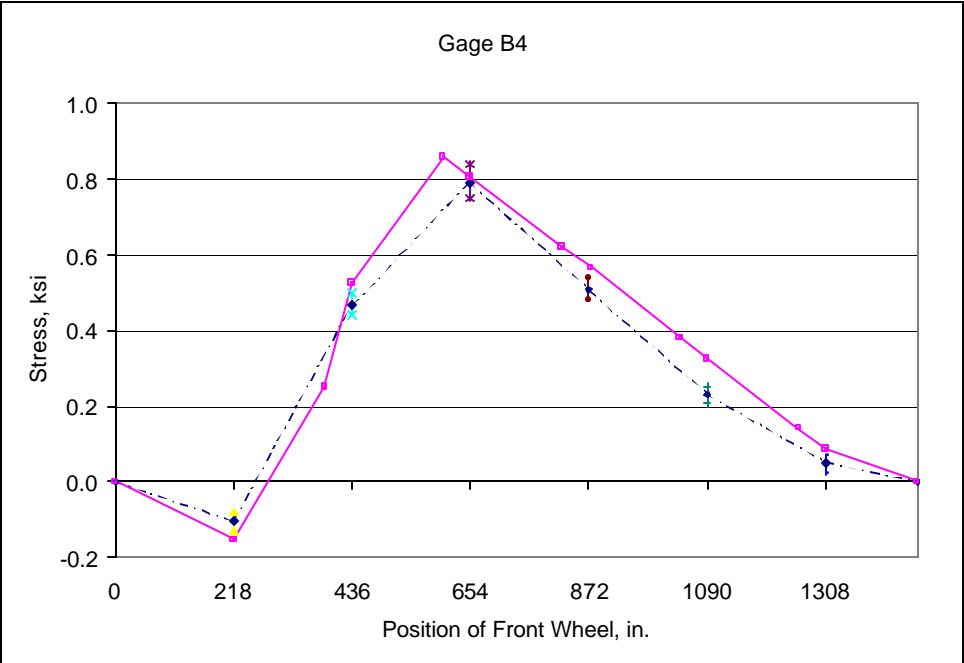
Graph F.73: Diagonal member L2U1



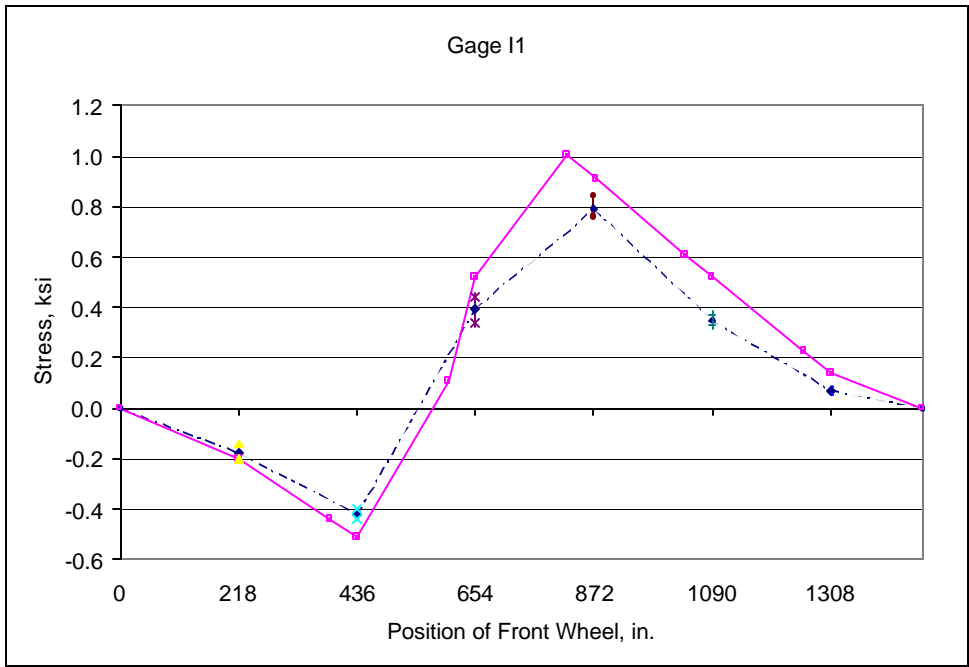
Graph F.74: Diagonal member L2U1



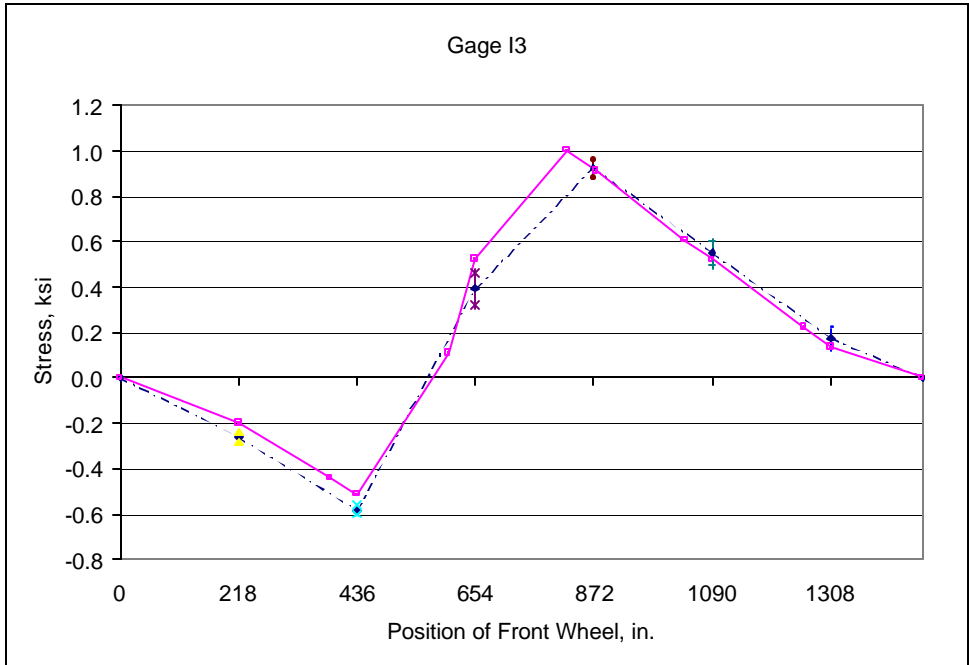
Graph F.75: Diagonal member L2U1



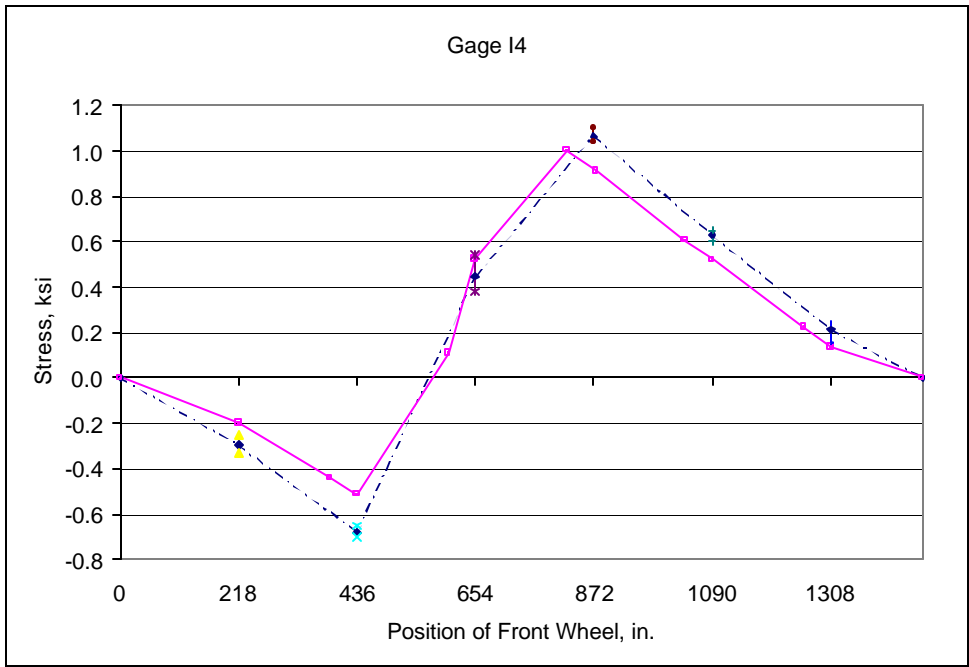
Graph F.76: Diagonal member L2U1



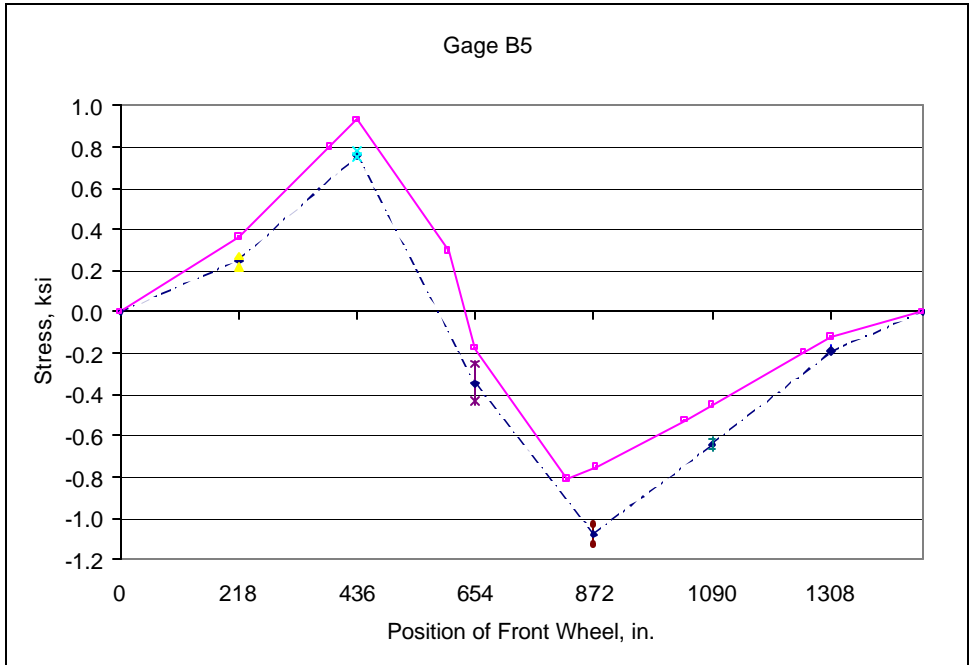
Graph F.77: Diagonal member L3U2



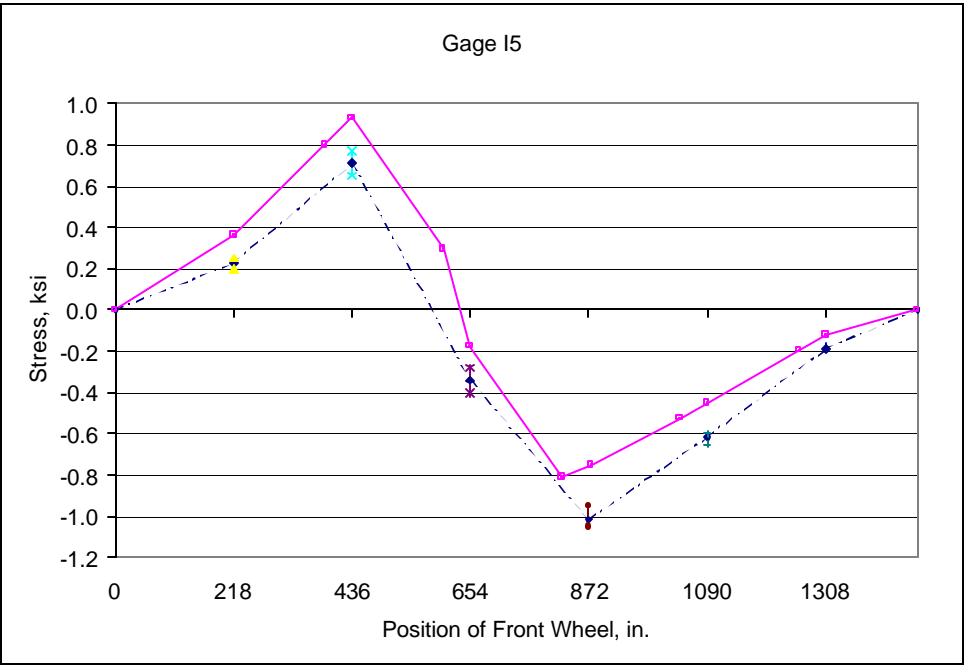
Graph F.78: Diagonal member L3U2



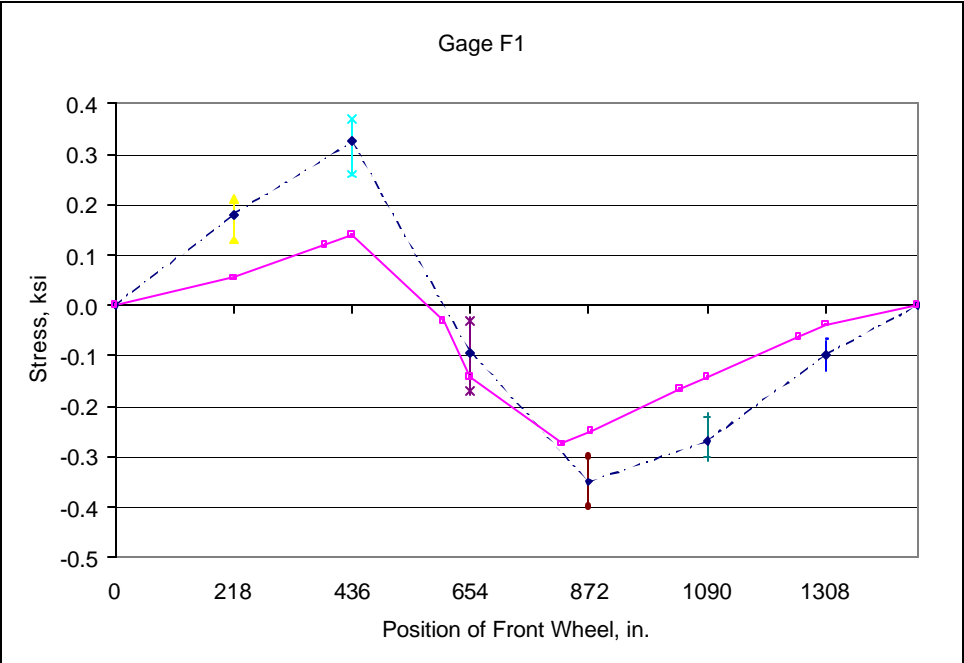
Graph F.79: Diagonal member L3U2



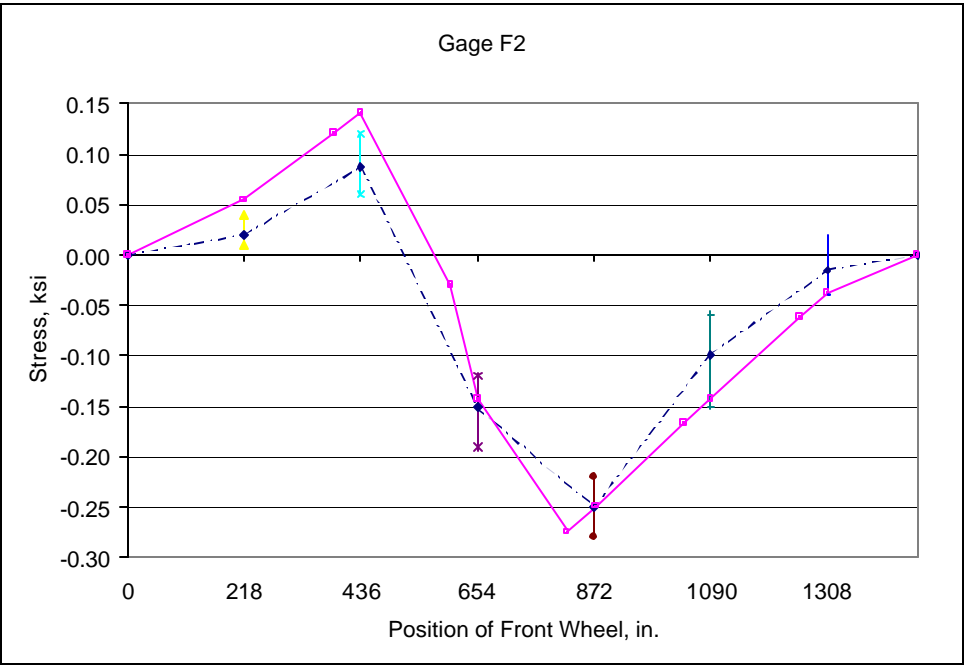
Graph F.80: Diagonal member L2U3



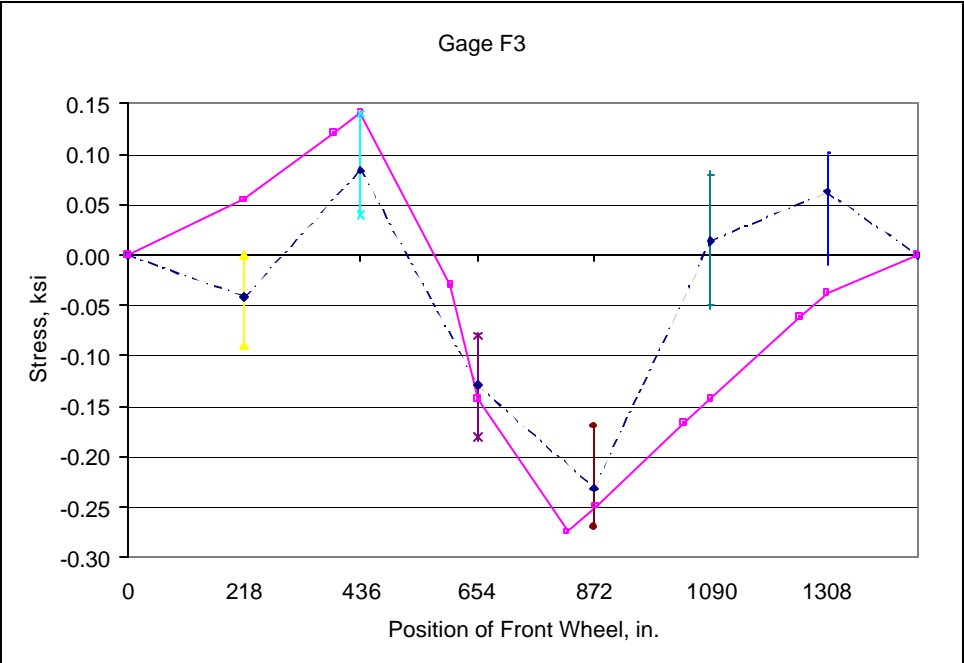
Graph F.81: Diagonal member L2U3



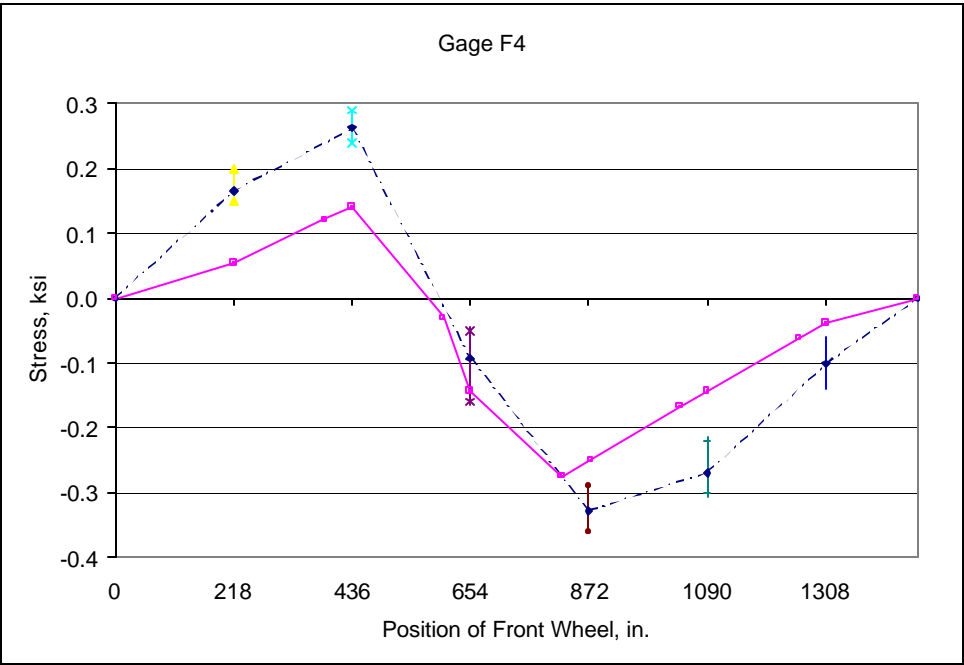
Graph F.82: Vertical member L2U2



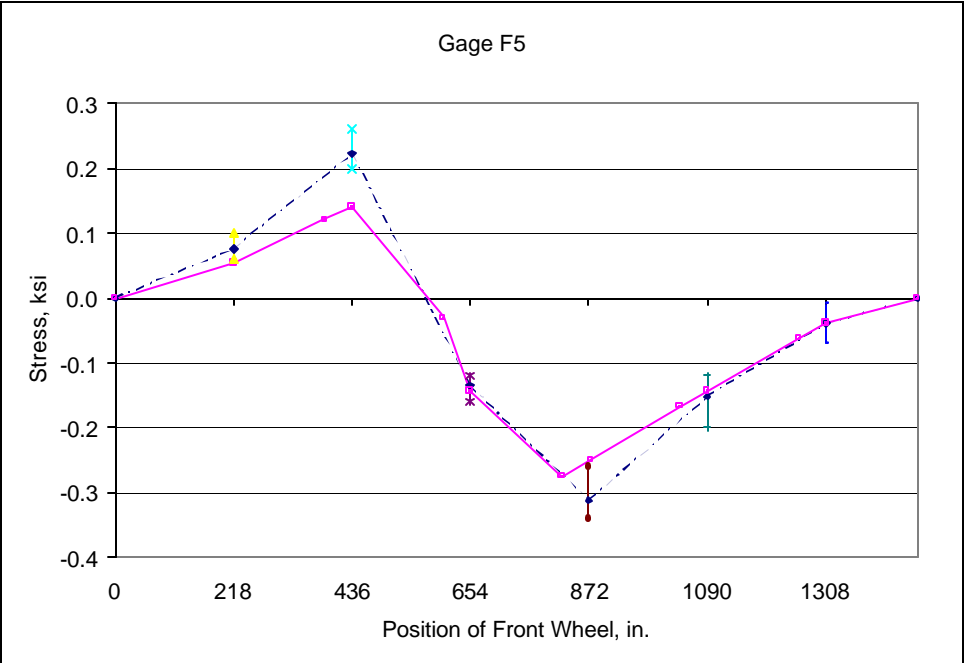
Graph F.83: Vertical member L2U2



Graph F.84: Vertical member L2U2



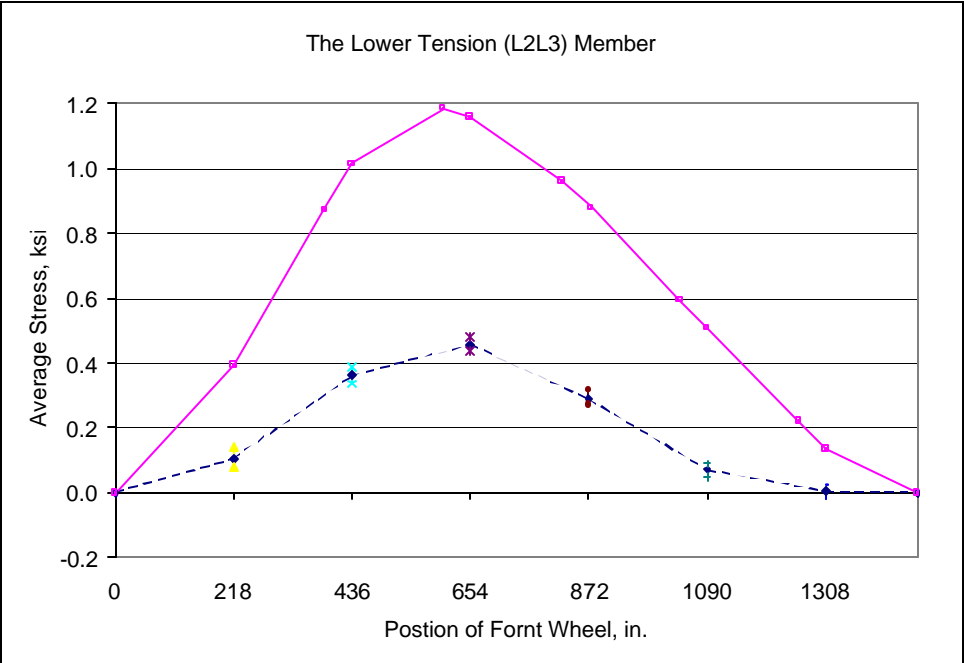
Graph F.85: Vertical member L2U2



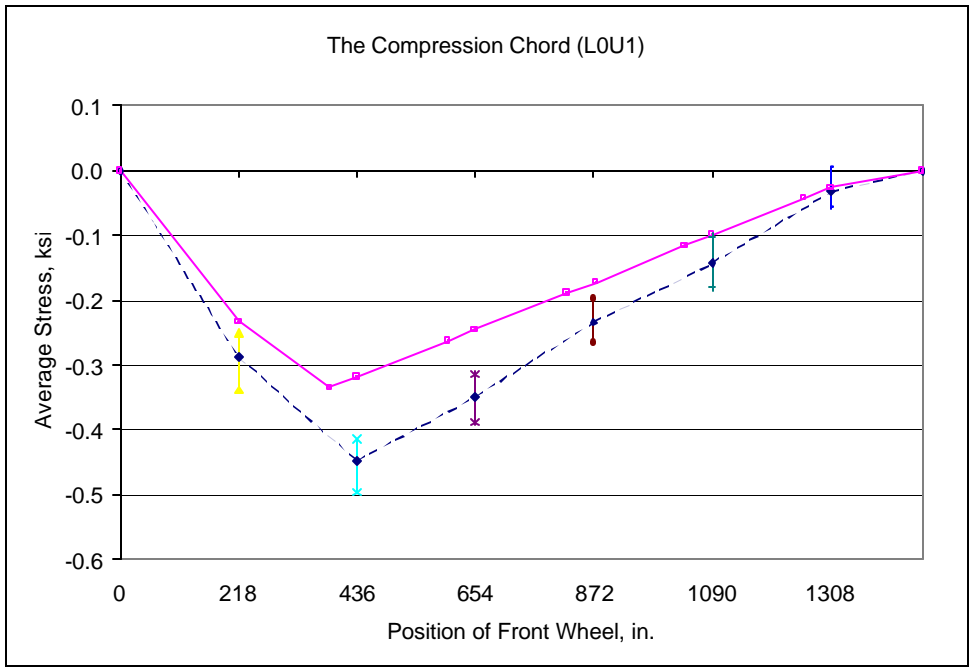
Graph F.86: Vertical member L2U2



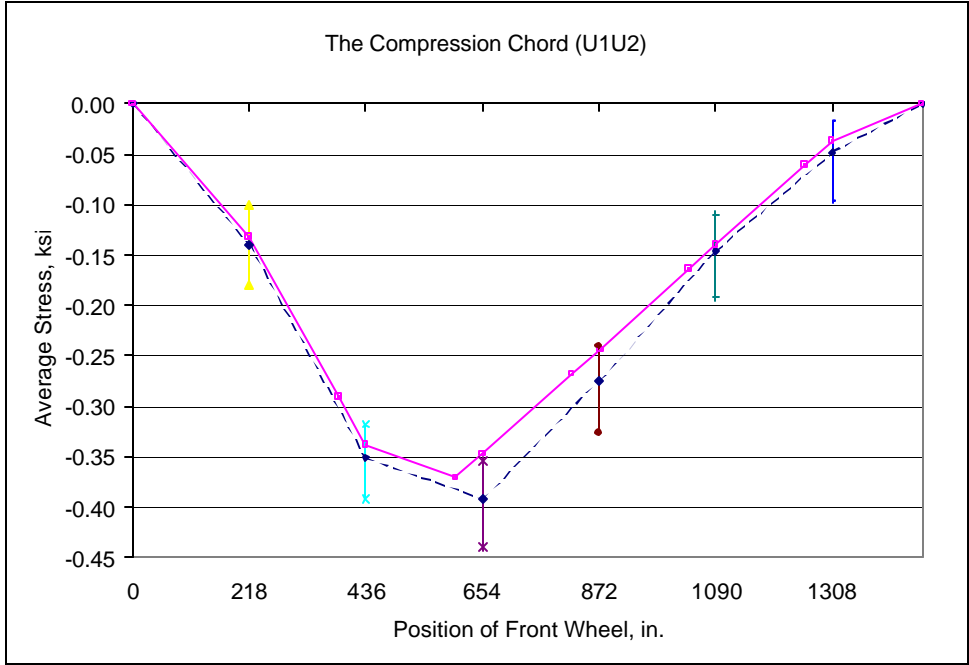
Graph F.87: Average stress: Bottom chord (L1L2)



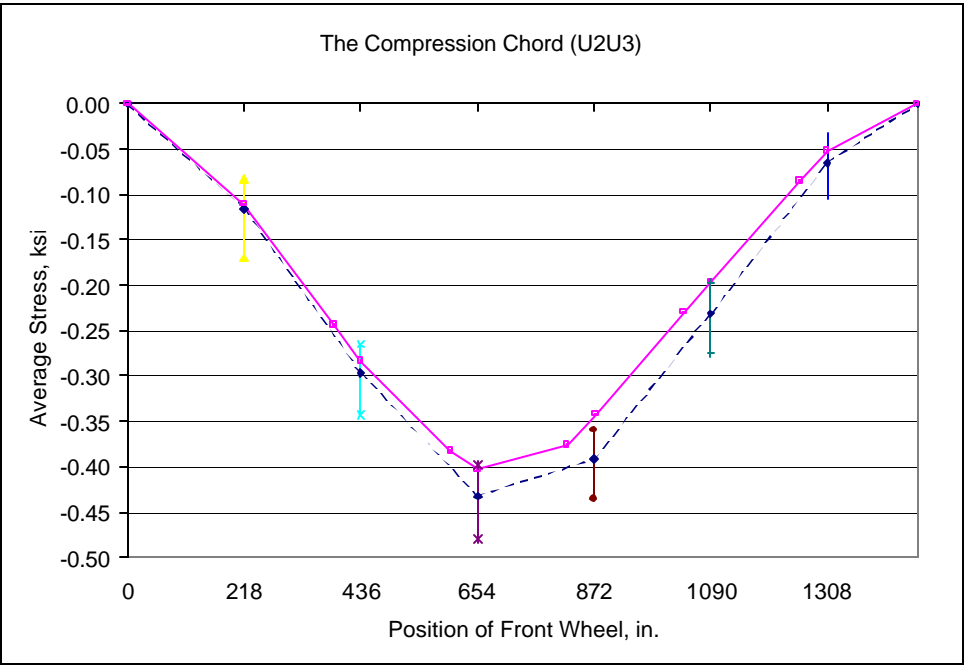
Graph F.88: Average stress: Bottom chord (L2L3)



Graph F.89: Average stress: Top Chord (L0U1)



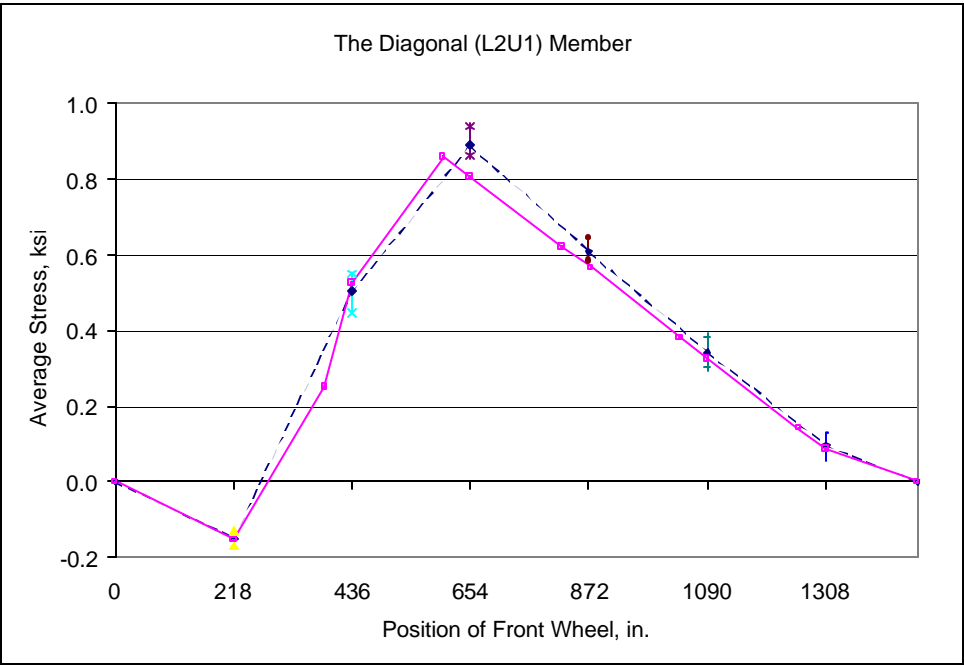
Graph F.90: Average stress: Top Chord (U1U2)



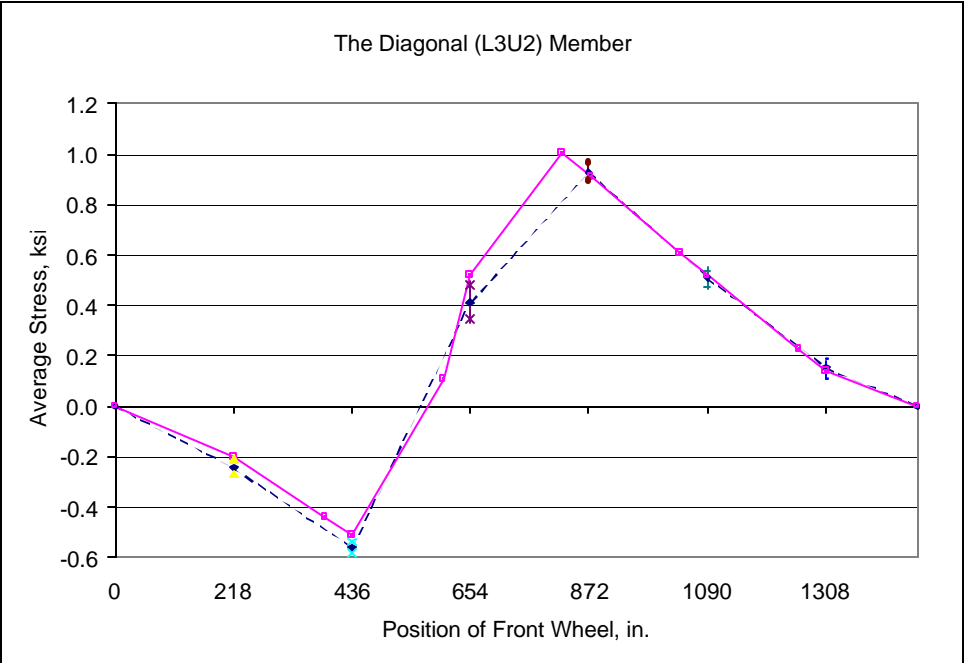
Graph F.91: Average stress: Top Chord (U2U3)



Graph F.92: Average stress: Vertical hanger (L1U1)



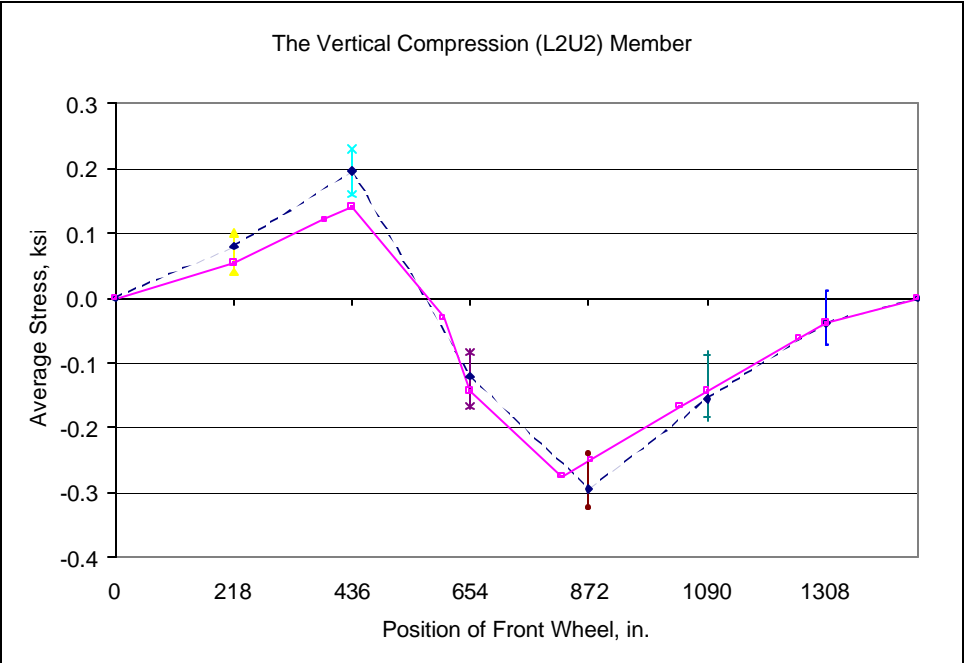
Graph F.93: Average stress: Diagonal member (L2U1)



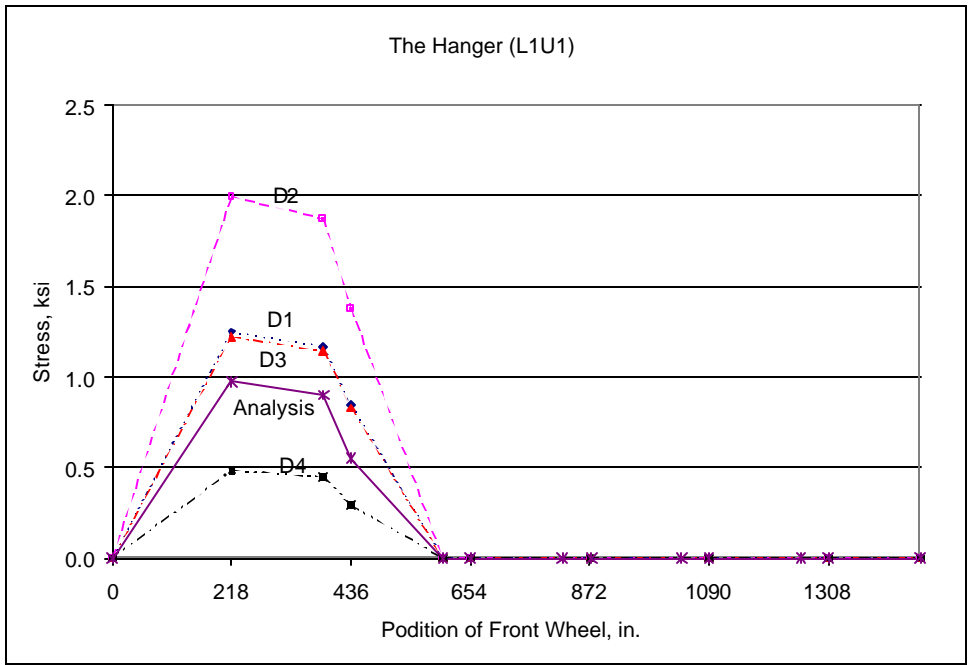
Graph F.94: Average stress: Diagonal member (L3U2)



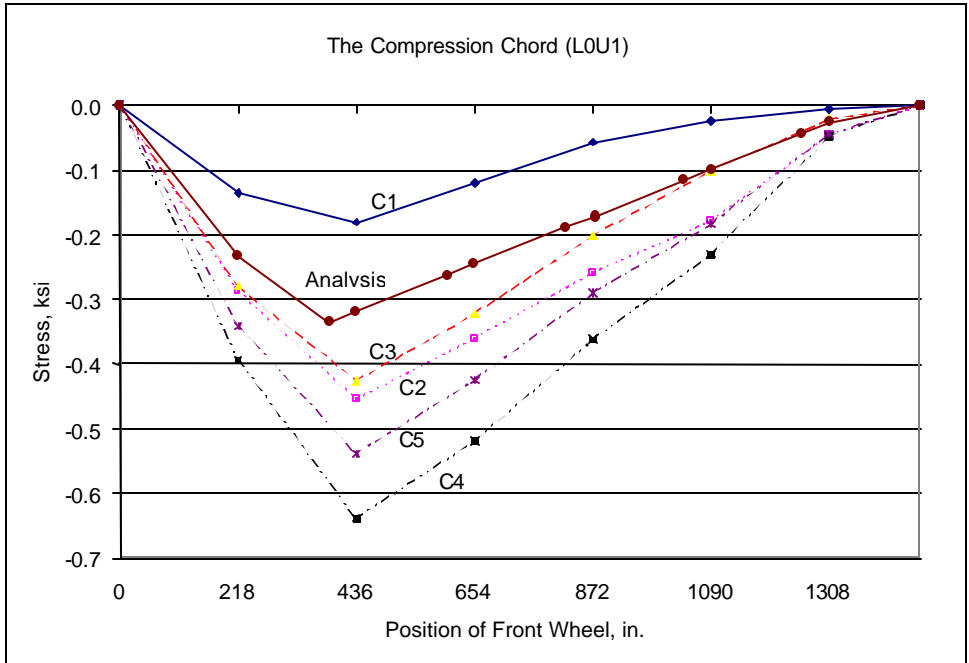
Graph F.95: Average stress: Diagonal member (L2U3)



Graph F.96: Average stress: Vertical member (L2U2)



Graph F.97: Stress variation: Vertical Hanger (L1U1)



Graph F.98: Stress variation: Top Chord (L0U1)

References

- Alibe, B. (1990). "Characteristics of columns with uncertain end restraint." *Journal of Structural Engineering*, 116 (6), 1522-1534.
- American Association of State Highway and Transportation Officials, (AASHTO). (1996). "Standard Specification for Highway bridges." Washington, D.C.
- American Association of State Highway and Transportation Officials, (AASHTO). (1994). "Manual for condition evaluation of bridges." Washington, D.C.
- American Association of State Highway and Transportation Officials, (AASHTO). (1989). "Guide specifications for strength evaluation of existing steel and concrete bridges." Washington, D.C.
- American Association of State Highway and Transportation Officials, (AASHTO). (1989a). "Guide specifications for fatigue design of steel bridges." Washington, D.C.
- American Concrete Institute, (ACI) (1985). "Rehabilitation, renovation, and preservation of concrete and masonry structures." Sabnis, G.M., editor, special publication No. 85.
- American Society of Civil Engineers, (ASCE). (1986). "Experimental assessment of performance of bridges." Wang, L.R.L. and Sabnis, G.M., editors.
- American Standards for Testing of Materials, (ASTM). (1973) "Metallography – A practical tool for correlating the structure and properties of material." special technical publication No. 557.
- Arnold, L. K. and Walker, R. E. (1953). "Wood Preservation." Iowa Engineering Experiment Station, LI (41), Department of Civil Engineering, Iowa State College, Ames, Iowa. Iowa Engineering Experiment Station Bulletin No. 174.
- Aston, J. (1936). "Wrought iron: Its manufacture, characteristics and applications." A. M. Byers, Pittsburgh, PA.

- Avent, R. R. (1985). "Decay, weathering and epoxy repair of timber." *The Journal of Structural Engineering*, 111 (2), 328-342.
- Avent, R.R. (1989). "Heat-straightening of steel: Fact and fable." *Journal of Structural Engineering*, 115 (11), 2773-2793.
- Ayyub, B.M., Ibrahim, A., and Schelling, D. (1990). "Posttensioned trusses: Analysis and design." *Journal of Structural Engineering*, 116 (6), 1491-1506.
- Ayyub, B.M. and Ibrahim, A. (1990). "Posttensioned trusses: Reliability and redundancy." *Journal of Structural Engineering*, 116 (6), 1507-1521.
- Badoux, M. and Sparks, P. 1998. (1998). "Fracture critical study of an historic wrought iron bridge." *Structural Engineering International*, 2, 136-139.
- Bahaa Machaly, E., (1986). "Buckling contribution to the analysis of steel trusses." *Computers and Structures*, 22 (3), 445-458.
- Bakht, B. and Csagoly, P.F. (1977). "Strengthening and widening of steel pony truss bridges." *Canadian Journal of Civil Engineering*, 4, 214-225.
- Bakht, B. and Jaeger, L.G. (1987). "Behavior and evaluation of pin-connected steel truss bridges." *Canadian Journal of Civil Engineering*, 14, 327-335.
- Bakht, B. and Jaeger, L.G. (1990). "Bridge testing – A surprise every time." *The Journal of Structural Engineering*, 116 (5), 1370-1383.
- Barr, B. I. G., Evans, H. R. and Harding, J. E. (1994). "Bridge assessment management and design." *Proceedings of the Centenary Year Bridge Conference*, Cardiff, UK, 26-30.
- Beauchamp, J.C., Chan, M.Y.T. and Pion, R.H. (1984). "Repair and evaluation of a damaged truss bridge – Lewes, Yukon River." *Canadian Journal of Civil Engineering*, 11, 494-504.
- Belenya, E.I. and Gorovskii, D.M. (1971/72). "The analysis of steel beams strengthening by a tie rod." *I.C.E. monthly*, 2 (9), 412-419.
- Bettigole, N. H. and Robinson, R. (1997). "Bridge decks: Design, construction, rehabilitation, and replacement." ASCE Press.

- Bondi, R.W. (1985). "Adding redundancy to fracture critical 2-eyebar members in a cantilever truss bridge." *Proceedings of second annual International Bridge Conference*, Engineers' Society of Western Pennsylvania, Pittsburgh, Pennsylvania.
- Bondi, R.W. (1985a). "Pin replacement on a 100-year-old Whipple truss bridge." *Proceedings of second annual International Bridge Conference*, Engineers' Society of Western Pennsylvania, Pittsburgh, Pennsylvania.
- Bousfield, B. (1992). "Surface preparation and microscopy of materials." John-Wiley & Sons, Inc.
- Boving, K. G. (1989). "NDE handbook: Non-destructive examination methods for condition monitoring." Bason, F., translator, Butterworths, England.
- Bray D. E. and McBride D. (1992). "Nondestructive testing techniques." John-Wiley & Sons, Inc.
- Brinckerhoff, P. (1993). "Bridge inspection and rehabilitation: A practical guide." Silano, L.G., Henderson, A.C., editors, John-Wiley & Sons, Inc.
- Cain, J. R. (1924). "Influence of sulfur, oxygen, copper and manganese on the red-shortness of iron." Department of Commerce, Bureau of Standards, Technologic papers of the bureau of standards, 18(261).
- Carver, D. R. and Hanson, N. W. (1953). "A determination of the stiffness factors of the upper chord of a continuous pony truss bridge." Engineering Experiment Station, Kansas State College Bulletin No. 68, Department of Applied Mechanics, Kansas State College, Manhattan, Kansas.
- Chajes, M.J., Kaliakin, V.N., Holsinger, S.D. and Meyer, A.J., Jr. (1995). "Experimental testing of composite wood beams for use in Timber bridges." *Fourth International Bridge Engineering Conference*, 2, 371-380.
- Clauser, H. R., Fabian, R., Peckner, D., and Riley, M. W. (1963). "The encyclopedia of engineering materials and processes." Reinhold Pub. Corp., New York.
- Clifton, J.R. (1985). "Nondestructive evaluation in rehabilitation and preservation of concrete and masonry materials." *Rehabilitation, Renovation, and Preservation of concrete and masonry structures*, ACI-SP-85, 19-29.

- Cole H. A, Jr. and Reed R. E. Jr. (1974). "Detection of structural deterioration in bridges." ASCE, *Specialty Conference on Metal Bridges*, 411-436.
- Column Research Council (CRC). (1966). "Guide to design criteria for metal compression members." Johnston, B. G., editor.
- Csagoly, P.F. and Bakht, B. (1978). "In-plane buckling of steel trusses." *Canadian Journal of Civil Engineering*, 5, 533-541.
- Ensminger, D. (1988). "Ultrasonics: Fundamentals, technology, and application." Marcel Dekker, Inc. New York.
- Fattal, S. G. and Cattaneo, L. E. (1975). "Evaluation of structural properties of masonry in existing buildings." US National Bureau of Standards Building Science Series No. 62.
- Fisher, J.W., Yen, B.T. and Wang, D. "Corrosion and its influence on strength of steel bridge members." Transportation Research Board 1290.
- Fisher, J.W. (1976). "Detection and repair of fatigue cracking in highway bridges." Transportation Research Board, Washington, D.C.
- Fisher, J.W. and Menzemer, C. (1990). "Bridge repair Methods: U.S./Canadian practice." *Bridge Evaluation, Repair and Rehabilitation*, Nowak, A.S., editor, 495-512, Kluwer Academic Publishers.
- Frangopol, D.M. and Nakib, R. "Effects of damage and redundancy on the safety of existing bridges." Transportation Research Board 1290, 9-16.
- Frank, K. H. (1974). "Mechanical and chemical properties of selected steels used in bridge structures." FHWA-RD-75-79.
- Ghosn, M. (1995). "Redundancy in highway bridge superstructure." *Fourth International Bridge Engineering Conference*, 2, 338-348.
- Goebbels, K. (1994). "Material characterization for process control and product conformity." CRC Press.
- Green, M. (1985). "Masonry rehabilitation: Practice and research." Rehabilitation, Renovation, and Reconstruction of Buildings, ASCE, 84-92.

- Griffith, J. H. and Bragg, J. G. (1918). "Tests on large bridge columns." Technologic Papers of the Bureau of Standards No. 101, Department of Commerce, Washington, D.C.
- Hambly, E.C. (1979). "Bridge foundation and substructure." Department of the Environment, Building Research Establishment Report.
- Harding, J. E., Parke, G. E. R. and Ryall M. J. (1996). "Bridge Management 3: Inspection, Maintenance, Assessment and Repair." E & FN SPON.
- Historic American Engineering Record, (HAER). 1996. "Fort Griffin Iron Truss Bridge", HAER No. TX-63, the report prepared as a part of the Texas Historic Bridge Recording Project sponsored by the Texas Department of Transportation.
- Holt, E. C. Jr. (1956). "The lateral stability of Pony truss bridge chords." PhD thesis, Department of Civil, Environmental, and Architectural Engineering, The Pennsylvania State University.
- International Bridge Conference. (1986). "Proceedings of Third Annual International Bridge Conference." Engineers' society of western Pennsylvania, Pittsburgh.
- Jáuregui, D.V. (1999). "Measurement-based evaluation of non-composite steel girder bridges." PhD thesis, Department of Civil Engineering, The University of Texas at Austin, Austin, Texas.
- Jones, J.S. (1995). "Alternatives to riprap as a scour countermeasure." *Fourth International Bridge Engineering Conference*, 2, 261-278.
- Kehl G. L. (1949). "The principles of metallographic laboratory practice." The McGraw-Hill Book Co., New York.
- Kent, W. (1916). "The mechanical engineers' pocket-book." John-Wiley & Sons, Inc.
- Kerekes, F and Hulsbos, C. L. (1954). "Elastic Stability of the top chord of a three-span continuous pony truss bridge." Iowa Engineering Experiment Station, LIII (1), Department of Civil Engineering, Iowa State College, Ames, Iowa. Iowa Engineering Experiment Station, Bulletin No. 177.

- Kim, J.B., Brungraber, R.J., and Yadlosky, J.M. (1984). "Truss bridge rehabilitation using steel arches." *Journal of Structural Engineering*, 110 (7), 1589-1597.
- Kingsley, G. R. and Noland, J. L. (1988). "Nondestructive methods for evaluation of masonry structures." Agbablan, M.S. and Maari, S.F., editors, *Proceedings of the International Workshop on Nondestructive Evaluation for Performance of Civil Structures*, Los Angeles, California, 252-261.
- Lash, S. D. and Joyce, T. C. R. (1962). "Laboratory tests of a full scale pony truss bridge part 1: Test with a laminated timber deck." Department of Civil Engineering, Queen's University, Kingston, Ontario, Canada, Ontario Joint Highway Research Program Report No. 16.
- Li, G. (1987). "Analysis of box girders and truss bridges." China Academic Publisher and Springer-Verlag, New York.
- Mack, R.C., de Teel, P.T. and Askins, J.S. (1980). "Repointing mortar joints in historic brick buildings." *Preservation Briefs: 2*, HCRS, US Department of the Interior.
- Mark, L.S. (1930). "Marks' mechanical engineering handbook." The McGraw-Hill Co., New York.
- Martin, R.A. and Iffland, J.S.B. (1983). "Marine Parkway bridge truss member replacement." *Journal of Structural Engineering*, 10 (7), 1602-1616.
- Mazurek, D. F. and DeWolf, J. T. (1990). "Experimental study of bridge monitoring technique." *The Journal of Structural Engineering*, 116 (9), 2532-2549.
- Melaragno, M. (1998). "Preliminary design of bridges for architects and engineers." Marcel Dekker, Inc.
- Mills, A. P., Hayward, H. W., Rader, L. F. (1939). "Material of construction: Their manufacture and properties." John-Wiley & Sons, Inc., New York.
- Miner, D. F. and seasstone, J. B. (1955). "Handbook of engineering materials." John-Wiley & Sons, Inc.
- Narayanan, R. (1988). "Axially compressed structures: Stability and strength." Applied Science Publisher.

- National Academy of Science (1952). "Distribution of load stresses in highway bridges." National Research Council Publication No. 253.
- National Cooperative Highway Research Program, NCHRP #222. 1980. "Bridges on secondary highways and local roads." Transportation Research Board, Washington, D.C.
- National Cooperative Highway Research Program, NCHRP #271. 1984. "Guidelines for evaluation and repair of damaged steel bridge members." Transportation Research Board, Washington, D.C.
- National Cooperative Highway Research Program #293. 1987. "Methods of strengthening existing highway bridges." Klaiber, F.W., Dunker, K.F., Wipf, T.J., and Sanders W.W., authors, Transportation Research Board, Washington, D.C.
- NDTech. "Operating instructions for the MiniBrineller™ portable hardness tester." NDTech, New Jersey.
- Nowak, A.S. and Ritter, M.A. (1995). "Load and Resistance factor design code for wood bridges." *Fourth International Bridge Engineering Conference*, 2, 351-357.
- Organization for Economic Cooperation and Development (1979). "Evaluation of load carrying capacity of bridges." Road Research, Paris.
- Planck, S.M., Klaiber, F.W. and Dunker, K.F. (1993). "Postcompression and superimposed trusses for bridge rehabilitation." *Journal of Structural Engineering*, 119 (3), 978-991.
- Pullaro, J.J. and Sivakumar, B. (1990). "Increasing the capacity of bridge truss tension members via post tensioning strands." Proceedings of second workshop on bridge engineering research in progress, National Science Foundation and Civil Engineering Department, University of Nevada, Reno, 107-109.
- Rawdon, H. S. and Epstein, S. (1924). "The nick-bend test for wrought iron." Department of Commerce, Bureau of Standards, Technologic papers of the bureau of standards, 18(252).
- Rawdon, H. S. (1917). "Some unusual features in the microstructure of wrought iron." Department of Commerce, Bureau of Standards, Technologic papers of the bureau of standards, 97.

- Ritter, M.A., Wacker, J.P. and Tice, E.D. (1995). "Design, construction, and evaluation of timber bridge constructed of cottonwood lumber." *Fourth International Bridge Engineering Conference*, 2, 358-370.
- Ryder, G.H. 1957. "Strength of Materials." Claver-Hume Press, London.
- SAP2000 *analysis reference vol. I and II – version 6.1.* (1997). Computers and Structures, Inc., Berkeley, California.
- Saraf, V.K. and Nowak, A.S. (1996). "Bridge evaluation using proof load testing." *Recent advances in bridge engineering*, Casas, J.R., Klaiber, E.W., and Mari, A.R., editors, CIMNE, Barcelona, Spain.
- Sedlacek, G., Hensen, W., and Axchen, R. (1992). "New design methods for the rehabilitation of old steel bridges." *Proceedings of the Third International Workshop on Bridge Rehabilitation*, Gert König and A.S.Nowak, editors, The Technical University of Darmstadt and The University of Michigan, 301-317.
- Seong, C.K., Ward, B.A., Yen, B.T. and Fisher, J.W. "Behavior of truss bridges as three dimensional structures." *International Bridge Conference*, IBC-84-30, 203-207.
- Society for Experimental Mechanics, Inc. (1996). "Handbook of measurement of residual stresses." Lu, J., editor, The Fairmont Press, Inc.
- Taly, N (1998). "Design of modern highway bridges." The McGraw-Hill Co., Inc.
- Taavoni, S. "Upgrading and recycling of pin-connected truss bridges by pin replacemmnet." Transportation Research Board 1465, 16-21.
- Tarnai, T. (1977). "Lateral buckling of plane trusses with parallel chords and hinged joints." *Acta Technica Academiae Scientiarum Hungaricae*, Tomus 85 (1 –2), 179-196.
- Texas Department of Transportation, (TxDOT). "Shackelford County Bridge, County Road 188 at Clear Fork of Brazos River."
- Thiel, M.E. (1998). "Preservation alternatives for historic metal truss bridges: Survey of literature and current practices." Master's thesis, Department of Civil Engineering, The University of Texas at Austin, Austin, Texas.

- Trautner, J. J. (1989). "Computer Modeling and Reliability Evaluation of Truss Bridges." PhD thesis, Department of Civil Engineering, The University of Colorado.
- Troitsky, M. S. (1990). "Prestressed steel bridges: Theory and design." Van Nostrand Reinhold Co., New York.
- Vegesna, S. and Yura, J. A. (1992). "An ultimate load test to study bracing effects of bridge decks." The University of Texas at Austin, Research Report No. 1239-2.
- Vishay Measurements Group. (1992). "Student manual for strain gage technology." Bulletin 309D, Vishay Measurements Group, Inc.
- Webb, S. T. and Yura, J. A. (1992). "Evaluation of bridge decks as lateral bracing for supporting steel stringers." Center for Transportation Research, Bureau of Engineering Research, The University of Texas at Austin, Research Report No. 1239-3.
- White, K. R., Minor, J. and Derucher, K. N. (1992). "Bridge maintenance, inspection and evaluation." Marcel Dekker, Inc., New York.
- Willson F. (1984). "Building material evaluation handbook." Van Nostrand Reinhold.
- Witmer, R. W. Jr., Manbeck, H. B., and Janowiak, J. J. (1999). "Partial composite action in hardwood glued-laminated T-beams." *The Journal of Bridge Engineering*, 4 (1), 23-29.
- Zobel, H. (1995). "Determination of heat-straightening parameters for repair of steel pedestrian bridge." *Fourth International Bridge Engineering Conference*, 2, 26-32.
- Zuk, W. and McKeel, W.T., Jr. "Adaptive use of historic metal truss bridges." Transportation Research Board 834.
- Zulfiquar, K. (1998). "Preservation alternatives for the historic metal truss bridges: Literature survey." Master's report, Department of Civil Engineering, The University of Texas at Austin, Austin, Texas.

Vita

Dilip Maniar was born on August 17, 1973 in Bombay, India to Rugnathbhai and Heeragauri Maniar. Dilip attended Smt. J.B.Khot High School and completed his secondary school in May 1988. He entered Victoria Jubilee Technical Institute (VJTI), Bombay where he studied Licentiate Civil and Sanitary Engineering (LCSE). Dilip graduated in the May of 1992. Dilip reentered VJTI to get bachelors degree in civil engineering. He graduated BSCE, with honors from the University of Bombay in the May of 1995. He awarded three gold medals, one silver medal, two bronze medals, two silver trophies and numerous other prizes for his academic excellence. Dilip worked with Tata Consulting Engineers for one year and with Tata Consultancy Services for another year. He joined The University of Texas at Austin in the August of 1997 to get master of science in civil engineering. Dilip graduated in the August of 2000. Dilip will be continuing for doctoral studies at The University of Texas at Austin from the August of 2000.

Permanent address: B/3, Sajag Apartments, Shimpoli Road,
Borivali (West), Mumbai – 400 092. India.

This thesis was typed by the author.